Atmospheric Particle Production from Freshwater and Oceanic Wave-breaking

by

Nathaniel W. May

A dissertation submitted in partial fulfillment
of the requirements for the degree of
Doctor of Philosophy
(Chemistry)
in the University of Michigan
2018

Doctoral Committee:

Assistant Professor Kerri Pratt, Chair
Assistant Professor Andrew Ault
Professor Joel Blum
Professor Robert Kennedy
Assistant Professor Ginger Shultz

Nathaniel W. May

maynate@umich.edu
nathanielwmay@gmail.com

ORCID iD: 0000-0002-8913-4827

Acknowledgements

I first need to thank Dr. Kerri Pratt, my advisor. My growth as a scientist and resulting accomplishments over these last five years would not have been possible without your mentorship. You pushed me to do more than I ever thought I was capable of. In addition, I am forever grateful to you for the opportunity to conduct field research in Michigan and the Arctic, and for the freedom to pursue my passion for education. I would also like to thank my committee members – Dr. Andrew Ault, Dr. Joel Blum, Dr. Ginger Shultz, and Dr. Robert Kennedy – for their guidance and support. Individually, I would like to thank Dr. Ault for his mentorship and support in my research into the exciting new field of lake spray aerosol. I would also like to thank Dr. Shultz, who has been an invaluable mentor in my foray into the world of education research, I have learned so much from you about teaching and learning that I will carry with me into the future.

Next, I would like to extend my deepest appreciation to Dr. Steven Suljak, my undergraduate research advisor at Santa Clara University. It was in your laboratory that I discovered my passion for research and working with chemical instrumentation. Your mentorship empowered me as an undergraduate researcher and I would not have made it through my doctoral career without your continued support. Speaking of Santa Clara, I would be remiss if I did not acknowledge the best friends I could ever ask for - the Skrilla Villains. You reminded me that I was more than just a scientist, that there was a life outside of graduate school, and that there was always sunshine in California – I cannot thank you enough for that.

To the members of the Ault and Pratt labs, who were invaluable as both labmates and friends, I am truly grateful. I would not have made it through these past years without the help of both past and present labmates. From the Pratt lab I would like to extend my thanks to Dr. Matt Gunsch, Eric Boone, Stephen McNamara, Rachel Kirpes, Dr. Peter Peterson, Dr. Siyuan Wang, Ryan Cook, and Jeffrey Spencer. From the Ault lab I would like to extend my thanks to Dr. Rebecca Craig, Nicole Olson, Dr. Amy Bondy, and Dr. Jessica Axson. No matter if it was preparing for our numerous field studies, giving feedback at countless practice talks, fixing instruments, commiserating at happy hour, or celebrating each other's accomplishments with large

volumes of sugary alcohol, we were always in it together. This comradery was always a light in the dark and I hope it never leaves our labs. In this spirit, I would like to extend a special thanks to Dr. Craig - we entered into graduate school at the same time and "I won't quit if you won't quit" was said amongst us more times than I could count, but here we are five years later. I would also like to extend my gratitude to the high school and undergraduate students I have mentored, who have conducted impressive work as young scientists, made important contributions to several of my papers, and inspired me with their excitement for science. In addition, I would like to extend my sincerest thanks to all of the undergraduates I have had the honor of teaching during my time as a graduate student instructor. I discovered my life's true passion with you in the classroom and for that I am eternally grateful.

Last, but most important, my family. First to my brother, Dr. James May (he's the "real doctor" of the family) - we both started our respective journeys towards becoming doctors in the Fall of 2013 and the knowledge that together we were working to achieve our respective dreams, although thousands of miles apart, always reassured me that I was on the right path. To my parents, words cannot express my gratitude for your unwavering love and support, and for giving me "roots and wings." Dad – you instilled in me a love for the environment at an early age and opened so many doors for me to discover my own passion for science. I was always so proud to have Dr. Christopher May as my dad, you were my inspiration for pursuing a Ph.D. and it was an honor to follow in your footsteps. Mom – I want you to know how much I appreciate all the things you have done for me over these last five years, which include, but are not limited to: the countless boxes of homemade jam and chocolate chip cookies, putting print-outs of my papers up on the fridge back at home, sending me letters with comforting or inspiring words just when I needed it most, and the homemade knitwear that kept me warm during the cold Midwest winters. More importantly, you helped me keep it all in perspective and were always there to talk when I needed. Finally, I would like to thank my supportive, understanding, and loving partner Gloria. I consider it life's greatest miracles that we found each other in Michigan of all places and I would not have made it through these last, hard years without you. Whether it was camping next to Lake Michigan, driving to Detroit for the day, or just spending a quiet weekend at home with Gaston, our time together always helped me remember what was truly important in life. To all my family and loved ones, thank you – I owe everything to you.

Table of Contents

List of Figures

List of Tables

List of Equations

Abstract

Wave-breaking in natural bodies of water forms bubbles that burst at the air-sea interface to produces atmospheric particles, known as sea spray aerosol (SSA) in marine environments and lake spray aerosol (LSA) in freshwater environments. While the properties and associated health and climate impacts of SSA have been widely reported, the impacts of SSA on atmospheric composition far from the ocean remain uncertain. In comparison, few studies of LSA exist. In this dissertation, the production and physiochemical properties of LSA and SSA at coastal and inland environments were examined. The results of this work increase our understanding of the atmospheric impacts of wave-breaking particle production from varied aquatic environments. In addition, this dissertation details efforts to integrate environmental chemistry research into introductory chemistry curricula to increase student engagement in the sciences.

A laboratory-based LSA generator was constructed to produce and analyze particles from freshwater in a controlled environment for the first time. To evaluate the LSA generator, bubble and aerosol number size distributions were measured for salt solutions representative of freshwater and seawater, and a freshwater sample from Lake Michigan. The LSA generator was then utilized to produce particles from freshwater samples with varying blue green algae concentrations with analysis by single particle microscopy and mass spectrometry. Notably, the number fraction of LSA with organic carbon increased with decreasing diameters and the total number fraction of LSA with biological material increased directly with increased blue green algae concentration. During summertime ambient aerosol sampling conducted in northern Michigan, both SSA and LSA were observed by single particle microscopy and mass spectrometry. Air mass back trajectory analysis indicated that SSA originated from Hudson Bay, Canada and LSA originated from the Great Lakes, >700 km and >25 km from the sampling site, respectively. These results represent the furthest inland quantification of SSA particle mass contributions by single particle analysis and the first confirmation of the inland transport of LSA.

Rapid sea ice loss is dramatically changing the Arctic surface, with increasing SSA production expected from newly exposed ocean surface. Multi-year bulk atmospheric particle inorganic ion concentrations, local sea ice conditions, and meteorology at Utqiaġvik, AK were

combined to investigate the dependence of SSA mass concentrations on Arctic sea ice coverage and wind speed. Supermicron (1–10 μm) SSA mass concentrations increased in the presence of nearby leads (fractures in the sea ice) and wind speeds greater than 4 m s^{-1}. SSA produced from leads has the potential to alter the chemical composition of the Arctic atmosphere and snowpack. To investigate impacts of SSA production from Arctic sea ice leads on snow chemistry, a course based undergraduate research experience (CURE) centered on Arctic snow chemistry was implemented in an existing introductory general chemistry laboratory course. Survey evaluation results indicate students in the snow chemistry CURE experienced greater gains in confidence of research skills and general attitudes towards chemistry compared to a traditional course. To increase the accessibility of the environmental chemistry CURE, a research-based laboratory experiment for the determination of chloride content in snow and other environmental samples with basic laboratory equipment was designed for the high school classroom. The positive impacts on undergraduates of the snow chemistry CURE, and the potential for its translation into the high school classroom, motivates further incorporation of environmental research experiences at an early academic career stage.

Chapter 1 Introduction

1.1. Atmospheric Particles

Atmospheric particles have a profound impact on climate and human health (Pöschl 2005, Calvo et al. 2013, Pöschl and Shiraiwa 2015). Atmospheric particles impact climate by altering the balance between the energy the Earth receives from incoming solar radiation and that which it radiates back into space, known as radiative forcing (Boucher et al. 2013). The total radiative forcing due to atmospheric particles, estimated to be -0.9 ± 0.8 W m^{-2} (Boucher et al. 2013), is directly impacted by atmospheric particles either scattering or absorbing incoming solar radiation, and is indirectly impacted by atmospheric particles acting as cloud condensation nuclei (CCN) or ice nucleating particles (INP) (Boucher et al. 2013). Atmospheric particles represent the largest source of uncertainty in global radiative forcing predictions due to their complex and dynamic physiochemical properties, as well as their high temporal and spatial variability (Boucher et al. 2013). In addition to impacting climate, increased concentrations of atmospheric particles are linked to reduced air quality and negative health effects (Pope and Dockery 2006), with over 3 – 5 million premature deaths attributed annually to atmospheric particles worldwide (Lelieveld et al. 2015, Cohen et al. 2017).

Atmospheric aerosol particles range in size from 1 nm – 100 μm and contain hundreds to thousands of different chemical species (Prather et al. 2008). The size and chemical composition (physiochemical properties) of individual atmospheric particles largely determines their climate and health properties (Brook et al. 2004, Pöschl 2005, Furutani et al. 2008, Calvo et al. 2013, Fierce et al. 2016). Typically, atmospheric particles with diameters >100 nm will act as CCN at lower water vapor super saturation than atmospheric particles with diameters <100 nm (Dusek et al. 2006). Cloud formation by atmospheric particles is also influenced by composition, with particles composed of more hygroscopic material (i.e. ammonium sulfate) more readily taking up water to act as CCN compared to particles composed of less hygroscopic material (i.e. hydrophobic organic carbon) (Seinfeld and Pandis 2016). Atmospheric particle composition also affects the nature of their direct interactions with incoming solar radiation, with particles composed of

absorbing material (e.g. black carbon) resulting in a positive radiative forcing (warming) and particles composed of scattering material (e.g. organic carbon) resulting in a negative radiative forcing (cooling) (Kopp and Mauzerall 2010). In regards to health implications, atmospheric particles with diameters less than 100 nm, which represent the majority of atmospheric particles by number (Seinfeld and Pandis 2016), can enter the lungs and bloodstream, resulting in a larger impact on health than particles with larger diameters that are deposited in the upper respiratory system (Brook et al. 2004, Pope and Dockery 2006). The inclusion of transition metals and certain organic compounds can increase the negative health impacts of these atmospheric particles (Valavanidis et al. 2008). Atmospheric particle composition, and associated climate and health properties, can be altered by heterogeneous reactions and gas-particle partitioning (Moffet and Prather 2009, Riemer and West 2013) during atmospheric transport away from their source (Uno et al. 2009). Characterizing the size and chemical composition of atmospheric particles, as well as the changes in these properties during their lifetime in the atmosphere, is thus necessary to predict climate and air quality impacts (Calvo et al. 2013).

1.2. Production and Characteristics of Wave Breaking Particles

Wind-induced wave-breaking in marine environments, which directly emits sea spray aerosol (SSA), is one of the largest natural sources of atmospheric particles (Lewis and Schwartz 2004, Andreae and Rosenfeld 2008). Wave-breaking entrains air beneath the water's surface, forming bubbles that rise to the surface and burst to eject droplets that result in SSA after the evaporation of water (Lewis and Schwartz 2004). As the bubble-bursting droplet production mechanism is a function of wind-induced wave-breaking, the production flux of SSA is modelled as a function of increasing wind speed (Lewis and Schwartz 2004). Two distinct mechanisms in the bubble bursting process dominate the production of SSA (Blanchard and Woodcock 1957). First, the fragmentation of the top of the bubble membrane produces film drops. After the bubble membrane top bursts, droplets of water are flung upward from the bubble bottom during the collapse of the remaining cavity, producing jet drops. After evaporation of water, film drops mainly result in submicron particles and jet drops generally result in supermicron particles (O'Dowd et al. 1997). However, recent work has demonstrated that small bubbles (radius < 20 μm) produce jet drops that contribute a significant portion of submicron SSA (~20-40% by number) dependent on seawater composition (Wang et al. 2017).

Reflective of the composition of their seawater origin (Pilson 2013), SSA is composed primarily of NaCl and other inorganic salts, as well as organic compounds and biological material (Prather et al. 2013). The bubble bursting particle production method determines the distribution of inorganic salts, organic compounds, and biological material across the population of SSA (i.e. mixing state) (Prather et al. 2013, Wang et al. 2017). Understanding the bubble bursting particle production method is thus vital in determining the health and climate properties of SSA (Collins et al. 2013, Prather et al. 2013, Collins et al. 2014, Guasco et al. 2014). Hydrophobic organic matter accumulates at the surface of bubbles as they rise through the water column (O'Dowd et al. 2004, Keene et al. 2007, Bigg and Leck 2008, Facchini et al. 2008) and is further enriched by the sea surface microlayer, which contains a higher concentration of organics than bulk seawater (Zhang 2003, Hawkins and Russell 2010). The concentration of organics at the bubble surface is then translated to an enrichment of organics in SSA resulting from the fragmentation of the bubble film cap (Blanchard and Syzdek 1975, Cheng et al. 2007, Backer et al. 2008, Backer et al. 2010, Wood and Dietrich 2011). The addition of less water soluble organic species to SSA resulting from film drops decreases SSA overall hygroscopicity and increases their CCN activation diameter (Andreae and Rosenfeld 2008). SSA resulting from jet drops are more representative of the inorganic-rich bulk seawater solution (Lewis and Schwartz 2004) and contain a higher concentration of biological material, as well as water soluble organic compounds, when produced from marine algal blooms (Blanchard and Syzdek 1972, Matthias-Maser et al. 1999, Aller et al. 2005, McCluskey et al. 2017). The enrichment of biological matter and hydrophilic organic matter in SSA resulting from jet drops, as well as their larger size, increase their propensity to act as INP (DeMott et al. 2015, Wilson et al. 2015, Ladino et al. 2016, McCluskey et al. 2017, Vergara-Temprado et al. 2017, Wang et al. 2017). In addition to climate impacts, SSA can present an inhalation exposure risk if it contains organic and biological material from toxin containing marine algal blooms, most commonly from red tide containing brevotoxins (Cheng et al. 2005, Cheng et al. 2005, Cheng et al. 2010, Kirkpatrick et al. 2011).

The production of particles from wave-breaking in freshwater environments, including the Laurentian Great Lakes, has been far less studied. Slade et al. (2010) first observed the production of atmospheric particles from the surface of Lake Michigan as a function of wind speed. Based on these observations, Chung et al. (2011) conducted the first regional chemical transport modelling that incorporated a freshwater particle source and predicted that the wind-dependent production of

atmospheric particles from the Great Lakes could affect aerosol number and CCN concentrations throughout the surrounding region. Motivated by these findings, Axson et al. (2016) first determined the chemical signature for atmospheric particles produced by freshwater wave-breaking. These particle, termed lake spray aerosol (LSA), were determined to be primarily composed of calcium carbonate, along with contributions from other inorganic ions and organic material (Axson et al. 2016), reflective of the composition of their freshwater origin (Chapra et al. 2012). The identification of calcium particles in Great Lakes region clouds (Lasher-Trapp et al. 2008, Twohy and Anderson 2008), alongside previous studies of the cloud formation properties of $CaCO_3$ particles (Gibson et al. 2006, Sullivan et al. 2009), suggests that the newly identified LSA may impact climate through participation in cloud formation. Freshwater wave-breaking may also impact climate through the introduction of INP active biological species (D'Souza et al. 2013, Pietsch et al. 2015, Pietsch et al. 2017), which are two to three orders of magnitude higher in concentration in freshwater than in seawater (Moffett 2016). In addition, investigations of aerosol production by bubble-bursting action from recreational activity in freshwater harmful algal blooms (HABs), composed primarily of microcystin producing cyanobacteria (blue-green algae), reported measurable concentrations of aerosolized toxins associated with human health impacts (Cheng et al. 2007, Backer et al. 2008, Backer et al. 2010, Wood and Dietrich 2011). Therefore, the production of organic and biological containing LSA from HABs, which are increasing in occurrence and severity in the Great Lakes (Michalak et al. 2013), should be considered for their potential impacts on both air quality and climate.

As LSA has only recently been identified, the discussion of the methods for physiochemical analysis of wave-breaking particles presented here will focus primarily on SSA. Traditionally, SSA was studied through offline bulk particle measurements achieved through filter-based sampling, followed by extraction and analysis (Shaw 1991, Quinn et al. 1998, Gustafsson and Franzén 2000, Quinn et al. 2002, Hara et al. 2004, Silva et al. 2007, Manders et al. 2010, Santos et al. 2012, Udisti et al. 2012, Chalbot et al. 2013, Makowski Giannoni et al. 2016). However, traditional offline bulk particle measurements have significant analytical limitations. Time resolution of bulk particle methods is constrained by how often the filter is changed, typically multiple hours to days, which limits observation of changes in particles due to rapidly shifting conditions, such as shifts in wind direction or speed. In addition, bulk particle methods only provide an average chemical composition and cannot determine if a particle population exists as

an internal mixture, where all particles have all components and are well-mixed, or an external mixture, where individual components are present in separate particles (Riemer and West 2013, Ault and Axson 2017). Understanding chemical mixing state in a population of atmospheric particles is vital in determining climate and health properties (Jacobson 2001, Zaveri et al. 2010). Bulk methods also cannot determine the spatial distribution of chemical species within a particle, which can alter their climate properties (Ryder et al. 2015, Nguyen et al. 2017). Therefore, single particle techniques that can measure chemical species between and within individual particles are needed to address the complex and dynamic atmospheric particle populations present in the ambient atmosphere to fully understand their climate and health impacts.

1.3. Chemical Characterization of Individual Wave Breaking Particles

For offline measurements of individual SSA and LSA, particles are collected on substrates using an impactor, such as a multiple orifice uniform deposition impactor (MOUDI, MSP Corp.) or a microanalysis particle sampler (MPS, California Instruments) that collect particles on size-resolved stages. Particle morphology can then be measured by microscopy techniques, such as scanning electron microscopy (SEM) and transmission electron microscopy (TEM) (Ault and Axson 2017). SEM measures the reflection of a beam of electrons off the particle (Ault and Axson 2017) to collect detailed morphological images of single particles down to ~100 nm (Laskin and Cowin 2001). TEM can also collect morphological images of particles; however, these images are derived from the electrons transmitted through the particle and offer a higher spatial resolution (<0.1 nm) (Ault et al. 2013, Prather et al. 2013). The addition of computer-controlled automation to SEM allows for a larger number of particles to be analyzed (Laskin and Cowin 2001). TEM and SEM analysis have demonstrated that the morphology of SSA is typically cubic under vacuum, but can become more circular with greater total organic carbon concentrations in seawater (Ault et al. 2013) or after heterogeneous reaction with HNO_3 (Ault et al. 2013). These microscopy techniques of have also identified cubic morphology in ambient and laboratory generated LSA under vacuum (Axson et al. 2016), which, in both LSA and SSA, is the result of inorganic salts crystalizing after drying on the substrate.

When SEM and TEM are coupled with energy dispersive X-ray (EDX) spectroscopy, semi-quantitative chemical information can be obtained by measuring element specific X-rays emitted during interactions between the particle and the electron beam (Ault and Axson 2017). EDX coupled with microscopy has been used to analyze the composition and morphology of SSA in

both field (Allen et al. 2015, Chi et al. 2015, Bondy et al. 2017, Gunsch et al. 2017, Kirpes et al. 2018) and laboratory studies (Ault et al. 2013, Ault et al. 2013, Prather et al. 2013, Ault et al. 2014, Guasco et al. 2014, Patterson et al. 2016), as well as both ambient and laboratory generated LSA (Axson et al. 2016). The elemental composition data from SEM-EDX and TEM-EDX allows for the differentiation of wave-breaking particles from their respective aquatic sources, with LSA characterized by the predominance Ca, C, and O (Axson et al. 2016), reflective of the high $CaCO_3$ content of Great Lakes freshwater (Chapra et al. 2012), and SSA characterized by the predominance of Na and Cl (Laskin et al. 2002, Kirpes et al. 2018), reflective of the NaCl content of seawater (Pilson 2013).

Demonstrating the capability of EDX coupled with microscopy to determine size-dependent chemical mixing state, SEM-EDX and TEM-EDX analysis of laboratory generated SSA showered that internal mixtures of inorganic salts and organic material are externally mixed with particles composed primarily of organic carbon, with organic carbon particles predominating at smaller sizes (<200 nm) in a manner consistent with the enhancement of organic material in film drops (Ault et al. 2013, Prather et al. 2013). SEM-EDX and TEM-EDX has also been used to demonstrate that heterogeneous reaction with HNO_3 redistributes the NaCl core and Mg ring, typical of fresh SSA (Ault et al. 2013), evenly within the particle core and results in a more concentrated layer of organic matter at the surface (Ault et al. 2013, Chi et al. 2015, Kirpes et al. 2018). However, as an offline technique, the utility of traditional SEM-EDX and TEM-EDX in assessing the native state of atmospheric particles can be limited by physicochemical changes that occur during storage and in the vacuum environment of a conventional electron microscope (Laskina et al. 2015). Recently, a modification of traditional TEM-EDX was introduced in an attempt to overcome these challenges. Cryogenic transmission electron microscopy (cryo-TEM), wherein SSA particles are flash frozen in their native state immediately following collection on substrates and before analysis by TEM, allows for the detection of whole hydrated bacteria, diatoms, virus particles, marine vesicles (Patterson et al. 2016). In general, single particle microscopy techniques coupled with EDX offer the advantage of the nondestructive analysis of chemical species between and within individual particles, but can only determine elemental composition and require impaction prior to analysis, which can limit time resolution and lead to artifacts (Ault and Axson 2017).

Single particle mass spectrometers simultaneously measure the size and chemical composition of individual atmospheric particles in real-time (Murphy 2007, Pratt and Prather 2012). One such single particle mass spectrometer is the aerosol time of flight mass spectrometer (ATOFMS), which was one of the first online single particle mass spectrometers developed (Prather et al. 1994) and has since incorporated technological advancements to increase analytical and field deployment capabilities (Pratt et al. 2009). Briefly, particles enter the ATOFMS through a nozzle or aerodynamic lens system, accelerating the particles to terminal velocity and focusing them in a beam. The particle beam then continues into the sizing region of the instrument, which consists of two continuous wave lasers spaced a set distance apart. The velocity of individual particles are measured based on the time it takes to pass between the two lasers and is calibrated to particle diameter based on the measured velocity of polystyrene latex spheres of a known size. After the sizing region individual particles are desorbed and ionized by a 266nm Nd:YAG laser triggered based on the particle velocity calculated in the sizing region. Generated ions enter the dual-polarity time-of-flight mass spectrometer, which produces individual particle positive and negative ion mass spectra.

To date, the ATOFMS has been used to analyze SSA from both field (Gard 1998, Pratt and Prather 2009, Gaston et al. 2010, Qin et al. 2012, Gunsch et al. 2017) and laboratory studies (Prather et al. 2013, Collins et al. 2014, Guasco et al. 2014, Lee et al. 2015, Sultana et al. 2017, Sultana et al. 2017), as well as laboratory generated LSA (Axson et al. 2016). Similar to single-particle micro-spectroscopy techniques, single-particle mass spectrometry can be utilized to determine size-dependent mixing state (Prather et al. 2008). ATOFMS analysis of laboratory generated SSA demonstrated that particles composed primarily of inorganic material (NaCl) and particles enriched in biological materials predominated at diameters > 1 μm (Prather et al. 2013, Collins et al. 2014), reflective of the origin of larger SSA as inorganic and biological rich jet drops. ATOFMS analysis of laboratory generated SSA has also identified the increased predominance of internal mixtures of inorganic salts and organic material (SS-OC) with decreasing diameters < 1 μm (Prather et al. 2013, Collins et al. 2014), reflective of the origin of smaller SSA as organic rich film drops. By varying the ionization laser energy the presence of organic rich coatings around an NaCl core can be identified by ATOFMS in both ambient and laboratory generated SSA (Sultana et al. 2017).

The higher time resolution of ATOFMS (> 1 Hz), compared to offline micro-spectroscopy techniques (multi-hour sampling), enables the examination of changes in the composition of SSA with changes in seawater composition in laboratory studies (Collins et al. 2013, Guasco et al. 2014, Forestieri et al. 2016, Sultana et al. 2017). Measurements of seawater biological and organic content over the course of an induced algal bloom can be coupled with online analysis of generated SSA organic content by ATOFMS (Guasco et al. 2014, Sultana et al. 2017), alongside measurements of particle climate properties (Collins et al. 2013). In doing so, the impact of biological-mediated changes in seawater organic content on the climate properties (Cochran et al. 2017) of particles can be studied more directly in a controlled environment. Field-study deployment of ATOFMS enables the real-time examination of changes in ambient SSA composition, such as the liberation of chlorine to the gas phase by heterogeneous reactions (Gard et al. 1998), and concentrations due to shifts in meteorological conditions (Qin et al. 2012, Gunsch et al. 2017). Coupling single-particle analysis of wave-breaking particles with measurements of their climate properties, alongside meteorological observations, represents an important means for better understanding their impacts on air quality and reducing the uncertainty due to atmospheric particles in global radiative forcing predictions (Boucher et al. 2013).

1.3. Science Education Reform

Numerous national reports conclude that reform is needed in science, technology, engineering, and mathematics (STEM) education (The Boyer Commission on Educating Undergraduates in the Research University 1998, National Research Council 1999, National Research Council 2011, National Research Council 2012, Olson and Riordan 2012, NGSS Lead States 2013, U.S. Department of Education 2016). This conclusion is largely a response to concerns that current STEM educational models are not retaining and training citizenry prepared to contribute to an increasingly technologically driven economy (Baldwin 2009). In addition, STEM educational reform is cited as a means to create a more "just and inclusive society" for women and minorities (Olson and Riordan 2012), who exhibit particularly low participation and achievement in STEM (Griffith 2010, Graham et al. 2013, Lewis 2014, Shedlosky-Shoemaker and Fautch 2015). Improvements in STEM education are also needed to better produce citizenry who possess the scientific literacy necessary to "address the global challenges that humanity now faces and that only science can explain and possibly mitigate, such as global warming, as well as to make wise decisions, informed by scientific understanding, about issues such as genetic

modification," as noted by Nobel laureate Carl Wieman (Wieman 2007). Therefore, educators must confront this great challenge and offer an improved experience in STEM for a new generation of students.

Poor teaching practices in college STEM courses appear to lie at the heart of some of these problematic STEM retention and training trends (Seymour and Hewitt 1997). These problems are more pronounced in introductory courses, as the majority of students, especially underrepresented minorities (Griffith 2010, Graham et al. 2013, Lewis 2014, Shedlosky-Shoemaker and Fautch 2015), leave STEM majors by their second year of undergraduate education (Chen 2013). Introductory undergraduate STEM education often occurs in large halls and is heavily lecture based (Stains et al. 2018). In this setting, students are largely passive learners that rely heavily on memorization to pass tests and experience increased course failure rates (Freeman et al. 2014). The traditional lecture is thus an ineffective means for students to master the basic scientific concepts essential to advanced study and work in STEM fields (Wieman 2007). As a result, students who drop out of STEM after introductory courses are left with little understanding or appreciation of the true nature of science (Seymour and Hewitt 1997).

Replacing standard laboratory courses with discovery-based research courses is listed amongst the President's Council of Advisors on Science and Technology top five recommendations for preparing a scientifically literate population prepared to excel in tomorrow's STEM workforce and address global challenges (Olson and Riordan 2012). Such courses expose participating students to science as it is practiced in the real-world through collaborative, first hand engagement in the process of finding evidence-based answers to problems in the natural world for which no single correct answer exists (Chinn and Malhotra 2002). Course-based undergraduate research experiences (CUREs), in which whole classes of students address a research question (Auchincloss et al. 2014, Chase et al. 2017), have recently gained increased notice as a means for implementing discovery-based research experiences into the undergraduate classroom. CUREs have primarily been implemented in the fields of biology (Lopatto et al. 2014, Bakshi et al. 2016, Kowalski et al. 2016, Rodenbusch et al. 2016) and chemistry (Clark et al. 2016, Kerr and Yan 2016, Chase et al. 2017). Increased implementation of such courses is supported by assessment data that demonstrate significant benefit to of participation in CUREs for both undergraduate students and faculty members (Auchincloss et al. 2014, Hanauer et al. 2016, Shortlidge et al. 2016). However, loss of student interest and engagement in STEM begins before students begin their

undergraduate education, with a decline in the attitudes of students' towards science reported from age 11 onwards (Osborne et al. 2003). The Next Generation Science Standards (NGSS Lead States 2013) attempt counteract this trend through the incorporation of discovery-based curriculum that incorporates authentic science practices into K-12 curricula. However, K-12 teachers often lack scientific research experience and feel unprepared to lead students in activities that are central to inquiry based learning, such as student led question formulation, experimental design, and data interpretation (Singer et al. 2000, Windschitl 2003). Therefore, future work is needed to support the implementation of discovery-based research experiences into K-12 science classrooms in order to fully address the decline in students choosing to pursue academic degrees in STEM fields and produce a population more prepared to address the scientifically challenging future.

1.4. Goals of Dissertation

This dissertation focuses on using bulk and single particle chemical composition measurements to investigate wave breaking particles, as well the integration of environmental chemistry research into the introductory chemistry classroom. Chapter 2 describes the construction of a laboratory LSA generator and characterization of bubbles and aerosol size distributions produced from freshwater samples and model salt solutions. Chapter 3 details the chemical characterization by single particle microscopy and mass spectrometry of particles produced in the laboratory from freshwater samples collected from Great Lakes locations with varying concentrations of blue green algae. Chapter 4 describes the characterization of long-range transported sea spray and lake spray aerosols in remote northern Michigan using single particle microscopy and mass spectrometry. Chapter 5 details the multi-year dependence of bulk sea salt mass concentrations on sea ice coverage and wind speed in the Alaskan coastal Arctic. Chapter 6 describes the implementation and outcomes of an Arctic snow chemistry themed CURE in an introductory general chemistry laboratory course. Chapter 7 details a research-based laboratory experiment for the determination of chloride content in authentic environmental samples with basic laboratory equipment for classrooms with fewer resources, including high school. Finally, Chapter 8 concludes the dissertation and discusses the proposed future directions of on-going projects.

Chapter 2 Lake Spray Aerosol Generation: A Method for Producing Representative Particles from Freshwater Wave Breaking

Atmospheric Measurement Techniques, 9, 4311–4325, 2016.
DOI:10.5194/amt-9-4311-2016

2.1. Introduction

Particles produced from wave breaking in marine environments, known as sea spray aerosol (SSA), are one of the largest sources of naturally generated aerosol to the atmosphere (Lewis and Schwartz 2004, Andreae and Rosenfeld 2008). SSA contribute to both direct and indirect radiative forcing on a global scale (Murphy et al. 1998, Lohmann and Feichter 2005). Aerosol generation from freshwater sources, such as the Laurentian Great Lakes, has been far less studied, with only a single ambient measurement (Slade et al. 2010) and modelling study (Chung et al. 2011) having examined the process to our knowledge. Slade et al. (2010) observed the production of ultrafine (< 40 nm) aerosol, which increased in concentration as a function of wind speed, during periods of white-capped waves over Lake Michigan. Through regional chemical transport modelling, Chung et al. (2011) found that these particles could slightly increase surface level aerosol number concentrations, by ~20% over the remote northern Great Lakes and by ~5% over other parts of the Great Lakes, potentially affecting cloud nuclei (CCN) concentrations over the Great Lakes region. However, the study was challenging due to the need to use SSA-based parameterizations derived from bubble bursting of higher salinity seawater due to the lack of a bubble bursting parameterization for lower salinity freshwater. Due to their inherent differences from SSA, the term lake spray aerosol (LSA) is proposed to refer to aerosol formed from breaking waves in freshwater. Based on the intrinsic differences between SSA and LSA, and the heterogeneous water properties between and within the Great Lakes, methods are needed to understand aerosol production across a wide range of ionic and organic concentrations (Chapra et al. 2012, Shuchman et al. 2013).

Breaking waves caused by winds that entrain air beneath the water's surface, form bubbles that rise to the surface and burst to eject droplets into the atmosphere (Lewis and Schwartz 2004).

Therefore, droplet production flux is generally modelled as a function of increasing wind speed (Lewis and Schwartz 2004). Higher wind speeds are necessary to generate whitecaps, the product of bubbles formed by breaking waves rising to the surface, over freshwater compared to seawater (Monahan 1969). The minimum wind speed necessary for freshwater whitecap production was observed by Monahan (1969) to be 7-8 m s^{-1} over the Laurentian Great Lakes, compared to a threshold wind velocity for seawater whitecap production at 3-4 m s^{-1} (Blanchard 1963). However, wind speeds greater than this minimum wind speed necessary to produce breaking waves are still observed on large freshwater bodies of water such as the Laurentian Great Lakes (Monahan 1969, Slade et al. 2010), which have a yearly mean wind speed > 6.6 m s^{-1} at a height of 10 m above the lake surface for the majority of the Laurentian Great Lakes (Doubrawa et al. 2015). In addition to differences in differences in the dependence of wind speed on whitecap formation, the lifetime of freshwater whitecaps is shorter than saltwater whitecaps (Monahan and Zietlow 1969). Combined, the higher minimum wind speed necessary for whitecap formation and shorter whitecap lifetime in freshwater compared to seawater whitecap will likely lead to less aerosol produced from bubble bursting in freshwater than seawater.

To produce aerosols from freshwater using this mechanism, inorganic ions or other non-volatile material must be present in the droplets to form a dry particle after water evaporation. The Laurentian Great Lakes contain inorganic ions (Chapra et al. 2012) and dissolved organic carbon (DOC) (Shuchman et al. 2013), though differing in concentration and composition from that found in the ocean. Figure 2—1 shows the concentrations of a range of important ions and total organic carbon as a function of total water conductivity (Biddanda and Cotner 2002, Repeta et al. 2002, Chapra et al. 2012, Pilson 2013, Shuchman et al. 2013). Three key aspects of Great Lakes freshwater highlight the differences from seawater: 1) 2-5 orders of magnitude lower inorganic ions concentrations, 2) different relative concentrations of key inorganic ions ($Ca^{2+} > Mg^{2+} \approx Na^{+} \approx Cl^{-} > SO_4^{2-} > K^{+}$), and 3) total organic carbon (TOC) concentrations on the same order of magnitude as total inorganic ion concentrations. These differences in ion concentrations and ratios between seawater and freshwater will lead to important differences in the properties of bubbles from wavebreaking formed in the Great Lakes and thus lead to different physical and chemical properties of the resulting aerosol, in comparison to SSA.

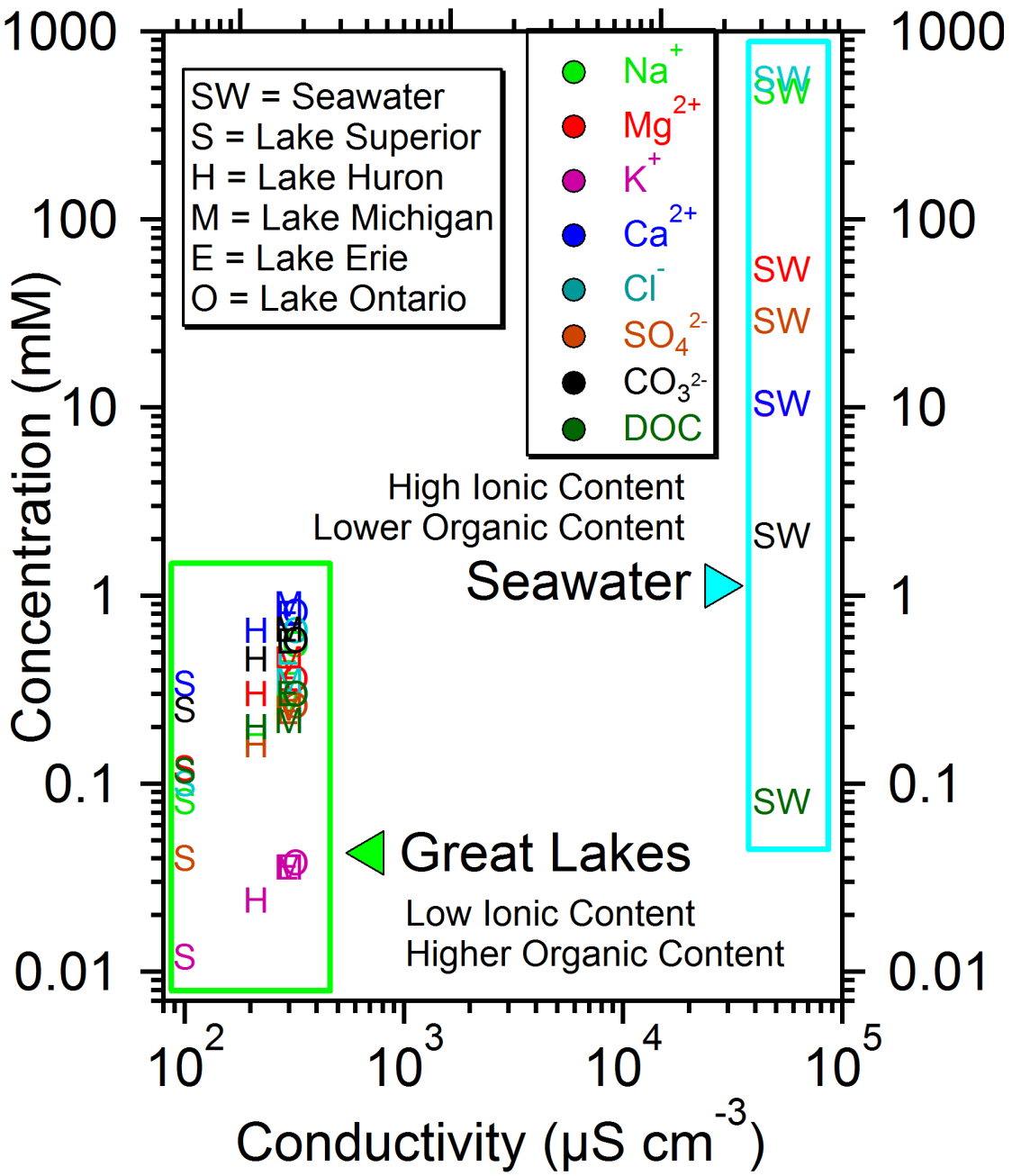

Figure 2—1. Concentration versus conductivity versus of important ions (Na^+, Mg^{2+}, K^+, Ca^{2+}, Cl^-, SO_4^{2-}, and CO_3^{2-}) for freshwater (Great Lakes) and mean seawater, as well as DOC. Great Lakes ion concentrations and conductivity are from Chapra et al. (2012), and seawater ion concentrations and conductivity are from Pilson (2013). TOC values for the Great Lakes are from Repeta et al. (2002), Shuchman et al. (2013), and Biddanda and Cotner (2002), while the TOC value for seawater is from Repeta et al. (2002). Note: K^+ is fully obscured for seawater by Ca^{2+}.

Previous work determined the bubble size distributions present in the water column for freshwater and seawater during laboratory simulations of wave breaking (Monahan and Zietlow 1969, Carey et al. 1993, Spiel 1994, Slauenwhite and Johnson 1999, Blenkinsopp and Chaplin 2011). An increase in the concentration of < 1 mm bubbles in seawater compared to freshwater primarily is thought to be due to differences in bubble coalescence (Monahan and Zietlow 1969, Carey et al. 1993, Blenkinsopp and Chaplin 2011). The higher ion concentrations in seawater inhibit bubble coalescence, leading to a higher proportion of small bubbles. In contrast, bubble coalescence occurs more freely in fresh water due to lower ion concentrations, leading to a higher proportion of large bubbles (Lessard and Zieminski 1971). Slauenwhite and Johnson (1999) suggest that, in addition to coalescence, increases in the initial break up of bubbles in seawater when compared to freshwater cause variation in the bubble size distributions. As droplet, and subsequent dry particle, production is in part dependent on the bubble size distribution (Prather et al. 2013, Stokes et al. 2013), the increase in smaller bubbles in seawater compared to freshwater translates into a different number size distribution of droplets, and therefore aerosol, produced by bubble bursting in freshwater compared to seawater. However, the bubble size distribution does not fully control the number size distribution of aerosols produced by bubble bursting. The concentration and composition of freshwater and seawater will further alter the dry particle formation by controlling the mass that remains, and thus the size, of a dry particle resulting from a droplet produced from bubble bursting. Droplets produced by bubble bursting in freshwater will have a lower solute concentration, and will form a dry particle of smaller size than those produced by bubble bursting in seawater, if the initial droplet is the same size (Slade et al. 2010).

To examine aerosol production from freshwater wave-breaking, a LSA generator was constructed based on design elements from multiple previous laboratory SSA generators (Sellegri et al. 2006, Facchini et al. 2008, Fuentes et al. 2010, Hultin et al. 2010, King et al. 2012, Zábori et al. 2012, Stokes et al. 2013, Salter et al. 2014). The LSA generator can produce aerosols from a relatively small amount of freshwater, lowering the limitations surrounding the collection, transport, storage, and analysis of large surface lake water samples. This increases the possible number and variety of environmental samples that can be analyzed in a region with heterogeneous water properties. Systematic experiments were conducted in the LSA generator to determine the relationship between bubble size distributions and the resulting aerosol size, concentration, and composition. The bubble and aerosol properties were tested for simple salt solutions (NaCl and

$CaCO_3$), simulated inorganic seawater and freshwater solutions, and a surface water sample from Lake Michigan. This study establishes a method to probe LSA with an interdisciplinary approach that draws from atmospheric science (production fluxes), physical oceanography (bubble measurements), atmospheric chemistry (aerosol physicochemical properties), and limnology (Great Lakes water properties). This work will broaden understanding of the effect of ion concentration and composition on aerosol production and properties, allowing for improved parameterization of LSA production from the Laurentian Great Lakes and other bodies of freshwater.

2.2. Materials and methods

2.2.1. Materials

Synthetic seawater was produced using Instant Ocean™ (Atkinson and Bingman 1997) prepared with 18.2 MΩ ultrapure water. All remaining standard solutions were prepared using 18.2 MΩ ultrapure water and anhydrous analytical grade inorganic salts (NaCl ≥ 99% and $CaCO_3$≥ 99%; Fisher Scientific). A solution of 1 mmol Ca^{2+}, 1 mmol CO_3^{2-}, 0.4 mmol Mg^{2+}, 0.4 mmol SO_4^{2-}, 0.3 mmol Na^+, 0.3 mmol Cl^-, and 0.02 mmol K^+ was prepared as synthetic freshwater based on Lake Michigan ion concentrations reported by Chapra et al. (2012). Freshwater was collected from the surface of Lake Michigan near Muskegon, Michigan (N 43˚14'21.545, W 86˚20'45.153) on July 26, 2015 in an 8 L LDPE carboy. During freshwater sampling, a multi-parameter water quality sensor (Professional Plus, YSI, Inc.) was used to measure freshwater properties, including temperature, pH, salinity, and dissolved oxygen, and a handheld spectrophotometer (AquaFluor 8000) was used to measure blue green algae content. The freshwater was frozen after sampling for storage and thawed prior to analysis. Analysis of frozen freshwater samples that have been thawed and analyzed by nanoparticle tracking analysis did not show changes in size or number concentration of insoluble components compared to unfrozen samples, indicating the sample was likely not significantly modified by freezing (Axson et al. 2016).

2.2.2. Aerosol generation

A LSA generator (Figure 2—2) was constructed based a design incorporating elements from previously published laboratory SSA generators (Sellegri et al. 2006, Fuentes et al. 2010, Hultin et al. 2010, Stokes et al. 2013, Salter et al. 2014). The LSA generator consists of an acrylic box with a total volume of 18 L (30 x 20 x 30 cm) and a water circulating system controlled using

a diaphragm pump (ShurFlo 2088). Water was circulated from the tank and cycled back into the tank at a rate of 2 L min^{-1} as plunging jets from four tubes (1/8" inner diameter) arranged in a square pattern 5 cm apart at the top of the tank, approximately 20 cm above the water surface (depending on fill level). Air was entrained by the plunging jets, creating a bubble plume of approximately 5 cm in depth with 5 cm between the plume and the base of the chamber, analogous to the wave breaking mechanism observed in nature (Fuentes et al. 2010). The four tubes were capped with mesh to break up the flow and increase the surface roughness of the plunging jet before it hit the water surface in order to obtain an accurate bubble size distribution (Zhu et al. 2000, Stokes et al. 2013). Prior to each experiment, the LSA generator was rinsed with 18.2 MΩ ultrapure water. Prior to and during operation, HEPA-filtered particle free air was pulled through the LSA generator to prevent ambient particle contamination as flow was pulled to the instruments. The LSA generator was maintained at positive pressure with a constant overflow of 0.2 L min^{-1}. All experiments were performed at room temperature, approximately 22.0 °C, and the relative humidity (RH) within the tank was maintained at ~85%, the standard RH for ambient and laboratory SSA generation (Lewis and Schwartz 2004).

A major advantage of the LSA generator system is that it needs a relatively small volume of water (4 – 6 L) compared to other SSA generation systems (100 L) (Stokes et al. 2013, Salter et al. 2014). However, the shallow bubble plume generated in plunging water jet systems of reduced dimensions such as the one discussed in this study (5 cm), and others (Sellegri et al. 2006, Fuentes et al. 2010, Hultin et al. 2010), limits bubble plume lifetime, as discussed in detail by Fuentes et al. (2010). Large volume plunging jets with plume depths > 0.5 m are expected to be representative of the lifetime of oceanic plumes (Stokes et al. 2013), but those are only suitable when large amounts of sample are available. Due to difficulties in obtaining and storing large volume freshwater samples from multiple collection sites, these types of large-scale aerosol generation methods are not suitable for our research. In addition, work by Fuentes et al. (2010) demonstrated that the shortened bubble plume lifetime does not affect the adsorption of marine surfactant to rising bubbles in small volume SSA generation methods and these systems are appropriate for studying the effects of marine organics on SSA. Therefore, the LSA generator presented in this work, despite its reduced dimensions, should be suitable for the study of the

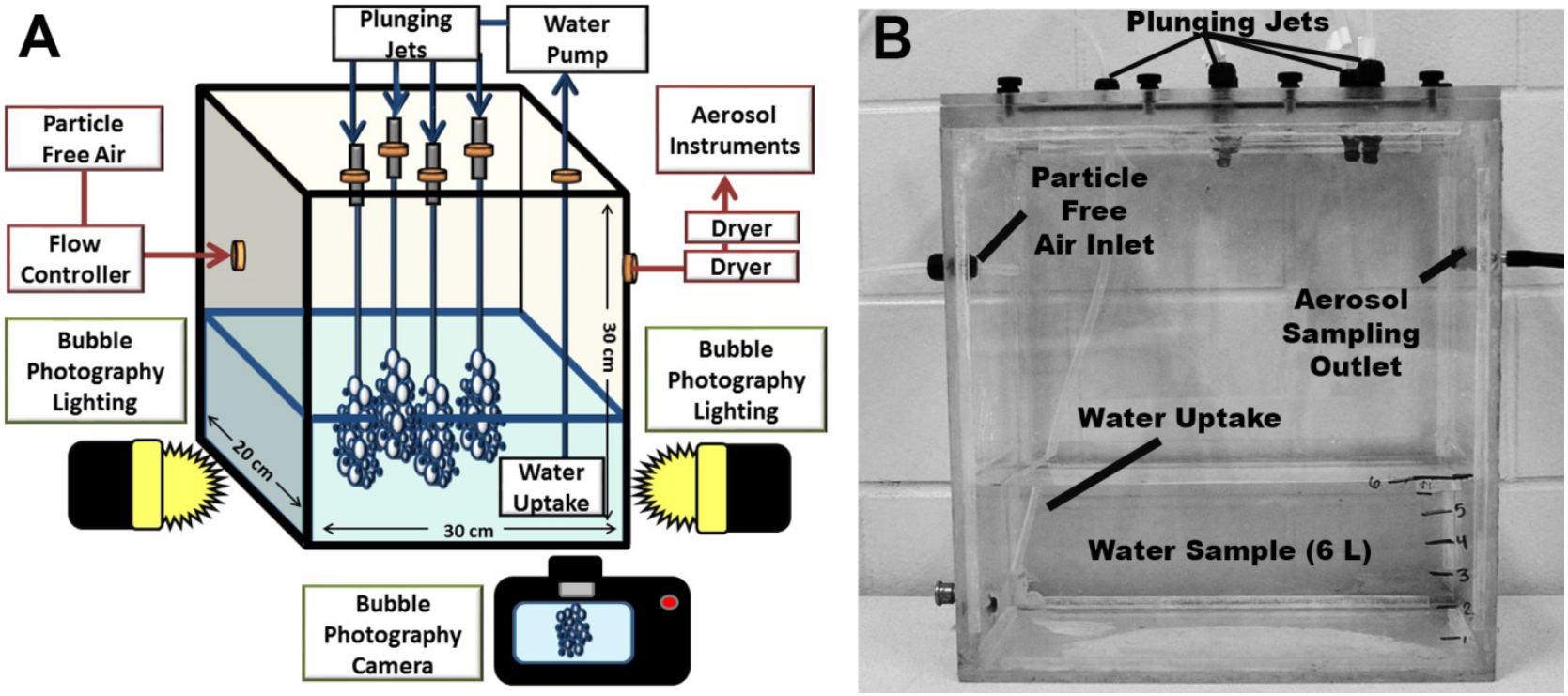

Figure 2—2. The constructed lake spray aerosol generator shown as a (A) schematic and (B) photograph with functional components labelled. Not all components of the LSA Generator shown in the (A) schematic are visible in the (B) photograph.

effect freshwater composition on LSA production.

2.2.3. Bubble size distribution measurements

Digital high-speed photographs of the LSA generator plunging jet bubble plume were collected to examine the bubble size distributions. The bubbles were photographed using a Nikon D100 camera fitted with an AF Nikkor 24 – 50 mm lens and placed approximately 45 cm from the front of the tank to capture side profiles of the bubble plume. An aperture of 4.5 was used to achieve the narrowest depth of field possible in the resulting images. To increase bubble clarity, two light sources (Ring 48, Neewer) were placed to the right and left of the tank illuminating the bubbles (Figure 2—2). Photographs were obtained at intervals > 60 seconds to ensure each bubble was counted only once (Salter et al. 2014).

ImageJ was used to determine the bubble plume size distribution in each photograph. Individual bubbles were manually identified and a circle was fit to each bubble (Schneider et al. 2012). The bubble dimensions obtained in pixels were converted to mm by a scaling factor calculated for individual photographs in the ImageJ software from measurements of a portion of the tank with known length visible in the photograph. The area was then converted to diameter, reported here in mm, assuming the bubbles to be circular (Lewis and Schwartz 2004). In determining the bubble volume density, the volume of the bubble plume was calculated from measurements of plume photographs in ImageJ. Due to interferences of light diffraction in the LSA generator and limitations in the camera, such as pixel size and resolution, bubbles < 100 μm in diameter could not be distinguished accurately from the background of the photograph and are not included in the analysis. Another limitation inherent in this method is that it is possible that not all bubbles were counted due to being obscured by other bubbles.

2.2.4. Aerosol size distribution measurements

Aerosols generated by bubble bursting exited the LSA generator and passed through two silica gel diffusion dryers to achieve a RH of ~15%, similar to the RH of previous measurements of aerosol size distributions of laboratory SSA (Fuentes et al. 2010, Stokes et al. 2013, Salter et al. 2014). After exiting the diffusion driers, the aerosol number size distributions and total aerosol concentrations produced for each solution in the LSA generator were measured using a scanning mobility particle sizer (SMPS), consisting of a differential mobility analyzer (DMA; model 3082, TSI Inc.) and condensation particle counter (CPC; model 3775, TSI Inc.), as well as an

aerodynamic particle sizer (APS; model 3321, TSI Inc.). The SMPS operated at a sample flow rate of 0.3 L min^{-1} and sheath flow of 3 L min^{-1} and a scan rate of 5 minutes to obtain a size distribution for particles with an electrical mobility diameter (d_m) between 14.1 - 736.5 nm. The APS was operated at a flow rate of 5.0 L min^{-1}, with an aerosol and sheath flow of 1.0 and 4.0 L min^{-1} respectively, and a scan rate of 30 sec to obtain a size distribution for particles with an aerodynamic diameter (d_a) between < 0.52 - 19.8 µm. For each sample solution, SMPS and APS particle size distributions were collected over a 3-hour period and averaged. In order to merge the SMPS and APS size distribution, measurements recorded in d_m and d_a, respectively, were converted to physical (geometric) diameters (d_p) (Khlystov et al. 2004). The relation:

Equation 2—1 $$\boldsymbol{d_m = d_p}$$

was used to convert particles sized by the SMPS, under the assumption that the particles were spherical. Particles sized by the APS were assigned an effective density (ρ_{eff}) of 1.2 - 1.6 g cm^{-3}, a value determined experimentally for particles produced from each individual solution, allowing for conversion based on the following relation:

Equation 2—2 $$\boldsymbol{d_p = \frac{d_a}{\sqrt{\frac{\rho_{eff}}{\rho_0}}}}$$

where ρ_0 is equal to unit density (1 g cm^{-3}). The SMPS has a tendency to undercount particle concentrations at the highest particle diameter bins, due to the cut-off from the particle impactor, and the APS has a tendency to undercount particle concentrations at the lower diameter bins, due to the poor scattering efficiency of the lowest particle diameter bins. To compensate for these limitations, the highest and lowest particle diameter bins of the SMPS and APS, respectively comprising the overlapping diameters of the two methods, were removed when stitching (Stokes et al. 2013). Aerosol blank measurements conducted before experiments by circulating 18.2 MΩ ultrapure water through the LSA generator showed that the background aerosol number concentrations were < 20 cm^{-3}, compared to an average of 350 cm^{-3} during freshwater samples.

2.2.5. Scanning electron microscopy

Particles generated from the different solutions run in the LSA generator were impacted onto Carbon Type-B (Formar film coated with carbon on copper grid) transmission electron microscopy (TEM) grids, (01910-F, Ted Pella, Inc.) using a three stage Microanalysis Particle Sampler (MPS; model MPS-3, California Measurements, Inc.). Particles were examined from the

third (smallest) stage, with a size cut of < 700 nm. Scanning electron microscopy with energy dispersive x-ray (SEM-EDX) measurements were made at the Michigan Center for Materials Characterization $(MC)^2$ located at the University of Michigan in Ann Arbor. An FEI Helios with environmental dual focused ion beam/scanning electron microscope (FIB/SEM) was used to obtain images of the particles. The FEI Helios was equipped with a Schottky field emitting source operating at an accelerating voltage of 15 kV and current of 0.58 nA. Scanning transmission electron microscopy (STEM) was conducted and a high-angle annular dark field (HAADF) electron detector was used to collect Z-dependent dark-field images of individual particles.

2.3. Results and discussion

2.3.1. Comparison of seawater and freshwater bubble plume size distributions

Photographs of bubble plumes generated from synthetic seawater, synthetic freshwater, and Lake Michigan freshwater were collected to observe visual changes in bubble plumes and to determine their respective bubble plume size distributions (Figure 2—3). There was an observed decrease in the concentration of smaller bubbles in freshwater when compared to synthetic seawater, which has been observed in previous studies (Monahan and Zietlow 1969, Carey et al. 1993, Spiel 1994, Slauenwhite and Johnson 1999, Blenkinsopp and Chaplin 2011). The visual differences in the images were reflected in the measured bubble size distributions (Figure 2—3d), with the synthetic freshwater and Lake Michigan freshwater sample producing a similar total bubble concentration that was only 12% and 8% (Figure 2—3e), respectively, of the total bubble concentration produced from the synthetic seawater solution. Bubble size distributions generated from synthetic seawater showed that bubbles were produced up to 4 mm in radius in the LSA generator (Figure 2—3d), similar to measurements of bubble size distributions for ocean waves (Deane 1997, Deane and Stokes 1999, Bowyer 2001, Deane and Stokes 2002).

The production of bubbles with radii > 1 mm are important because droplet production from bubble bursting, and the resulting dry particle size distribution, is dependent on bubble size (Collins et al. 2014). The bubble bursting process in seawater ejects two types of droplets into the atmosphere: film and jet droplets (Blanchard and Woodcock 1957, Blanchard and Syzdek 1975). Film and jet droplets typically range in size from 0.2 – 10 μm and 1 – 200 μm, respectively (Lewis and Schwartz 2004). The number of film and jet droplets produced from a single bubble in seawater is dependent on the size of the bubble, and bubbles with radii > 1 mm

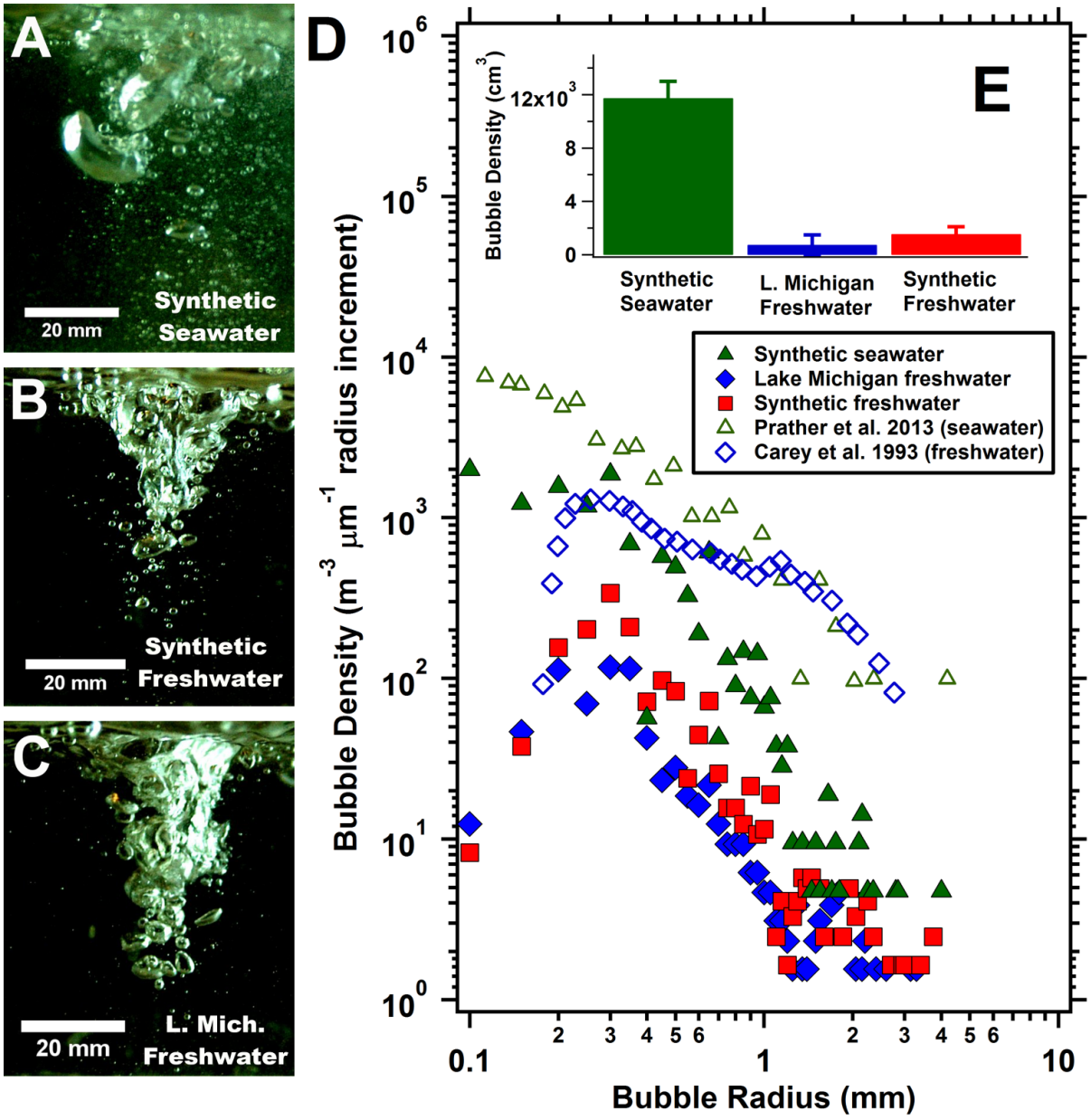

Figure 2—3. Digital images of a bubble plume generated by one plunging jet in the LSA generator with (A) synthetic seawater, (B) synthetic freshwater, and (C) Lake Michigan freshwater, with brightness/contrast adjusted to increase bubble clarity. (D) Bubble number size distributions and (E) bubble concentrations generated by the LSA generator using synthetic seawater, synthetic freshwater, and Lake Michigan freshwater measured by the bubble photography method, as well as previously measured bubble size distributions generated from synthetic seawater with a plunging waterfall (Prather et al. 2013) and freshwater with a tipping trough (Carey et al. 1993).

produce more film drops and bubbles < 1 mm produce jet drops in quantities greater than 1 per bubble (Lewis and Schwartz 2004). In addition, jet drop size is directly correlated to bubble size (Lewis and Schwartz 2004). If bubbles > 1 mm are not produced by a generation method, then a higher proportion of jet droplets will be formed shifting the aerosol size distribution mode and modifying the aerosol chemical composition (Stokes et al. 2013, Collins et al. 2014). The replication of this power law decrease in bubble concentrations at larger radii using the LSA generator is therefore critical for the accurate reproduction of SSA (Prather et al. 2013, Stokes et al. 2013) and LSA.

The lognormal radius mode for the synthetic freshwater and Lake Michigan freshwater bubble size distributions were observed at 280 ± 70 μm and 250 ± 60 μm, respectively (Figure 2—3D). This is consistent with freshwater laboratory measurements by Carey et al. (1993), which show a mode of 300 μm and a steep drop in bubble concentration for radii below 300 μm (Figure 2—3d). This bubble size mode is much larger than that observed for seawater, for which bubble size distributions typically peak at a radius between 40 - 80 μm (Sellegri et al. 2006, Fuentes et al. 2010, Hultin et al. 2010, Prather et al. 2013, Stokes et al. 2013). This means the peak mode for the synthetic seawater bubble size distribution produced in the LSA generator was below the detectable bubble size limit of the photographic technique used in this study. Indeed, the LSA generator bubble size distribution for seawater in Figure 2—3d has a peak mode lower than that for freshwater and is < 100 μm. Previous work examining seawater bubble size distributions have encountered this same measurement limitation (Carey et al. 1993, Deane and Stokes 2002, Hultin et al. 2010), which was resolved by comparing the power law dependent decrease in bubble concentrations at higher radii to confirm the accuracy of bubble size distribution. Results from this comparison are consistent with previous observations and confirm that the LSA generator produces bubble plumes representative of both oceanic and freshwater wave breaking. However, the concentration of bubbles produced from both freshwater and seawater samples in the LSA generator were lower than the concentrations representative of freshwater (Carey et al. 1993) and seawater (Stokes et al. 2013) wave breaking previously reported (Figure 2—3d). Further, the lower concentration of bubbles compared to previous measurements is more pronounced at larger radius (>1 mm) bubbles. This limitation of the LSA generator is likely due to its reduced dimensions compared to the bubble generation methods used for comparison (Carey et al. 1993, Stokes et al.

2013), which allows for small sample volume but limits the lifetime of the bubble plume (Fuentes et al. 2010), as discussed in Section 2.2.2.

2.3.2. Aerosol generation from seawater and freshwater

2.3.2.1. Validation of aerosol generated with synthetic seawater

To both characterize the LSA generator and compare freshwater aerosols to those generated from seawater, aerosol size distributions generated from synthetic seawater, synthetic freshwater, and Lake Michigan freshwater were measured (Figure 2—4). The aerosol size distribution generated for synthetic seawater produced a total number concentration of 1195 cm^{-3} and exhibited a single lognormal mode at a diameter of 110 ± 4 nm, with a geometric standard deviation (σ) of 1.52, and an amplitude of 1620 cm^{-3} (Table 2—1). This SSA lognormal mode is in agreement with the primary diameters of SSA lognormal modes, which ranged from 60 - 200 nm, determined using various laboratory generation techniques (Sellegri et al. 2006, Fuentes et al. 2010, Hultin et al. 2010, Stokes et al. 2013, Collins et al. 2014, Salter et al. 2014). It was determined that the LSA generator successfully reproduced seawater bubble and aerosol size distributions such that the system can be used to test other applications.

2.3.2.2. Characteristics of aerosol generation from freshwater

The synthetic freshwater and Lake Michigan freshwater produced 67% and 33% lower total (d_p = 0.018-18 μM) aerosol number concentrations, compared to the synthetic seawater, respectively (Figure 2—4b). The lower total aerosol number concentration produced from the freshwater solutions, in comparison to the synthetic seawater, is a reflection of the lower bubble concentrations produced from the freshwater solutions in comparison to synthetic seawater (Figures 2—3b & 2—4). However, it is important to note that the Lake Michigan freshwater produced a larger total aerosol concentration normalized by the total bubble concentration generated than both the synthetic freshwater and the synthetic seawater solution, which were both similar (Figure 2—4c). In contrast to the unimodal synthetic seawater aerosol size distribution, both the synthetic freshwater and Lake Michigan freshwater aerosol size distributions were bi-modal (Figures 2—4a & Table 2—1). The primary lognormal mode observed for the synthetic freshwater and Lake Michigan freshwater occurred at a diameter of 300 ± 40 nm and 180 ± 20 nm, respectively, which are larger than the dominant lognormal diameter mode observed for synthetic seawater (110 ± 4 nm). The secondary lognormal mode

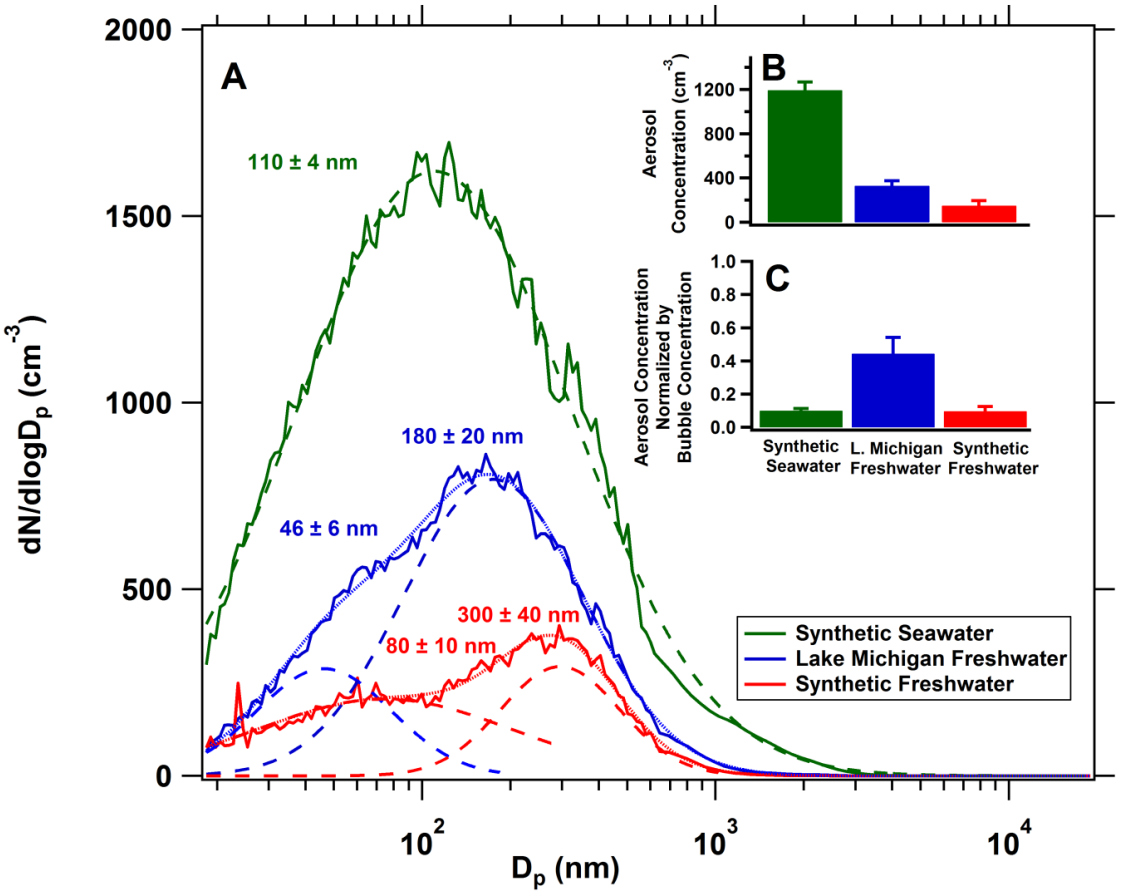

Figure 2—4. (A) Average aerosol number size distributions fitted with lognormal peaks, (B) average total aerosol number concentration, and (C) average total aerosol number concentration normalized by average total bubble concentration produced by the LSA generator from synthetic seawater, synthetic freshwater, and Lake Michigan freshwater.

Table 2—1. Aerosol size distribution characteristics obtained from lognormal fitting for LSA generated from synthetic seawater, synthetic freshwater, and L. Michigan freshwater.

Solution	Mode	Diameter (nm)	Standard Deviation (σ)	Amplitude (cm^{-3})
Synthetic Seawater	Primary	110 ± 4	1.52	1620
Synthetic Freshwater	Primary	300 ± 40	1.00	292
	Secondary	80 ± 10	0.75	206
L. Michigan Freshwater	Primary	180 ± 20	0.66	794
	Secondary	46 ± 6	1.42	286

was observed at a diameter of 80 ± 10 nm for the synthetic freshwater and 46 ± 6 nm for the Lake Michigan freshwater sample. The LSA secondary lognormal mode for the Lake Michigan freshwater is similar to previous aircraft measurements by Slade et al. (2010), who observed a 15 – 40 nm particle lognormal diameter mode over Lake Michigan. Slade et al. (2010) performed calculations of expected dry particle diameter based on typical droplet size produced from oceanic wave-breaking and total dissolved ion content of freshwater. These calculations indicated that the aerosol size distribution of LSA would peak at a diameter smaller than SSA, and this would explain the measured secondary lognormal diameter mode generated from freshwater solutions in this study that was lower in diameter than the primary lognormal diameter mode of SSA (see Section 2.2.3). These results indicate that wave breaking induced bubble bursting of freshwater in the Great Lakes can produce aerosols through mechanisms analogous to wave breaking on open oceans, but the size distribution of LSA has different characteristics than that of SSA.

The increased total particle concentration and as well as the shift in lognormal diameter mode to smaller sizes, for the Lake Michigan freshwater sample compared to the synthetic freshwater points to the possible additional influence of organic carbon present in the Lake Michigan freshwater sample. While the synthetic freshwater was a simplified mixture of inorganic ions representing freshwater, the Lake Michigan freshwater contained a more complex mixture of inorganic ions, as well as organic and biological material present in the surface water during collection. Like the synthetic freshwater, the synthetic seawater is a simplified mixture of inorganic ions representing seawater. The higher total particle concentration normalized by total

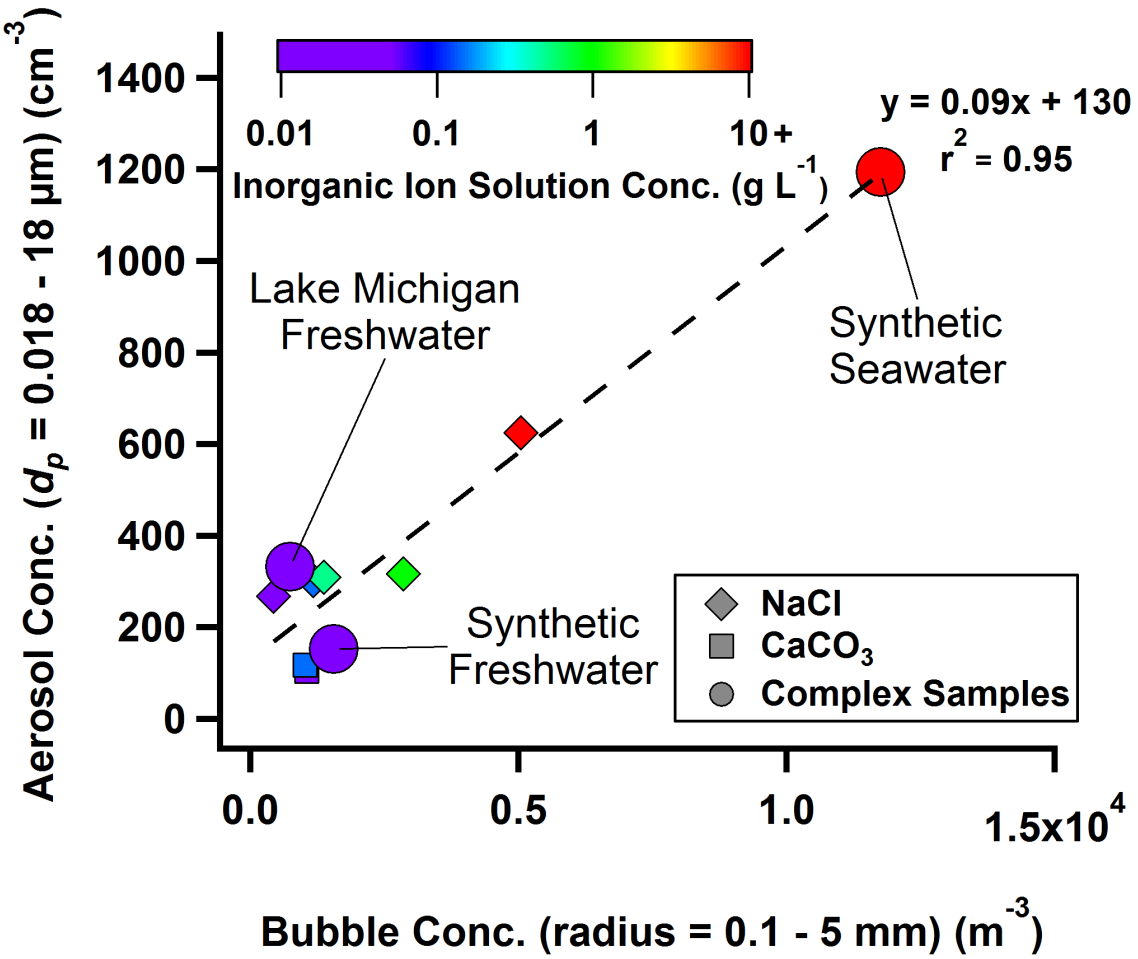

Figure 2—5. Aerosol vs. bubble concentrations produced by the LSA generator from solutions of NaCl and $CaCO_3$ of varying concentrations, Lake Michigan freshwater, synthetic freshwater, and synthetic seawater. A best-fit line is shown for the empirical relationship between aerosol and bubble concentrations.

bubble concentration observed for the Lake Michigan freshwater sample, compared to the total particle concentration normalized by total bubble concentration for the synthetic freshwater and synthetic seawater, further demonstrates the possible influence of organic carbon present in the Lake Michigan freshwater sample. The presence of biological material in the freshwater sample was confirmed by spectrophotometric measurements of bulk water at the site during sample collection, which indicated 57.2 ppb of blue green algae present. Given that the Lake Michigan freshwater sample was frozen prior to analysis, it is likely that the sample did not contain substantial living biological material when run in the LSA generator. To further determine the influence of organic carbon between the Lake Michigan freshwater sample aerosol populations, impacted particles were analyzed by SEM to determine circularity (Figure 2—6). Particles generated from the Lake Michigan freshwater sample showed median circularity values closer to 1, indicative of a perfect circle (and thus spherical particle in the atmosphere), compared to particles generated from the synthetic freshwater sample for all size ranges measured (< 0.5 μm, 0.5 – 1.0 μm, and > 1 μm). This increase in circularity is likely due to disruption of crystallization of the inorganic salts by the higher organic and biological content of the Lake Michigan freshwater sample, compared to the synthetic freshwater. Previous work has shown that the circularity of SSA particles increases with increased total organic carbon concentrations in seawater (Ault et al. 2013). In addition, the complex salt mixture in the Great Lakes, where most ion concentrations are within an order of magnitude of each other, is likely to affect crystallization more than for seawater, where Na^+ and Cl^- are present in order of magnitude higher concentrations than any other inorganic ion (Figure 2—1). Future efforts will involve systematic studies of aerosols generated from freshwater samples with a range of inorganic, organic, and biological components.

2.3.2.3. Freshwater droplet size distribution to freshwater aerosol size distributions

Calculations of the relationship between dry particle diameter and initial drop diameter were explored for seawater and freshwater to determine the effect of the initial droplet size distribution on aerosol formation. The physical diameter of a dry (RH = 0%) SSA particle (d_p) will typically be ~4x smaller than the diameter of the droplet of seawater (d_d) it originated from (Veron 2015). Therefore, the d_p = 110 ± 4 nm lognormal aerosol mode generated from the synthetic seawater in the LSA generator would have resulted from a roughly d_d = 440 nm initial synthetic seawater lognormal droplet mode (Table 2—2). In contrast, due to the lower

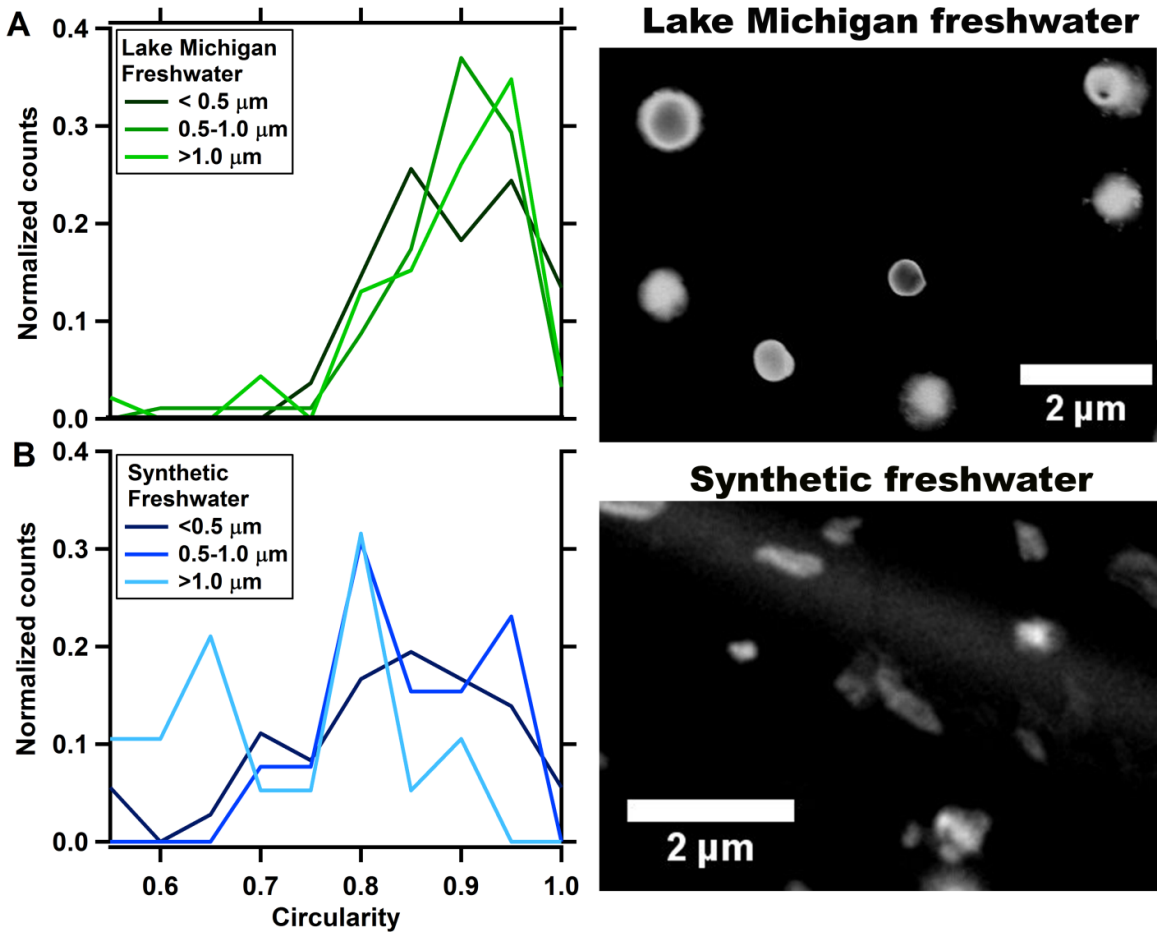

Figure 2—6. Circularity of (A) Lake Michigan freshwater particle sample and (B) synthetic freshwater particles as a function of diameter from the LSA generator, as well as example SEM images of the impacted particles used in the analysis.

concentration of dissolved components in freshwater, the d_p of an LSA particle is predicted to be ~20x smaller than the d_d of the freshwater droplet it originated from (Slade et al. 2010) (Table 2—2). Using this relationship Slade et al. (2010) predicted that the size distribution of LSA shifts towards smaller, ultrafine diameters in comparison to the size distribution of SSA. However, these calculations were made under the assumption freshwater and seawater bubble bursting produce the same d_d size distributions, which may not be accurate as there are differences in bubble size distributions generated in freshwater and seawater solutions (Figure 2—3d).

Previous work, while limited, has shown differences in the size distribution of droplets produced from freshwater bubble bursting in comparison to droplet production from seawater bubble bursting (Resch 1986). Resch (1986) observed that film drops produced from freshwater are larger than those usually reported for seawater, which for SSA can range in d_{80} from 0.02 to 200 μm (Lewis and Schwartz 2004). Therefore, the first lognormal diameter mode of the Lake Michigan freshwater aerosol size distribution (46 ± 6 nm) observed in this study could be the result of a freshwater film lognormal droplet mode of d_d = 920 nm that is larger than the $d_d \approx 400$ nm synthetic seawater film droplet mode (Table 2—2). The second lognormal mode (175 nm) of the observed Lake Michigan freshwater sample aerosol size distribution is likely the result of an even larger lognormal film droplet mode at d_d = 3.5 μm. This second lognormal diameter mode is unlikely to be the result of jet drop production as bubble bursting, in seawater, typically produces jet drops with a d_d that are 10% of the bubble diameter (d_{bub}) (Lewis and Schwartz 2004), and individual bubbles in freshwater and seawater produce jet drops at similar numbers and sizes from bubbles with radii of 300 - 1500 μm (Spiel 1994). Therefore, even the smallest freshwater bubble measured in this study (d_{bub} = 0.2 mm) would likely only produce jet drops of d_d = 20 μm and d_p = 1 μm, a far higher diameter than the second lognormal diameter

Table 2—2. Fresh- and seawater droplet diameters (d_d) calculated from the mass (assuming particle density is 1.2 g/mL) of the dominant dry particle diameter (d_0) modes produced from synthetic seawater (SSA) and the Lake Michigan freshwater sample (LSA).

Observed Dry Diameter (d_0)	**Droplet Diameter (d_d)**
0.110 μm SSA	0.440 μm Seawater
0.046 μm LSA	0.92 μm Freshwater
0.175 μm LSA	3.5 μm Freshwater

mode observed in the aerosol size generated the freshwater samples (175 nm) (Figure 2—4).work is needed to determine the differences in film droplet production between fresh and seawater bubble bursting to fully connect bubble and aerosol size distributions observed in this study.

2.3.3. Aerosol & bubble generation from standard salt solutions

2.3.3.1. Bubble size and concentration from standard salts

To determine the influence of the dominant inorganic ions, and their concentrations, in freshwater and seawater (Figure 2—1) on bubble production, bubble size distributions for NaCl (seawater proxy) and $CaCO_3$ (freshwater proxy) solutions were determined as a function of solution concentration (Figures 2—7a & 2—7b). The lognormal radii modes of the bubble size distributions produced from $CaCO_3$ solutions of 0.05 g kg^{-1} and 0.15 g kg^{-1} (230 ± 90 μm) (Figure 7a) were similar to the synthetic freshwater (280 ± 70μm) and Lake Michigan freshwater sample (250 ± 60 μm) bubble size distributions (Figure 2—3d). This similarity in bubble size distribution lognormal radii modes is consistent with Ca^{2+} and CO_3^{2-} being the dominant cation and anion respectively in the calcareous Great Lakes (Chapra et al. 2012). No solutions of $CaCO_3$ of concentration greater than 0.15 g kg^{-1} could be analyzed for bubble size distributions due to solubility limits.

For NaCl solution concentrations 0.05 g kg^{-1} to 35 g kg^{-1}, total bubble density increased with solution concentrations. The largest increase in bubble density (2-3 orders of magnitude) primarily occurred for the bubble size range smallest bubbles (radii < 0.3 mm) (Figure 2—7b), which is the same that the largest increase (2-3 orders of magnitude) in bubble density between freshwater and seawater solutions was observed (Figure 2—3d). This observed increase in bubble density from freshwater to seawater concentration solutions is likely the result of bubble coalescence inhibition at higher ionic concentration (Slauenwhite and Johnson 1999), as the two electrolyte combinations tested in this study ($CaCO_3$ and NaCl) are known to exhibit concentration dependent bubble coalescence effects (Craig et al. 1993, Craig et al. 1993, Henry et al. 2007). Typically, increasing the solution salt concentration up to 0.01 M leads to minimal decreases in bubble coalescence relative to pure water (Henry et al. 2007). As a result, total bubble number concentrations increased only gradually for NaCl when solution concentrations

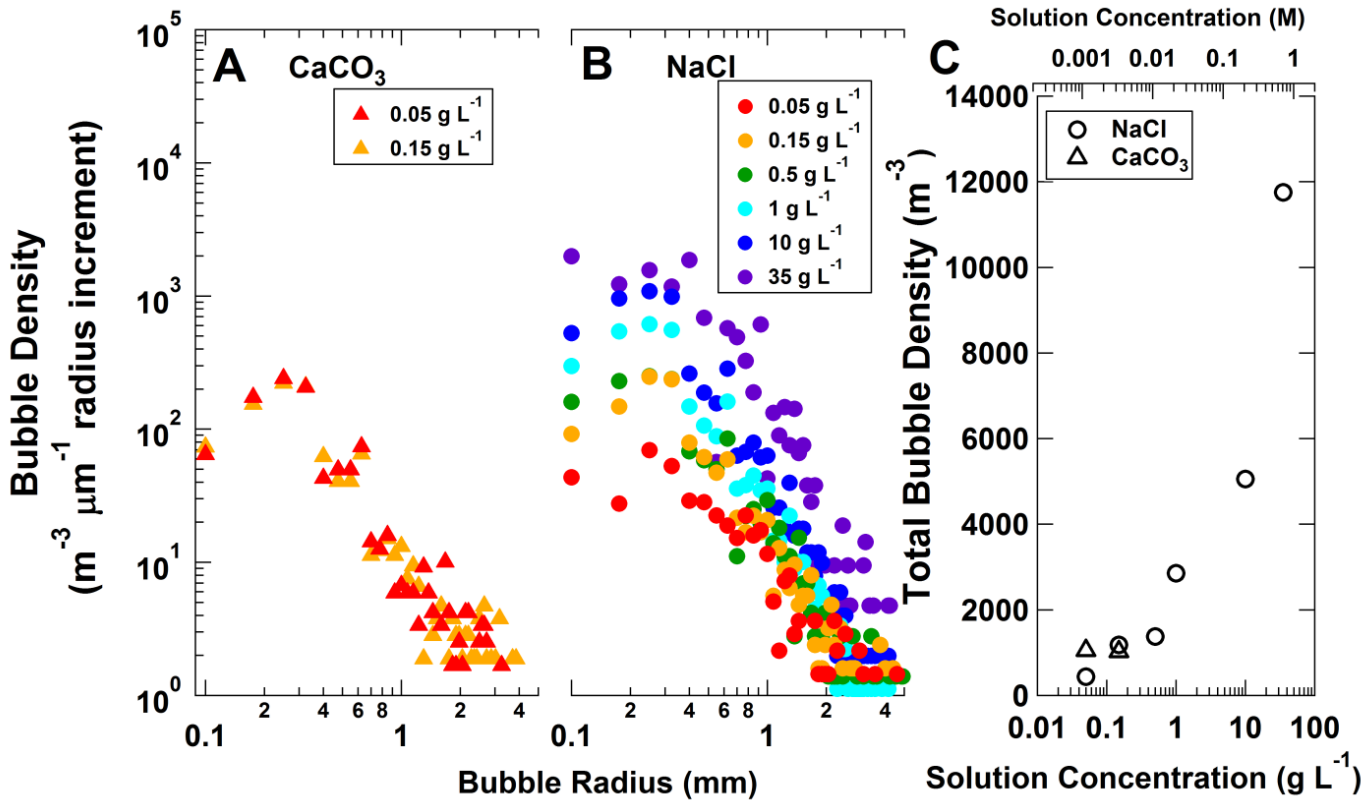

Figure 2—7. Bubble size distributions (density vs. bubble radius) generated by the LSA generator as a function of solution concentration for (A) $CaCO_3$ and (B) NaCl, as well as (C) total bubble density as a function of ion composition for $CaCO_3$ and NaCl.

in the LSA generator increased from 0.05 g kg^{-1} to 1 g kg^{-1} NaCl (0.00086 – 0.017 M). However, when the solutions entered the 0.01 – 0.2 M solution concentration range (1 – 35 g kg^{-1} NaCl), where bubble coalescence is known to decrease significantly (Sovechles and Waters 2015), a greater rate of increase in total bubble number concentration with increased solution concentration was observed (Figure 2—7c). These results indicate that the different ionic concentrations affected bubble coalescence and bubble concentrations in this study, which in turn influenced aerosol concentrations produced by bubble bursting.

2.3.3.2. Aerosol generation from standard salts

The aerosol size distributions for the two standard salt solutions representative of seawater (NaCl) and freshwater ($CaCO_3$) were measured as a function of solution concentration (Figures 2—8a & 2—8b) to examine the effect of the dominant ion present, and ionic concentration, in solution on aerosol production. At concentrations representative of the Great Lakes, 0.05 and 0.15 g kg^{-1}, aerosol size distributions generated from solutions of NaCl and $CaCO_3$ exhibited two lognormal diameter modes (Figures 2—8a & 2—8b). The primary aerosol lognormal modes produced from the 0.05 - 0.15 g kg-1 NaCl and $CaCO_3$ solutions were larger in diameter than the secondary aerosol lognormal modes (Figures 2—8a & 2—8b). This is consistent with the bimodal lognormal aerosol size distributions generated from the synthetic freshwater (total inorganic ion content = 0.12 g kg^{-1}) and Lake Michigan freshwater (total inorganic ion content = 0.14 g kg^{-1}), which also exhibited primary aerosol lognormal modes higher in diameter than the secondary aerosol lognormal modes (Section 2.2.2). At higher concentrations (0.5 - 35 g kg^{-1}) more representative of seawater total inorganic ion content (35 g kg^{-1}), the NaCl solutions produced unimodal lognormal size distributions (Figure 2—8b), consistent with the unimodal lognormal number size distribution produced from synthetic seawater (Figure 2—4a). The bimodal lognormal aerosol number size distribution that was observed for all freshwater concentration (0.05 - 0.15 g kg^{-1}) standard salt solutions (Figures 2—8a & 2—8b) and the freshwater solutions (Figure 2—4a) indicates that solution concentration is important in determining aerosol size distribution.

Solution composition, as well as concentration, was observed to the affect aerosol size distribution (Figure 2—8). The two lognormal modes of the aerosol size distribution produced from the 0.05 g kg^{-1} concentration solutions were located at a higher diameters for $CaCO_3$ (83 ± 8 nm; 340 ± 20 nm) compared to NaCl (55 ± 9 nm; 210 ± 20 nm). When $CaCO_3$ and NaCl solution

concentrations increased from 0.05 to 0.15 g kg^{-1}, the $CaCO_3$ lognormal modes (60 ± 10 nm; 290 ± 10 nm) remained at higher diameters than the NaCl lognormal modes (40 ± 6 nm; 140 ± 10 nm), but all lognormal modes shifted to smaller diameters (Figure 2—9b). The lognormal modal diameter of the 35 g kg-1 NaCl solution (81 ± 3 nm) was smaller than the lognormal modal diameter of the NaCl dominant synthetic seawater solution (110 ± 4 nm), suggesting that mixtures of ions affect aerosol size distributions. In addition, the lognormal modal diameters produced from the 0.15 g kg^{-1} $CaCO_3$ solution (60 ± 10 nm; 290 ± 10 nm) were slightly smaller in comparison to the synthetic freshwater aerosol size distribution lognormal modes (80 ± 10 nm; 300 ± 40 nm), again indicating that mixtures of ions affect aerosol size distributions. As the Great Lakes have a wide and evolving range of inorganic ion compositions and concentration (Figure 2—1) (Chapra et al. 2012), the dependence of aerosol size distributions on solution composition and concentration observed in this study could significantly impact the range of LSA size distributions in the atmosphere.

The total aerosol concentrations generated from $CaCO_3$ and NaCl solutions increased with solution concentration (Figure 2—8) in a similar manner to the increase in total bubble concentrations generated with increased solution concentration (Figure 2—7). The total aerosol concentration increased slowly between solution concentrations of 0.05 – 1.0 g kg^{-1}, reflecting the low increase in bubble concentrations over this concentration range (Figure 2—7). At solution concentrations greater than 1.0 g kg^{-1} a shift to a larger increase in total aerosol concentration with increased solution concentration occurred. The change in relationship between solution and aerosol concentration at solution concentrations above 1.0 g kg^{-1} (NaCl = 0.017 M) reflects the change in bubble concentration above 1.0 g kg^{-1} (NaCl = 0.017 M) observed in this study (Figure 2—8c) and the known transition in bubble coalescence behavior that occurs above ionic concentrations of 0.01 M (Sovechles and Waters 2015). Further, the direct relationship between bubble and aerosol concentrations for the increasing standard salt solution concentrations aligns well with the direct relationship in bubble and aerosol concentrations for freshwater and seawater solutions (Figure 2—5). These results confirm that there is a direct relationship between solution concentration, bubble concentration, and aerosol concentration that will result in the production of a lower number of particles from wave breaking in low salt concentration freshwater compared to wave breaking in high salt concentration seawater.

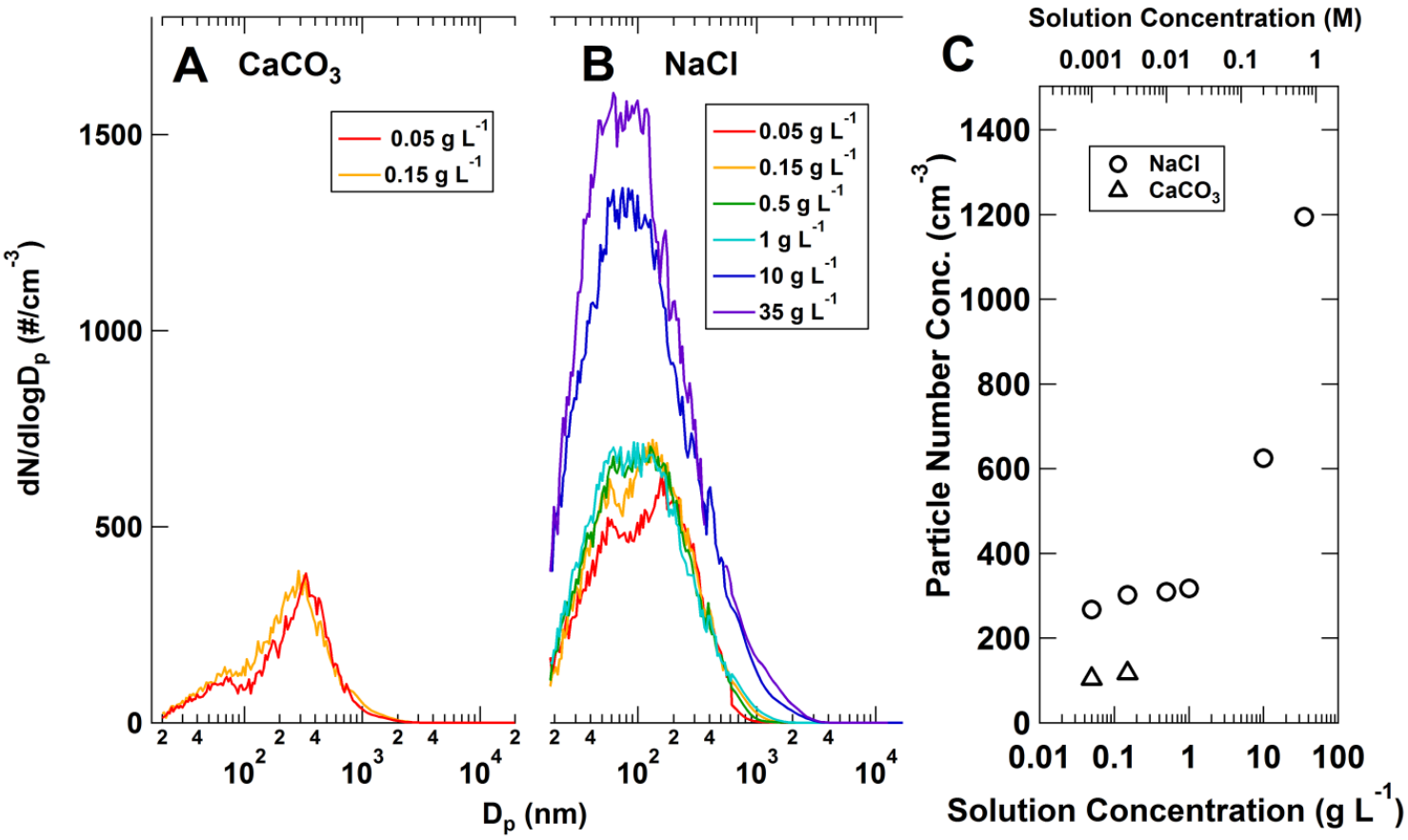

Figure 2—8. Average aerosol number concentration generated by the LSA generator as a function of solution concentration for (A) $CaCO_3$ and (B) NaCl, as well as (C) total aerosol number concentration as a function of ion composition for $CaCO_3$ and NaCl.

2.4. Conclusions

We have constructed and demonstrated the capabilities of the newly developed LSA generator to reproduce SSA using marine salinities and to probe LSA generation under freshwater-relevant low salt concentrations. The LSA generator utilizes plunging jets to entrain air and generate bubbles, similar to other SSA generation techniques, but with modifications, such as the addition of mesh caps on the plunging jet outlets to obtain more accurate air entrainment by increasing surface roughness of the plunging jet (Zhu et al. 2000, Stokes et al. 2013). The LSA generator requires lower sample volume to generate aerosols compared to other plunging jet SSA generators (Salter et al. 2014). The lower solution volume requirement (4 L) allowed for generation of LSA from a variety of samples, including a freshwater sample collected from Lake Michigan. This increases the ease of analyzing a large number of freshwater samples, which will be necessary to probe how the differences in composition between freshwater locations (Chapra et al. 2012, Shuchman et al. 2013) affect aerosol generation.

This LSA generator-enabled laboratory study of LSA production allowed a direct investigation into the influence of salt concentration and composition on aerosol production from bubble bursting in freshwater and simplified model systems. The results show that freshwater bubble bursting, expected during periods of high winds and high waves over freshwater environments such as the Laurentian Great Lakes, will produce LSA. Distinct differences in the production and properties of LSA compared to SSA from marine environments are observed. For example, the lower concentration of salts in freshwater compared to seawater leads to lower number concentrations of bubbles in freshwater compared to seawater, such that a lower number concentration of LSA is produced compared to SSA. In addition, the differences in salt concentration and composition between seawater and freshwater leads to a size distribution of LSA that is bimodal compared to the unimodal SSA. The primary and secondary lognormal modes of the aerosol size distribution generated from the Lake Michigan freshwater sample were centered at larger diameters (180 ± 20 nm, 46 ± 6 nm) than the aircraft-measured lognormal mode (15-40 nm) over Lake Michigan by Slade et al. (2010). Lower RH aloft and the presence of other aerosol present near the modes of the LSA size distribution in the ambient atmosphere sampled by Slade et al. (2010) could explain the discrepancy with this laboratory study in reported LSA diameter modes. The larger LSA observed in this study could better act as CCN (Lewis and Schwartz 2004)

than the smaller LSA observed by Slade et al. (2010) and the smaller SSA observed in this study and others; however, further studies are needed.

While this laboratory study represents a fundamental exploration of the role of inorganic salts in LSA production, the role of organic and biological material present in lake water in determining LSA production and properties is currently poorly understood. Organic and biological content of seawater is known to affect SSA production and properties (Facchini et al. 2008, O'Dowd et al. 2008, Ault et al. 2013, Prather et al. 2013, Burrows et al. 2014, Quinn et al. 2014, Lee et al. 2015), and thus, organic and biological components of lake water are likely to affect LSA production, properties, and heterogeneous chemistry (Ault et al. 2013, Ault et al. 2014, Ryder et al. 2014). This study observed the effect of organic and biological materials in lake water on LSA through the differences in the aerosol size distributions and aerosol circularity generated from the organic and biological rich Lake Michigan freshwater sample, and the organic and biological free synthetic freshwater. Lake water has a higher ratio of organic to inorganic content than seawater (Chapra et al. 2012, Pilson 2013), so the organic content in lake water likely plays a larger role in LSA than the organic content in SSA. In addition, recent increases in toxic cyanobacteria blooms in the Great Lakes (Michalak et al. 2013) may impact air quality if toxic components are aerosolized with LSA, as has been observed for marine algal blooms (i.e. red tides) (Woodcock 1948, Cheng et al. 2010). Therefore, future studies are needed to determine the effect of the organic and biological content in freshwater on aerosol production and resulting properties.

The impact of LSA on radiative forcing and precipitation in the Great Lakes region is currently uncertain (Chung et al. 2011). For example, SSA impacts radiative forcing directly through scattering and indirectly by acting as CCN, which influences cloud properties and precipitation patterns (Wise et al. 2009), and LSA could have a similar effect. The Great Lakes' impact on downwind cloud cover and precipitation, known as lake effect, is well known and LSA could play a role in this process (Scott and Huff 1996). The contribution of LSA to regional aerosol concentrations may have seasonality, with the highest production likely occurring in the fall and late spring when wind speeds are highest and the lakes are not covered in ice. With global climate change predicted to decrease ice extent during winter (Wang et al. 2012) and observed increases in wind speed, linked to warming temperatures (Desai et al. 2009), the impact of LSA is expected to increase in the future.

2.5. Acknowledgements

Dr. Jessica L. Axson, Alexa Watson, and Prof. Andrew P. Ault are thanked for their contributions in freshwater sample collection, design and construction of the LSA generator, and the collection and analysis of bubble and particle measurements. The University of Michigan Water Center and Dow Sustainability Fellows Program at the University of Michigan provided funding for this work. The authors would like to thank the University of Michigan, College of Literature, Science, and the Arts Instrument Shop for helping with construction of the LSA generator and the Michigan Center for Materials Characterization, $(MC)^2$, at the University of Michigan is acknowledged for assistance with electron microscopy. Grant Deane of Scripps Institute of Oceanography at the University of California - San Diego is thanked for discussions regarding bubble plume analysis.

Chapter 3 Aerosol Emissions from Great Lakes Harmful Algal Blooms

Reprinted (adapted) with permission from:
Environmental Science & Technology, 52, 2, 397–405, 2017.
DOI: 10.1021/acs.est.7b03609.

3.1. Introduction

Eutrophication of freshwater resulting from increased anthropogenic nutrient loading has led to a global increase in harmful algal blooms (HABs), which are typically caused by *Cyanobacteria* (blue-green algae) (Smith 2003). Biogenic organic toxins (e.g. microcystis) contained within, and introduced into the aquatic environment by, blue-green algae (BGA) are a threat to both human and animal health through direct ingestion (Carmichael and Boyer 2016). Marine wave breaking under HAB conditions introduces toxic marine HAB products into the atmosphere alongside sea spray aerosol (SSA), with air concentrations of toxins as low as 2 – 7 ng m^{-3} inducing upper respiratory symptoms (Cheng et al. 2005, Kirkpatrick et al. 2011), suggesting the same process could occur in freshwater. Since freshwater recreational activity aerosolizes toxic HAB products (0.1 – 0.4 ng m^{-3}) (Backer et al. 2008, Backer et al. 2010), it is likely that freshwater wave breaking producing LSA under HAB conditions may be a previously unrecognized exposure route for HAB toxins. However, the only previous measurements of LSA chemical composition, which showed that the inorganic composition of LSA is reflective of freshwater, occurred during a period of low biological activity in Lake Michigan (Axson et al. 2016). As a result, there is currently a lack of understanding of how freshwater HABs affect the incorporation of biological material in LSA.

The relationship between seawater composition and SSA (Prather et al. 2013, Quinn et al. 2015) can inform our currently limited understanding of the links between the compositions of freshwater and LSA. Organics present in SSA are enriched relative to bulk seawater due to two mechanisms in the bubble bursting particle production method. Hydrophobic organic matter first accumulates at the surface of bubbles as they rise through the water column (O'Dowd et al. 2004, Keene et al. 2007, Bigg and Leck 2008, Facchini et al. 2008), and then organics in the sea surface

microlayer (60 μm thick) (Zhang 2003) are added to the bubble surface (Hawkins and Russell 2010). The concentration of organics at the bubble surface is then translated to an enrichment of organics in particles formed from droplets produced from the fragmentation of the bubble film cap (Blanchard and Syzdek 1975). It is likely, given that organic material is also concentrated in films at the surface of freshwater (100 μm thick) (Andren et al. 1976, Fuhs 1982, Meyers and Kawka 1982), that LSA also become enriched in organics relative to bulk freshwater concentrations through the same mechanisms identified for SSA. Dissolved organic content in freshwater without algal blooms (10−180 μM C) (Biddanda and Cotner 2002, Repeta et al. 2002, Shuchman et al. 2013) and with algal blooms (400 μM C) (Cory et al. 2016) is similar in concentration to seawater without and with algal blooms (80 and 50−300 μM C, respectively) (Ittekkot 1982, Repeta et al. 2002, Pilson 2013). The lower inorganic ion concentration in freshwater (0.05 – 0.15 g L^{-1}) (Chapra et al. 2012) compared to seawater (35 g L^{-1}) (Pilson 2013) results in a higher ratio of organic to inorganic content in freshwater compared to seawater (May et al. 2016). Therefore, organics may comprise a larger fraction by mass in LSA compared to SSA, likely impacting particle hygroscopicity and reactivity (Andreae and Rosenfeld 2008, Forestieri et al. 2016). The enrichment of organics in particles affects cloud condensation nuclei (CCN) activity of SSA, and possibly of LSA, as the addition of less water soluble organic species to salt particles decreases the overall hygroscopicity and increases the diameter at which particles can activate as CCN (Andreae and Rosenfeld 2008). In addition, organic compounds and biological material aerosolized from marine algal blooms by bubble bursting (Matthias-Maser et al. 1999, Aller et al. 2005, McCluskey et al. 2017) contribute to marine ice nucleating particle (INP) populations (DeMott et al. 2015, Wilson et al. 2015, Ladino et al. 2016, McCluskey et al. 2017, Vergara-Temprado et al. 2017), and organic compounds and biological material aerosolized from freshwater algal blooms may do the same in freshwater environments. Furthermore, biological species in freshwater with the potential to act as INP (D'Souza et al. 2013) are two to three orders of magnitude higher in freshwater than in seawater (Moffett 2016). These potential climate impacts of LSA may be reduced, compared to SSA, by the lower concentration of particles produced from bubble-bursting in freshwater compared to seawater (May et al. 2016). However, the distribution of organic and biological material across the population of bubble bursting particles (i.e. mixing state) plays an important role in determining their climate properties (Collins et al. 2013, Prather et al. 2013, Collins et al. 2014, Guasco et al. 2014).

Blue-green algae are the most widespread and common cause of HABs in the Laurentian Great Lakes of North America and have become increasingly important due to their significant resurgence near population centers (Steffen et al. 2014, Carmichael and Boyer 2016). The Great Lakes are characterized by large surface area, frequent high wind speeds, and significant fetch, leading to extensive wave breaking, which is conducive to LSA production (Doubrawa et al. 2015). LSA with variable biological content could be produced throughout the region due to the variability in the BGA concentration across the Great Lakes (Carmichael and Boyer 2016). Since the Laurentian Great Lakes system is a contiguous body of water, the effect of blue-green algae concentrations on LSA composition can be examined using samples collected from different lakes because of their similar inorganic ion composition (Chapra et al. 2012). In this study, freshwater samples were collected from Lake Erie and Lake Michigan from three locations with varying levels of BGA (Marion et al. 2012). The freshwater samples were used to generate LSA in the laboratory using a recently constructed laboratory LSA generator with a plunging jet system (May et al. 2016) that produces particles analogous to natural wave-breaking (Fuentes et al. 2010). Individual particles were analyzed using single-particle mass spectrometry and microscopy to determine size-resolved chemical composition. Chemical signatures of individual LSA particles were identified based on inorganic, organic, and biological ion markers. For each of the three freshwater samples, the relationship between freshwater BGA concentration and LSA chemical composition was examined. Fluorescence microscopy provided additional confirmation of the incorporation of biological material within individual particles. This information can be used for future identification of atmospheric LSA produced from freshwater of varying HAB content through field studies.

3.2. Experimental Methods

3.2.1. Freshwater Sample Collection & Aerosol Generation

Freshwater was collected from the top ~5 cm of the surface of three Great Lake sites in 8 L LDPE carboys. The three samples and corresponding collection times were as follows: 1) Lake Erie - Maumee Bay State Park, Oregon, Ohio (N 41.686365, W -83.372286) collected on September 12, 2014, 2) Lake Erie - Catawba Island State Park, Port Clinton, Ohio (N 41.573131, W -82.857192) collected on September 12, 2014, and 3) Lake Michigan – Washington Park Beach, Michigan City, Indiana (N 41.727573, W -86.909516) collected on October 12, 2014. An

additional freshwater sample was collected from the Lake Erie - Maumee location on September 20, 2017 to test the effect of freshwater sample freezing on LSA composition. Figure 3—1 shows the sampling locations on a NASA MODIS satellite image from September 17, 2014, the nearest clear sky day that allowed for a full visualization of the Great Lakes; photographs of the surface freshwater at the three sites at the time of collection are also shown. For comparison, Figure 3—2 shows NASA MODIS satellite images from October 12, 2014 and September 22, 2017, the nearest clear sky days that allowed for a full visualization of the Great Lakes; a photograph of the September 20, 2017 Lake Erie – Maumee surface freshwater is also shown. During freshwater sampling, a handheld spectrophotometer (AquaFluor 8000) measured BGA content through phycocyanin fluorescence, which serves as an indicator for algal cell and microcystin concentrations (Marion et al. 2012).

The three 2014 freshwater samples were frozen (-20 ˚C) after sampling for storage over a period of 20 months and thawed prior to aerosol generation in a laboratory LSA generator. Half of the 2017 Lake Erie - Maumee freshwater sample was used for aerosol generation in the laboratory LSA generator on the day of collection. The other half of the 2017 Lake Erie - Maumee freshwater sample was frozen (-20 ˚C) after sampling for storage over a period of 24 hours and thawed prior to aerosol generation in the laboratory LSA generator. Details of the LSA generator construction, operation, and validation studies are provided by May et al. (2016). Briefly, the LSA generator circulates 4 L of freshwater sample at 2 L min^{-1} via a diaphragm pump into four plunging jets, which creates bubbles that burst at the freshwater sample surface to generate aerosol particles. During all experiments the tank was kept at room temperature (23 ± 1 °C) with a relative humidity (RH) of 85%. Generated freshwater aerosols were passed through two silica gel diffusion dryers to achieve a relative humidity of ∼15% before measurement to reduce the suppression of negative ion mass spectra by particle phase water in the single-particle mass spectrometer (Neubauer et al. 1997). Prior to particle generation, particle-free air (Pall, HEPA Capsule Filter) was cycled through the LSA generator. Background particle concentrations were negligible (<20 particles cm^{-3}; <5%), in comparison to the average total particle concentration generated from the freshwater samples (∼750 particles cm^{-3}), and below sizes (d_a <250 nm) chemically analyzed by single particle analysis. The aerosol number size

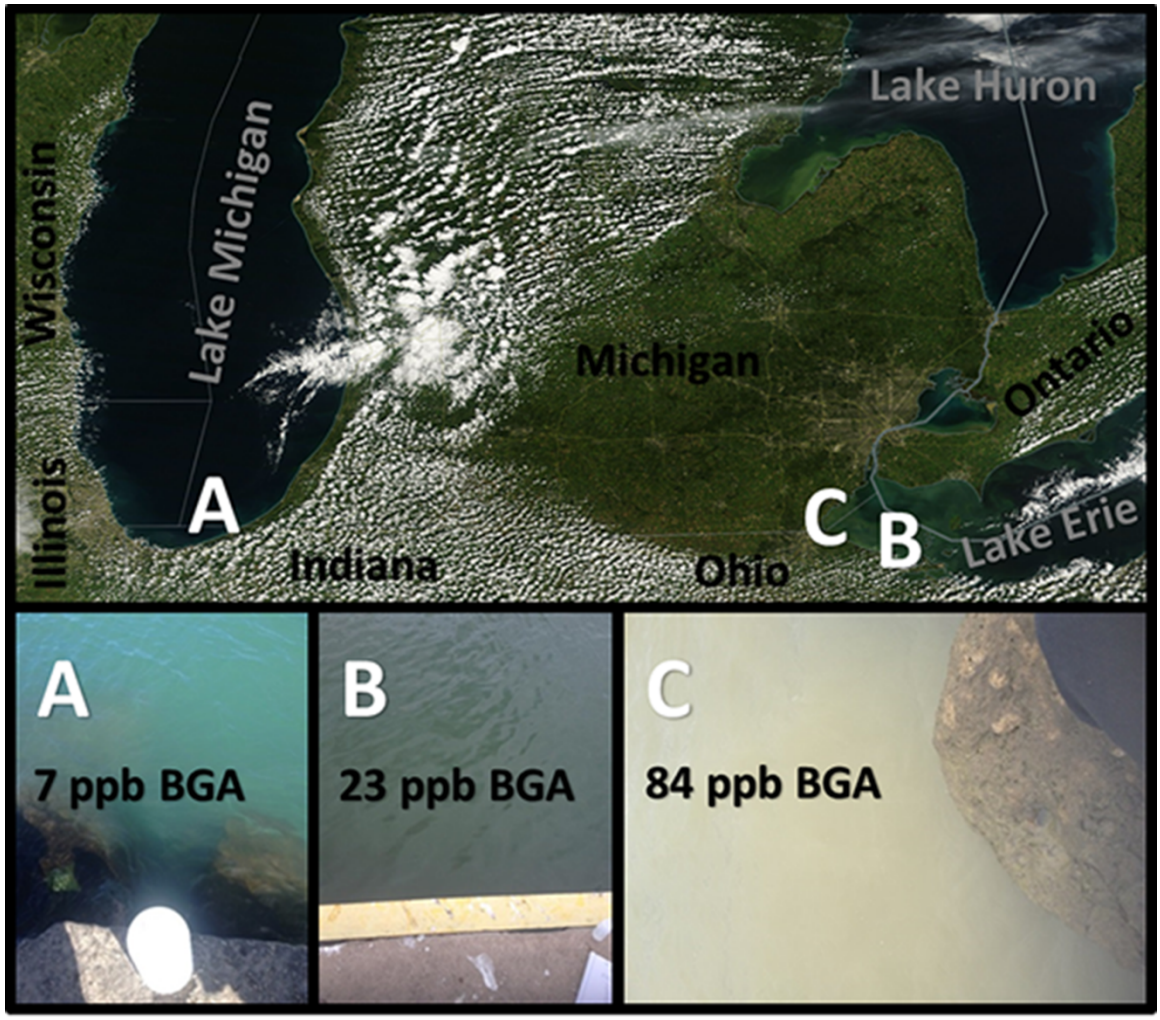

Figure 3—1. NASA MODIS satellite images of the Great Lakes region on September 17, 2014 with locations of Great Lakes surface freshwater sampling locations: (A) Lake Michigan – Michigan City, (B) Lake Erie – Catawba, and (C) Lake Erie – Maumee, with corresponding photographs of surface freshwater at sampling locations with blue green algae concentrations measured inset.

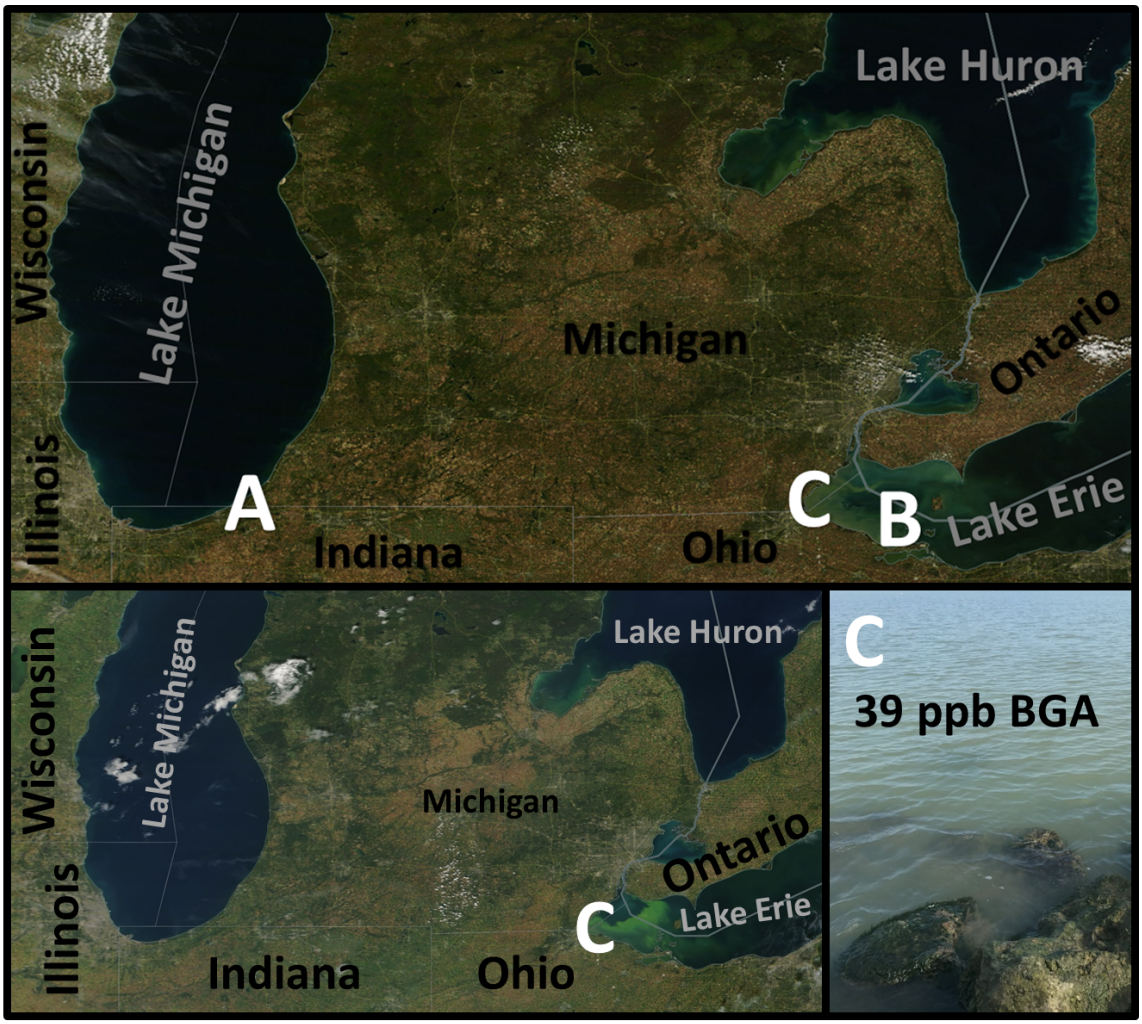

Figure 3—2. NASA MODIS satellite imagery of the Great Lakes region on (top) October 12, 2014 and (bottom left) September 22, 2017 with locations of Great Lakes surface freshwater sampling locations: (A) Lake Michigan – Michigan City (N 41.727573, W -86.909516), (B) Lake Erie – Catawba (N 41.573131, W -82.857192), and (C) Lake Erie – Maumee (N 41.686365, W -83.372286). (Bottom right) Photograph of 2017 surface freshwater at the Lake Erie – Maumee (N 41.686365, W -83.372286) with the measured blue green algae concentration noted.

distributions and total aerosol concentrations (Figure 3—3) for each LSA sample were measured by a scanning mobility particle sizer (SMPS), consisting of a differential mobility analyzer (DMA; TSI Inc., model 3082) and a CPC (TSI Inc., model 3775) for particles with electrical mobility diameters (d_m) between 14.1 and 736.5 nm, as well as an aerodynamic particle sizer (APS; TSI Inc., model 3321) for particles with aerodynamic diameters (d_a) between 0.52 and 19.8 μm.

3.2.2. Single Particle Analysis

An aerosol time-of-flight mass spectrometer (ATOFMS) was used for the real-time analysis of the size and chemical composition of individual LSA particles ranging from vacuum aerodynamic diameters of 0.25−1.5 μm (Pratt et al. 2009). Briefly, particles enter the instrument through an aerodynamic focusing lens creating a narrow particle beam. Particles are then accelerated to terminal velocities, which are measured by the time a particle takes to pass between two continuous wave lasers, with wavelengths of 488 and 405 nm, respectively, separated by 6 cm. Particle aerodynamic diameter is obtained by calibrating size dependent particle terminal velocity using polystyrene latex spheres of known diameter (0.1−2.5 μm) and density (1 g/cm^3). Individual particles entering the mass spectrometer are desorbed and ionized by a 266 nm Nd:YAG laser (1.2 mJ) generating positive and negative ions. Ions are detected using a dual polarity time-of-flight mass spectrometer. All particle measurements discussed here describe nascent LSA, sampled less than 10 s following production, thus minimizing subsequent chemical processing of these particles. 8,857 particles were chemically analyzed by ATOFMS for the 2014 Lake Michigan – Michigan City sample, 11,407 particles for the 2014 Lake Erie – Maumee sample, and 9,827 particles for the 2014 Lake Erie – Catawba sample. 4,651 particles were chemically analyzed by ATOFMS for the 2017 Lake Erie – Maumee sample pre-freeze particles and 5,255 particles for the 2017 Lake Erie – Maumee sample post-freeze particles. Mass spectral peak identifications correspond to the most probable ion(s) for a given *m/z* ratio based on previous studies (Prather et al. 2013, Guasco et al. 2014, Cahill et al. 2015, Axson et al. 2016). Relative peak area searches for combinations of inorganic, organic and biological marker ions within single-particle mass spectra were completed using the MATLAB toolkit FATES (Flexible Analysis Toolkit for the Exploration of Single-particle mass spectrometry data) (Sultana et al. 2017) to identify and separate the distinct single-particle types observed.

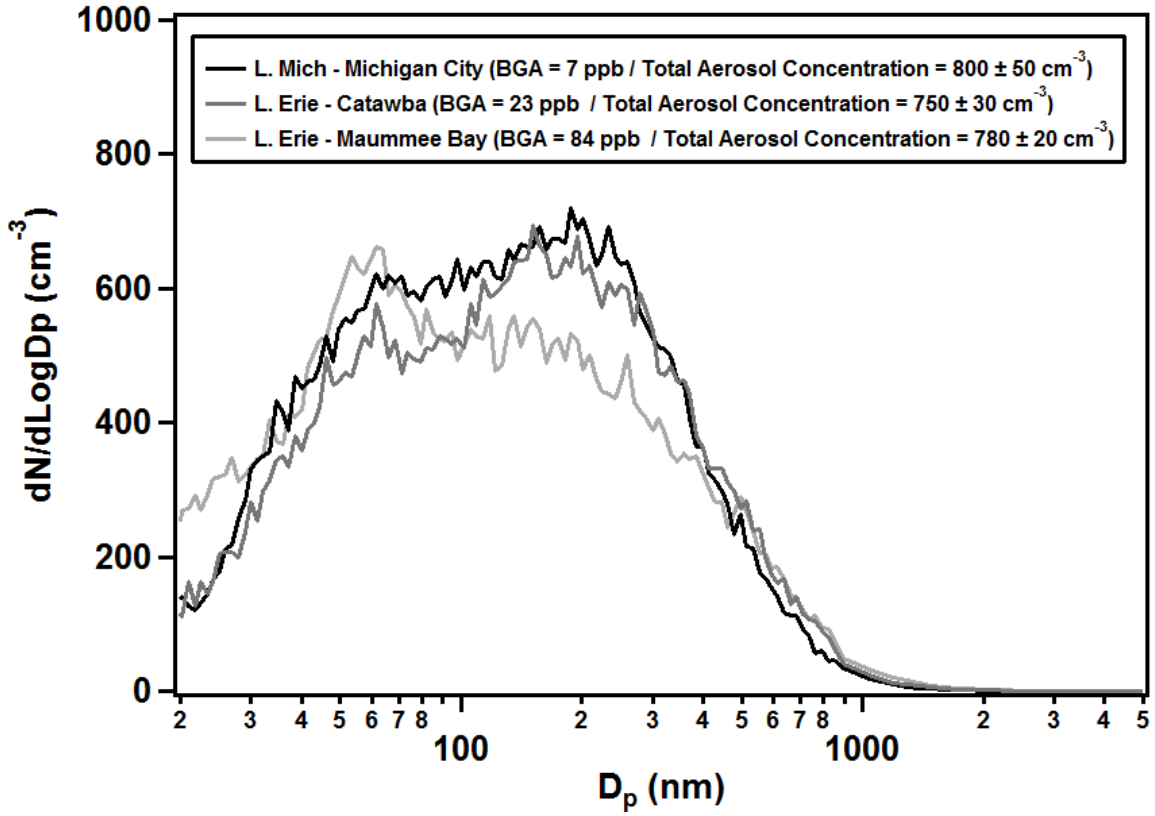

Figure 3—3. Average aerosol number size distributions produced by the LSA generator from the Lake Michigan – Michigan City, Lake Erie – Catawba, and Lake Erie – Maumee freshwater samples collected in 2014.

A microanalysis particle sampler (MPS, California Measurements, Inc.) was used to impact particles from the three 2014 freshwater samples onto Formvar coated copper microscopy grids (Ted Pella, Inc.) for analysis by scanning electron microscopy (SEM) and onto aluminum foil for fluorescence analysis. The MPS is operated at 2 L min^{-1} and consists of 3 stages with aerodynamic diameter size cuts of 2.5-5.0 μm for stage 1, 0.7-2.5 μm for stage 2, and <0.7 μm for stage 3. Aerosols collected on stage 3 of the MPS were analyzed using a Quanta environmental scanning electron microscope (ESEM, FEI). The FEI Quanta was operated at 20 kV and used a high angle annular dark field (HAADF) detector and an EDAX energy dispersive X-ray spectroscopy (EDX) detector to collect images and EDX spectra of 30 individual particles, respectively. In addition, particle circularity distributions were determined using SEM for 1,250 particles from the Lake Michigan – Michigan City sample, 2,016 particles from the Lake Erie – Catawba sample, and 1,766 particles from the Lake Erie – Maumee sample, from stages 2 and 3 of the MPS.

Aerosols from the three 2014 freshwater samples collected on stage 2 of the MPS were analyzed with a Raman microspectrometer (Horiba LabRAM HR Evolution) with a confocal microscope (100x objective) and a Nd:YAG laser (532 nm, 50 mW) for fluorescence analysis. The Raman spectrometer was operated in Swift mode with a 600 groove/mm grating and used a CCD detector. Fluorescence spectra were acquired from 545 to 605 nm over an area of 50 x 53 μm with a step size of 0.5 μm using 0.1 s acquisitions to create fluorescence maps of individual particles. The summed fluorescence intensities of 5 maps, each with ~20 particles, for each sample were averaged together and normalized to the highest average fluorescence intensity sample.

3.3. Results & Discussion

3.3.1. LSA Particle Chemical Composition & Morphology

Three distinct individual types of particles were identified by ATOFMS from the LSA generated in the laboratory from the freshwater surface samples. These three individual particle types are identified as: LSA primarily composed of inorganic salts (LSA-Salt), LSA with elevated organic carbon content (LSA-Organic), and LSA with biological material (LSA-Bio). This classification of LSA particle types is consistent with previous single particle mass spectrometry studies of laboratory generated SSA, which defined particle types on a scale of increasing organic and biological content: sea salt (SS), sea salt with organic carbon (SS-OC), bioparticles (Bio), and organic carbon (OC) (Prather et al. 2013, Guasco et al. 2014) (Lee et al. 2015). The seawater-

sourced OC particles are typically smaller in diameter (< 0.2 μm) (Guasco et al. 2014) than the lower size limit (0.25 μm) of the ATOFMS used in this study, such that freshwater-sourced OC particles may not be expected to be detected herein, as observed. Average dual polarity mass spectra from all three freshwater samples are shown for each of the three particle types, with major ions labeled, in Figure 3—4. Difference mass spectra, calculated as the difference between the average mass spectra between pairs of particle types, highlight the major changes in composition between the three particle types and are shown in Figure 3—5.

The individual LSA-Salt particle mass spectra were characterized by *m/z* 40 [Ca^+] as the highest intensity peak (Figure 3—4A), reflective of calcium as the highest concentration cation in Great Lakes freshwater (Chapra et al. 2012) and consistent with previous ATOFMS analyses of LSA generated from Lake Michigan freshwater with low BGA concentration (11 ppb) (Axson et al. 2016). Minor inorganic ion peaks included *m/z* +23 [Na^+], +24 [Mg^+], +39 [K^+], and +56 [CaO^+]. The LSA-Salt particle mass spectra were further defined by the lack of significant organic ions in the positive ion mass spectra. The LSA-Salt particle type negative ion mass spectrum was characterized by *m/z* -26 [CN^-] and -42 [CNO^-], representative of organic nitrogen (Guasco et al. 2014), as the most prominent peaks, consistent with our previous ATOFMS study of laboratory generated LSA from a Lake Michigan freshwater sample (Axson et al. 2016).

The individual LSA-Organic particle mass spectra (Figure 3—4b) exhibited similar inorganic ions as the LSA-Salt particle mass spectra, again with *m/z* +40 [Ca^+] as the most prominent peak in the positive ion mass spectrum. However, the LSA-Organic particle mass spectra were differentiated from the LSA-Salt particle mass spectra by the presence of significant *m/z* +66 [$CaCN^+$] and +82 [$CaCNO^+$] peaks, consistent with enhanced organic nitrogen content (Guasco et al. 2014). Additional significant organic ions were detected: *m/z* +74 [$N(CH_3)_4^+$]) and negative (*m/z* -45 [$CHOO^-$], -59 [CH_3COO^-], and -71 [$C_3H_3O_2^-$] (Figure 3—4) (Cahill et al. 2015). Therefore, similar to the classification of ATOFMS particles in SSA studies, the LSA-Organic particles are similar to the LSA-Salt particles, but with an enrichment in organic carbon internally mixed with the salt particles (Prather et al. 2013, Guasco et al. 2014).

The individual LSA-Bio particles (Figure 3—4c) exhibited similar organic ions as the LSA-Organic particle mass spectra. However, as shown in the mass spectral difference plots

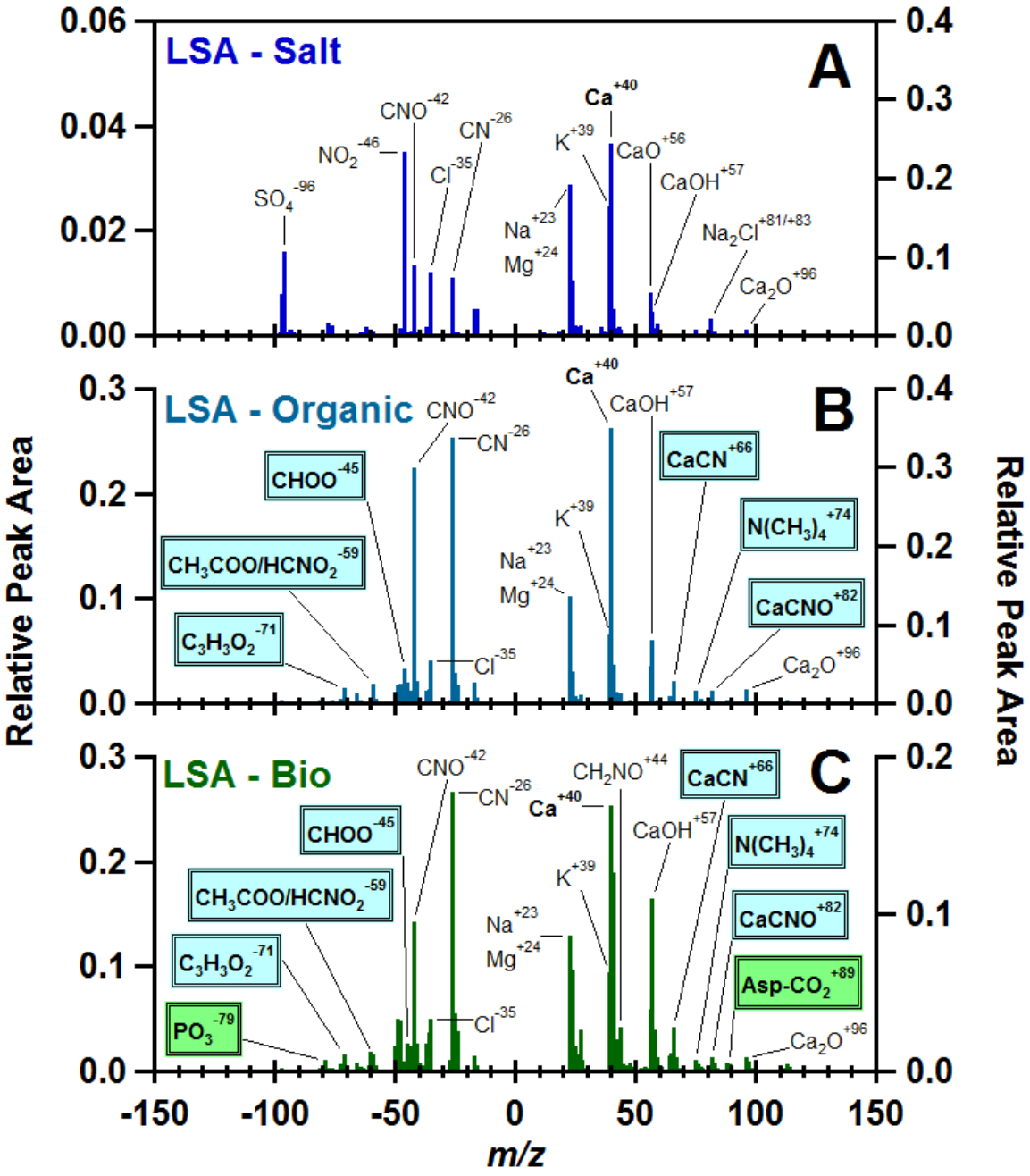

Figure 3—4. Average negative (left) and positive (right) mass spectra of individual particles defined as: (A) LSA – Salt, (B) LSA – Organic, and (C) LSA – Bio. Ions significantly enhanced in LSA-Organic and LSA-Bio, compared to LSA-Salt, particles are highlighted in blue, and ions significantly enhanced in LSA-Bio, compared to LSA-Organic and LSA-Salt, particles are highlighted in green; for comparison, mass spectral difference plots are shown in Figure A—4.

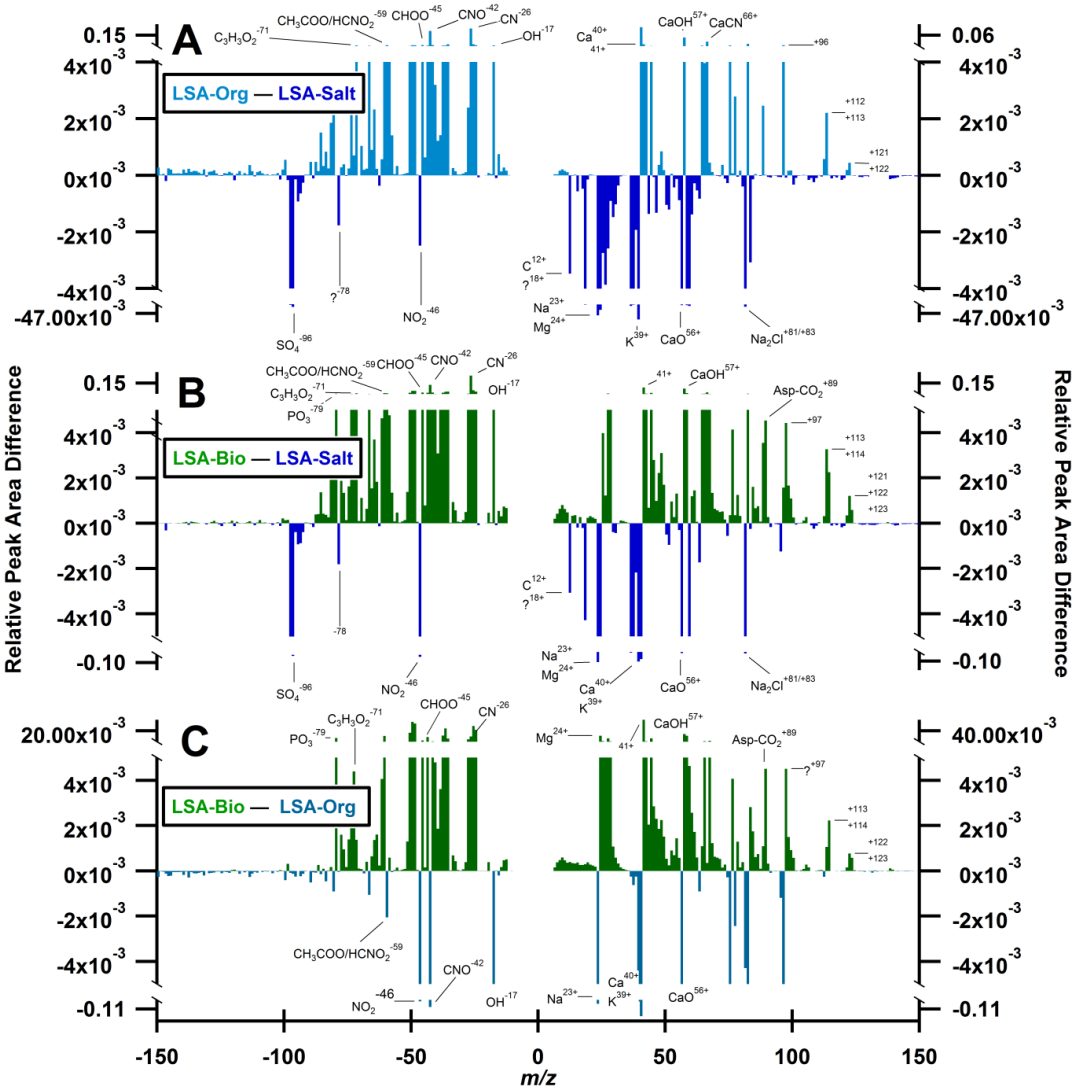

Figure 3—5. Mass spectral subtraction plots of relative peak areas for average mass spectra: A) LSA – Organic minus LSA – Salt, B) LSA – Bio minus LSA – Salt, and C) LSA – Bio minus LSA – Organic.

and highlighted in Figure 3—4, the LSA-Bio particles were distinguished from the LSA-Salt and LSA-Organic particles by the significant presence of *m/z* +89, suggested to be the common amino acid aspartic acid observed as [Asp – CO_2], based on previous bio-aerosol studies (Russell et al. 2004). The LSA-Bio particle mass spectra were further defined by the presence of a significant phosphate ion peak (*m/z* -79 [PO_3^-]) (Figure 3—5), which previous ATOFMS studies have found to be unique to particles containing primary biological material, when combined with organic nitrogen ion markers (*m/z* -26 [CN^-] and -42 [CNO^-]) (Pratt et al. 2009, Guasco et al. 2014, Sultana et al. 2017). Similar to the established marine biological aerosol mass spectral signature (Guasco et al. 2014), this LSA-Bio mass spectral signature likely represents fragments of BGA cells, which are typically 3 – 7 μm (Yan and Jameson 2004), as well as BGA exudates. Therefore, the LSA-Bio particles could potentially contain toxins from the BGA measured in the freshwater samples. Future measurements to differentiate between toxic and non-toxic biological species in particles are needed to assess the toxicity and public health impacts of the individual LSA-Bio particles.

The identification of the LSA-Salt, LSA-Organic, and LSA-Bio particles by ATOFMS was complemented by EDX analyses of single particle elemental composition (Figure 3—6). The EDX spectrum of a representative LSA-Salt particle was characterized by inorganic elements Na and Mg, with Ca as the highest intensity peak (Figure 3—6a), consistent with the ATOFMS mass spectra (Figure 3—4) and Great Lakes freshwater composition (Chapra et al. 2012). This Ca-dominant elemental composition and cubic morphology is similar to previous SEM-EDX analyses of ambient LSA collected on the coast of Lake Michigan and LSA generated in the laboratory from Lake Michigan freshwater of low BGA concentration (Axson et al. 2016). The EDX spectrum of a LSA-Organic particle was also characterized by Ca as the highest intensity peak (Figure 3—6b), consistent with the LSA-Organic ATOFMS mass spectra (Figure 3—4) and Great Lakes freshwater (Chapra et al. 2012); however, this particle had lower relative contributions from other inorganic elements present in the EDX spectra of LSA- Salt particles. While the C peak in the EDX spectrum is partly due to contributions from the microscopy substrate, the lack of other elements present suggests that carbon and oxygen from organic compounds comprised a significant fraction of the LSA-Organic particle mass. The LSA-Bio particle was further differentiated from the LSA-Organic particle by the presence of N

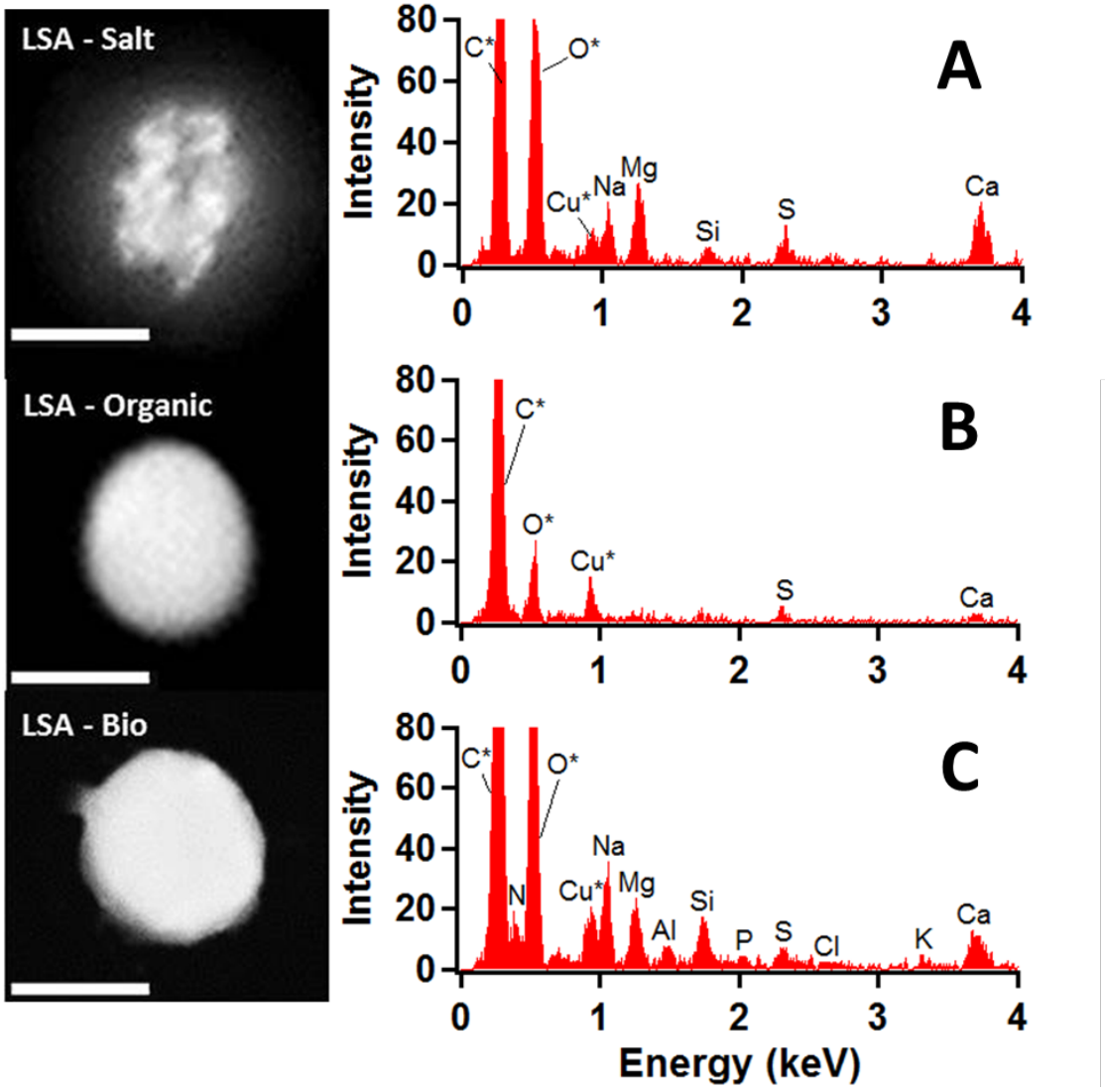

Figure 3—6. Scanning electron microscopy images with 1 µm scale bars (left) and corresponding energy dispersive X-ray spectra (right) of representative individual particles defined as: (A) LSA – Salt, generated from the 2014 Lake Michigan – Michigan City freshwater sample, (B) LSA – Organic, generated from the 2014 Lake Michigan – Michigan City freshwater sample, and (C) LSA – Bio, generated from the 2014 Lake Erie – Maumee freshwater sample.

and P, known markers of biological content (Mensah-Attipoe et al. 2016), in the EDX spectra (Figure 3—6c) and consistent with the ATOFMS spectra.

The identification of the individual LSA-Salt, LSA-Organic, and LSA-Bio particles by EDX analysis of single particle elemental composition was further supported by SEM analysis of single particle morphology (Figure 3—6). The LSA-Salt particle was defined in SEM images by a cubic core surrounded by a circular shell, the result of water loss from the particle after deposition to form a salt crystal (Ault et al. 2013). Increased total organic carbon concentration in seawater has been shown to disrupt the crystallization of salts in SSA during drying on the substrate resulting in more circular particles (Ault et al. 2013). In addition, previous SEM analysis demonstrated that LSA generated from Lake Michigan freshwater exhibited increased circularity compared to LSA generated from a synthetic freshwater representative of Great Lakes inorganic ion content without organic content (May et al. 2016). Therefore, the increased circularity of the LSA-Organic particle type observed in the SEM image, in comparison to the LSA-Salt particle type, further supports the increased incorporation of organic carbon identified by EDX analysis. The LSA-Bio particle type exhibited similar circularity to the LSA-Organic particle type, which is consistent with transmission electron microscopy studies of laboratory generated SSA that found biological particles to be circular (Patterson et al. 2016).

3.3.2. Effect of Blue Green Algae Content on LSA Composition

A direct relationship was observed between the BGA content of the 2014 surface freshwater samples and the submicron and supermicron ATOFMS number fractions of individual LSA-Bio particles (Figure 3—7). The low biological activity Lake Michigan – Michigan City sample (7 ppb BGA) produced the lowest LSA-Bio submicron (1 ± 1% (standard error)) and supermicron (3 ± 1%) particle number fractions. The Lake Erie – Catawba sample, which had the second highest biological activity (23 ppb BGA), produced the second highest submicron (11 ± 1%) and supermicron (34 ± 1%) number fractions of LSA-Bio particles. The highest biological activity Lake Erie – Maumee sample (84 ppb BGA) produced the correspondingly highest submicron (17 ± 1%) and supermicron (44 ± 1%) particle number fractions of LSA-Bio particles. A similar positive association between seawater biological content and SSA biological particle type number fraction was shown in a laboratory SSA generation study, where increasing seawater biological content (chlorophyll-a: 0.5 to 5 mg/m^3; heterotrophic bacteria 1x10^6 to 7x10^6 cells/mL) corresponded to the SSA-Bio number fraction

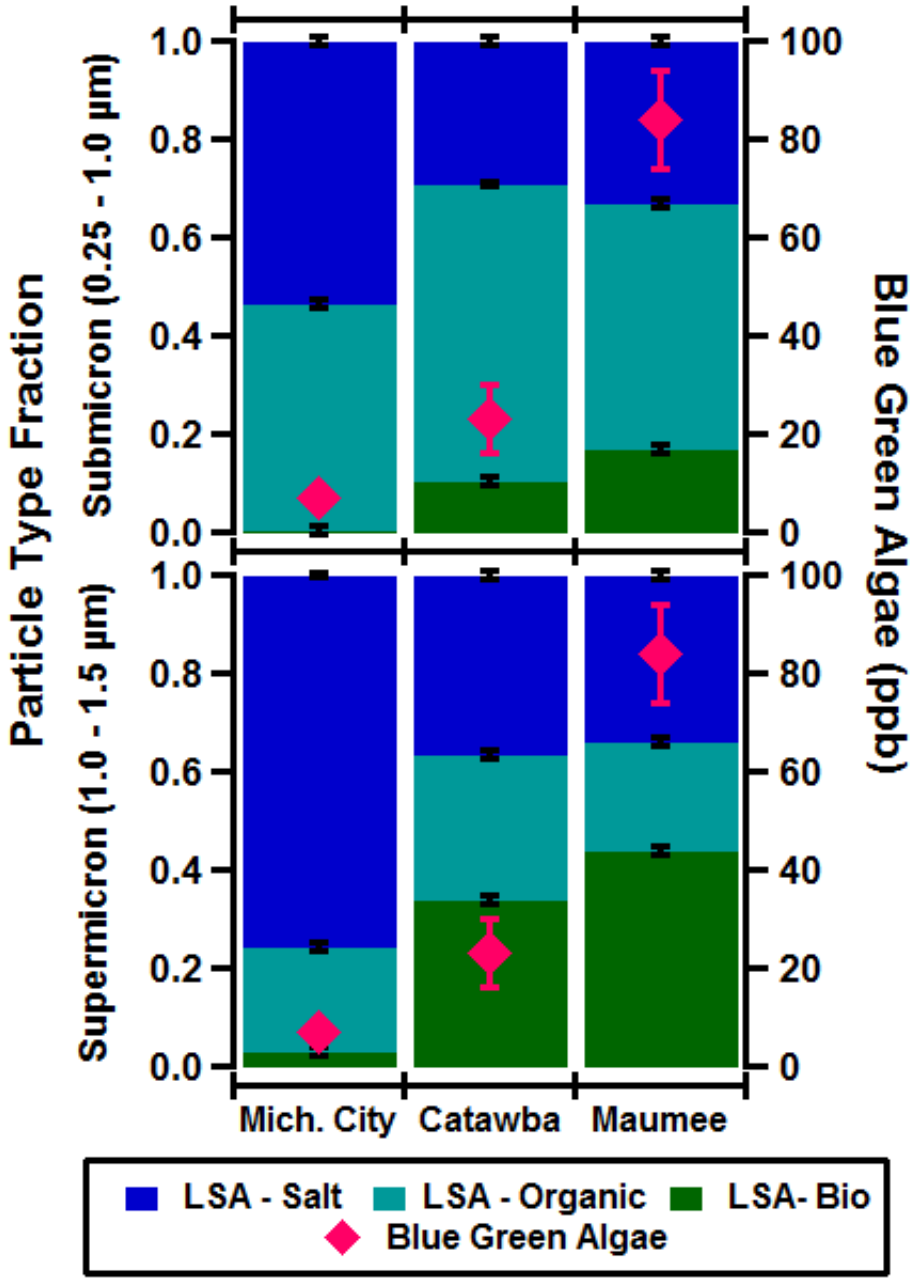

Figure 3—7. Number fractions of ATOFMS particle types, with standard errors shown, for submicron (0.25-1.0 µm) (top) and supermicron (1.0-1.5 µm) (bottom) particles generated in the laboratory from freshwater samples collected in 2014 from Lake Michigan – Michigan City (left), Lake Erie – Catawba (center), and Lake Erie – Maumee (right). Average blue green algae concentrations, with standard deviations shown, of the freshwater samples measured at the time of collection are also shown.

increasing from 18% to 30% (using ATOFMS to probe 0.5 – 3.0 μm particles) (Guasco et al. 2014). Therefore, the increase in the number fractions of individual LSA-Bio particles with increasing measured BGA concentration further demonstrates the incorporation of biological material in LSA.

As shown in Figure 3—8, similar size dependence was observed in the number fractions of LSA-Bio and LSA-Salt particles produced by the three 2014 freshwater samples. For the elevated biological content Lake Erie – Catawba (23 ppb) and Lake Erie – Maumee (84 ppb) freshwater samples, the number fraction of individual LSA-Bio particles increased substantially as particle diameters increased from 0.4 μm to 1.5 μm (1% to 40% and 3% to 50%, respectively). While evident, this increase was less substantial for the low biological content (7 ppb) Lake Michigan – Michigan City freshwater sample, with the number fraction of individual LSA-Bio particles increasing from 0.6% to 6% for particle diameters from 0.4 μm to 1.5 μm. Consistent with this size-dependent trend, previous ATOFMS measurements of laboratory generated SSA from an induced phytoplankton bloom observed the greatest contribution of biological aerosols at supermicron diameters (Prather et al. 2013, Collins et al. 2014, Sultana et al. 2017), which was attributed to the enrichment of biological material in marine jet drops (Blanchard and Syzdek 1972). Since the LSA-Bio particles primarily exist at larger diameters resulting from freshwater jet drops (May et al. 2016), the jet drop aerosol generation process likely leads to the enrichment of biological material within LSA, similar to SSA. Following a similar process, LSA-Salt particles were also primarily observed in particles at larger diameters, regardless of freshwater sample (Figure 3—8). For the low biological content (7 ppb BGA) Lake Michigan – Michigan City freshwater sample, the LSA-Salt particle number fraction increased substantially as particle diameters increased from 0.25 μm to 1.5 μm (26% to 76%). A previous ATOFMS study of laboratory generated SSA observed a comparable increase in inorganic-rich sea salt particles as particle diameters increased from 0.55 to 3 μm (Prather et al. 2013, Collins et al. 2014). The increase in the number fraction of inorganic-rich aerosols at larger diameters in both SSA and LSA is attributed to their production by jet drops (Kientzler et al. 1954), which are larger and more representative of the inorganic-rich bulk solution than film drops (Lewis and Schwartz 2004).

The size dependence of LSA-Organic particle number fractions produced from all three 2014 freshwater samples, characterized by greater contributions to smaller particles, is distinct

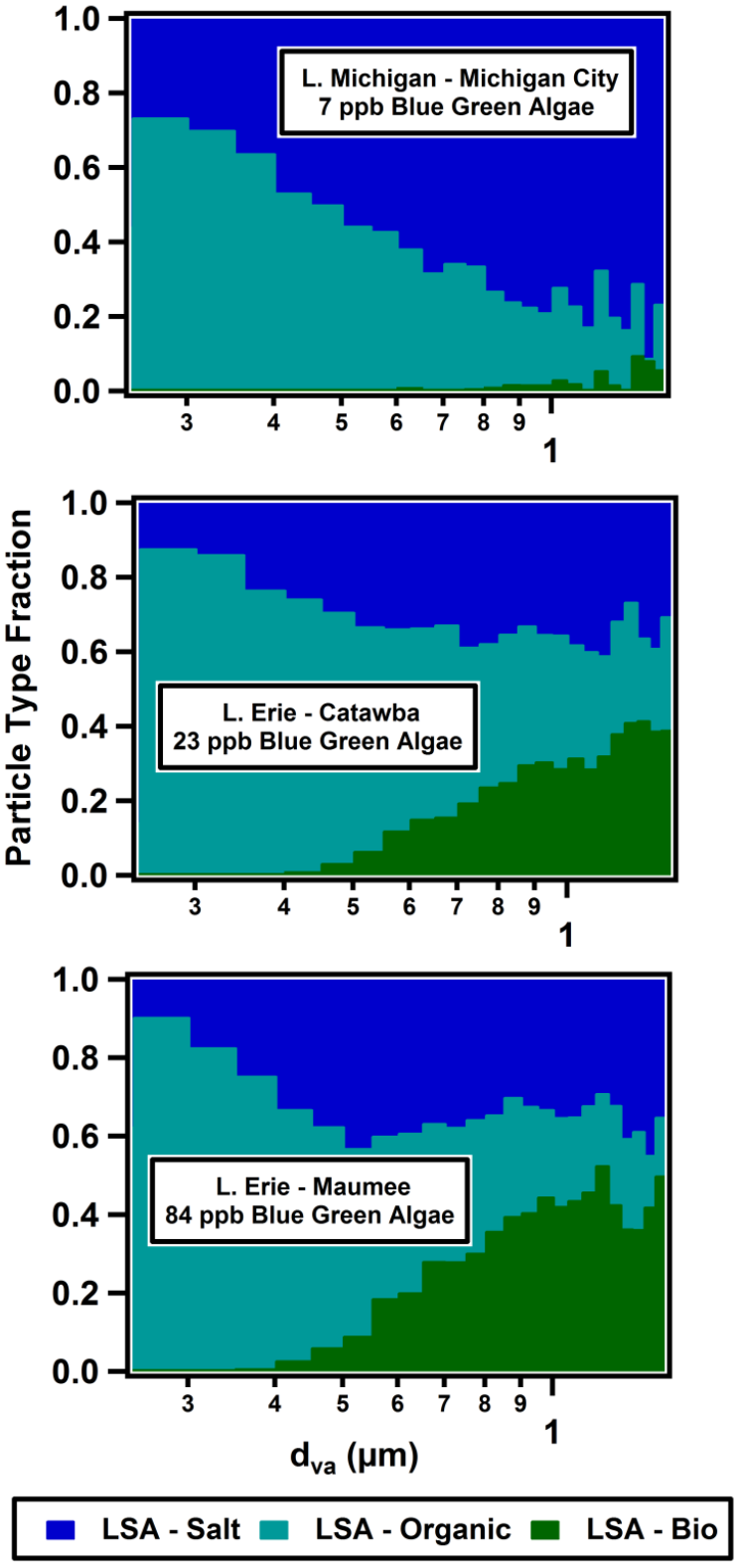

Figure 3—8. Size-resolved (0.25 – 1.5 µm) particle type number fractions measured by ATOFMS for particles generated in the laboratory from freshwater samples collected in 2014 from Lake Michigan – Michigan City (top), Lake Erie – Catawba (middle), and Lake Erie – Maumee (bottom).

from the size dependence of LSA-Salt and LSA-Bio particles. The LSA-Organic particle number fraction decreased as particle diameters increased from 0.25 μm (Lake Michigan – Michigan City = 74%; Lake Erie – Catawba = 88%; Lake Erie – Maumee = 90%) to 1.5 μm (Lake Michigan – Michigan City = 18%; Lake Erie – Catawba = 30%; Lake Erie – Maumee = 15%) for all three 2014 freshwater samples (Figure 3—8), similar to studies of laboratory generated SSA that observed a decrease in SSA-Organic particle type number fractions from 0.3 to 1.5 μm in diameter (Prather et al. 2013). In the marine environment, smaller particles resulting from film drops in the bubble bursting process are enriched in organic compounds due to the high concentration of organics at the surface of seawater and bubbles (Lewis and Schwartz 2004). Therefore, increase in the LSA-Organic particle number fractions at smaller particle diameters is consistent with an enrichment in organics at the surface of freshwater (Andren et al. 1976, Fuhs 1982, Meyers and Kawka 1982), leading to an enrichment in smaller LSA particles resulting from the freshwater bubble bursting process. All freshwater samples produced higher total number fractions (46-60%) of LSA-Organic particles, compared to the total number fractions (23-27%) of SSA-Organic particles generated from subsurface seawater enriched in organic material by a laboratory induced phytoplankton bloom (Collins et al. 2014). This is likely due to the higher proportion of organic material relative to inorganic material present in freshwater (Biddanda and Cotner 2002, Repeta et al. 2002, Chapra et al. 2012, Shuchman et al. 2013), compared to seawater, even under phytoplankton bloom conditions.(Repeta et al. 2002, Pilson 2013) Particle circularity distributions (measured from SEM images), shown in Figure 3—9, demonstrate that, for all three freshwater samples, the distribution maximum was close to 1, indicative of primarily spherical particles. These data are consistent with circularity distributions of particles previously generated from a Lake Michigan freshwater sample (May et al. 2016) and suggest that all of the freshwater samples are comprised of sufficient organic matter to disrupt cubic crystal formation within the LSA (Ault et al. 2013, May et al. 2016).

Normalized average fluorescence intensity derived from fluorescence microspectroscopy mapping of impacted particles (Figure 3—10 & 3—11) further suggests a direct relationship between the increased contributions of individual LSA-Bio particles with measured BGA concentration. For the lowest BGA concentration (7 ppb) Lake Michigan – Michigan City freshwater sample, the lowest normalized average fluorescence intensity (0.34 ± 0.09 (standard deviation)) was observed. The Lake Erie – Catawba freshwater sample (23 ppb BGA) was

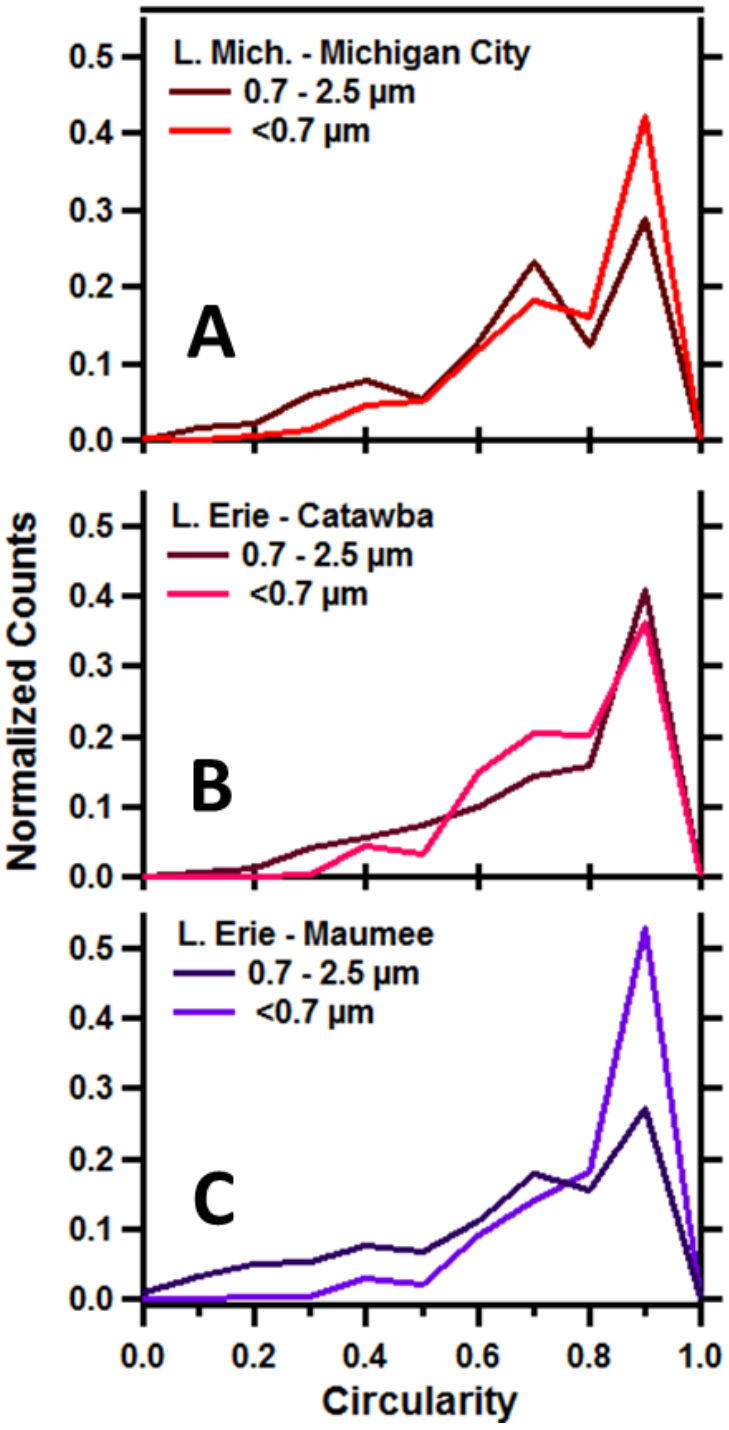

Figure 3—9. Circularity distributions as a function of aerodynamic particle diameter, where a value of 1 is indicative of a perfect circle, of particles produced from the 2014 (A) Lake Michigan – Michigan City, (B) Lake Erie – Catawba, and (C) Lake Erie – Maumee freshwater samples, as measured by SEM.

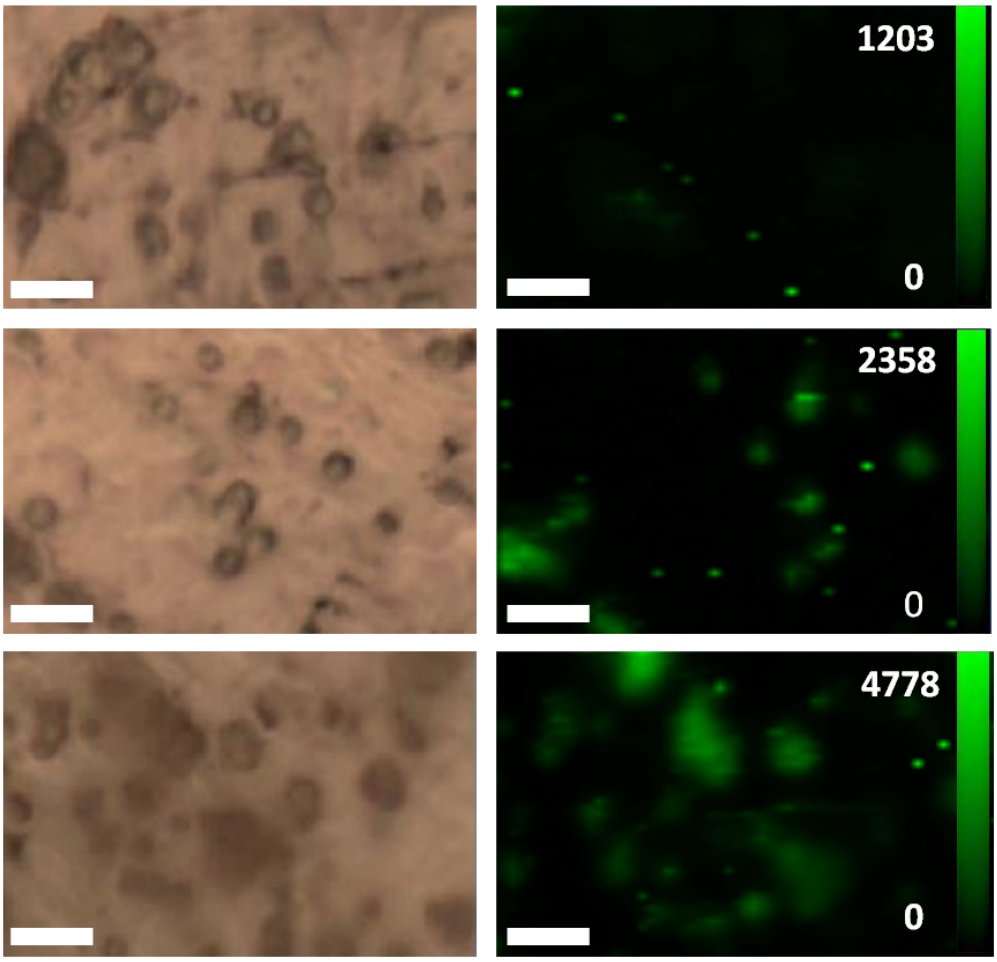

Figure 3—10. Optical images (left) and fluorescence maps with fluorescence intensity scales in counts, (right), of particles generated from the Lake Michigan – Michigan City (top), Lake Erie – Catawba (middle), and Lake Erie – Maumee (bottom) freshwater samples collected in 2014, as a function of freshwater blue green algae concentrations measured at the time of collection. All scale bars are 5 μm.

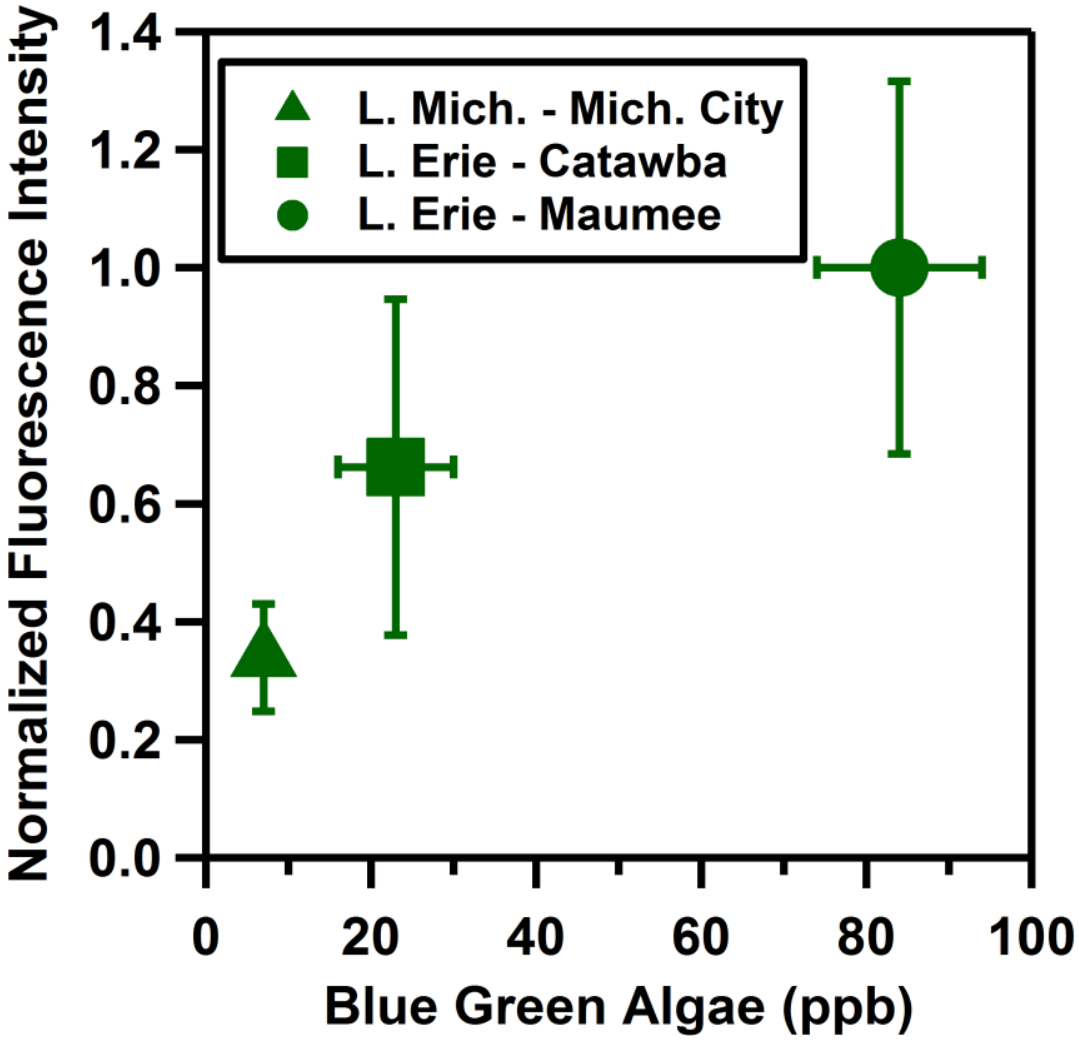

Figure 3—11. Normalized fluorescence intensity, an indicator of biological content, for particles generated from the Lake Michigan – Michigan City, Lake Erie – Catawba, and Lake Erie – Maumee freshwater samples collected in 2014, as a function of blue green algae concentrations of the freshwater samples at the time of collection. Error bars shown are standard deviations.

characterized by an intermediate normalized average fluorescence intensity (0.7 ± 0.3), and the Lake Erie – Maumee freshwater sample, with the highest BGA concentration (84 ppb), exhibited the highest normalized average fluorescence intensity (1.0 ± 0.3). While a statistically significant increase in fluorescence intensity of particles was only observed between the lowest (7 ppb BGA) and highest (84 ppb BGA) biological content samples, it is supportive of the statistically significant increase in the LSA-Bio particle number fractions with increasing freshwater BGA concentration, and provides further evidence of the bubble bursting production of bioaerosols from freshwater environments, with a dependence on biological activity. The increased fluorescence of particles associated with increased BGA concentration is indicative of increased biological particle content as organic molecules of biological origin, such as proteins and coenzymes, exhibit intrinsic fluorescence, providing a means for bioaerosol detection (Pöhlker et al. 2012, Lee et al. 2015).

3.3.3. Effect of Freezing on LSA Composition

The 2017 Lake Erie – Maumee freshwater sample was used to test for differences in BGA concentration and LSA composition prior to freezing and after 24 h frozen and then thawed. The measured BGA concentration of 39 ppb did not change with freezing. The trends in the size dependence of the number fractions of all three particle types (LSA-Salt, LSA-Organic, and LSA-Bio) produced by the pre- and post-freeze 2017 Lake Erie – Maumee freshwater samples (Figure 3—12) are consistent that observed for the LSA produced from the three 2014 freshwater samples (Figure 3—5). For both the pre- and post-freeze 2017 Lake Erie – Maumee freshwater samples, the number fraction of individual LSA-Bio particles increased as particle diameters increased from 0.4 μm to 1.5 μm (pre-freeze = 18% to 35%; post-freeze = 15% to 27%, Figure 3—12). Similarly, the number fraction of individual LSA-Salt particles increased as particle diameters increased from 0.25 μm to 1.5 μm (pre-freeze = 10% to 38%; post-freeze = 5% to 33%). Similar to the 2014 samples, the size dependence of the number fraction of individual LSA-Organic particles produced from the pre- and post-freeze 2017 Lake Erie – Maumee freshwater samples freshwater samples was distinct from the size dependence of LSA-Salt and LSA-Bio particles. The number fraction of individual LSA-Organic particles for both the pre- and post-freeze 2017 Lake Erie – Maumee freshwater samples decreased as particle diameters increased from 0.25 μm to 1.5 μm (pre-freeze = 80 ± 1% - 27 ± 1%; post-freeze = 87 ± 1% - 38 ± 1%). These

results indicate that freezing of freshwater samples does not affect the size dependent trends and relative order of abundance in the number fractions of individual LSA particles produced.

The number fraction of individual submicron LSA-Organic particles increased from 52 ± 1% to 62 ± 1% from pre- to post-freeze for the 2017 Lake Erie – Maumee sample (Figure 3—13). This ~10% increase in the number fraction of individual submicron LSA-Organic particles may be the result of the release of organic material from cell lysis during the freeze-thaw process, as suggested by the concurrent decrease in the number fraction of individual submicron (19 ± 1% to 15 ± 1%) and supermicron (36 ± 2% to 28 ± 2%) LSA-Bio particles from pre- to post-freeze for the 2017 Lake Erie – Maumee sample (Figure 3—13). Therefore, it is possible that the number fraction of submicron LSA-Organic particles generated from the three 2014 freshwater samples post-freeze was biased higher than the number fraction of individual submicron LSA-Organic particles that would have been generated from the three 2014 freshwater samples pre-freeze. Correspondingly, the number fraction of individual submicron and supermicron LSA-Bio particles generated from three 2014 freshwater samples post-freeze was biased lower than the number fraction of individual submicron and supermicron LSA-Bio particles that would have been generated from the three 2014 freshwater samples pre-freeze. However, the relative abundance and size-dependent trends in the LSA-Organic and LSA-Bio particles hold when comparing pre- and post-freeze samples, providing support for the findings from the 2014 samples. When possible, future experiments should not freeze freshwater samples prior to LSA generation.

The 2017 Lake Erie – Maumee sample confirmed the direct relationship between BGA content and the submicron (and total) ATOFMS number fractions of LSA-Bio particles. In the context of the 2014 samples, the post-freeze 2017 Lake Erie – Maumee (39 ppb BGA) was the third highest biological activity freshwater sample, and it produced the third highest submicron number fraction of LSA-Bio particles (15%) (see Figure 3—7 for comparison). Similarly, this sample produced the third highest total number fraction of LSA-Bio particles (17%) (for comparison: 2014 Lake Michigan – Michigan City (7 ppb BGA) = 1%; 2014 Lake Erie – Catawba (23 ppb BGA) = 12%; 2014 Lake Erie – Maumee (84 ppb BGA) = 33%). However, the post-freeze 2017 Lake Erie – Maumee sample (39 ppb BGA) produced a lower number fraction

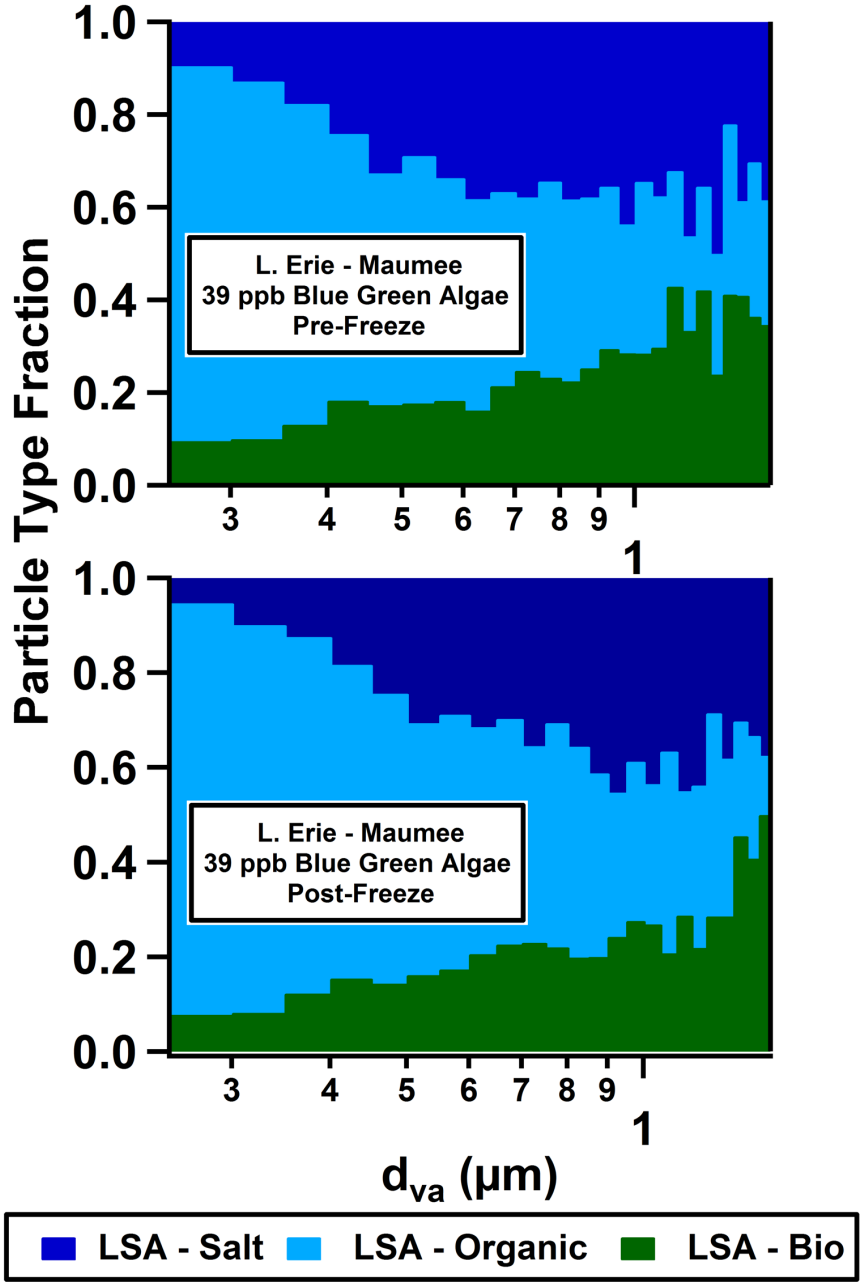

Figure 3—12. Size-resolved (0.25 – 1.5 µm) particle type number fractions measured by ATOFMS for particles generated in the laboratory from the pre- (top) and post-freeze (bottom) Lake Erie – Maumee freshwater samples collected in 2017. Measured blue green algae concentrations pre- and post-freeze are noted.

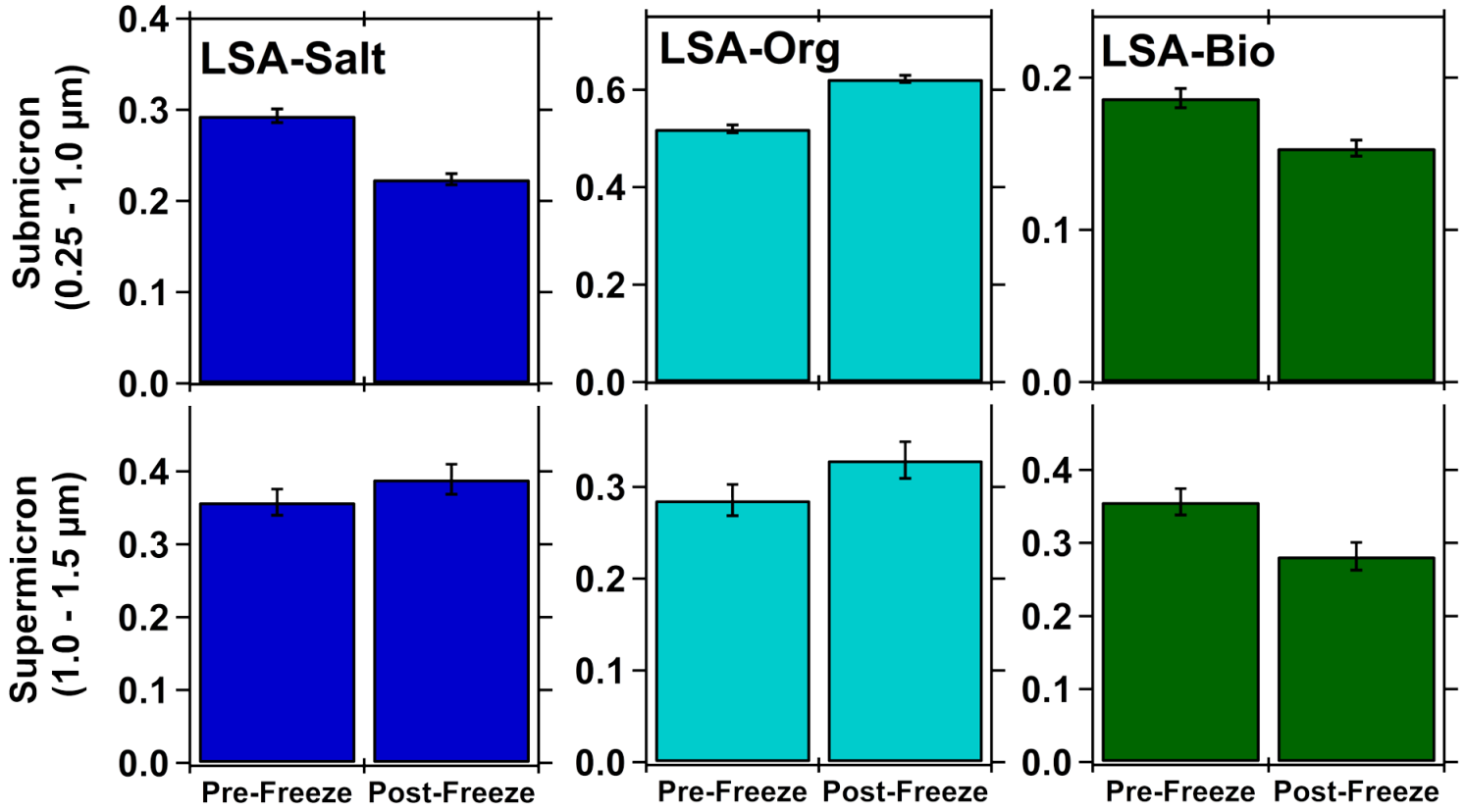

Figure 3—13. Number fractions of ATOFMS particle types, with standard errors shown, for submicron (0.25-1.0 µm) (top) and supermicron (1.0-1.5 µm) (bottom) particles generated in the laboratory from the pre- and post-freeze Lake Erie – Maumee freshwater samples collected in 2017.

of supermicron LSA-Bio particles (28%) than the lower biological activity 2014 Lake Erie – Catawba sample (23 ppb BGA; 34%). In addition, higher contributions of the LSA-Bio particle type were observed for number fractions of 0.25 – 0.4 μm particles for the pre- and post-freeze 2017 freshwater sample (11% and 9%, respectively) compared to the three 2014 freshwater samples (all <1%). Recent work has shown that variations over the course of phytoplankton blooms significantly changes the contribution of jet drops and associated biological material to the submicron SSA population (Pham et al. 2017, Wang et al. 2017). Therefore, the decrease in LSA-Bio particle number fractions at supermicron diameters in the 2017 samples and simultaneous increase in LSA-Bio particle number fractions at smaller (0.25 – 0.4 μm) diameters suggests that HAB variations (e.g. bloom progression), which were not assessed through BGA measurements, may affect the contribution of freshwater jet drops to the submicron LSA population, similar to SSA, and therefore, explain the observed differences in LSA-Bio contributions. Future studies of the size dependent composition of LSA over the development and decay of HABs, similar to seawater mesocosm studies of SSA (Forestieri et al. 2016, Jayarathne et al. 2016, Pham et al. 2017), are needed to understand variations in how biological material is incorporated in LSA impacts toxicity and climate properties.

3.4. Atmospheric Implications

This study examined the individual particle chemical composition of LSA generated from freshwater of varying BGA content. Individual LSA particles primarily composed of inorganic salts, inorganic salts with organic compounds, and inorganic salts with biological material were identified, with the biological content of individual LSA particles increasing with freshwater BGA content. This information is essential for improving our currently limited understanding of the potentially wide ranging atmospheric impacts of LSA, particularly in regions with large freshwater surface area, high wind speeds, and increasing HAB severity, such as the Great Lakes (Chung et al. 2011, Michalak et al. 2013, Doubrawa et al. 2015). The identification of biological material associated with individual LSA particles and its relation to BGA concentration in this

study demonstrates that freshwater wave breaking should be further studied as a vector for the introduction of aquatic toxins into the atmosphere. The LSA-Bio ATOFMS spectra characterized in this study could thus be used in future field measurements to identify the presence in the ambient atmosphere of potentially toxic bioaerosols produced by wave breaking induced bubble bursting from freshwater containing HABs. However, as the species present in freshwater algal blooms can range in toxicity,(Gobler et al. 2016) LSA produced by wave breaking induced bubble bursting from freshwater containing HABs also needs to be studied with techniques that can assess the molecular composition and toxicity of HAB products present to fully assess the public health impacts of freshwater wave breaking (Msagati et al. 2006, Gambaro et al. 2012).

The identification of biological material associated with individual LSA particles demonstrates freshwater wave breaking as a potentially important process for the introduction of freshwater biological INP into the atmosphere (D'Souza et al. 2013, Pietsch et al. 2015, Moffett 2016). The relative enrichment of organic compounds in smaller diameter LSA, similar to SSA, is also important to consider in predicting cloud droplet formation. Previous SSA studies have concluded that particles composed mostly of hygroscopic salts will activate into cloud drops at relatively smaller sizes, with the addition of less soluble organic species decreasing the overall hygroscopicity and increasing the size at which the particles can activate (Prather et al. 2013). However, studies on the effect of the distribution of inorganic and organic material on the hygroscopic properties of SSA may not be able to fully predict LSA climate impacts because of the differences in inorganic and organic species and associated concentrations present between freshwater and seawater (May et al. 2016). Laboratory measurements of the relationship between freshwater biological activity and LSA INP and CCN activity are needed to improve prediction of LSA climate impacts in models. In addition, field measurements of the size-dependent fluxes of LSA, including those particles containing biological material, from the freshwater to the atmosphere need to be conducted across various stages of freshwater algal bloom development to improve understanding of LSA production and air quality model simulations.

3.5. Acknowledgements

Nicole E. Olson, Dr. Jessica L. Axson, Peter S. Tirella, Dr. Rebecca L. Craig, and their advisor Prof. Andrew P. Ault, are thanked for assistance in freshwater sample collection, as well as laboratory aerosol generation and analysis. Mark Panas, Rachel M. Kirpes, and Dr. Matthew J. Gunsch are thanked for their assistance in laboratory aerosol analysis. The University of Michigan Water Center provided funding for freshwater collection. Dr. Swarup China and Prof. Alexander Laskin are thanked for their assistance in SEM-EDX analyses performed at the Environmental Molecular Sciences Laboratory (EMSL), a national scientific user facility located at the Pacific Northwest National Laboratory (PNNL) and sponsored by the Office of Biological and Environmental Research of the U.S Department of Energy (DOE). PNNL is operated for DOE by Battelle Memorial Institute under Contract No. DE-AC06-76RL0 1830. N.E. Olson's travel to Pacific Northwest National Laboratory was partially supported by a University of Michigan Rackham Graduate School Research Grant. J.L. Axson was partially supported through the University of Michigan Dow Sustainability Postdoctoral Fellows Program. M. Panas was supported by the University of Michigan, Department of Chemistry National Science Foundation Research Experience for Undergraduate program (CHE-1460990).

Chapter 4 Unexpected Contributions of Sea Spray and Lake Spray Aerosol to Inland Particulate Matter

Submitted to *Environmental Science & Technology: Letters*

4.1. Introduction

Sea spray aerosol (SSA) produced from oceanic wave breaking impact climate by scattering solar radiation, acting as cloud condensation nuclei (CCN), and serving as a source of reactive halogen gases (Andreae and Rosenfeld 2008, Quinn et al. 2015). SSA is primarily observed over marine and coastal locations, where it dominates particle mass concentrations (Ault et al. 2009, Grythe et al. 2014). Remote and rural inland regions often have fewer local PM sources than urban or coastal regions, such that, under certain meteorological conditions, transported particles from distant sources contribute significantly to PM mass (Sheesley et al. 2004, Spak and Holloway 2009, Allen et al. 2015, Bondy et al. 2017). Bulk PM measurements have demonstrated that SSA undergoes long-range transport to inland regions 100 – 1,100 km from the ocean (Shaw 1991, Gustafsson and Franzén 2000, Hara et al. 2004, Silva et al. 2007, Manders et al. 2010, Santos et al. 2012, Udisti et al. 2012, Chalbot et al. 2013, Makowski Giannoni et al. 2016). However, these methods rely on Na^+, Mg^{2+}, and Cl^- ratios, which can lead to an underestimation of inland SSA concentrations due to contributions from other particle sources (e.g. dust) (Sullivan et al. 2007, Pratt et al. 2010) and changes in initial source ratios due to multiphase reactions causing Cl^- depletion (Pakkanen 1996, Bondy et al. 2017).

The atmospheric abundance and climate impacts of lake spray aerosol (LSA) produced from freshwater wave breaking are more uncertain (Slade et al. 2010, Chung et al. 2011, Axson et al. 2016, May et al. 2016). Ambient identification of LSA is restricted to one aircraft study over portions of northern Lake Michigan and Lake Huron (Slade et al. 2010) and one ground-based coastal Lake Michigan study (Axson et al. 2016). However, previous identification of calcium-containing particles in clouds over the Great Lakes region (Lasher-Trapp et al. 2008, Twohy and Anderson 2008) suggests participation of calcium-rich LSA (Axson et al. 2016) in cloud droplet

formation. LSA may also have potential climate (Pietsch et al. 2015, Moffett 2016, Pietsch et al. 2017) and health (Cheng et al. 2007, Backer et al. 2008, Backer et al. 2010) implications due to the incorporation of organic and biological material from harmful algal blooms (HABs) (May et al. 2018). Identification and quantification of LSA in the atmosphere has been limited as chemical characterization of LSA has only occurred recently (Axson et al. 2016, May et al. 2018), and differentiating LSA from other sources of calcium-containing particles using bulk analytical measurements can be difficult (Sullivan et al. 2007, Allen et al. 2015). Herein, we show periodic contributions of transported SSA and LSA to ambient PM in northern Michigan during July 2014, motivating further study of the impacts of wave breaking particles on inland atmospheric composition, climate processes, and air quality.

4.2. Methods

4.2.1. Aerosol Measurements

Atmospheric measurements were conducted from July 13-24, 2014 at the University of Michigan Biological Station (UMBS) near Pellston, MI, >700 km from the nearest seawater source (Hudson Bay) and >25 km from Great Lakes sources (Lake Michigan = 25 km; Lake Superior = 100 km). Instrumentation was located within a laboratory at the base of a 30 m tall tower (45°33'31"N, 84°42'52"W) and individually connected by insulated 0.79-cm I.D. copper tubing to a manifold that sampled air at ambient relative humidity (RH) from 34 m above ground level (AGL) through insulated 1.09-cm I.D. copper tubing at a flow rate of 9.25 L min^{-1} (laminar) with a residence time of 15 s (Carroll et al. 2001), as described in detail by Gunsch et al. (2018). An aerosol time-of-flight mass spectrometer (ATOFMS, TSI 3800) (Gard et al. 1997, Dall'Osto et al. 2004) measured the size and chemical composition of 11,430 individual atmospheric particles ranging from 0.5 – 2 μm (vacuum aerodynamic diameter, d_{va}) in real-time, with particle losses in the sampling inlet tubing calculated to be <5% over this size range. An ART-2a algorithm clustered individual particle dual-polarity mass spectra (Song et al. 1999). Differences in the ion identities and intensities, the SSA and LSA individual particle mass spectra, discussed here, were separated by the ART-2a clustering. Additional resulting particle types are described by Gunsch et al. (2018), in which SSA and LSA were discussed as the combined Na/Ca Salt particle type. No internal mixtures of SSA and LSA identified. Size-resolved ATOFMS particle counts were scaled with size-resolved number concentrations of 0.5 – 2.0 μm aerodynamic diameter (d_a) particles,

measured by an aerodynamic particle sizer (APS, TSI model 3321), to obtain chemically-resolved particle number concentrations, following the method in Qin et al. (2006). The conversion of number to mass concentrations assumed spherical shape, as observed for the particles by scanning electron microscopy (SEM) (Figure 4—1). As wave breaking forms wet aerosols and RH was high enough to avoid efflorescence (ambient RH range: 40-80%) (Gunsch et al. 2018), a density of 1.5 g cm^{-3} was used for the SSA and LSA conversions of number to mass concentrations, based on the assumption of considerable aerosol liquid water (Moffet et al. 2008). Mass concentrations were also calculated assuming the material densities of NaCl (2.16 g cm^{-3}) and $CaCO_3$ (2.71 g cm^{-3}), with the understanding that this represents an upper bound for aerosols with low liquid water content.

For off-line analysis of individual particles, a micro-orifice uniform deposit impactor (MOUDI, MSP Corp., model 110) (Marple et al. 1991) impacted particles onto transmission electron microscopy (TEM) grids (Cu 400 mesh, Carbon type-B, Ted Pella, Inc.). 409 ambient particles collected on stage 4 (1 – 1.8 μm d_a) on July 16, 2014 (9:00-21:00 EDT) were analyzed by computer-controlled scanning electron microscopy with energy dispersive X-ray (CCSEM-EDX) spectroscopy to determine particle size, morphology, and elemental composition. K-means clustering of individual particle EDX spectra was used to identify the sources of particles present (Ault et al. 2012, Axson et al. 2016, Shen et al. 2016).

In addition to ambient sampling, particles were produced in a LSA generator (May et al. 2016) from freshwater samples collected August 1 and 2, 2014 in 8 L LDPE carboys from the surfaces of Lake Superior and Lake Michigan at sites upwind of UMBS. An ATOFMS, based on the design of Pratt et al. (2009), measured the size and chemical composition of 337 (Lake Superior) and 396 (Lake Michigan) laboratory generated particles (0.25 − 1.5 μm d_{va}). A three-stage microanalysis particle sampler (MPS-3, California Measurements, Inc.) impacted particles onto TEM grids (Cu 400 mesh, Carbon type-B, Ted Pella, Inc.) for analysis by CCSEM-EDX to determine single particle size, morphology, and elemental composition (Ault et al. 2012, Axson et al. 2016). The composition of LSA generated from these August 2014 freshwater samples can be compared to the July 2014 ambient LSA composition because significant changes in inorganic ion composition over a period of < 1 month are not expected (Chapra et al. 2012).

4.2.2. Backward Air Mass Trajectory Analysis & Wave Conditions

72 h backward air mass trajectories arriving at UMBS at heights of 100, 200, 500, 1000, and 3000 m AGL were calculated for every 12 h of the field study using the NOAA HYSPLIT4.8 (Hybrid Single-Particle Lagrangian Integrated Trajectory) model with 1˚ GDAS (Global Data Assimilation System) meteorology (Stein et al. 2015). Changes in measured particle composition associated with air mass transport pathways were investigated through potential source contribution function (PSCF) analysis, which combines backward air mass trajectories and atmospheric chemistry (ATOFMS particle type number fractions) to determine the probabilities of geographical areas being source locations of the measured chemical components (Polissar et al. 2001, Yu et al. 2016). Hudson Bay wind speed data at Fort Severn, Ontario (56°01'08" N 87°40'34" W) (wave height data not available) were provided by Environment Canada (https://www.canada.ca/en/services/environment.html). Lake Superior and Lake Michigan wind speed and wave height data at Stations 45001 (48°3'41" N 87°47'33" W) and 45024 (43°58'24" N 86°33'23" W), respectively, were from the NOAA National Data Buoy Center (http://www.ndbc.noaa.gov/).

4.3. Results & Discussion

4.3.1. Identification and Quantitation of Sea Spray Aerosol

On multiple occasions during the northern Michigan study, SSA were identified by ATOFMS based on comparison of individual particle dual-polarity mass spectra (Figure 4—2) with previous SSA ATOFMS mass spectra (Prather et al. 2013). While SSA negative ion mass spectra did not exhibit significant *m/z* -35 (Cl^-), characteristic of fresh SSA (Prather et al. 2013), nitrate markers, *m/z* -46 (NO_2^-) and -62 (NO_3^-), were observed, indicative of the multiphase reactions of $HNO_{3(g)}$ and/or $N_2O_{5(g)}$ that liberate chlorine to the gas phase (Gard et al. 1998, Ault et al. 2014). The SSA mass concentration mode identified by ATOFMS was >1 μm (Figure 4—2c), consistent with previous SSA observations (Lewis and Schwartz 2004, Ault et al. 2009, Qin et al. 2012). Consistent with the ATOFMS results, CCSEM-EDX also identified SSA particles based on elemental composition similar to seawater (Ault et al. 2013, Ault et al. 2013, Prather et al. 2013) following chloride depletion (Ault et al. 2013, Ault et al. 2014, Bondy et al. 2017). The EDX spectrum and elemental map of a representative individual SSA particle are shown in Figures 4—2d and 4—1, respectively, and are consistent with previous observations of the distribution of

major elements in SSA (Ault et al. 2013, Ault et al. 2013). The average SSA single particle Mg/Na elemental mole ratio (0.11 ± 0.07) was consistent with seawater (0.11) (Pilson 2013), and the

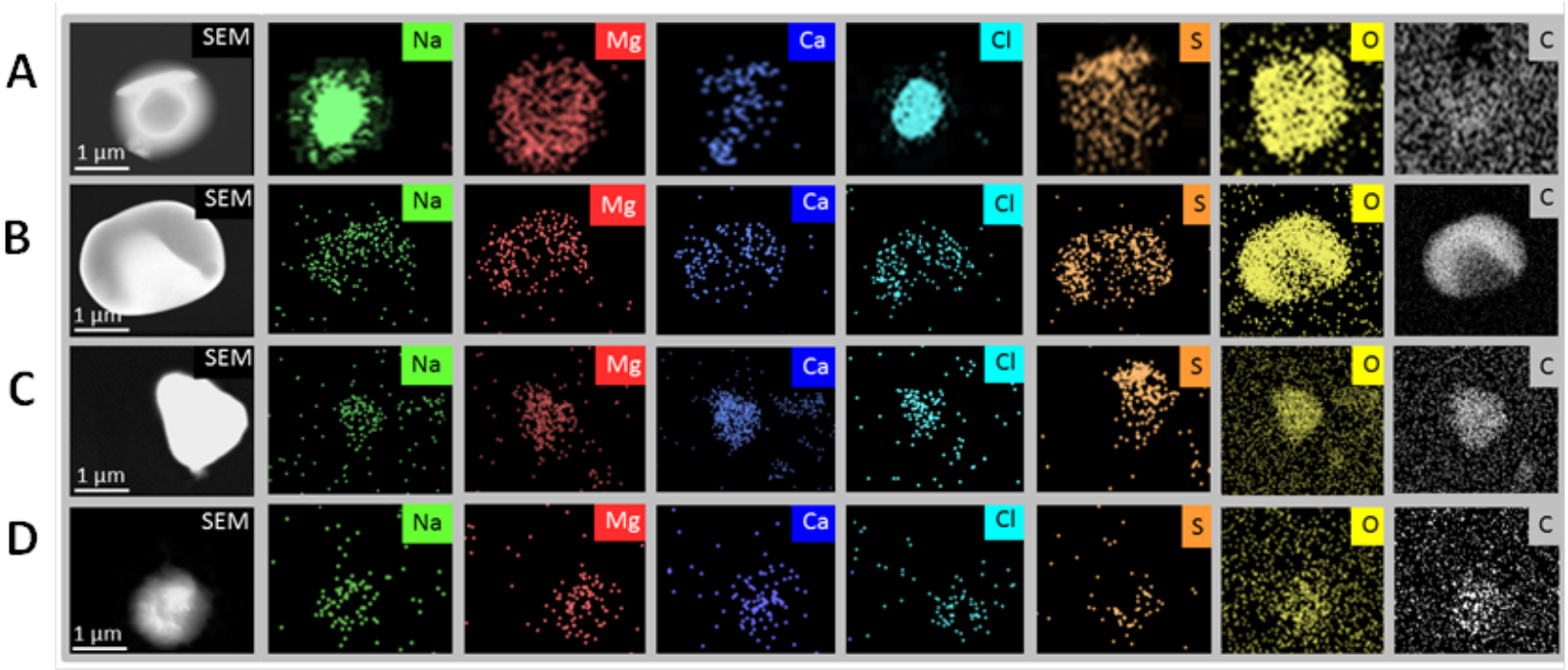

Figure 4—1. SEM images and EDX elemental maps of representative: (A) SSA and (B) LSA particles collected at UMBS on July 16, 2014 9:00 – 21:00 EST, as well as LSA generated in the laboratory from (C) Lake Superior and (D) Lake Michigan freshwater sample.

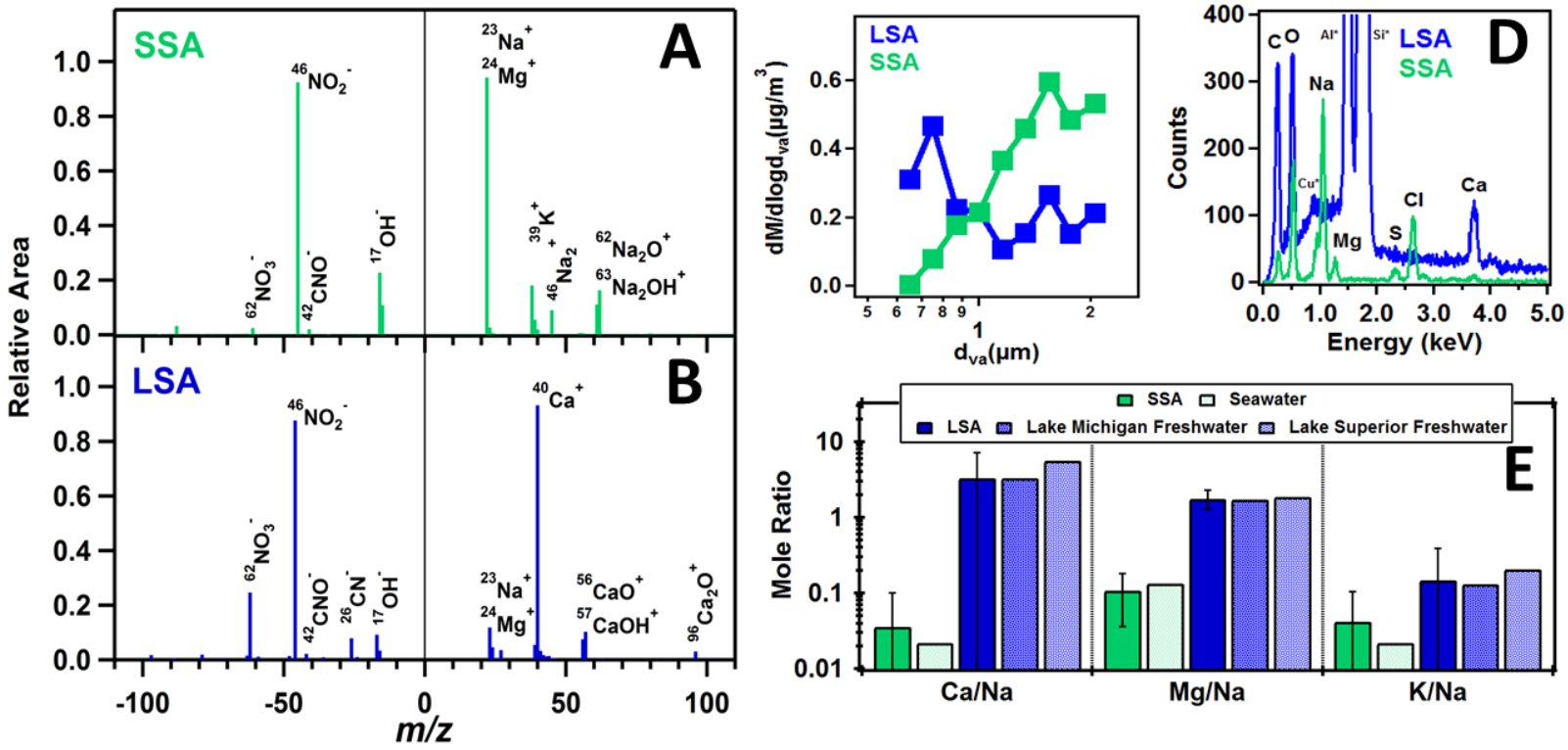

Figure 4—2. Average ATOFMS positive and negative ion mass spectra of individual ambient (A) sea spray aerosol (SSA) and (B) lake spray aerosol (LSA). (C) Average size-resolved aerosol mass distributions of ambient SSA and LSA, calculated from ATOFMS and APS data. (D) Representative EDX spectra of individual ambient SSA and LSA, with sample holder and substrate contributions (Al, Si, Cu) to the spectra denoted with asterisks. (E) Comparison of seawater, Lake Michigan freshwater, Lake Superior freshwater, ambient SSA, and ambient LSA elemental mole ratios. Ambient SSA and LSA mole ratios were calculated from the atomic weight percentages of each element measured by CCSEM-EDX with respect to the 15 elements that were analyzed (C, N, O, Na, Mg, Al, Si, P, S, Cl, K, Ca, Ti, Fe, Zn). Seawater, Lake Michigan freshwater, and Lake Superior freshwater mole ratios were calculated from ion concentrations reported by Pilson (2013) and Chapra et al. (2012).

average SSA particle Ca/Na (0.04 ± 0.06) and K/Na (0.04 ± 0.06) elemental mole ratios were also within error of seawater (both 0.02) (Pilson 2013) (Figure 4—2e). Overall, 35% and 65% of individual SSA particles, by number (measured by CCSEM-EDX), were aged (Cl/Na mole ratios < 0.1) or partially aged (1 ≥ Cl/Na ≥ 0.1) (Bondy et al. 2017), respectively (Figure 4—3). No SSA particles were observed without at least some chloride depletion. The capability of both single particle measurement techniques (ATOFMS and CCSEM-EDX) to identify individual SSA, even after Cl depletion, and differentiate between multiple sources contributing to Na and Mg (Gard et al. 1998, Allen et al. 2015, Bondy et al. 2017) , provides an advantage over bulk methods relying on average elemental ratios (Pakkanen 1996), which hinder accurate identification and quantification of inland SSA.

The PSCF trajectory domain of the observed SSA extended north and northeast of the UMBS sampling site to Hudson Bay (Figure 4—4), where wind speeds capable of producing SSA (> 3 m s^{-1}) (Lewis and Schwartz 2004, Stokes et al. 2013) were present for 78% of the July 2014 sampling period (Figure 4—5). As the nearest point of Hudson Bay is over 700 km away from UMBS, the SSA particles underwent long-range transport (>48 h), providing time for chloride depletion (Gard et al. 1998) by reaction with HNO_3 and N_2O_5. As shown by Gunsch et al. (2018), this air mass was also impacted by Canadian wildfire smoke, the long-range transport of which is associated with elevated NO_x levels (Dreessen et al. 2016). SSA contributions to particle mass concentrations were largest during two separate periods of Hudson Bay influenced air masses (Figures 4—5 & 4—6), as determined by 72 h HYSPLIT backward air mass trajectories arriving at UMBS at 100 m AGL. During these two periods (7/15/2014 12:00 - 7/18/2014 0:00 EST & 7/23/2014 0:00 - 7/25/2014 0:00 EST), SSA comprised 20 ± 10% (0.06 ± 0.04 μg m^{-3}) and 15 ± 6% (0.09 ± 0.04 μg m^{-3}) of 0.5 – 2 μm particle mass on average, corresponding to number concentrations of 0.03 ± 0.02 and 0.06 ± 0.02 particles cm^{-3}, respectively (Figure 4—5). Elevated wind speeds capable of producing SSA (Lewis and Schwartz 2004, Stokes et al. 2013) (5 ± 2 m s^{-1} and 5 ± 2 m s^{-1}, respectively) were present over Hudson Bay when these two air masses crossed over the water (Figure 4—5). Outside of these periods, SSA mass contributions were minor (average 3 ± 3%; 0.03 ± 0.02 μg m^{-3}), although number concentrations were similar (0.03 ± 0.02 particles cm^{-3}). Air mass PSCF analysis, in combination with ATOFMS and CCSEM-EDX data, suggests that SSA produced over Hudson Bay contributed to atmospheric particle mass

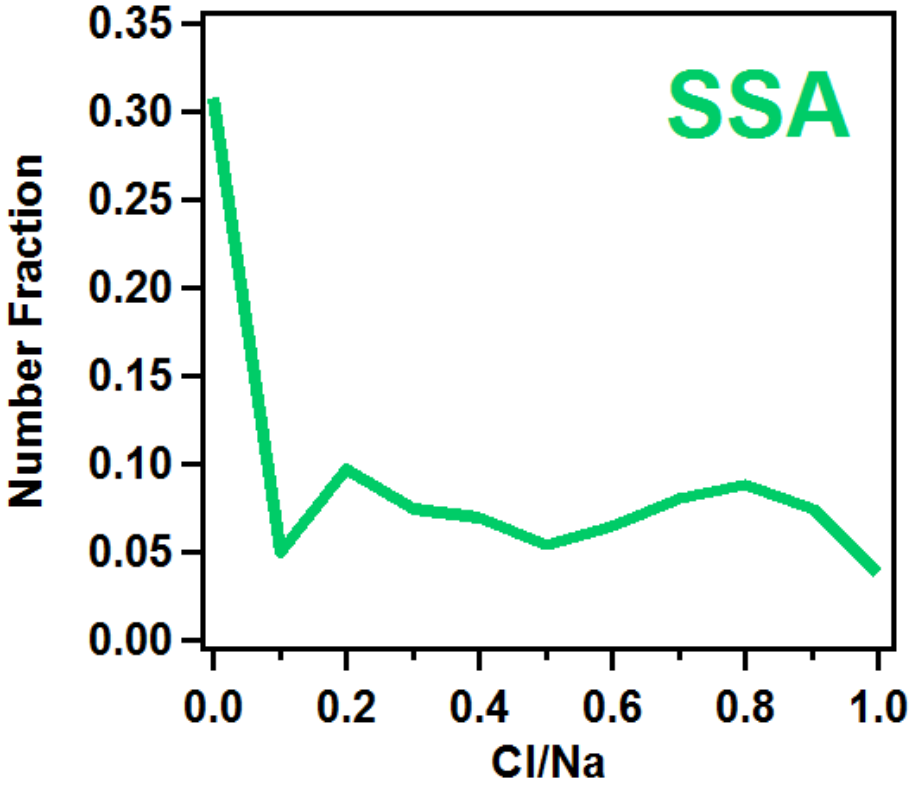

Figure 4—3. Cl/Na elemental mole ratio distribution for individual ambient sea spray aerosol (SSA), as measured by EDX. Ambient SSA mole ratios were calculated from the atomic weight percentages of each element measured by CCSEM-EDX with respect to the 15 elements that were analyzed (C, N, O, Na, Mg, Al, Si, P, S, Cl, K, Ca, Ti, Fe, Zn).

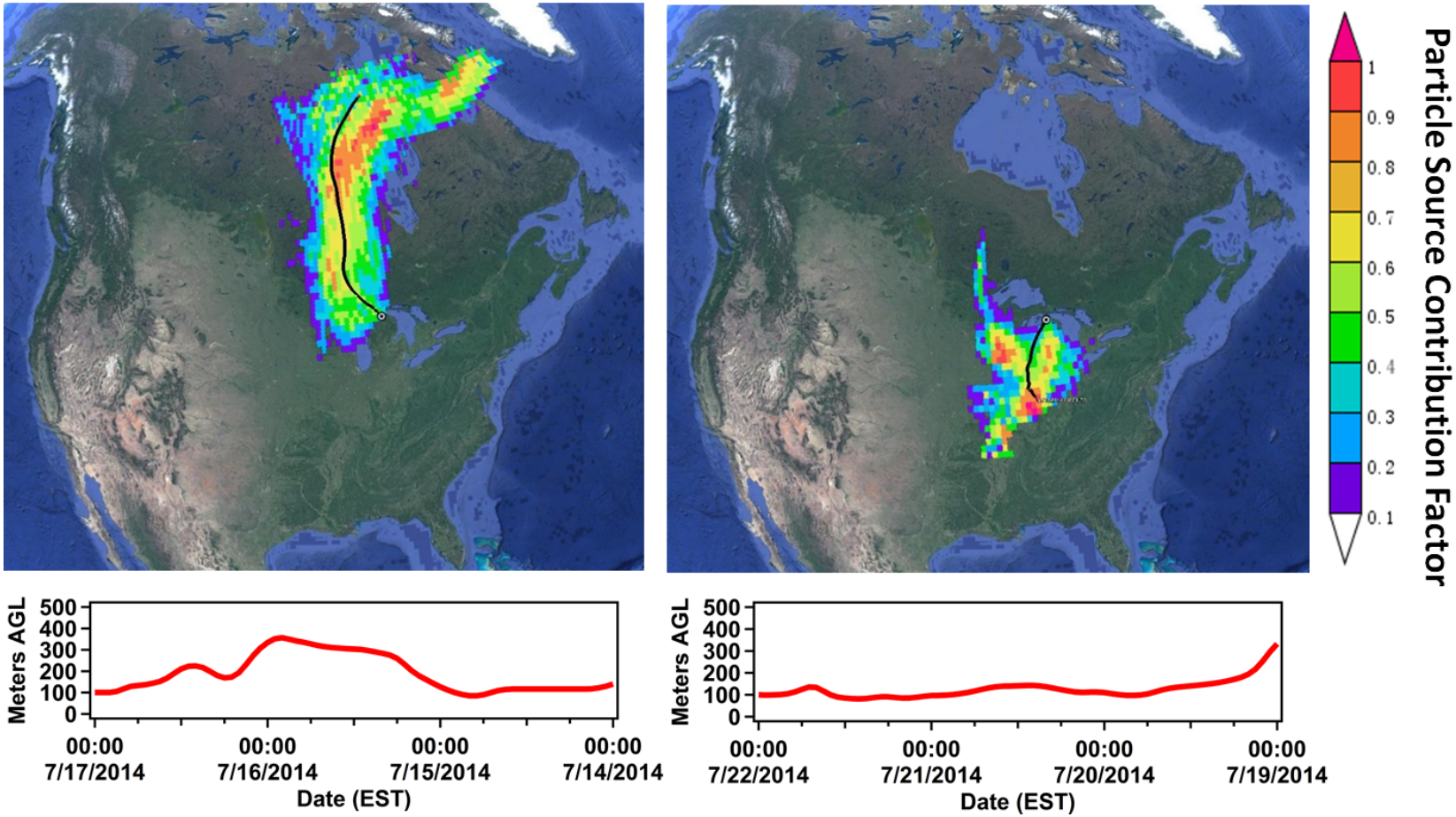

Figure 4—4. (Top) Particle source contribution factor (PSCF) maps, with representative 72 h 100 m AGL HYSPLIT backward trajectories (black lines) and (Bottom) heights (red lines), associated with (A) SSA and (B) LSA levels observed at UMBS (white circle). Imagery adapted from Landsat, NOAA, Data SIO, NOAA, U.S. Navy, NGA, GEBCO. Map data adapted from Google. Copyright 2016.

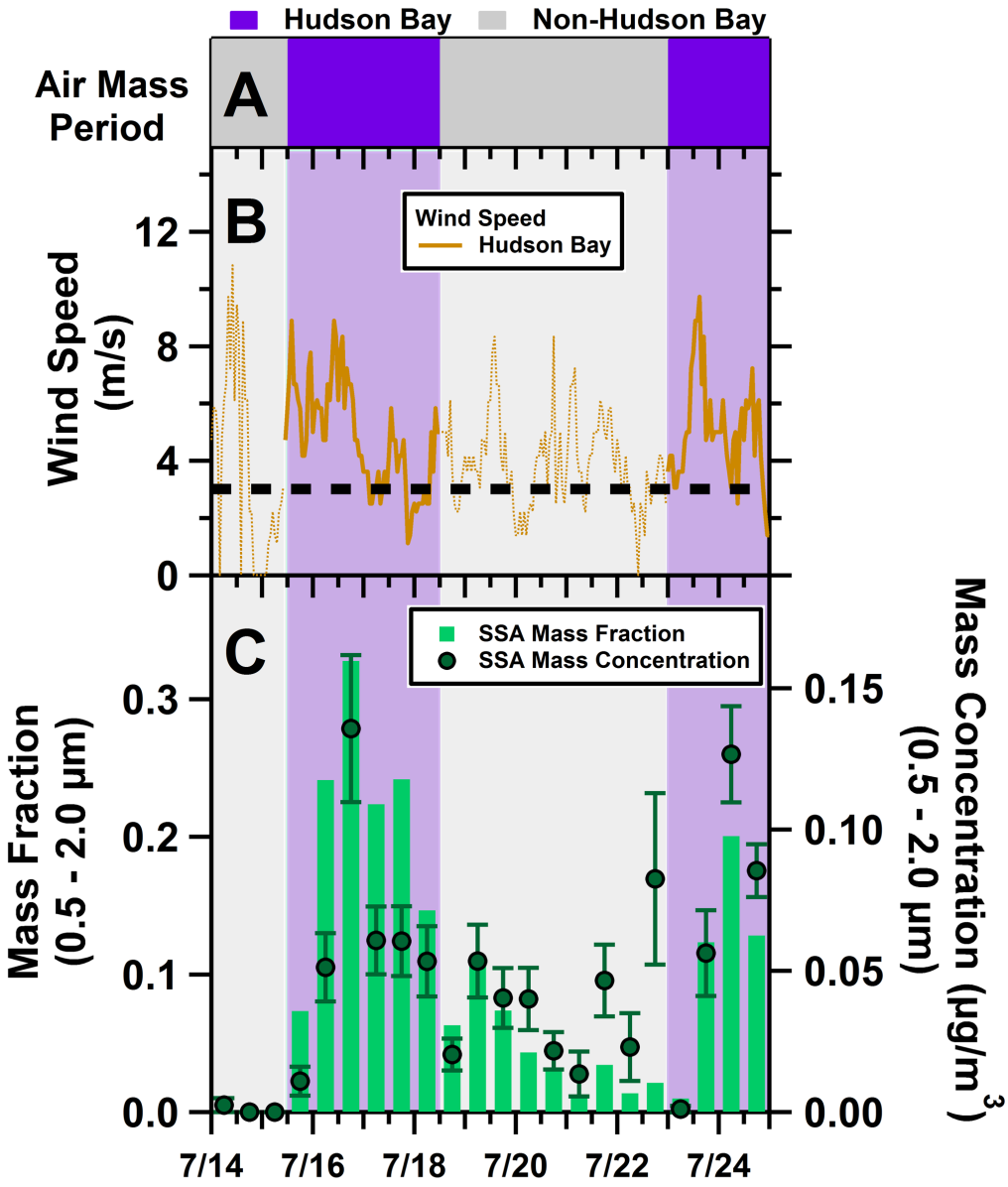

Figure 4—5. (A) Air mass period classification from HYSPLIT modeling and (B) Hudson Bay wind speed, with the minimum wind speed necessary for SSA production(Lewis and Schwartz 2004) denoted with the black dashed line, shown as a bolded line during Hudson Bay influenced air mass periods. To account for transport time to the sampling site, wind speed data were offset by -48 hours. (C) 12 h time resolution SSA mass fractions and concentrations (0.5 – 2 µm) measured by ATOFMS.

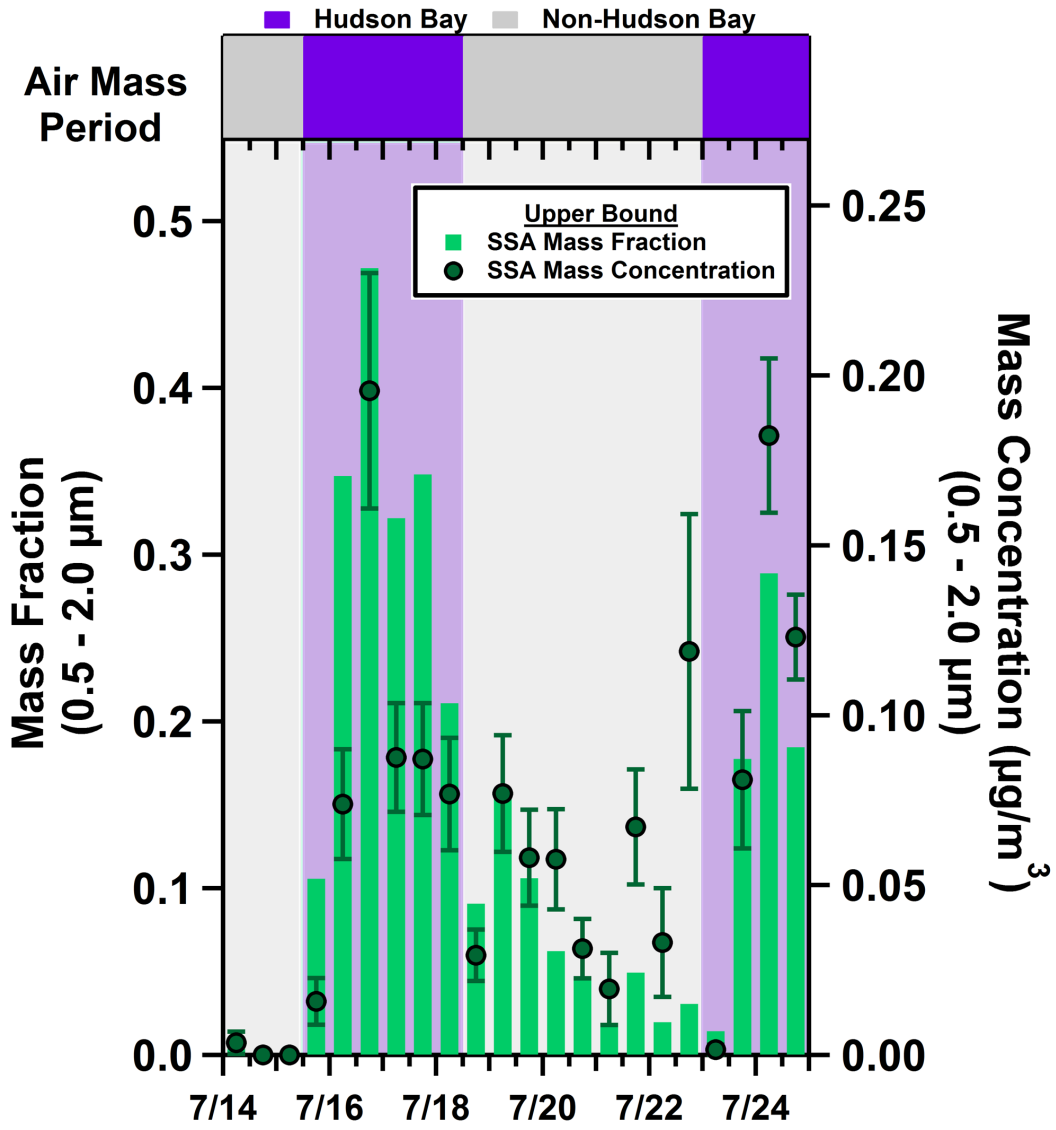

Figure 4—6. 12 h time resolution SSA upper bound mass fractions and concentrations, along with air mass period classification from HYSPLIT analysis. SSA upper bound mass fractions and concentrations (0.5 – 2 µm) were measured by ATOFMS using the material density of NaCl (2.16 g cm^{-3}).

concentrations in the upper Midwestern United States. The results presented here represent the furthest inland quantification of SSA particle mass contributions by single particle analysis (Bondy et al. 2017) and support previous bulk particle measurements that suggested long-range transport of SSA >500 km inland (Shaw 1991, Hara et al. 2004, Udisti et al. 2012, Chalbot et al. 2013).

4.3.2. Identification and Quantitation of Lake Spray Aerosol

LSA were identified by ATOFMS based on individual particle dual-polarity mass spectra consistent with previous LSA studies (Axson et al. 2016), as well as LSA generated in the laboratory from freshwater collected from both Lake Michigan and Lake Superior during this study (Figures 4—2b & 4—7). Calcium is the highest concentration cation in freshwater from the calcareous Great Lakes (Chapra et al. 2012), and both the ambient and laboratory-generated LSA were characterized by *m/z* +40 (Ca^+) as the highest intensity positive ion (Figures 4—2b & 4—7). Minor inorganic ion peaks included *m/z* +23 (Na^+), +24 (Mg^+), +39 (K^+), and +56 (CaO^+) (Figures 4—2b & 4—7). The significant presence of organic nitrogen (*m/z* -26 (CN^-)) is consistent with mass spectra of LSA generated in the laboratory in this study, and previously, from Lake Michigan freshwater (Axson et al. 2016, May et al. 2018). The laboratory-generated LSA mass spectra also showed a minor contribution from a nitrate marker at *m/z* -46 (NO_2^-). However, the average relative peak area ratio of *m/z* -46 (NO_2^-) / *m/z* -26 (CN^-) was lower in the mass spectra of individual LSA generated in the laboratory from Lake Michigan (1.0 ± 0.4) and Lake Superior (0.2 ± 0.2) freshwater (Figure 4—7), compared to the ambient LSA mass spectral ratio (11 ± 5) (Figure 4—2b). Similar to SSA, the enriched presence of nitrate markers, *m/z* -46 (NO_2^-) and -62 (NO_3^-),(Ault et al. 2014) suggests atmospheric processing of ambient LSA particles during transport, as shown in laboratory studies of calcite (Sullivan et al. 2009). This result suggests the ambient LSA had undergone multiphase reactions, with the formation of nitrate increasing its ratio relative to organic nitrogen, during transport inland. Similar to calcite dust aging (Gibson et al. 2006), LSA aging could impact particle optical properties and cloud activation efficiencies. Since soil in the region is rich in Fe (Cahill 1981), the observed LSA was differentiated from mineral dust (Axson et al. 2016) based on the lack of iron (*m/z* +54 (Fe^+) (Sullivan et al. 2007)) in the ambient mass spectra (Figure 4—2b) and EDX spectra (Figure 4—2d). In addition, the ambient LSA mass distribution identified by ATOFMS peaked near 0.7 μm d_a (Figure 4—2c), consistent with previous

measurements of laboratory generated LSA (mass distribution mode of 0.75 μm) (Axson et al. 2016) and distinct from mineral dust (mass distribution mode >1 μm) (Mahowald et al. 2014).

CCSEM-EDX analysis further confirmed the identification of LSA particles with elemental composition consistent with Lake Michigan and/or Lake Superior freshwater sources (Figure 4—2e). As observed previously on the shore of Lake Michigan by Axson et al. (2016), the LSA EDX spectra are defined by calcium with abundant carbon and oxygen (Figure 4—2d), due to the presence of carbonate in Great Lakes freshwater (Chapra et al. 2012). Ca, Mg, Na, K, C, and O were evenly distributed across the individual ambient and laboratory generated LSA particles (Figure 4—1). The average ambient LSA Mg/Na mole ratio (1.8 ± 0.5) is consistent with that of Lake Michigan (1.72) and Lake Superior (1.88) freshwater (Chapra et al. 2012). Similarly, the average ambient LSA K/Na and Ca/Na mole ratios (0.2 ± 0.2; 3 ± 3) were both consistent with the corresponding ratios in Lake Michigan (0.13; 3.31) and Lake Superior (0.21; 5.48) freshwater, respectively (Chapra et al. 2012).

The PSCF trajectory domain of ambient LSA extended to the west over the Great Lakes region of the upper Midwestern United States (Figure 4—4). While all air masses during the sampling period crossed over Lake Michigan and/or Lake Superior, wind speeds capable of producing LSA (> 3.5 m s^{-1}) (Slade et al. 2010, Axson et al. 2016) were present for 68% and 51% of this period for each lake, respectively (Figure 4—8). The highest contributions of LSA to 0.5 – 2 μm PM mass concentrations (6 ± 1%; 0.2 ± 0.1 μg m^{-3}) and number concentrations (0.5 ± 0.3 particles cm^{-3}) occurred during a period (7/22/2014 0:00 – 7/23/2014 0:00 EST) of air transport over Lake Michigan (Figures 4—9 & 4—10) when elevated wind speeds (6 ± 2 m s^{-1}) and wave heights (1.0 ± 0.5 m) capable of producing LSA (Slade et al. 2010, Axson et al. 2016) were present across Lake Michigan (Figure 4—8). Since this period was also associated with elevated mass concentrations of urban pollution aerosols from Milwaukee and Chicago (Gunsch et al. 2018), the increase in LSA mass fractions, in comparison to other periods, was not proportional to the increase in LSA mass concentrations. During the remainder of the UMBS study (92% of the sampling time), the constant presence of lake-influenced air masses and elevated wind speeds resulted in a consistent background LSA contribution to 0.5 – 2 μm PM mass concentrations (average 3 ± 1%; 0.02 ± 0.01 μg m^{-3}) (Figure 4—9) and number concentrations (0.03 ± 0.03 particles cm^{-3}).

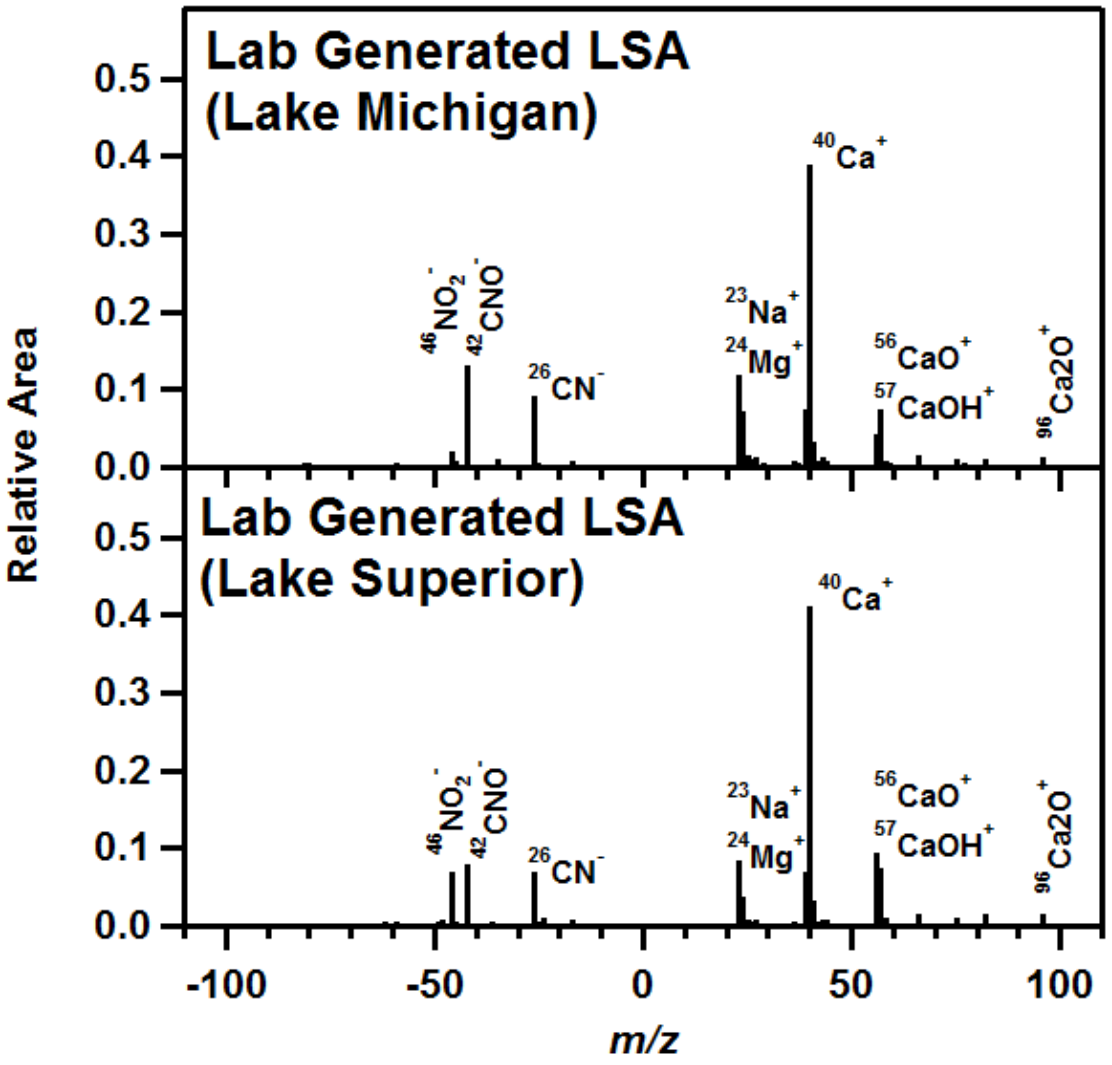

Figure 4—7. Average positive and negative ion single-aerosol mass spectra, with characteristic peaks labeled, of aerosol generated in the laboratory from (top) Lake Michigan and (bottom) Lake Superior freshwater.

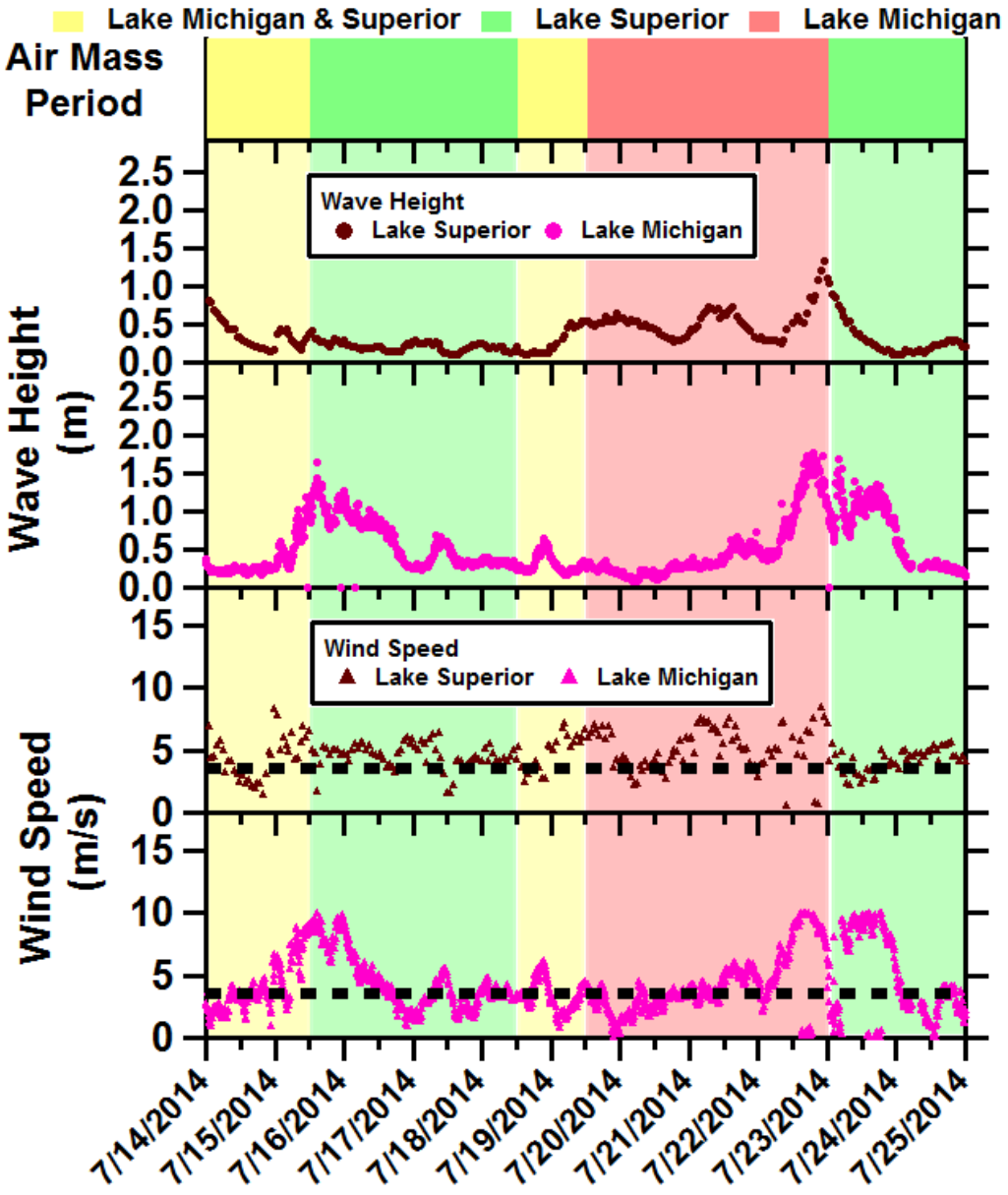

Figure 4—8. Air mass period classification from HYSPLIT analysis and Lake Superior and Lake Michigan wave heights and wind speeds, with the minimum wind speed necessary for LSA production (Slade et al. 2010) denoted with the black dashed line.

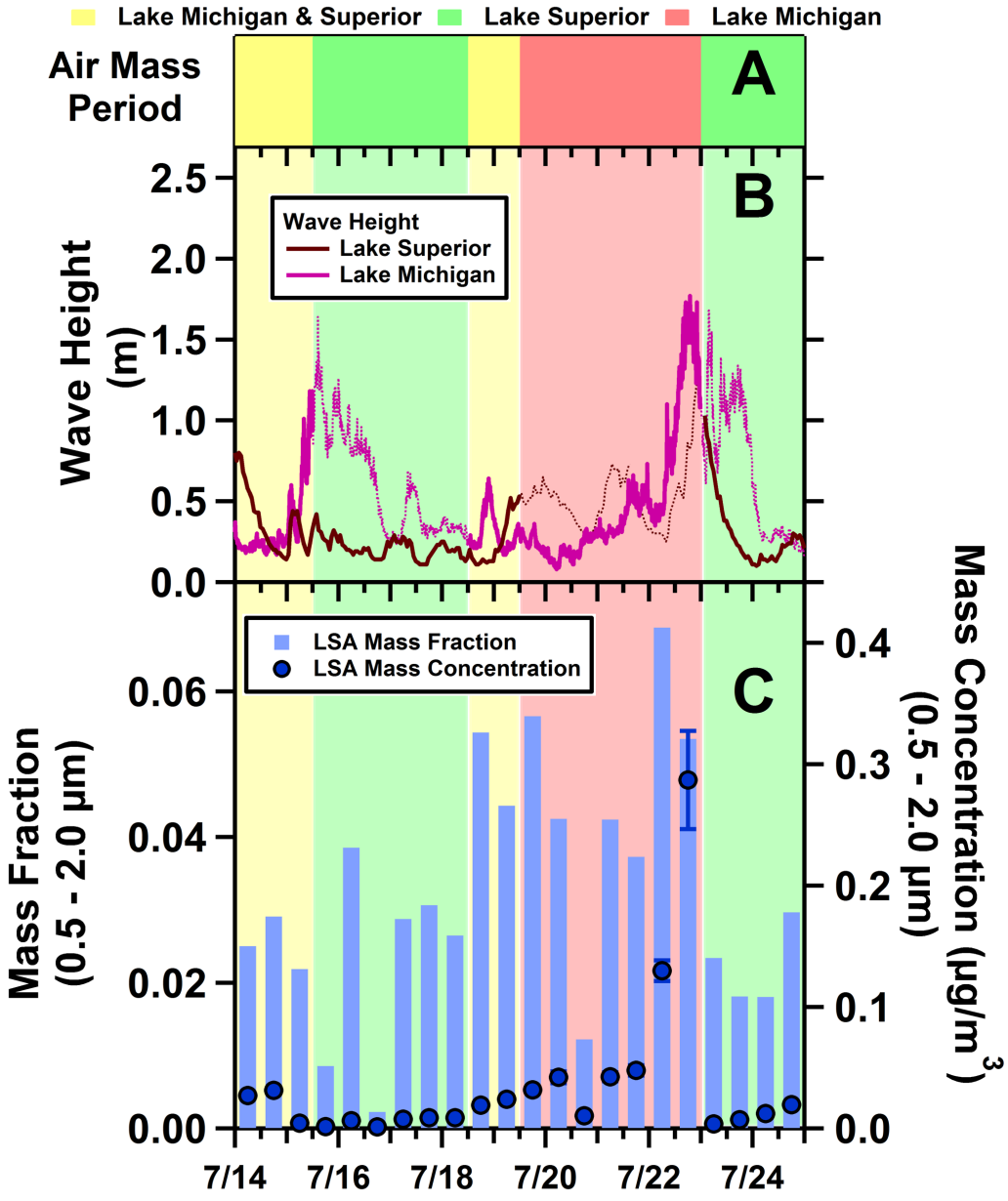

Figure 4—9. (A) Air mass period classification from HYSPLIT modeling and (B) Lake Superior and Lake Michigan wave heights, shown as bolded lines during air mass periods influenced by the respective lake(s). (C) 12 h time resolution LSA mass fractions and concentrations (0.5 – 2 µm) measured by ATOFMS.

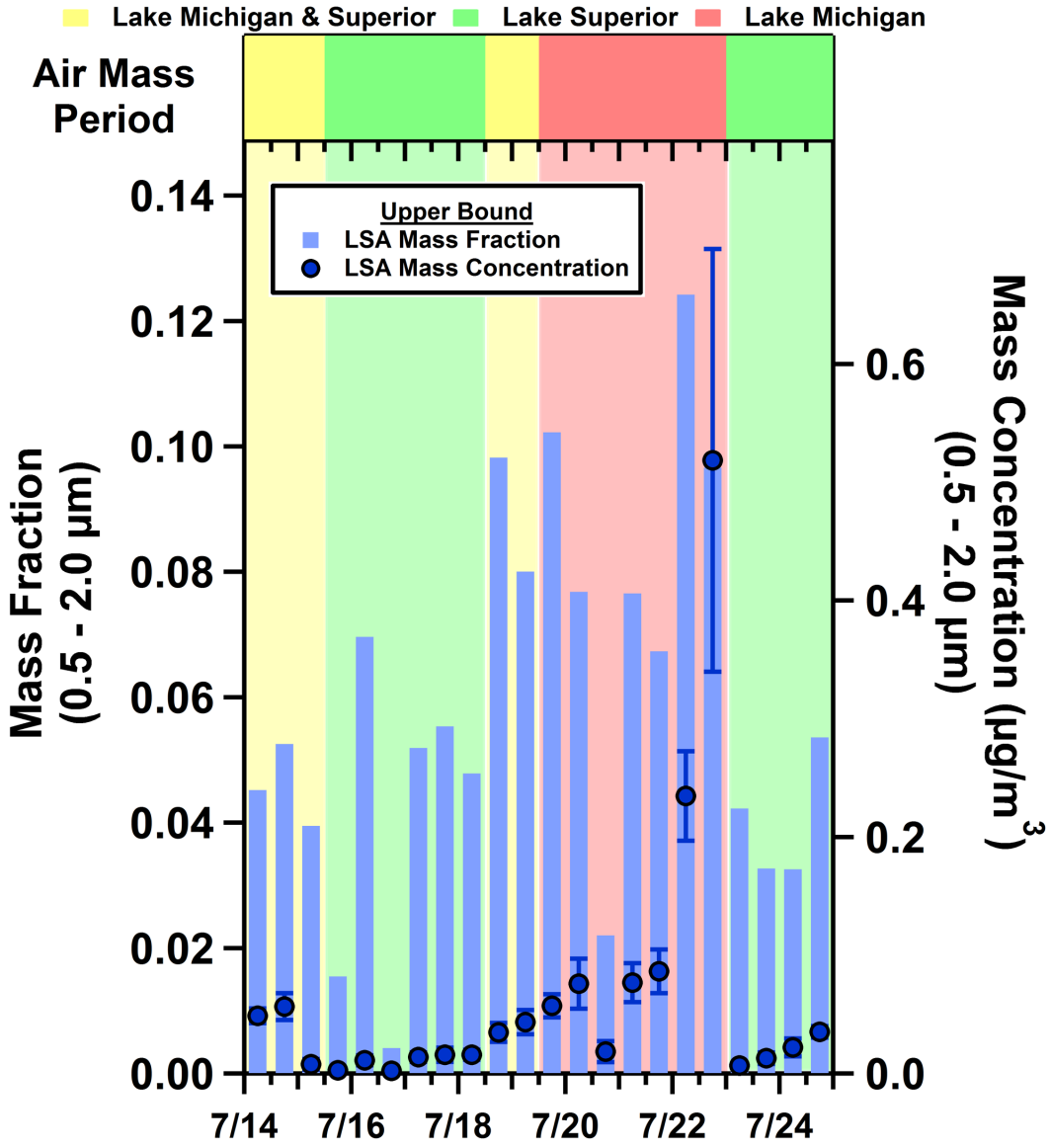

Figure 4—10. 12 h time resolution LSA upper bound mass fractions and concentrations, along with air mass period classification from HYSPLIT analysis. LSA upper bound mass fractions and concentrations (0.5 – 2 µm) were measured by ATOFMS using the material density of $CaCO_3$ (2.71 g cm^{-3}).

Inland contributions of LSA were thus determined for the first time, by single particle chemical analysis (ATOFMS and CCSEM-EDX) (Figures 4—2 & 4—9). The identification and quantification of inland LSA and SSA, and their differentiation from mineral dust, in this study further supports the previously demonstrated advantage of single particle measurements techniques to overcome complications in the use of ion ratios in bulk methods to accurately identify inland contributions of wave breaking particles (Pakkanen 1996, Bondy et al. 2017). Combined with previous identification of particles similar in composition to LSA in clouds over the Great Lakes region (Lasher-Trapp et al. 2008, Twohy and Anderson 2008) and the known participation of SSA in cloud formation (Cochran et al. 2017), the results herein motivate future study of the roles of LSA and SSA on inland environments. In particular, the impacts of inland LSA and SSA, which reached 0.5 – 2 μm PM number concentrations of 0.5 ± 0.3 particles cm^{-3} and 0.06 ± 0.02 particles cm^{-3}, respectively, on atmospheric composition and cloud formation may be important in the rural northern Great Lakes region (Chung et al. 2011) where low particle number concentrations (<1700 cm^{-3}) are present (VanReken et al. 2015). Clouds are highly sensitive to even low concentrations of ice nucleating particles (Ault et al. 2011, Creamean et al. 2013, Rosenfeld et al. 2014, Brooks and Thornton 2018), which are produced by marine wave breaking (DeMott et al. 2016) and present in high concentrations in freshwater (Moffett 2016) and aerosols produced from it (Pietsch et al. 2015, Pietsch et al. 2017). Future studies are also needed to measure the potential health implications of inland LSA modified by harmful algal blooms (HABs) (May et al. 2018). This will improve understanding of the impacts that freshwater wave breaking particles have in the upper Midwestern United States (Chung et al. 2011) and other regions with large freshwater lakes, such as eastern Africa (African Great Lakes), Canada (Lake Winnipeg, Great Bear Lake, Great Slave Lake), and Russia (Lake Baikal, Lake Ladoga, Lake Onega).

4.4. Acknowledgements

Dr. Matthew J. Gunsch, Nicole E. Olson, Dr. Amy L. Bondy, Rachel M. Kirpes, and Prof. Andrew P. Ault are thanked for their contributions in the collection and analysis of aerosol data. Prof. Philip K. Hopke and Prof. Steven B. Bertman are thanked for assistance in field measurements conducted at UMBS. Funding was provided by the University of Michigan MCubed program, the University of Michigan Rackham Graduate School, and the University of Michigan

Water Center. N.W. May and M.J. Gunsch were partially supported by UMBS graduate fellowships. Dr. Swarup China and Prof. Alexander Laskin are thanked for their assistance in CCSEM-EDX analyses performed at the Environmental Molecular Sciences Laboratory (EMSL), a national scientific user facility located at the Pacific Northwest National Laboratory (PNNL) and sponsored by the Office of Biological and Environmental Research of the U.S Department of Energy (DOE). PNNL is operated for DOE by Battelle Memorial Institute under Contract No. DE-AC06-76RL0 1830. The authors gratefully acknowledge the NOAA Air Resources Laboratory (ARL) for the provision of the HYSPLIT transport and dispersion model and READY website (http://www.ready.noaa.gov). Daniel Gardner and Stephanie Schmidt (University of Michigan) are thanked for assistance in atmospheric particle sampling.

Chapter 5 Multi-Year Study of the Dependence of Sea Salt Aerosol on Wind Speed and Sea Ice Conditions in the Coastal Arctic

Reprinted (adapted) with permission from:
Journal of Geophysical Research: Atmospheres, 121, 9208–9219, 2016.
DOI:10.1002/2016JD025273.

5.1. Introduction

Rapid sea ice loss is dramatically changing the Arctic surface (Serreze and Stroeve 2015). Mean September coverage of Arctic sea ice decreased by -13.3% dec^{-1} for the period of 1979-2014 (Serreze and Stroeve 2015), and complete summertime loss of sea ice is expected within 50 years (Overland and Wang 2013). In the winter-spring, the Arctic is becoming increasingly dominated by first-year sea ice cover (Maslanik et al. 2011). Thinner first-year sea ice is less structurally stable and more prone to fracturing, likely resulting in the formation of leads (transient areas of open water surrounded by sea ice), as well as more pancake ice (Stroeve et al. 2012). Increasing sea salt aerosol production is expected from the newly exposed ocean surface (Struthers et al. 2011, Browse et al. 2014). Sea ice loss is also expected to increase the emissions of marine primary organic aerosol and dimethyl sulfide, as well as lead to changes in aerosol processing and removal in the Arctic boundary layer through changing meteorology (Browse et al. 2014).

Atmospheric aerosols represent the largest source of uncertainty in global radiative forcing predictions (Boucher et al. 2013). An increase in sea salt aerosol emissions will increase Arctic aerosol optical depth, increasing the magnitude of aerosol direct radiative forcing (cooling) (Struthers et al. 2011). Sea salt aerosols can also indirectly alter radiative forcing by acting as cloud condensation nuclei (CCN) (Wise et al. 2009). Simulations by Browse et al. (2014) suggested that the CCN response to increased sea salt aerosol from the Arctic Ocean is weak due to efficient scavenging of particles and decreased new particle formation from a greater condensation sink. However, the predicted CCN response was spatially non-uniform, with coastal Arctic regions predicted to have a larger CCN response than the central Arctic Ocean (Browse et al. 2014). Further, deposition of sea salt aerosol to the snow surface contributes to springtime atmospheric

reactive bromine chemistry and ozone depletion (Pratt et al. 2013). However, due to limited Arctic aerosol measurements, the contributions and radiative impacts of sea salt aerosol under changing sea ice conditions are uncertain.

Under open ocean conditions, sea salt aerosol mass concentrations typically increase with increasing wind speed (Lewis and Schwartz 2004) and decreasing water temperature (Salter et al. 2015). Airborne sea salt aerosol particles are formed by two distinct processes when bubbles on the seawater surface burst (Blanchard and Woodcock 1957). The fragmentation of the top of the bubble membrane produces film drops. After the bubble membrane top bursts, droplets of water are flung upward from the bubble bottom, producing jet drops. Particles result from film and jet drops after evaporation, with film drops mainly resulting in submicron particles and jet drops generally resulting in supermicron particles (O'Dowd et al. 1997). Over the open ocean, the bubble-bursting production of sea salt aerosol is driven by wind-induced wave breaking that entrains air underneath the ocean surface. However, there is still uncertainty regarding the mechanism of aerosol production from leads. Nilsson et al. (2001) and Leck et al. (2002) measured wind-dependent number fluxes of particles, likely produced through the bubble-bursting mechanism, from open leads at a rate ~10 times less than the open ocean, which was attributed to the decreased fetch over the open leads. However, Nilsson et al. (2001) found that an additional particle emission mechanism was needed to explain the particle number fluxes at low wind speeds. Studies conducted under lower wind speed conditions have proposed emission mechanisms, including the transport of bubbles to the surface by increased turbulence caused by supercooling conditions (Grammatika and Zimmerman 2001), gas released from melting ice (Leck and Bigg 1999, Nilsson et al. 2001), phytoplankton respiration (Johnson and Wangersky 1987), and a surface heat flux driven mechanism (Norris et al. 2011).

Sea salt aerosol is a significant contributor to Arctic particle mass (Quinn et al. 2002). Given the impacts of sea salt aerosol on climate and the changing sea ice surface, it is imperative to evaluate the contribution of sea salt aerosol produced from leads. Previous Arctic spring (Scott and Levin 1972, Radke et al. 1976) and summer (Leck and Persson 1996, Leck and Bigg 1999, Nilsson et al. 2001, Leck et al. 2002, Held et al. 2011, Held et al. 2011, Leck and Svensson 2015) short-term intensive studies measured the direct flux of particles from leads over the pack ice. However, significant uncertainty remains regarding the extent leads currently influence Arctic particle mass concentrations over multiple seasons and at coastal locations. Therefore, to build on

previous work on the production of aerosols from leads and to probe the wind dependence of sea salt aerosol production from Arctic leads across multiple seasons and years, we present an examination of sea salt concentrations near Barrow, Alaska under varying local sea ice and wind speed conditions from April 2006 to December 2009.

5.2. Methods

5.2.1. Meteorology

Wind speed and wind direction were monitored with 1 min resolution at the NOAA Barrow Observatory (71° 32′ 30″ N, 156° 61′ 14″ W) at 10 m above ground. The meteorological data used in this study can be found on the NOAA Barrow, Alaska Observatory website (http://www.esrl.noaa.gov/gmd/obop/brw/). Given that wind speeds ≥ 4 m s^{-1} over open ocean are typically associated with the formation of bubbles responsible for sea salt aerosol production (Monahan and O'Muircheartaigh 1986), wind speed data were divided into three average wind speed categories: 1) "low" < 4 m s^{-1} , 2) "moderate" 4-7 m s^{-1} , and 3) "high" >7 m s^{-1}. As there are no direct measurements of wind speed over the adjacent Arctic Ocean available, it is assumed that local measured wind speed is representative of the wind speed over the nearby sea ice and open water. The local wind speeds observed in this study are consistent with previous observations of Arctic wind speeds over sea ice (Tjernström et al. 2012), with low or moderate wind speeds present for 22% and 62% of supermicron, respectively, and 29% and 48%, respectively, of submicron particle sampling periods.

5.2.2. Sea Ice Radar

The coverage of local near-shore sea ice at Barrow, AK was determined by examination of radar backscatter maps (http://seaice.alaska.edu/gi/data/barrow_radar) produced from a Furuno 10 kW, X-band marine radar, which provides high spatial resolution sea ice imaging during dark periods (Figure 5—1). The radar operated atop a building in downtown Barrow (71° 17′ 33″ N, 156° 47′ 17″ W) 22.5 m above sea level, with a range of up to 11 km to the northwest (Druckenmiller et al. 2009, Eicken et al. 2011). While the radar only covered sea ice conditions to the northwest in this analysis, any lead activity observed within the 11 km range analyzed

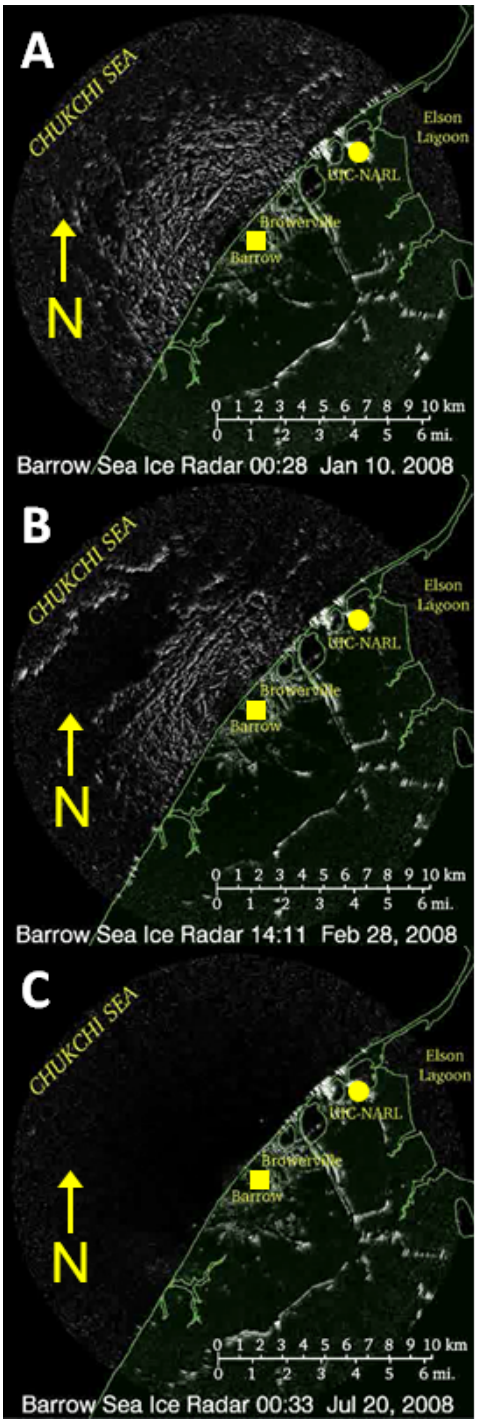

Figure 5—1. Representative radar backscatter maps of local near-shore sea ice at Barrow, AK. The yellow arrow indicates direction of north, the aerosol sampling location is marked by a yellow circle, and the radar backscatter location is marked with a yellow square. Land is colored green, white is indicative of sea ice, and black is shown for open water. Sea ice conditions include: (A) full sea ice coverage, indicated by the full coverage of the white signal indicative of sea ice, (B) leads present, identified from the area of dark signal in the upper left indicative of open ocean present in the middle of the white signal indicative of sea ice, and (C) open ocean, identified from the full coverage of the dark signal indicative of open ocean.

in this study was assumed to reflect lead activity along the coast to the southwest and northeast, as observed frequently by Mahoney et al. (2014). Radar backscatter maps were manually analyzed to divide the observed local sea surface into three categories: 1) full sea ice cover present, when local sea ice cover was complete and no areas of exposed ocean surface were present, 2) leads present, when local sea ice cover with areas of exposed ocean surface was present, 3) open ocean, when no major local sea ice cover was observed on the radar map (Figure 5—1).

5.2.3. Aerosol Chemical Composition

Atmospheric particles were sampled at the NOAA Barrow Observatory 10 m above the surface from April 2006 to December 2009. Real-time wind direction was used to sample only from the clean air sector (0˚-129˚) to avoid influence from local pollution (Quinn et al. 2002). The Beaufort and Chukchi Seas are 2-25 km upwind of the aerosol sampling site in the clean air sector, so all air sampled is assumed to be of direct marine origin. A Berner type multijet cascade impactor operating at a sample flow rate of 30 L min^{-1} with 50% cut points at aerodynamic diameters (D_{50}) of 10 μm and 1 μm was used to collect particles with aerodynamic diameters < 1 μm (referred to as submicron particles) and 1-10 μm (referred to as supermicron particles). Particles with diameters < 1 μm passed through an impactor to a rotating filter carousel housing 8 Millipore Fluoropore filters (1.0 mm pore size). For every revolution of the rotating submicron filter carousel, 7 filters were sampled individually, with sampling time varying depending on season and particle loadings, and one filter, exposed to ambient air for 10 s, served as a blank. Particles with aerodynamic diameters between 1 and 10 μm were collected on Tedlar films over the course of one revolution of the rotating submicron filter carousel, with one additional film collected as a blank for every supermicron sample collected. To minimize bounce of large particles onto downstream submicron filters, a 12 mm grease cup coated with silicone grease and a film coated with silicone spray were placed on the 10 μm jet (Quinn et al. 2002). Sample air was heated to maintain a stable reference relative humidity (RH) of 40% despite changes in ambient RH. The stable sampling RH allows for a constant instrumental size segregation, and all measurements are reported at the reference RH (Quinn et al. 2002). Submicron and supermicron particle sampling periods ranged from 1-11 days and 5-35 days, respectively. After collection, sealed filters and films were shipped to the National Oceanic and Atmospheric Administration (NOAA) Pacific Marine Environmental Laboratory for analysis.

For inorganic ion analysis, filters and films were first wetted with 1 mL of spectral grade methanol. 5 mL of distilled deionized water was then added to the solution, and the samples were extracted by sonicating for 30 min. Concentrations of major cations (Na^+, NH_4^+, K^+, Mg^{2+}, Ca^{2+}) and anions ($CH_3SO_3^-$, Cl^-, Br^-, NO_3^-, SO_4^{2-}, $C_2O_4^{2-}$) extracted from each submicron and supermicron particle sample were measured by ion chromatography (Quinn et al. 1998). Details of the inlet, sampling procedures, and chemical analyses can be found in *Delene and Ogren (2002)* and *Quinn et al. (2002)*. Based on the aerosol sampling flow rate (30 L min^{-1}) and typical sampling time, the detection limits calculated as two times the standard deviation of the blank for the major sea salt ions of interest, Na^+ and Cl^-, were both 0.0002 μg m^{-3}. For periods that were below the detection limit, a value of half the detection limit (0.0001 μg m^{-3}) was substituted for calculations. Periods below the detection limit constituted 0% of supermicron and 12% submicron sampling periods for Na^+ and 3% of supermicron and 20% submicron sampling periods for Cl^-. Na^+ mass concentration is a conservative tracer for sea salt mass (Legrand et al. 2016) and will be discussed henceforth in the place of sea salt mass to avoid biases from varying chloride depletion. While sea spray aerosol is a complex mixture of inorganic salts and organic compounds, the distribution of which alters the chemical and physical properties of the particle, sea spray aerosol is primarily (>60%) composed of inorganic salt (Quinn et al. 2015). All Na^+ is assumed to be derived from seawater (Quinn et al. 2002), as Sirois and Barrie (1999) showed that the majority of Na^+ in the Arctic is associated with sea salt aerosol. Error was calculated as the standard error of the mean and is not shown for periods when only one sampling period fell into the given sea surface and wind speed category.

5.3. Results & Discussion

5.3.1. Sea Salt Mass Concentrations

A clear dependence of supermicron (1-10 μm) Na^+ (sea salt) mass concentrations on the combination of local sea ice coverage and wind speed was observed (Figure 5—2a). There was little difference in the supermicron Na^+ mass concentrations observed for periods with no leads present and low (< 4 m s^{-1}) (0.04 ± 0.01 μg m^{-3}) or moderate (4-7 m s^{-1}) (0.03 μg m^{-3}) wind speeds compared to periods with leads and low wind speeds (0.026 ± 0.009 μg m^{-3}). However, for periods characterized by moderate wind speeds, supermicron Na^+ mass concentrations were higher when leads were present (0.11 ± 0.03 μg m^{-3}) compared to when full sea ice cover was

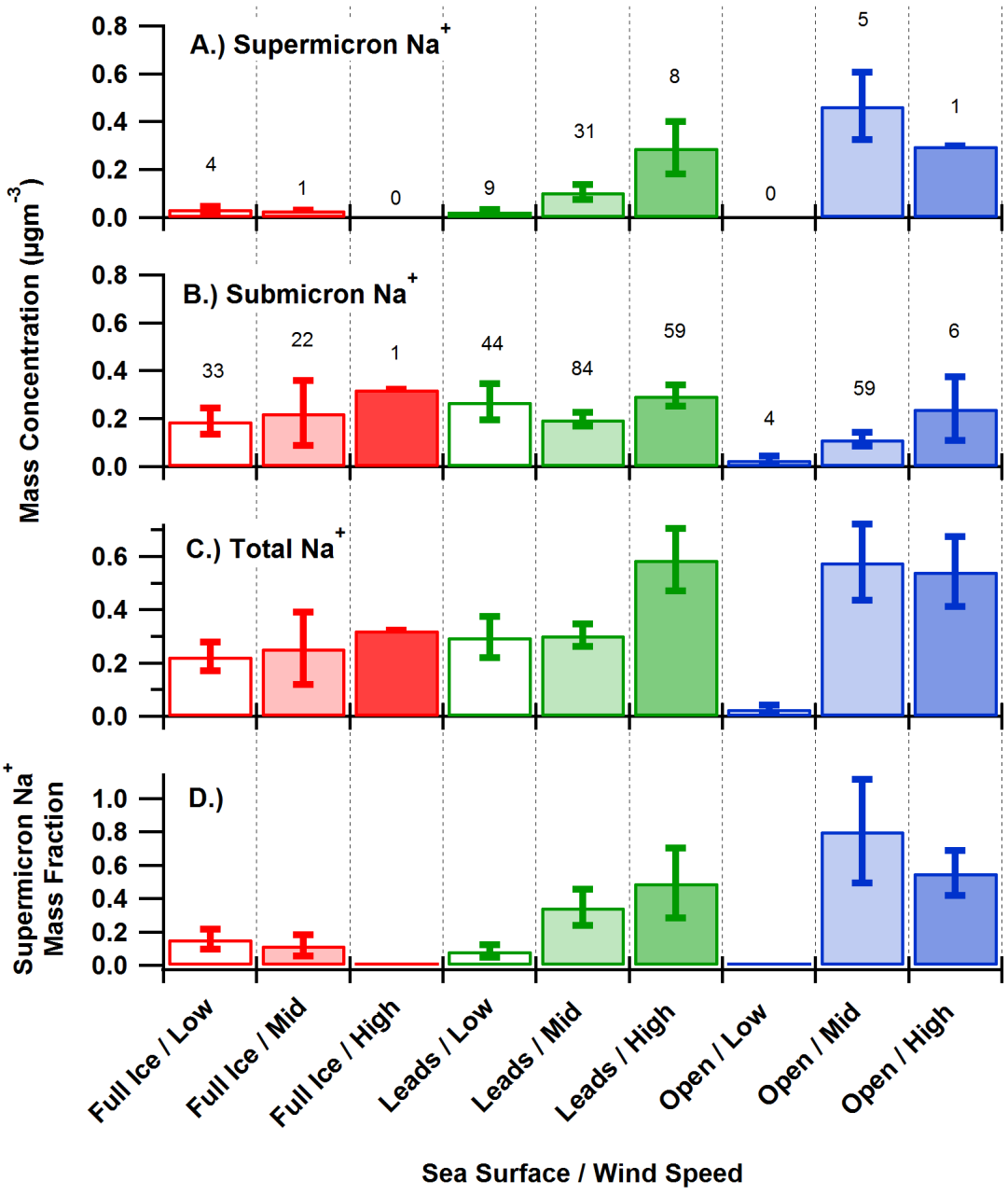

Figure 5—2. Average mass concentrations of Na+ for the supermicron (1-10 µm) (A), submicron particle (<1 µm) (B) size ranges, and (C) total respectively, and (d) the fraction of the total Na+ mass that was observed in the supermicron size range, separated into 9 bins based on local sea ice extent and wind speed. Sea ice extent categories include: full ice, leads present, and open water. Wind speed categories include: low (<4 m s-1), mid (4-7 m s-1), and high (>7 m s-1). All error bars were calculated as the standard error of the mean, and the numbers above each category indicate the number of samples in that category.

present (0.03 μg m^{-3}). Unfortunately, no supermicron sampling periods of full sea ice coverage with high wind speeds (>7 m s^{-1}) were present for comparison to periods of leads present with high wind speeds.

When leads were present, supermicron Na^+ mass concentrations were 4 and 10 times greater for periods with moderate (0.11 ± 0.03 μg m^{-3}) and high (0.3 ± 0.1 μg m^{-3}) wind speeds, respectively, in comparison to low wind speeds (0.03 ± 0.01 μg m^{-3}) (Figure 5—2a). This is consistent with wind-driven sea salt aerosol number fluxes from leads observed directly by Nilsson et al. (2001) and Leck et al. (2002). Local leads, when observed by the sea ice radar, are the most likely source for the wind dependent supermicron Na^+ mass observed in this study, as the lifetime of supermicron aerosols in the boundary layer is typically < 12 hours (Williams et al. 2002). The short lifetime of these supermicron particles limits the distance from which the majority of these particles could have originated, for the wind speeds observed, to a scale of a few hundred kilometers, which would fall within the area of Arctic sea
ice coverage in the winter-spring and for which the sea ice radar is representative of ice fracturing conditions (Mahoney et al. 2014).

The highest supermicron Na^+ mass concentrations are expected for open ocean and high wind speeds, as sea salt aerosol production generally increases with increasing wind speed and fetch (Lewis and Schwartz 2004). While no supermicron particle sampling periods occurred for open ocean and low wind speeds, periods of open ocean with moderate wind speeds showed supermicron Na^+ mass concentrations (0.5 ± 0.1 μg m^{-3}) 5 times greater than for periods when leads were present with moderate winds. Previously, sea salt aerosol number fluxes over leads were measured to be 10 times smaller than those over the open ocean at similar wind speeds, an observation which was attributed to the smaller fetch and area of exposed water (Nilsson et al. 2001, Leck et al. 2002). Therefore, these long-term measurements show that, while a smaller source than open water, leads are a significant wind-dependent source of supermicron sea salt particle mass in the Arctic. The supermicron Na^+ mass concentration for the one period of open ocean with high wind speeds (0.3 μg m^{-3}) was slightly lower than for periods of open ocean with moderate winds (0.5 ± 0.1 μg m^{-3}), contrary to that expected based on the dependence of sea salt aerosol mass over open ocean on wind speed (Lewis and Schwartz 2004). Only one open ocean aerosol sampling period was characterized by sustained high winds, imparting uncertainty in the trend that can be attributed to the small sample size and natural variability in meteorological

conditions that would impact sea salt aerosol concentrations through deposition and marine boundary layer mixing (Lewis and Schwartz 2004). However, it is important to note that despite these confounding factors there are statistically significant trends overall in the dependence of supermicron sea salt concentrations on local sea ice extent and local wind speed.

There was no overall dependence of submicron (<1 μm) Na^+ mass concentrations on local sea ice coverage and wind speed (Figure 5—2b). Unlike supermicron Na^+ mass concentrations, submicron Na^+ mass concentrations did not increase substantially when leads were present. The average submicron Na^+ mass concentration when leads were present was 0.25 ± 0.03 μg m^{-3}, compared to 0.21 ± 0.06 μg m^{-3} when leads were not present. In further contrast to supermicron Na^+ mass concentrations, a wind speed dependence in submicron Na^+ mass concentration was not observed when leads were present (Figure 5—2b). In fact, open ocean periods with low or moderate wind speeds resulted in the lowest observed submicron Na^+ mass concentrations (0.03 ± 0.02 μg m^{-3} and 0.11 ± 0.03 μg m^{-3}, respectively). The lack of correlation of submicron Na^+ mass concentrations with local sea ice coverage and wind speed is most likely due to due to the longer atmospheric residence time of submicron sea salt particles, compared to supermicron sea salt particles (Gong et al. 2002, Williams et al. 2002). The shorter residence time of supermicron sea salt aerosol decreases the influence of long range transport, which significantly influenced the observed submicron sea salt aerosol, as discussed in section 3.2. The long range transport of submicron sea salt aerosol produced from high latitude open ocean sources to the Arctic could therefore have a significant influence on submicron Na^+ mass concentrations, as previously concluded (Sturges and Barrie 1988, Barrie and Barrie 1990, Barrie et al. 1994, Sirois and Barrie 1999, Quinn et al. 2002).

During periods of full sea ice cover and open ocean, submicron Na^+ mass concentrations exhibited a correlation with wind speed. For full sea ice periods, submicron Na^+ mass concentrations increased from low (0.19 ± 0.05 μg m^{-3}) and moderate (0.2 ± 0.1 μg m^{-3}) to high wind speed (0.3 μg m^{-3}), although the increase from moderate to high wind speed was not statistically significant, in part due to the availability of only one sampling period at high wind speed for comparison (Figure 5—2b). Under full ice conditions, a non-wave breaking source of Na^+, as discussed in section 3.4, could potentially contribute, in addition to long-range transport, as discussed in section 3.2. For open ocean periods, submicron Na^+ showed a greater dependence on local meteorology. Submicron Na^+ mass concentrations increased from low (0.03 ± 0.01 μg m^{-}

^{3}) to moderate (0.11 ± 0.03 μg m^{-3}) and high (0.2 ± 0.1 μg m^{-3}) wind speeds. However, the increase from moderate to high wind speeds was not statistically significant. The higher sea salt concentrations under these open ocean conditions, along with the decrease in the fraction of aged submicron sea salt periods discussed in Section 3.2, suggests the influence of submicron sea salt production from local wind-driven wave breaking processes.

Overall, the supermicron fraction of the total Na^+ mass concentration increased with decreasing sea ice coverage and, in the presence of leads, increasing wind speed (Figure 5—2c and 2—2d). Supermicron Na^+ mass concentrations comprised less than 20% of the total Na^+ mass concentrations for periods with full sea ice cover and with leads and low winds. In the presence of leads, the supermicron Na^+ mass fraction increased with increasing wind speed. At moderate wind speeds the supermicron Na^+ mass concentration comprised 40% of the total Na^+ mass concentration for periods with leads, ~4 times greater than periods with leads and low wind speeds. Then, for periods with leads and high wind speeds, the supermicron Na^+ mass fraction increased to 50% of the total Na^+ mass concentration. Finally, the supermicron Na^+ mass fraction was the most dominant for periods with open ocean, comprising 60-80% of the total Na^+ mass concentration. The dependence of supermicron Na^+ mass fraction on local sea ice coverage and wind speed highlights that the supermicron sea salt aerosol population is more directly influenced by local sea ice coverage and wind speed than the submicron sea salt aerosol population, as expected due to the longer atmospheric residence time of submicron sea salt particles (Gong et al. 2002, Williams et al. 2002).

5.3.2. Contributions of Aged Sea Salt Aerosol

Cl^-/Na^+ molar ratios were calculated to investigate sea salt aerosol lifetime and chemical processing, a measure of the influence of long-range transport. Sea salt aerosol retains the Cl^-/Na^+ molar ratio of seawater (1.16) when introduced into the atmosphere (Keene et al. 1986). This ratio is altered in the atmosphere through the displacement of chlorine through reaction with acidic gases, such as H_2SO_4, or aqueous oxidation of $SO_{2(g)}$ (Keene et al. 1998). The extent of aging is thus dependent on atmospheric residence time, as well as the original particle mass and acidic precursor concentrations in the atmosphere (Leck et al. 2002). Previous work has shown that fine sea salt aerosol (aerodynamic diameter < 2.5 μm) are more likely to have greater chloride depletion than those of larger diameter coarse (aerodynamic diameter > 2.5 μm) sea salt aerosol (Barrie et al. 1994, Hara et al. 2002, Leck et al. 2002). In addition, previous work has shown sea salt aerosols

exhibit greater depletion following polar sunrise when production of sulfuric acid from the oxidation of $SO_{2(g)}$ occurs in the Arctic troposphere (Sirois and Barrie 1999). Using Cl^-/Na^+ molar ratios (Figure 5—3), fractions of sampling periods dominated by "aged" sea salt were calculated for each sea ice and wind speed category (Figure 5—4). "Aged" sea salt was defined as having a Cl^- enrichment factor < 0.75. Cl^- enrichment factor is determined by dividing the Cl^-/Na^+ ratio of the aerosol sample by the Cl^-/Na^+ ratio of bulk seawater (Newberg et al. 2005). Therefore an enrichment factor < 0.75 corresponds to the depletion of 25% or more of Cl^- from sea salt aerosol and represents particles that have undergone significant atmospheric processing. Sampling periods with a Cl^-/Na^+ enrichment factor > 0.75 were considered to consist primarily of "fresh" sea salt produced from local sources.

The average fraction of aged submicron sea salt periods (0.74 ± 0.07) across all local sea ice coverage and wind speed categories was higher than the fraction of aged supermicron sea salt periods (0.39 ± 0.06) (Figure 5—4). The median Cl^-/Na^+ molar ratios for submicron and supermicron sea salt aerosol sampling periods also exhibited a dependence on local sea ice coverage and wind speed (Figure 5—5). Overall, the median Cl^-/Na^+ molar ratio of submicron sea salt periods (0.62) was lower than the median Cl^-/Na^+ molar ratio for supermicron sampling periods (0.86) (Figure 5—5). This indicates that the atmospheric processing undergone by the submicron sea salt resulted in a greater Cl^- depletion than the supermicron sea salt, as expected since smaller particles have a longer residence time (Williams et al. 2002) and a higher surface area to volume ratio (McInnes et al. 1994).

The highest fractions (0.7-0.8) of aged sea salt sampling periods were observed when full sea ice cover with low and moderate wind speeds were present, consistent with the lack of a local sea salt source (Figure 5—6). The fractions of aged submicron and supermicron sea salt periods when leads or open ocean were present with low wind speed were similarly high (0.6-0.8). That some of the highest fractions of aged sea salt were observed under low wind conditions across all sea ice coverage categories indicates that the sea salt observed during low wind periods, regardless of sea ice coverage, experienced increased atmospheric processing, likely due to long range transport.

For periods with leads present, the fraction of aged submicron and supermicron sea salt periods, respectively, decreased from low (0.77 ± 0.06; 0.7 ± 0.2) to moderate (0.74 ± 0.05; 0.39

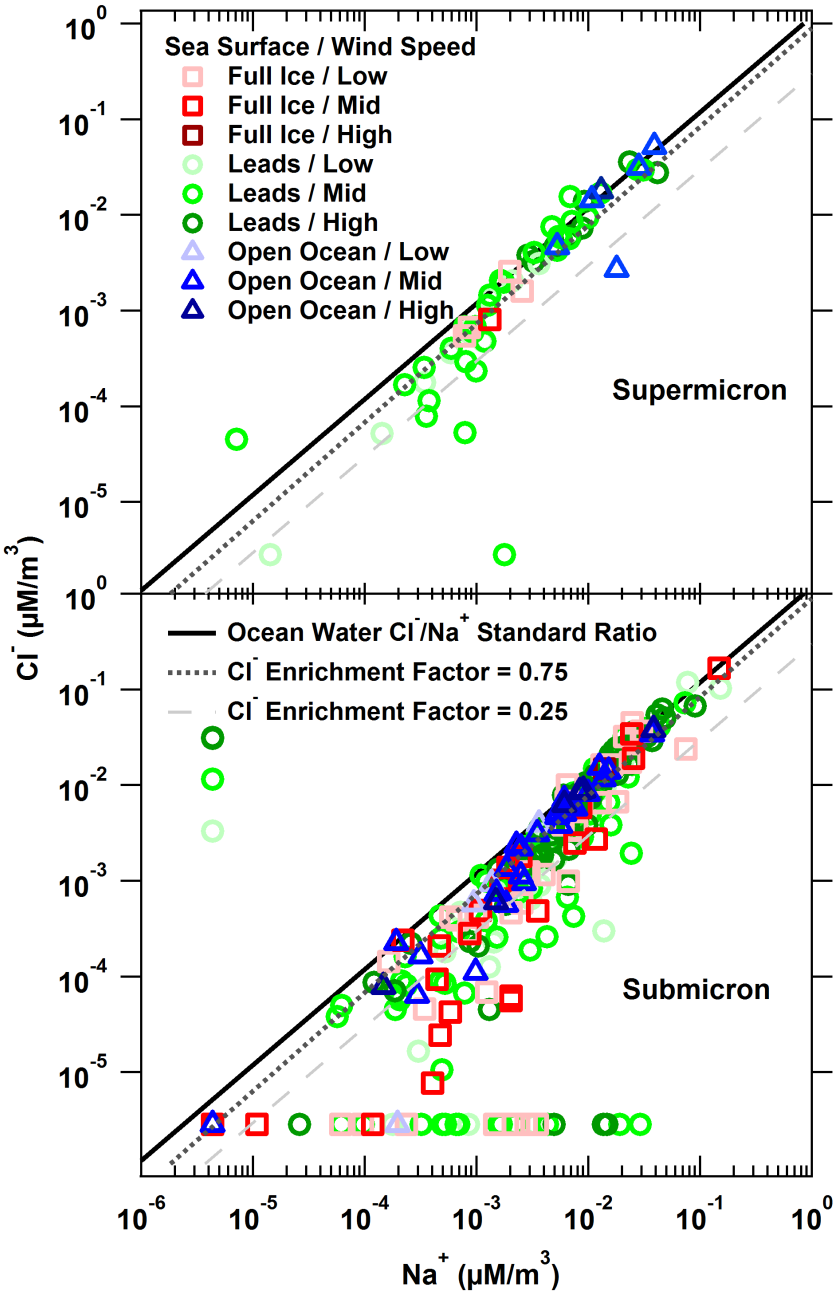

Figure 5—3. Cl- concentration vs. Na+ concentration for supermicron (top) and submicron (bottom) particle samples divided into categories based on sea ice conditions and wind speed. The Cl-/Na+ ratio of ocean water is shown in the solid black line, with points falling below the line representing periods where atmospheric Cl- depletion has occurred (Keene et al. 1986). The extent of Cl- depletion is denoted by the dotted dark grey line representing 25% depletion and the dashed light grey line representing 75% depletion.

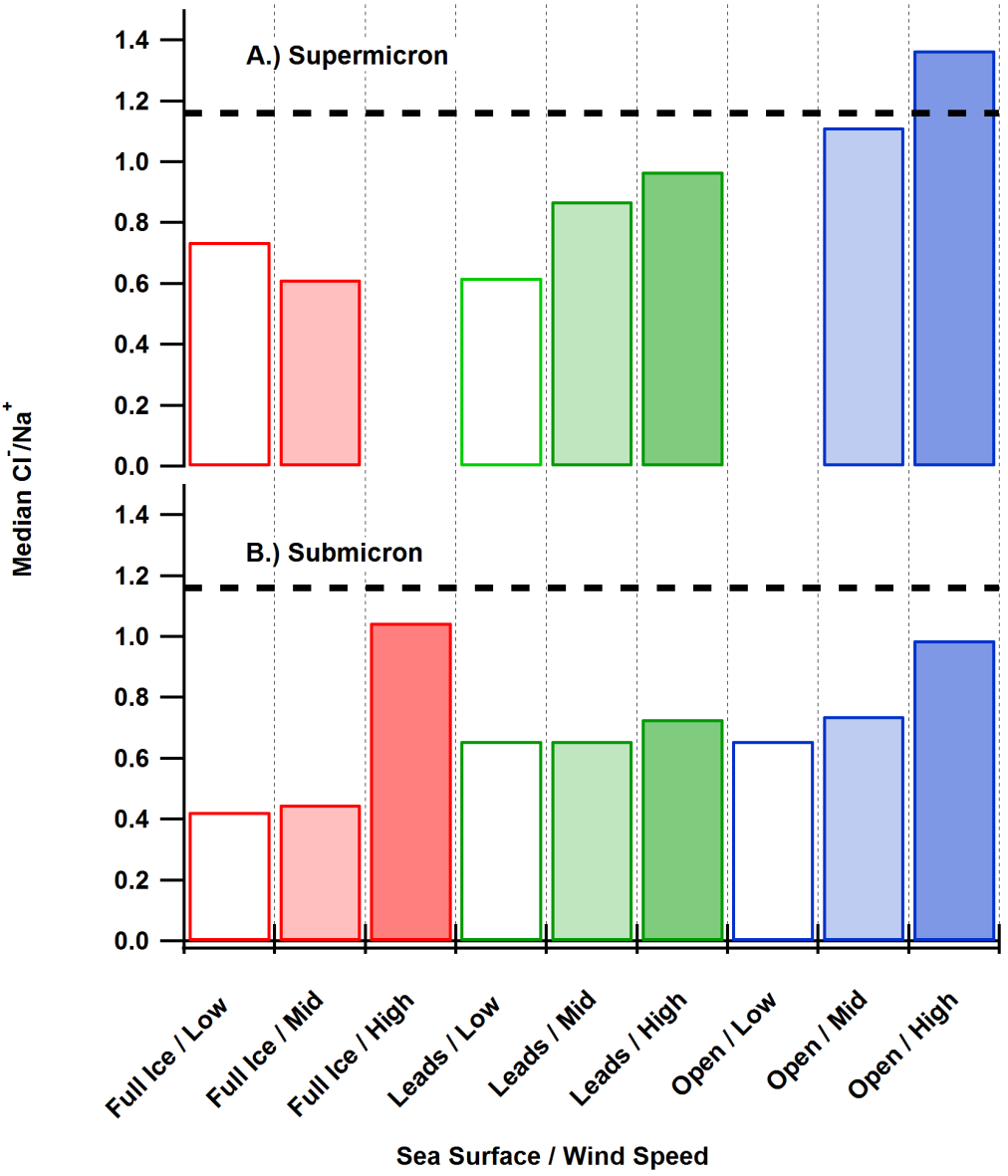

Figure 5—4. Median Cl-/Na+ molar ratios for the submicron (<1 µm) (S), and supermicron (1<10 µm) (B) particle size ranges separated into 9 bins based on local sea ice extent and wind speed, with the Cl-/Na+ ratio of ocean water shown in the dashed black line. Sea ice extent categories include: full ice, leads present, and open water. Wind speed categories include: low (<4 m/s), mid (4-7 m/s), and high (>7 m/s).

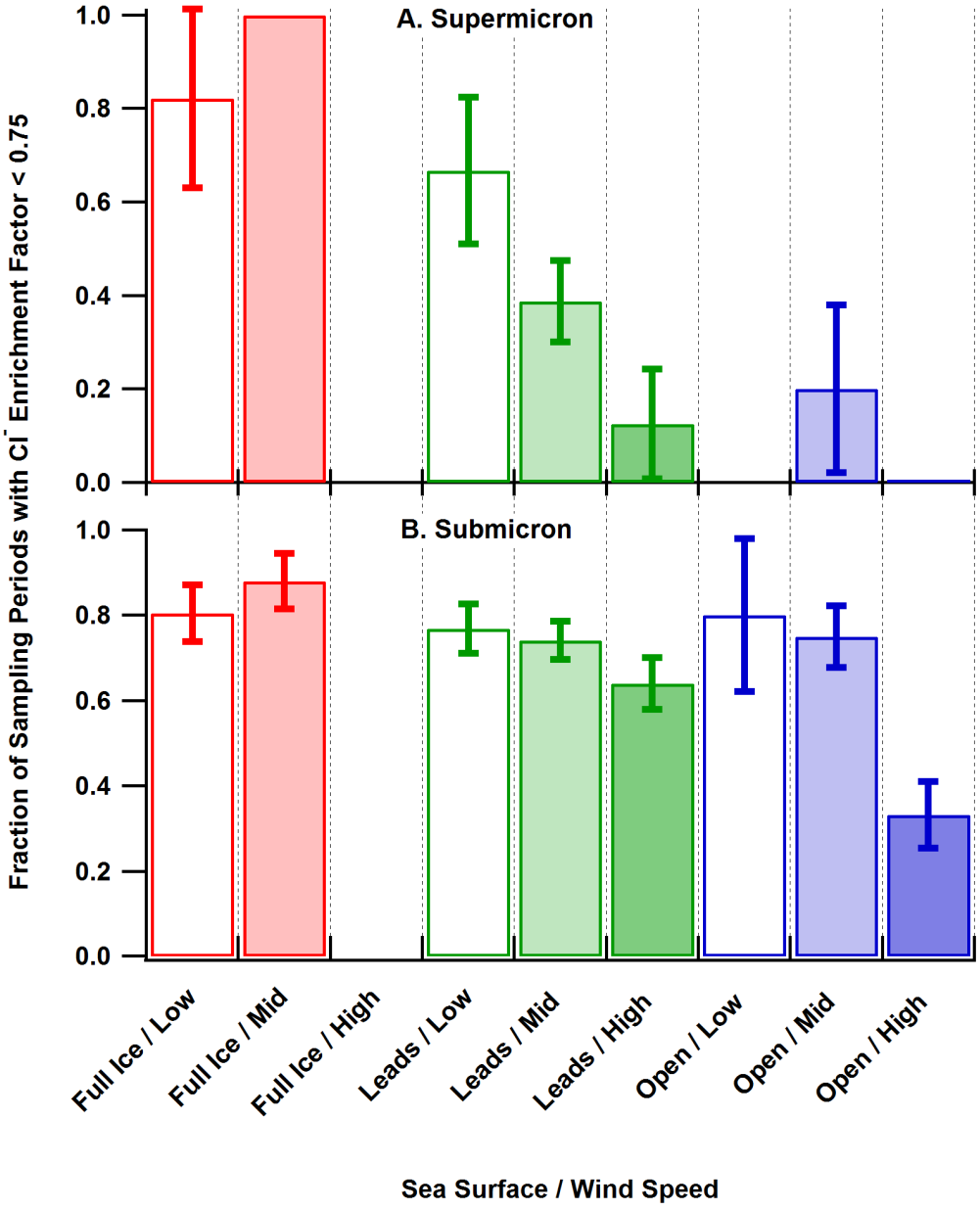

Figure 5—5. The fraction of sampling periods with a Cl^- enrichment factor < 0.75, corresponding to aged sea salt for supermicron (A) and submicron (B) size ranges, respectively, divided into categories based on sea ice conditions and wind speed.

± 0.09) to high wind speed (0.64 ± 0.06; 0.1 ± 0.1), consistent with greater contributions from a wind-dependent local sea salt aerosol source (Figure 5—5). However, this potential decrease in the fraction of aged submicron sea salt periods with increased wind speed, when leads were present, was partly within error. When open ocean was present, the fraction of aged submicron sea salt periods decreased, partly within error, with increasing wind speed (low wind speed = 0.8 ± 0.2; moderate wind speed = 0.75 ± 0.07; high wind speed = 0.3 ± 0.1), again consistent with a wind-dependent local sea salt aerosol source. These trends in sea salt aging are consistent with local sea salt aerosol production increasing with decreasing local sea ice coverage and increasing wind speed. This further supports wind-driven sea salt aerosol production, dominated by supermicron particles, from leads.

5.3.3. Difference in Particle Production from Leads versus Open Ocean

In addition to differences in particle lifetime between submicron and supermicron sea salt aerosol (Williams et al. 2002), differences in the production mechanisms of submicron and supermicron sea salt aerosol from leads likely also contributed to the observed trends in aged fractions and sea salt mass fractions. Leck et al. (2002) and Nilsson et al. (2001) hypothesized that, compared to open ocean production, film drop particle production from leads depends less on wind speed than jet drop particle production. As a result, the sea salt aerosol size distribution over pack ice is dominated by a larger particle diameter lognormal mode at ~2 μm, while over open ocean, a smaller particle diameter lognormal mode centered at 100 nm dominates (Nilsson et al. 2001). This is consistent with the lognormal size distribution of sea salt aerosol resulting from film and jet drops centered at ~100-200 nm and ~1-2 μm dry diameters, respectively, measured by O'Dowd et al. (1997). Thus, the larger contribution of fresh supermicron sea salt, compared to submicron sea salt, observed during periods with leads and moderate to high winds (Figure 5—5) is consistent with the hypothesis that jet drops are the dominant production mechanism of sea salt aerosol from leads. Additionally, the increased presence of smaller particles over open ocean observed by Nilsson et al. (2001) is evident in this study by the increased presence of fresh submicron sea salt during periods of open ocean and high wind speeds (Figure 5—5). These results therefore suggest that the differences in wind driven production of sea salt aerosol from leads, compared to open ocean, shifts the mass distribution of sea salt aerosol in the Arctic towards larger sizes when leads were present. This could impact radiative forcing and cloud processes in the Arctic as CCN efficiency is size dependent (Dusek et al. 2006).

5.3.4. Non-Wave Breaking Particle Sources

Sea salt aerosol production from local leads or open ocean appears to be the dominant contributor to sea salt mass concentrations in this study. However, submicron sea salt mass concentrations, sampled under conditions where local sea salt aerosol production are not expected [e.g., 0.21 ± 0.06 μg m^{-3} when full sea ice cover was present], were of equal to or greater than those from other categories where local sea salt production are expected (e.g., 0.12 ± 0.03 μg m^{-3} when open ocean was present). This suggests that there were sea salt aerosol sources even when no exposed ocean surface was present (Figure 5—2b). Frost flowers, highly saline ice crystals grown on rapidly freezing open leads, are a potential source for wind-driven sea salt aerosol production when no open ocean is present (Rankin et al. 2000). SO_4^{2-}/Na^+ molar ratios were calculated to determine the potential contribution of wind-blown frost flowers to the observed SSA mass concentrations. The SO_4^{2-}/Na^+ molar ratio of frost flowers in Barrow, AK was previously determined to be largely below 0.02 due to the precipitation of mirabilite (Na_2SO_4) at low temperatures (Douglas et al. 2012). In comparison, SO_4^{2-}/Na^+ ratios for fresh seawater and fresh SSA are ~0.06 (Keene et al. 2007). Therefore, the fractions of sampling periods with a SO_4^{2-}/Na^+ molar ratio < 0.02, suggesting possible significant frost flower aerosol influence, were calculated, as show in Figure 5—6. Very few sampling periods were characterized by these ratios. Sulfate-depleted periods were only observed for supermicron and submicron sampling periods, respectively, with leads present and moderate (0.03 ± 0.04; 0.02 ± 0.02) to high (0.1 ± 0.2; 0.02 ± 0.02) wind speeds (Figure 5—6). The presence of periods with SO_4^{2-}/Na^+ molar ratios < 0.02, as well as increased wind speed, is possibly indicative of aerosolized frost flowers from newly forming sea ice (Rankin et al. 2000). However, the increase in the fraction of potential frost flower influenced supermicron periods from low to moderate and high wind speeds when leads were present is not statistically significant, and the fraction of periods (0.02-0.1) is relatively low. Therefore, overall, the influence of wind-blown frost flowers on the SSA mass concentrations in this study was likely minor, and wave-breaking represents a greater influence on the local aerosol. Sulfate isotope analysis would be necessary to fully determine the influence of frost flowers, as anthropogenic sulfates can mask the sulfate depleted frost flower sea salt (Norman et al. 1999, Seguin et al. 2014).

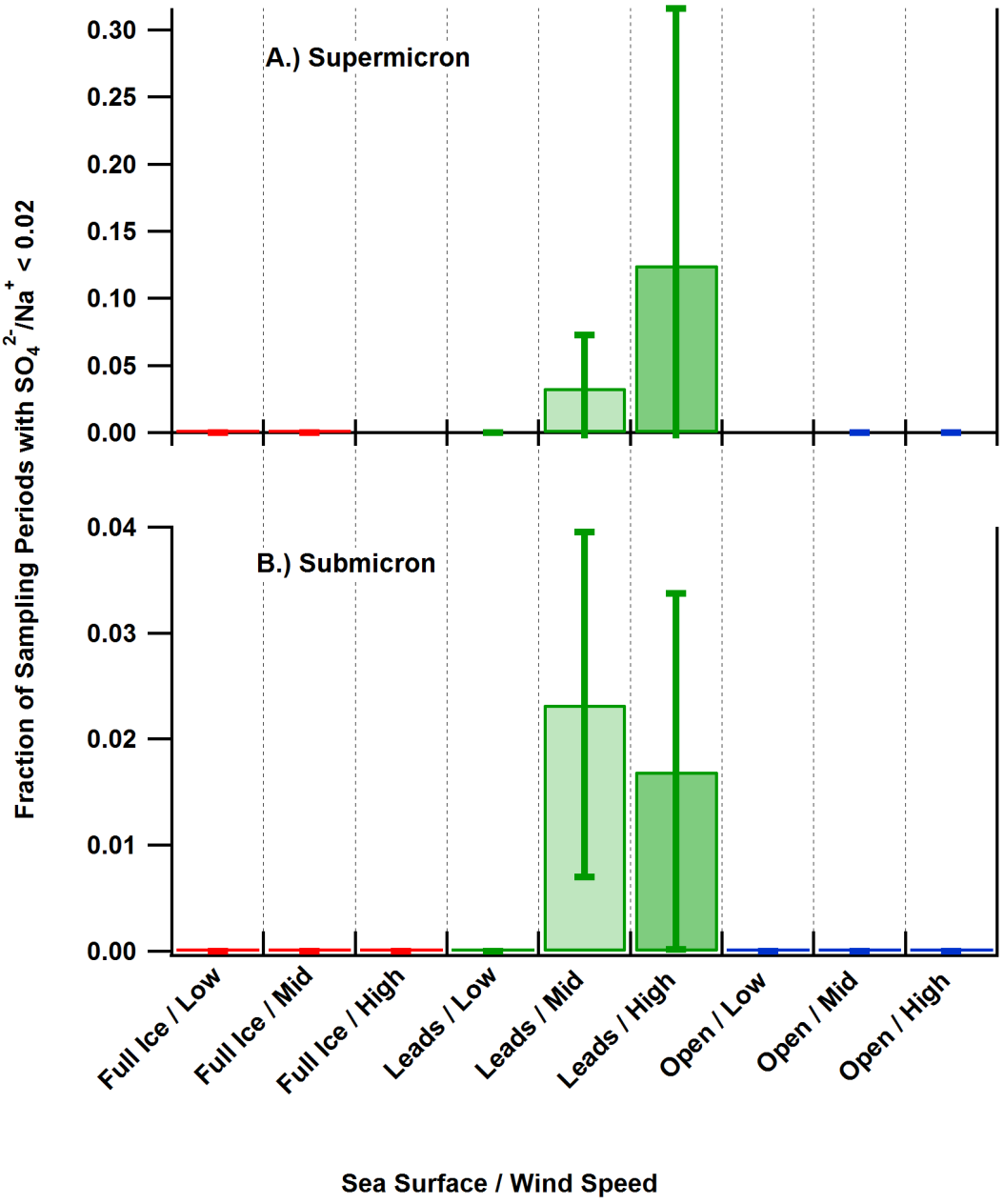

Figure 5—6. The fractions of sampling periods with SO42-/Na+ < 0.02, potentially indicative of aerosolized frost flowers, for supermicron (A) and submicron (B) particle size ranges, respectively, divided into categories based on sea ice conditions and wind speed.

High winds can also loft saline snow particles, which are suggested to form aerosols by sublimation (Yang et al. 2008, Lieb-Lappen and Obbard 2015). The increase in submicron Na^+ mass concentrations from low wind speed (0.19 ± 0.05 μg m^{-3}), to moderate wind speed (0.2 ± 0.1 μg m^{-3}), to high wind speed (0.3 μg m^{-3}) for periods with full sea ice cover was not also observed in the supermicron Na^+ mass concentrations. Therefore, additional detailed field measurements of aerosol size and chemical composition are required to examine the potential size-dependent production of aerosols from blowing snow. However, this increase in submicron Na^+ mass concentration was within error. In addition, the Cl^-/Na^+ ratio of blowing snow in Barrow, AK is expected to be similar to the ocean water ratio (Jacobi et al. 2012), such that any fresh sea salt observed during full ice periods can potentially be attributed to this source. Therefore, with less than 30% of the full sea ice cover submicron and supermicron sampling periods characterized by fresh sea salt, the contribution from blowing snow production to the observed Na^+ mass concentrations is likely minor with transported sea salt aerosol representing a greater contribution.

5.3.5. Seasonality of Sea Salt Aerosol Production

The Arctic sea ice coverage undergoes seasonal changes, with growth during winter, loss during summer, and pack ice movement due to winds and currents (Mahoney et al. 2014). In this study, particle sampling periods with local full sea ice cover occurred during the months of November through June (Figure 5—7). For these months, 11-36% and 0-25% of all submicron and supermicron particle sampling periods, respectively, corresponded to local full sea ice coverage. For Barrow, AK, Quinn et al. (2002) previously observed a winter maximum in submicron sea salt aerosol, attributed to long-range transport from high-latitude regions of the Pacific and Atlantic Oceans with seasonally high winds. This is consistent with the observations of the highest fractions of aged sea salt and submicron Na^+ mass concentrations during sampling periods with full sea ice cover, suggesting that the winter sea salt aerosol population had the longest transport time from its source. As expected, open ocean near Barrow was observed between July and November (Figure 5—7). The minimum fractions of aged sea salt and maximum supermicron Na^+ mass concentrations were observed during these periods of local open ocean, suggesting the sea salt aerosol population during summer had the shortest transport time from its source. The lower particle deposition velocity, and resulting longer particle lifetime, over sea ice compared to over open ocean in the Arctic may also have contributed to the

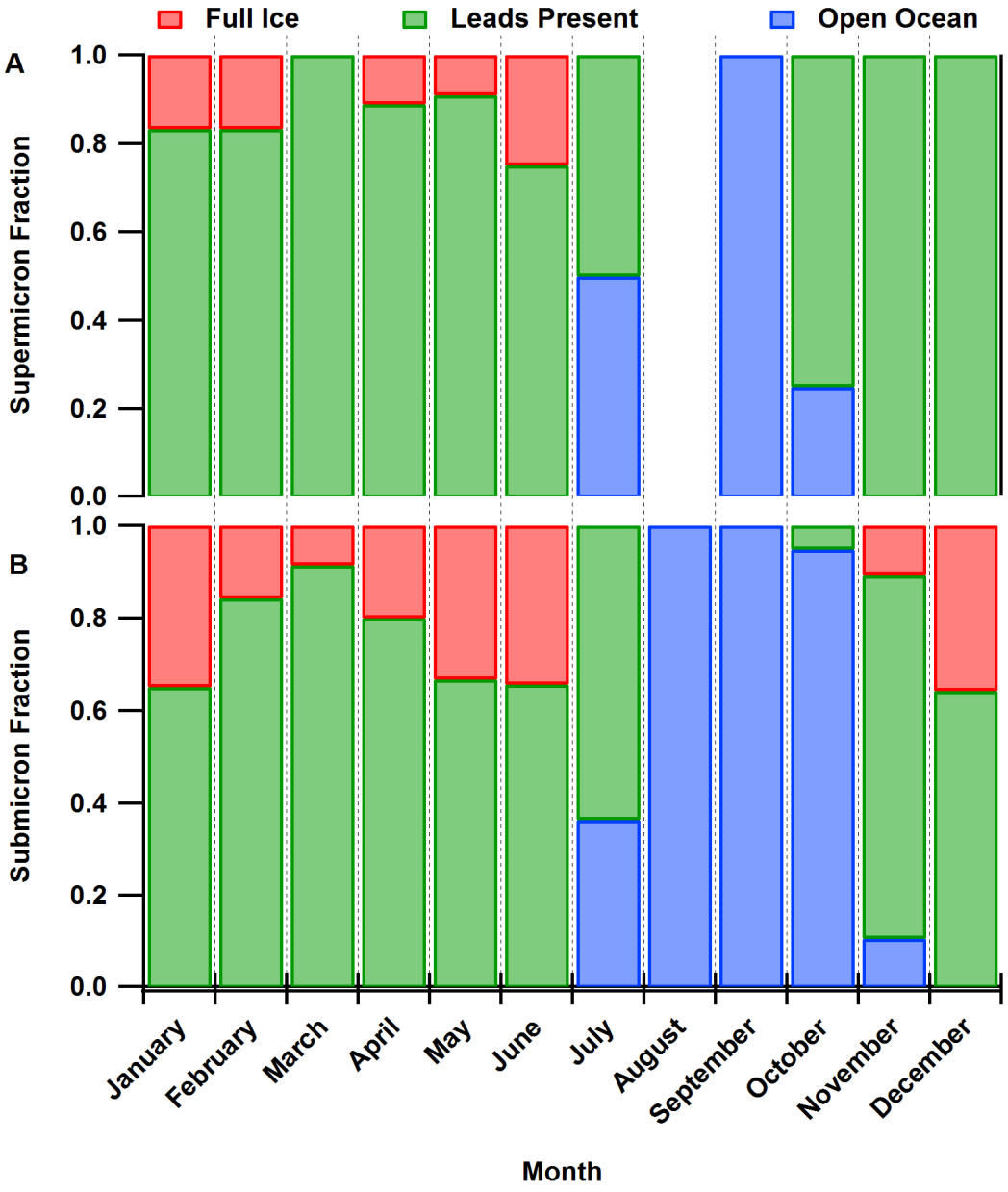

Figure 5—7. Fractions of supermicron and submicron sampling periods in the three local sea surface categories as a function of month.

higher fraction of aged sea salt and higher submicron Na^+ mass concentrations during sampling periods with full sea ice cover compared to periods of local open ocean (Nilsson and Rannik 2001). Nearby leads were observed to be present between October and July and were the dominant sea ice category over the entire study (Figure 5—7). Supermicron particle sampling periods with leads present comprised 50-91% of the supermicron particle sampling periods months of October to July. Submicron particle sampling periods with leads present comprised 64-91%, and 5%, of submicron particle sampling periods November to July, and October, respectively. This suggests that sea salt aerosol production from leads currently impacts sea salt aerosol mass concentrations, especially in the supermicron particle size range, in the Arctic atmosphere throughout the majority of the year.

5.4. Conclusions

This three-year study at Barrow, AK allowed a comprehensive investigation into the influences of sea ice coverage and wind speed on sea salt mass concentrations in the coastal Arctic. Wind-driven production of sea salt aerosol from leads contributes significantly to sea salt aerosol mass concentrations in the Arctic, but to a lesser extent than wind-driven production of sea salt aerosol from open ocean. This is consistent with previous short-term summertime number flux measurements of sea salt aerosol over open leads, where sea salt aerosol emissions were ~10 times smaller than the open ocean (Nilsson et al. 2001, Leck et al. 2002). The influence of sea salt aerosol production from open leads was most apparent in the supermicron size range, as evidenced by the strong dependence on wind speed of supermicron sea salt mass concentrations, which increased by a factor of 10 from periods with low wind speed to periods with high wind speeds, when leads were present. The increase in supermicron Na^+ mass concentration from 0.035 ± 0.007 μg m^{-3}, when leads were not present, to 0.12 ± 0.02 μg m^{-3} when leads were present, provides further evidence of the influence of sea salt aerosol production from leads. There was evidence of wind-driven submicron sea salt production from local leads, but submicron sea salt, depleted in chloride, from long range transport comprised the majority (~70%) of the submicron sea salt mass (Figure 5—3). The influence of long range transport was greatest when local sea salt aerosol production would not be expected, including periods of low winds and full sea ice cover.

This improves our knowledge of complex atmosphere-sea ice feedbacks (Shepson et al. 2012). Supermicron sea salt aerosol production from leads could increase direct radiative forcing,

as supermicron sea salt can contribute significantly to scattering in the remote marine boundary layer (Quinn et al. 1998). This supermicron sea salt aerosol could also impact indirect radiative forcing and cloud properties as giant CCN (2 – 10 μm), which can induce the formation of larger cloud droplets and accelerate precipitation in the presence of smaller particles (Yin et al. 2000). The CCN response to supermicron sea salt aerosol produced from leads may be reduced by the efficient removal of large particles in the highly scavenging nature of the Arctic atmosphere, particularly in summer (Browse et al. 2012). Supermicron sea salt aerosol emissions from leads would also increase the atmospheric condensation sink, which is predicted to suppress particle nucleation from dimethyl sulfide and reduce total CCN concentrations (Browse et al. 2014). Increased emissions of supermicron sea salt aerosol from leads thus plays an important role in controlling the CCN response to changes in sea ice (Browse et al. 2014). Supermicron sea salt aerosol could also alter snowpack and atmospheric halogen photochemistry, and therefore atmospheric oxidation, through heterogeneous reactions (Simpson 2005). The impacts of wind driven production of sea salt aerosol from leads could be particularly evident in winter and early spring when sea ice coverage is at its maximum and submicron sea salt mass concentrations are typically higher than supermicron sea salt mass concentrations due to a lack of local open ocean source (Quinn et al. 2002). Given decreasing multi-year sea ice extent and increasing ice fracturing (Stroeve et al. 2012), wind-driven production of supermicron sea salt aerosol from leads could therefore increase the supermicron sea salt aerosol mass fraction in the Arctic in the winter-spring, changing the annual contributions of sea salt aerosol to the atmosphere. In addition, lower particle scavenging efficiency and very stable thermal stratification in the boundary layer in the Arctic winter and early spring (Sirois and Barrie 1999) may further increase the atmospheric sea salt mass burden (Browse et al. 2012). To fully understand the influence of sea salt aerosol produced from leads, measurements of sea salt aerosol concentrations with higher time resolution must be combined with sea ice coverage measurements that take into account a larger area. Furthermore, to understand the long-term impacts of changing sea ice on the Arctic, decadal comparisons between sea ice conditions and sea salt aerosol are necessary.

5.5. Acknowledgments

Stephen M. McNamara is thanked for the analysis of sea ice radar backscatter maps. Dr. Patricia K. Quinn is thanked for help obtaining NOAA aerosol chemical composition data and for helpful discussions regarding the results of their analysis. We thank the NOAA personnel at

Barrow, AK for helping with sample collection and Kristen Schulz for sample analysis. The PMEL contribution number is 4408. The University of Michigan College of Literature, Science, and the Arts is thanked for funding this analysis. Hajo Eicken of the Sea Ice Group at the Geophysical Institute at the University of Alaska Fairbanks is thanked for discussions regarding, and assistance in obtaining, the sea ice radar backscatter maps. The meteorological data used in this study can be found on the NOAA Barrow, Alaska Observatory website (http://www.esrl.noaa.gov/gmd/obop/brw/) and sea ice radar backscatter maps can be found on the Sea Ice Group at the Geophysical Institute at the University of Alaska Fairbanks website (http://seaice.alaska.edu/gi/data/barrow_radar).

Chapter 6 Polar Plunge: Semester-Long Snow Chemistry Research in the General Chemistry Laboratory

Reprinted (adapted) with permission from:
Journal of Chemical Education, 2018.
DOI: 10.1021/acs.jchemed.7b00823.

6.1. Introduction

Concern has grown in the past decade in the science education community regarding the number of students who leave science, technology, engineering, and math (STEM) majors, especially among underrepresented minorities (Griffith 2010, Graham et al. 2013, Lewis 2014, Shedlosky-Shoemaker and Fautch 2015), by their second year of undergraduate education (Chen 2013). In response, introductory first- and second-year science courses have incorporated pedagogical techniques to increase student motivation and positive attitudes towards a subject (Williams and Bramwell 1989, Nagda et al. 1998, Russell et al. 2007, Canaria et al. 2012). The American Chemical Society Committee on Professional Training (ACS-CPT) (American Chemical Society 2015) advocates for incorporation of research into undergraduate chemistry curriculum to establish the relationship between content and the real-world (Kember et al. 2008, Williams and Williams 2011). In response, many introductory and upper level chemistry courses have integrated research (Williams and Bramwell 1989, Kharas 1997, Ford et al. 2008, Carpenter and Pappenfus 2009, Richter-Egger et al. 2010, Tomasik et al. 2014). Recently, course-based undergraduate research experiences (CUREs), where whole classes of students address a research question (Auchincloss et al. 2014, Chase et al. 2017), have been implemented in biological science courses (Lopatto et al. 2014, Bakshi et al. 2016, Kowalski et al. 2016, Rodenbusch et al. 2016), as well as introductory (Clark et al. 2016, Chase et al. 2017) and upper level chemistry courses (Kerr and Yan 2016). Compared to traditional undergraduate research experiences, in which undergraduates work one-on-one with a research mentor, CUREs offer the ability to scale up the research experience of a single professor's (principal investigator's, PI's) research group to involve more students (Auchincloss et al. 2014). The CURE format is a promising means for expanding

undergraduate involvement in chemistry research to a broader population and with a lower demand on resources (Bangera and Brownell 2014, Linn et al. 2015).

The integration of environmental topics in the classroom can provide a connection between the undergraduate chemistry curriculum and the natural world (Kegley and Stacy 1993, Swan and Spiro 1995, Mihok et al. 2006, Bachofer 2008, Richter-Egger et al. 2010, Robelia et al. 2010, Tomasik et al. 2013, Tomasik et al. 2014). This has previously been accomplished through the incorporation of experiments with environmental themes into pre-existing courses (Sinniah and Piers 2001, Salido et al. 2003, Bachofer 2008, Tomasik et al. 2013) and development of courses with environmental themes (Kegley and Stacy 1993, Tabbutt 2000, Mihok et al. 2006, Richter-Egger et al. 2010, Robelia et al. 2010). The combined incorporation of an environmental theme and research-based laboratory activities in an upper division analytical chemistry course positively impacted student attitudes towards chemistry (Tomasik et al. 2014). Similar introductory level courses could address student attrition from STEM majors prior to reaching upper level coursework (Chen 2013). Herein we describe a new environmental research-focused general chemistry laboratory course and investigate the impact of this pedagogical approach (CURE and an environmental theme) through pre- and post-semester surveys. In an attempt to improve STEM retention and prepare students to be active members of the scientific community, this introductory level, authentic research-based course aimed to engage students through exposure to all steps of the research process, while simultaneously teaching general chemistry skills. To our knowledge, this work represents the first semester-long environmental chemistry CURE in the general chemistry laboratory.

6.2. Course Description

At the University of Michigan – Ann Arbor (U-M), a semester-long general chemistry laboratory course with a focus on snow chemistry research (Chem 125–Snow) was designed and piloted during the Fall 2015 and 2016 semesters. Chem 125–Snow was implemented in conjunction with the University of Michigan Authentic Research Connection program (Vernon et al. 2016), which supports the integration of faculty-led semester-long research projects into introductory biology and chemistry laboratory courses and is examining the impacts of early research exposure on retention in STEM majors. This pilot course was run in parallel, and as an alternative, to the traditional general chemistry laboratory course (Chem 125–Traditional), which did not include a research project. Students are typically co-enrolled in a semester-long general

chemistry lecture course (Matz et al. 2012). Both Chem 125–Traditional and Chem 125–Snow are semester-long (12 week) 2-credit laboratory courses that include a 1 h pre-laboratory lecture given by the course instructor and a 3 h laboratory session, led by a graduate student instructors (GSIs), where students work in groups of three. Unlike Chem 125–Traditional, the Chem 125–Snow instructional team mirrored the composition of a multi-generational research group, and included the PI, one postdoctoral fellow, two graduate student instructors, and two-four undergraduate assistants. In both courses the pre-laboratory lecture introduces content and techniques for the upcoming laboratory session. In Chem 125–Snow, the pre-laboratory lecture was also used to provide background knowledge on the research topic (snow chemistry) and broader context (climate change). Chem 125–Snow mirrored the course structure and assessment, including pre-laboratory quizzes, post-laboratory written reports, and a midterm exam, used in Chem 125–Traditional.

As a pilot course, Chem 125–Snow engaged a smaller number of students in Fall 2015 (28 students) and Fall 2016 (35) split into 2 laboratory sections, compared to the number of students enrolled in Chem 125–Traditional (Fall 2015 = 1061; Fall 2016 = 1109) that were split into 48 and 49 laboratory sections, respectively (Table 6—1). Students enrolled in the general chemistry laboratory course are typically not prospective chemistry majors, as those students usually test out of general chemistry at U-M. For enrollment in Chem 125-Snow, students expressed interest in participation through a brief, online form. In 2015, all first and second year students who submitted requests were enrolled. In 2016, students were randomly selected among those who had applied, until reaching the criteria of 70% freshmen and 30% sophomores, reflective of Chem 125–Traditional demographics (Table 6—1). Chem 125–Snow uniquely featured a larger fraction of female students in both Fall 2015 (78%) and Fall 2016 (63%), compared to Chem 125–Traditional (Fall 2015 = 46%; Fall 2016 = 49%). The large percentage of female students in Chem 125–Snow provided a unique opportunity to use context-based content to positively impact (Machina and Gokhale 2010) a larger population of an underrepresented group in the sciences.

The structure of Chem 125–Snow, presented in Table 6—2 and discussed in detail in the following sections, was designed to provide all components of an authentic research experience wherein students investigated the chemical composition of snow, which influences its propensity to undergo photochemical reactions (Pratt et al. 2013). This research utilized ion

Table 6—1. Comparison of Student Demographics for the Snow Chemistry and Traditional General Chemistry Laboratory Courses.

Category	**Snow Chemistry Course (Respondents, *N*)**		**Traditional Chemistry Course (Respondents, *N*)**	
	2015	2016	2015	2016
Sections	2	2	48	49
Total Students, *N*	28 (22)	35 (34)	1061 (700)	1109 (920)
Class Standing				
Freshman	16 (12)	27 (26)	735 (488)	759 (634)
Sophomore	12 (10)	8 (8)	277 (181)	291 (241)
Junior	0 (0)	0 (0)	29 (17)	40 (29)
Senior	0 (0)	0 (0)	16 (11)	18 (15)
Undisclosed	0 (0)	0 (0)	4 (3)	1 (1)
Gender of Respondents				
Male	6 (4)	13 (12)	576 (349)	571 (454)
Female	22 (18)	22 (22)	485 (347)	538 (460)
Undisclosed	0 (0)	0 (0)	0 (4)	0 (6)

[a]Student survey response numbers shown in parentheses.

chromatography (IC) and was directly adapted from work in the PI's laboratory, where snow chemistry is actively investigated for its links to climate change (Domine et al. 2004, Jacobi et al. 2012, Krnavek et al. 2012, Pratt et al. 2013, Simpson et al. 2015). As an introductory general chemistry laboratory course, Chem 125–Snow also addressed key chemistry concepts and laboratory techniques, fulfilling the guidelines set by the ACS-CPT regarding general chemistry courses in that they are "hands-on, supervised laboratory experiences" where students were instructed in "basic laboratory skills such as safe practices, keeping a notebook, use of electronic balances and volumetric glassware, preparation of solutions, chemical measurements using pH electrodes and spectrophotometers, data analysis, and report writing" (American Chemical Society 2015). Discussion of these laboratory experiments (Laboratory sessions 1, 3, 5, 8, and 9), the general chemistry skills and concepts they addressed, as well as their connection to the snow chemistry research, are presented in the Laboratory Experiments section. Additional laboratory sessions (2, 4, 7, and 10) focused on exposure to individual components of an authentic research experience, including scientific literature, data processing, instrument calibration and operation, and Arctic snow composition analysis, are presented in the Arctic Snow Analysis section. The completion of the authentic research experience involved synthesis and public presentation of research results (Laboratory sessions 6, 11, and 12), as discussed here in the Synthesis & Presentation of Research Results section.

6.2.1. Laboratory Experiments

General chemistry concepts of measurements and uncertainty were explored in the first laboratory experiment session of Chem 125–Snow through experimental determination of water density. Lab. 1 was primarily intended to develop error propagation skills used throughout the course to calculate uncertainties for snow chemistry research data. Lab. 3 was designed to prepare students for their snow chemistry research through exposure, in a simplified manner, to calculating concentration, making solutions, and carrying out serial dilutions. This laboratory session, where students prepared dye solutions of varying concentration and related concentrations to absorbance spectroscopy measurements, was implemented for the first time in 2016 in response to observations of student difficulties with preparation of solutions for IC calibration in 2015 (Lab. 4, discussed in the Arctic Snow Analysis section). Lab. 1 and Lab. 3 were skill development based, and the post-laboratory worksheets assessed student understanding of laboratory procedures through calculations and short answer questions.

Table 6—2. Lab Experiments in the Snow Chemistry General Chemistry Laboratory Course, with Central General Chemistry Concepts Applications to Snow Chemistry Research

Lab Experiment	General Chemistry Concept	Snow Chemistry Research Application
Measurements and uncertainty	Use of glassware; Calculation of error; Accuracy and precision	Reporting ion composition and pH of snow samples with uncertainty
Scientific literature	Comprehension of technical writing	Interpretation of snow sample analysis data
Preparation of solutions, Part 1	Use of mass balances; Solution making; Dilutions; Absorbance spectroscopy	Preparation of anion and cation standard solutions for ion chromatography calibration
Preparation of solutions, Part 2: Ion chromatography calibration	Use of mass balances; Solution making; Dilutions	Preparation of anion and cation standard solutions for ion chromatography calibration
pH and Buffering	Techniques for pH measurements (indicator paper, digital meter); Buffering and titration	Buffering capacity and pH of ocean water and snowmelt
Poster design workshop	Presentation of results	Presentation of snow chemistry research
Data analysis	Calculations of concentration; Chemistry specific use of data analysis software	Construction of ion chromatography calibration curves; Interpretation of snow composition data
Quantification of Cl^- by Mohr method	Stoichiometry; Precipitation reactions; Titration	Determination of Cl^- content of snow
$Cl_2(g)$ synthesis and quantification	Redox reactions; Ideal gas laws; Absorbance spectroscopy	Quantification of the production of $Cl_2(g)$ for calibration of a chemical ionization mass spectrometer
Ion chromatography and pH analysis of Arctic snow	Concentration; Cations and anions; pH	Determination of ion composition and pH of snow samples
Creating research posters, Parts 1 and 2	Data synthesis and interpretation; Poster creation	Presentation of snow chemistry research
Research poster symposium	Presentation of results	Presentation of snow chemistry research

In Lab. 5, students were exposed to pH measurement through experimental determination of buffering capacity and pH (Ibanez et al. 2008) of melted snow samples and synthetic seawater (a solution that replicates the salt composition of the ocean, the main source of salts in Arctic snow). An understanding of, and ability to measure, pH is important because many reactions in Arctic snow are pH-dependent (Pratt et al. 2013). For Lab. 8, students examined Cl^- content in authentic snow samples by titration with the Mohr Method,(Ibanez et al. 2008) which involved the general chemistry concepts of molarity, stoichiometry, and precipitation reactions. Use of environmental samples in Lab. 5 and Lab. 8 exposed students to proper sample handling practices and created an exploratory laboratory experience as environmental samples are, by nature, not well-defined (Kegley and Stacy 1993). These exploratory laboratory experiences were extended in assigned written post-laboratory reports, for which students were required to critically interpret collected data to form independent conclusions on the chemistry of their snow samples.

In Lab. 9, students were exposed to general chemistry concepts of gas-phase and redox reactions, ideal gas laws, and absorbance spectroscopy, through the synthesis and measurement of $Cl_{2(g)}$. This laboratory experiment was based on procedures established for the calibration of a chemical ionization mass spectrometer (CIMS) (Liao et al. 2014), which is used in the PI's laboratory to study Arctic snowpack $Cl_{2(g)}$ production (Custard et al. 2017). Heightened safety concerns surrounding $Cl_{2(g)}$ were used to highlight the importance of laboratory safety (American Chemical Society 2015) through a pre-laboratory worksheet that assessed student understanding of safety data sheets. As a post-laboratory assignment, students demonstrated their understanding of the connection between measurements of standard concentrations of $Cl_{2(g)}$ and snowpack production of gas-phase halogens in a worksheet.

6.2.2. Arctic Snow Analysis

To interpret their Arctic snow chemistry data and place it in the context of previous work, students required a comprehension of scientific literature. Students were introduced to scientific literature in a laboratory session held in an on-campus computing facility (Lab. 2). Students received instruction, with assistance from a chemistry librarian, in the search for, and comprehension of, primary scientific literature. For the assigned research manuscript (Domine et al. (2004)), students identified important sections and specific concepts needed for their Arctic snow chemistry research project through a scavenger hunt activity and wrote a journal style introduction section as a post-lab assignment. The instructional staff provided feedback on the

introduction section to allow students to make revisions before its incorporation into their final research presentations. This laboratory session was designed to develop scientific literacy and establish a skill base in the use of primary literature to support data interpretation, while providing learning benefits of exposure to scientific literature (Ferrer-Vinent et al. 2015).

Data processing skills were also required for students to carry out their research. Most undergraduate students matriculate without spreadsheet experience,(Schlotter 2013) which increases the time required to complete coursework and detracts from learning.(Rubin and Abrams 2015) In response, students were introduced to data processing in Microsoft Excel in the on-campus computing facility in Lab. 7. Earlier in the course, using skills from Lab. 3, students prepared IC calibration standard solutions containing either seven anions (F^-, Cl^-, NO_2^-, SO_4^{2-}, Br^-, NO_3^-, PO_4^{3-}) or six cations (Li^+, Na^+, NH_4^+, K^+, Mg^{2+}, Ca^{2+}) (Lab. 4). Students were supplied in Lab. 7 with raw data from IC analyses of these calibration standards (IC analysis conducted by the course instructional staff due to time constraints) and followed a tutorial to construct calibration curves. Using these calibration curves, students practiced converting Arctic snow IC raw data, previously collected by the PI's laboratory, into concentrations and produced figures. During this laboratory session, instructors emphasized general data processing skills (spreadsheet organization, performing calculations within the software, constructing figures with proper labels and error shown) applicable to other data processing computer programs (e.g. KaleidaGraph (Synergy Software), Origin (OriginLab Corp.), IGOR Pro (WaveMetrics), R (rproject.org), Mathematica (Wolfram), and Matlab (Mathworks)). Students continued to utilize these data processing skills and their calibration curves throughout the course to process raw data generated in their independent IC analysis of Arctic snow (Lab. 10, described below) and construct figures to present their research. Similar to other CUREs, student involvement in data processing over multiple laboratory sessions increased the connection of the authentic research experience across the semester-long course and student ownership of research data (Bakshi et al. 2016).

To analyze students' individual Arctic snow samples by IC, Lab. 10 was held in the PI's laboratory, where students completed 1.5 h laboratory sessions scheduled at alternate times (individually in Fall 2015 and in pairs in Fall 2016). Students independently operated the ICs with course instructor guidance. To prepare students to conduct IC of melted Arctic snow, one lecture session prior to the laboratory session was devoted to IC fundamentals. For the Fall 2015 course, snow samples were collected in Feb. and Mar. 2015 during the day from locations on the Beaufort

Sea (Harrison Bay and Camden Bay) and Chukchi Sea by a collaborator. Following the first course pilot, two student alumnae and one GSI accompanied the PI to Utqiaġvik, AK in Feb. 2016 and collected snow samples during the day from locations on the Chukchi Sea, Elson Lagoon, and tundra surrounding Utqiaġvik, AK; these samples were used analyzed the Fall 2016 course. Snow was kept frozen during transport and stored at -40˚C until it was melted for analysis by anion and cation (Dionex ICS 2100 and 1100; Thermo Scientific) IC, as well as a digital pH meter. The use of IC in the snow chemistry research presented here introduced students to advanced instrumentation through a guided inquiry approach, a practice shown to improve student learning and problem solving skills.(Warner et al. 2016) In addition, snow composition data collected by students contribute to ongoing research on Arctic air-snow interactions in the PI's laboratory (Pratt et al. 2013).

6.2.3. Synthesis & Presentation of Research Results

Students completed the final components of the authentic research process through a series of laboratory sessions, in which they individually developed research questions to test with their data, analyzed and interpreted their data in this context, and then presented their research results through individual posters and written manuscripts. These final presentation forms were chosen because they are common mediums used to present research results in both the classroom, and professional scientific research settings (Kennedy 1985, Dunstan and Bassinger 1997, Sisak 1997, Marino et al. 2000, Whelan and Zare 2003, Wimpfheimer 2004, Raines et al. 2005, Squier et al. 2006, Dillner et al. 2011, Logan et al. 2015, Danowitz et al. 2016), allowing for evaluation of students' comprehension of their semester-long snow chemistry research experience. Incorporating science communication also served as a tool to engage students, promote critical thinking, and provide a method for student discovery and growth (Bressette and Breton 2001). The practice of communicating science among peers in a classroom setting may also help prepare students to communicate science in future research experiences (Logan et al. 2015) .

Lab. 11 focused on the integration and interpretation of data to develop and answer research questions. Data from individual student snow sample analyses were aggregated and made available to all students for their final research analysis. To aid in interpretation of snow sample data, supporting documentation was provided on the location and time of snow collection, as well as concurrent meteorological observations. In addition, students obtained satellite sea ice imagery from NASA MODIS Worldview to determine the local sea ice extent, which can influence snow

composition (Domine et al. 2004). The combination of snow inorganic ion composition, pH, and supporting information, as well as the knowledge of snow chemistry developed in lectures and the scientific literature laboratory session, allowed students to independently develop research questions to test with the available data. For example, some students investigated the relationship between the distance to the exposed ocean surface and snow chemical composition, to predict trace halogen gas production (Pratt et al. 2013) as a function of distance from open water. These students built upon previous studies of Arctic snow composition (Domine et al. 2004, Krnavek et al. 2012, Pratt et al. 2013) with their original research to examine whether increasing Arctic sea ice loss (Stroeve et al. 2011) will affect snow chemistry and air-snow interactions. The PI's laboratory is compiling the Arctic snow composition data and students' findings to produce a manuscript for submission to a peer-reviewed journal.

Similar to other CURE courses (Bakshi et al. 2016), a number of laboratory sessions were needed to help students translate the results and interpretation of their research into posters. First, a laboratory session was dedicated to the fundamentals of poster design (Lab. 6). The importance of the balance of text and graphs in posters (Furlan et al. 2007) was emphasized through an activity where students discussed the strengths and weaknesses of authentic scientific research posters, from both the PI's laboratory and outside sources. The final laboratory session(s) (one in Fall 2015; two in Fall 2016) were held at an on-campus computing facility where students constructed their research posters under the guidance of the course instructional staff (Lab. 11). The expansion of the research poster creation laboratory session into two laboratory sessions in Fall 2016 was intended to give students more time and guidance in the creation of their first research posters.

The student poster symposium was open to the public,(Logan et al. 2015) and each poster was judged three times for content and oral presentation by volunteers recruited from graduate students, postdoctoral researchers, and professors in the U-M Department of Chemistry (Lab. 12). In Fall 2015, individual written manuscripts were due one week after the poster symposium, allowing students to receive and incorporate poster feedback to make improvements to their manuscripts. This progression mirrored the traditional research process, wherein preliminary research results are often presented at scientific conferences before they are submitted to peer-reviewed journals. In contrast, the Fall 2016 poster session was held after the written manuscript was submitted, thereby allowing manuscript feedback to be incorporated into the posters. This

change was intended to make the poster session more satisfying for students as a culminating final experience. No assessment was conducted to compare these two approaches.

6.3. Results & Discussion

Quantitative and qualitative methods were used to investigate the impacts of Chem 125–Snow on students from the Fall 2015 and 2016 semesters. Responses to course specific survey questions (Table 6—3), the "Interest and Utility" factor (Bauer 2008) from the Attitude toward the Study of Chemistry Inventory (ASCI) (Table 6—4) (Xu and Lewis 2011) , and open-ended prompts were collected from participants who voluntarily responded (Fall 2015 = 79% response rate; Fall 2016 = 97%) (Table 6—1) (Vernon et al. 2016). Students in the concurrent Chem 125–Traditional, who received no exposure to snow chemistry or research, were designated as the control group and were surveyed in the same voluntary manner (Fall 2015 = 66% response rate; Fall 2016 = 83%) (Table 6—1). Institutional review board (IRB) approval and informed consent from participants were obtained before beginning this work (Vernon et al. 2016).

6.3.1. Survey Results

A series of survey questions were utilized pre- and post-course during the Fall 2016 semester to gauge student confidence in their familiarity with the snow chemistry research topic (Figure 6—1) and their ability to perform general research skills (Figure 6—3). The same series of survey questions were utilized only post-course during the Fall 2015 semester (Figures 6—2 & 6—4). Responses were recorded on a scale of 1 being "not confident" to 5 being "very confident." To test whether the Chem 125–Snow and Chem 125–Traditional student survey responses were significantly different, unpaired Student's t-tests ($\alpha = 0.05$) were applied, and Cohen's *d* effect sizes were calculated (Table 6—5). In response to all statements gauging student confidence in their familiarity with the snow chemistry research topic, the pre-course survey results for Fall 2016 Chem 125–Snow students showed no statistical difference compared to Chem 125–Traditional students, based on the t-test ($p > 0.05$), but the calculated effect size ($d < 0.35$) indicates a possible small difference (Figure 6—1). There was no statistical significance observed between students' pre-course confidence in general research skills for Fall 2016 Chem 125–Snow and Chem 125–Traditional courses ($p > 0.05$; $d < 0.2$) (Figure 6—3). This establishes that the two student populations are generally comparable in their self-reported confidence in their familiarity with the snow chemistry research topic and general research skills. While survey response data are not

available to assess the Fall 2015 student populations on their pre-course confidence, it is expected that the Fall 2015 students were also comparable because they were recruited in a similar manner from a similar population of students to Fall 2016.

For both Fall 2015 and 2016, post-course survey responses demonstrated that students who received lecture- and research-based instruction on snow chemistry exhibited significantly higher confidence, compared to Chem 125–Traditional students, in the fundamentals of snow chemistry research ($p < 0.001$; $d > 0.8$) (Figures 6—1 & 6—2). While it is unsurprising that Chem 125–Snow students' self-reported greater confidence towards their understanding of the techniques and concepts central to their snow chemistry research, confidence towards a subject is an important factor in student persistence in STEM (Dweck 1986, Graham et al. 2013). The significantly higher post-course survey responses of Chem 125–Snow students to the statement "I feel more informed about climate change" was an especially important finding because recent work has shown that the United States public is under-informed about climate change and its consensus in the scientific community (Leiserowitz et al. 2008, Leiserowitz et al. 2010, Leiserowitz et al. 2012). Chem 125–Snow lectures incorporated climate change science because of its important links to the research conducted by students (Domine et al. 2004, Jacobi et al. 2012, Krnavek et al. 2012, Pratt et al. 2013, Simpson et al. 2015) and a lack of climate change curriculum at all levels of education (Walz and Kerr 2007). Integrating climate change themes and instruction into existing courses,(Mahaffy et al. 2017, Versprille et al. 2017) as shown here, may contribute to efforts to improve climate change understanding amongst the United States public (Walz and Kerr 2007, Leiserowitz et al. 2008, Leiserowitz et al. 2010, Leiserowitz et al. 2012).

Notably, a significantly greater self-reported confidence in response to the statement "I can briefly describe the method of ion chromatography" was observed post-course for both the 2016 Chem 125–Traditional ($p < 0.001$) and Chem 125–Snow ($p < 0.001$) students, compared to their respective pre-course responses. However, the post-course increase in self-reported confidence towards understanding of ion chromatography in Chem 125-Snow (158% increase; d

Table 6—3. Summary of self-assessment survey questions used to gauge student confidence in their ability to perform general research skills and familiarity with the snow chemistry research topic. Survey were completed by students in the Fall 2015 and 2016 snow chemistry (Chem 125–Snow) and traditional (Chem 125–Traditional, control) general chemistry laboratory courses.

How confident do you feel about the following statements below:	
Creating and presenting a research poster.	(1) Not Confident : (5) Very Confident
Determining the main conclusions in a published journal manuscript.	(1) Not Confident : (5) Very Confident
I understand the likely origins of ions in snow.	(1) Not Confident : (5) Very Confident
I know examples of how snow influences the atmosphere.	(1) Not Confident : (5) Very Confident
I can briefly describe the method of ion chromatography.	(1) Not Confident : (5) Very Confident
I feel informed about climate change.	(1) Not Confident : (5) Very Confident

Table 6—4. Self-assessment survey questions from the "Interest and Utility" factor (Bauer 2008) of the Attitude toward the Study of Chemistry Inventory (ASCI) (Xu and Lewis 2011) that composed the "feelings about chemistry" survey category. Students in the Fall 2015 and 2016 snow chemistry (Chem 125–Snow) and traditional (Chem 125–Traditional, control) general chemistry laboratory courses completed the survey. The numerical scale was reversed for some questions during analysis to reflect a scale of 1 being a less positive attitude to 5 being a more positive attitude.

A list of opposing words appears below. Rate how well these words describe your feelings about chemistry. Think carefully and try not to include your feelings toward chemistry teachers or chemistry courses. For each line, choose a position between the two words that describes exactly how you feel. The middle position (3) is if you are undecided or have no feelings related to the terms on that line. Chemistry is:
(1) Worthless : (5) Beneficial
(1) Exciting : (5) Boring
(1) Good : (5) Bad
(1) Interesting : (5) Dull
(1) Worthwhile : (5) Useless

Table 6—5 . Summary of statistical analysis, including p values, Cohen's d effect size, and % changes marked with an asterisk to denote statistical significant changes at the 95% confidence interval, of all self-assessment survey data for students in the Fall 2015 and 2016 snow chemistry (Chem 125–Snow) and traditional (Chem 125–Traditional, control) general chemistry laboratory course.

	Survey Question																			
	I understand the likely origins of ions in snow			**I know examples of how snow influences the atmosphere**			**I can briefly describe the method of ion chromatography**			**I feel informed about climate change**			**Creating and presenting a research poster**			**Determine the main conclusions in a published journal manuscript**			**Attitudes towards chemistry**		
	p	**Change**	***d***	**p**	**Change**	***d***	**p**	**Change**	***d***	**p**	**Change**	***d***	**p**	**Change**	***d***	**p**	**Change**	***d***	**p**	**Change**	***d***
Traditional Pre vs. Snow Pre (2016)	0.75	-3%	-0.06	0.29	10%	0.17	0.06	-15%	-0.31	0.071	9%	0.33	0.95	0%	-0.01	0.75	2%	0.06	0.16	2%	0.11
Traditional Post vs. Snow Post (2016)	2.2 E-16	91%*	2.04	1.1 E-13	80%*	1.72	3.0 E-10	39%*	1.20	1.4 E-06	28%*	0.83	1.4 E-4	21%*	0.63	0.038	9%*	0.36	0.24	3%	0.09
Traditional Pre vs. Traditional Post (2016)	1.3 E-15	21%*	0.36	0.37	-2%*	-0.04	4.5 E-92	58%*	0.89	4.0 E-4	-5%*	-0.15	1.5 E-05	-7%*	-0.18	1.1 E-17	12%*	0.40	2.5 E-71	-10%*	-0.37
Snow Pre vs. Snow Post (2016)	8.8 E-17	139%*	3.08	1.1 E-07	61%*	1.41	3.1 E-20	158%*	4.03	0.079	11%	0.49	0.073	14%	0.44	0.005	21%*	0.74	2.1 E-4	-10%*	-0.44
Traditional Pre vs. Snow Pre (2015)	-	-	-	-	-	-	-	-	-	-	-	-	-	-	-	-	-	-	0.21	2%	0.11
Traditional Post vs. Snow Post (2015)	1.6 E-16	75%*	1.76	1.1 E-14	80%*	1.81	2.7 E-10	37%*	1.33	1.4 E-23	64%*	1.91	8.49 E-15	36%*	-	2.0 E-06	23%*	1.50	3.1 E-08	12%*	0.50
Traditional Pre vs. Traditional Post (2015)	-	-	-	-	-	-	-	-	-	-	-	-	-	-	-	-	-	-	9.0 E-33	-7%*	-0.29
Snow Pre vs. Snow Post (2015)	-	-	-	-	-	-	-	-	-	-	-	-	-	-	-	-	-	-	0.74	1%	0.05

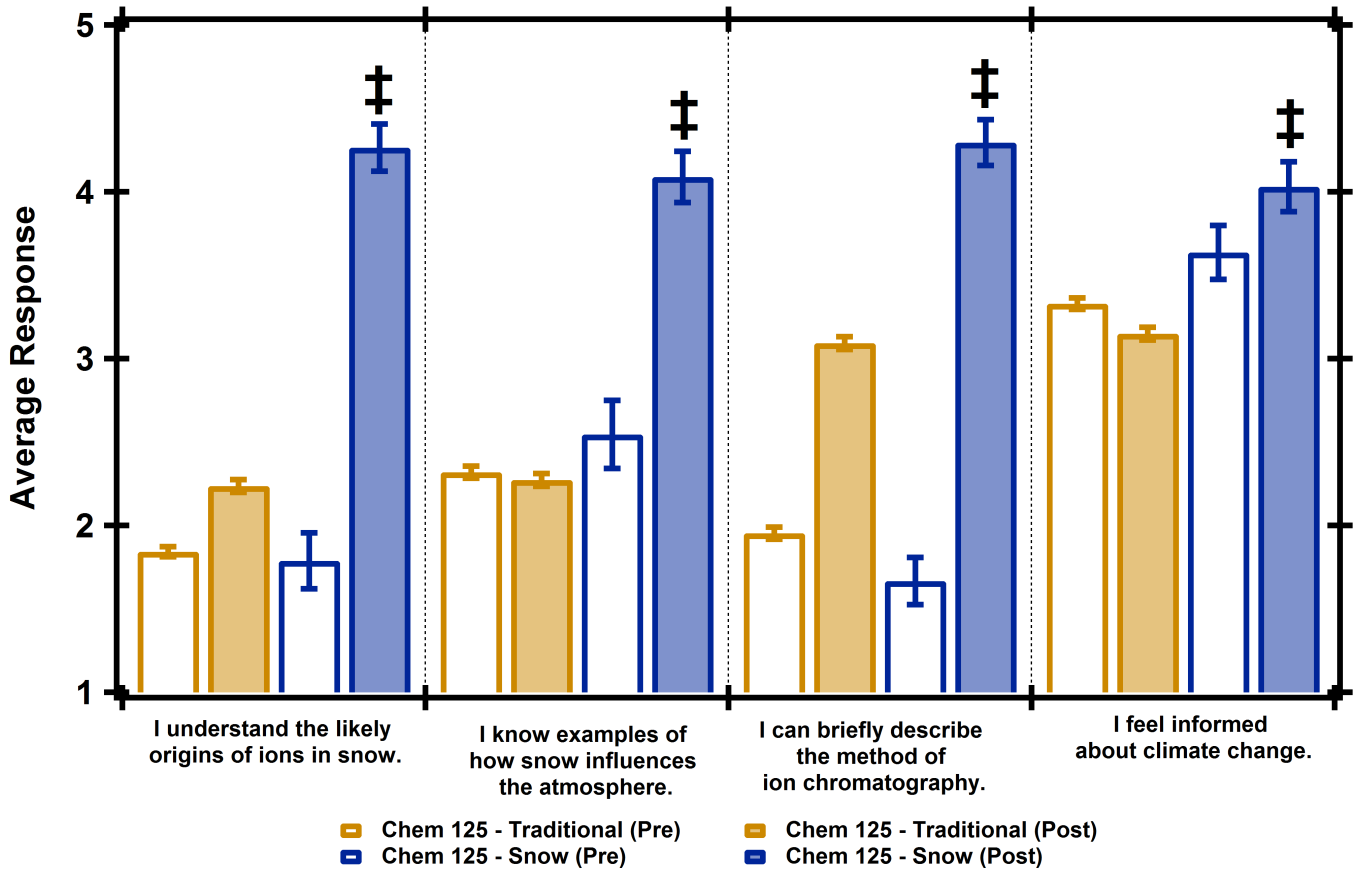

Figure 6—1. Average pre- and post-course responses to self-assessment survey questions regarding confidence in snow chemistry research topics, on a scale of 1 being "not confident" to 5 being "very confident" and with error bars shown as standard error of the mean, for students in the Fall 2016 snow chemistry (Chem 125–Snow; N = 34) and traditional (Chem 125–Traditional; N = 920) general chemistry laboratory courses (control). ǂ indicates pre-course and post-course responses for students in the snow chemistry course that are statistically significant at the 95% confidence interval compared to the traditional general chemistry laboratory course students.

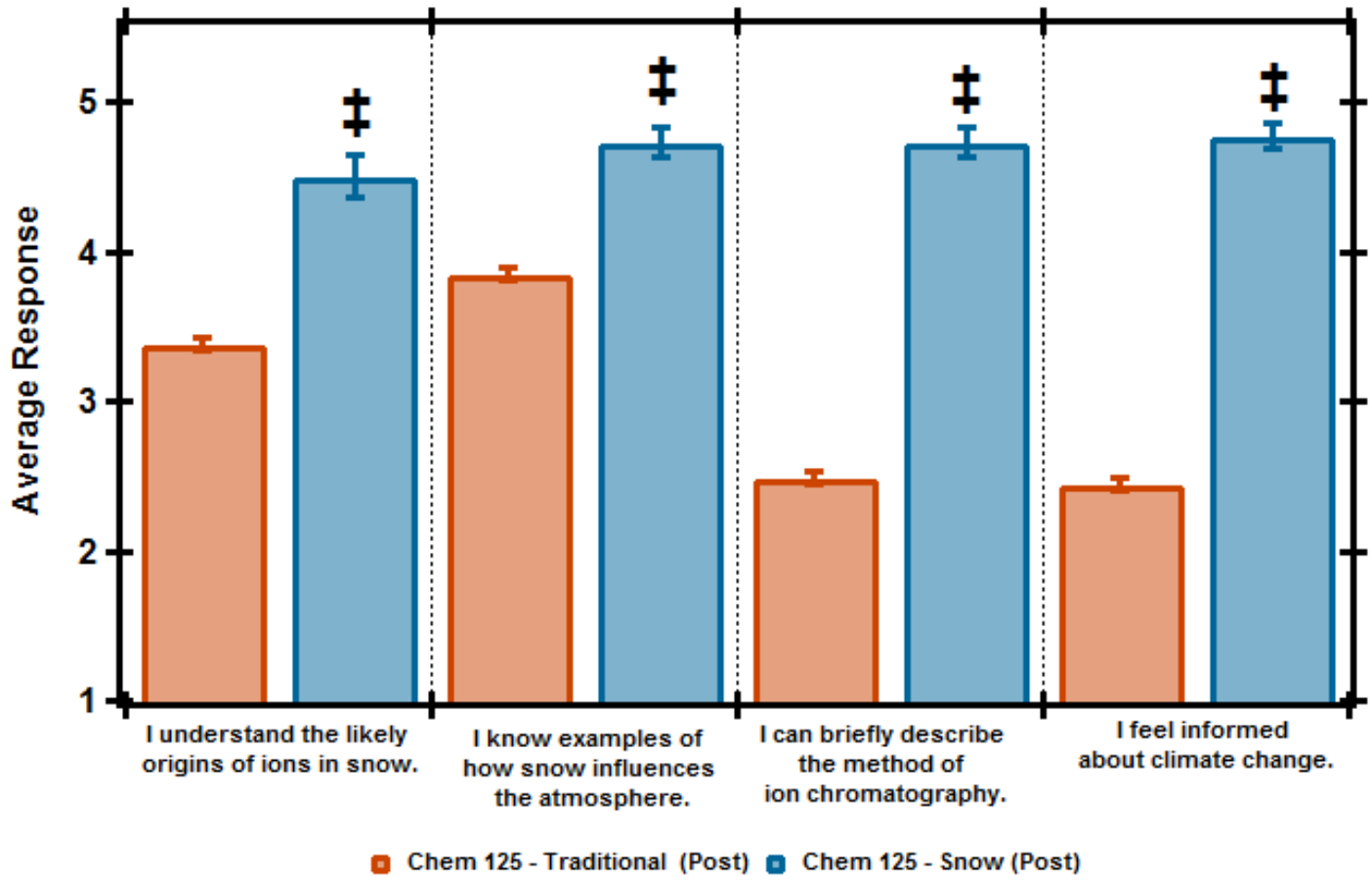

Figure 6—2. Average post-course responses to self-assessment survey questions regarding confidence in snow chemistry research topics, on a scale of 1 being "not confident" to 5 being "very confident", for students in the Fall 2015 snow chemistry (Chem 125–Snow) and traditional (Chem 125–Traditional, control) general chemistry laboratory courses. ǂ indicates responses for students in the snow chemistry course that are statistically significant at the 95% confidence interval compared to the traditional general chemistry

> 4) was much larger than the increase observed for the Chem 125-Traditional (58% increase; $d >$ 0.8). In addition, the self-reported confidence towards understanding of ion chromatography was significantly higher ($p < 0.001$; $d > 1$) post-course for Chem 125-Snow compared to Chem 125–Traditional. Therefore, we can conclude that the integration of ion chromatography into Chem 125-Snow had a measurable effect on student self-reported confidence. The significant increase in confidence in Chem 125–Traditional, which did not include ion chromatography, is possibly the result of the students' participation in a laboratory experiment on the use of thin layer chromatography that may have led to students to falsely state high confidence in other types of chromatography.

The post-course survey responses also indicated that Chem 125–Snow positively impacted students' confidence in general research skills (Figures 6—3 & 6—4). In particular, these students, who participated in a scientific literature laboratory session and incorporated scientific literature into their posters and manuscripts, had a significantly greater self-reported confidence ($p < 0.05$; $d > 0.3$) in utilizing scientific literature at the end of the semester compared to Chem 125–Traditional students, who had no formal instruction or practice with scientific literature. Similarly, Chem 125–Snow students, who received instruction on poster-making, made a poster, and then presented it at the public poster session, exhibited significantly higher self-reported confidence in creating and presenting a research poster at the end of the semester ($p < 0.001$; $d > 0.6$). Overall, the higher self-reported student confidence in research skills suggests that students left Chem 125–Snow more prepared than students in Chem 125–Traditional to be active members of the scientific community where these research skills are consistently utilized.

At the beginning and end of the Fall 2015 and 2016 courses, students were asked a series of questions, from the "Interest and Utility" factor (Bauer 2008) of the ASCI (Xu and Lewis 2011), about their feelings, on a scale of 1 being a less positive attitude to 5 being a more positive attitude, about chemistry. Unpaired Student's t-tests ($\alpha = 0.05$) were conducted, along with calculation of Cohen's d effect sizes, between Chem 125–Snow and Chem 125–Traditional student survey responses to determine if the responses of the two populations were significantly different (Table 6—5). The student responses to these questions regarding feelings about chemistry were averaged together (Figure 6—5), with individual questions shown in Table 6—4.

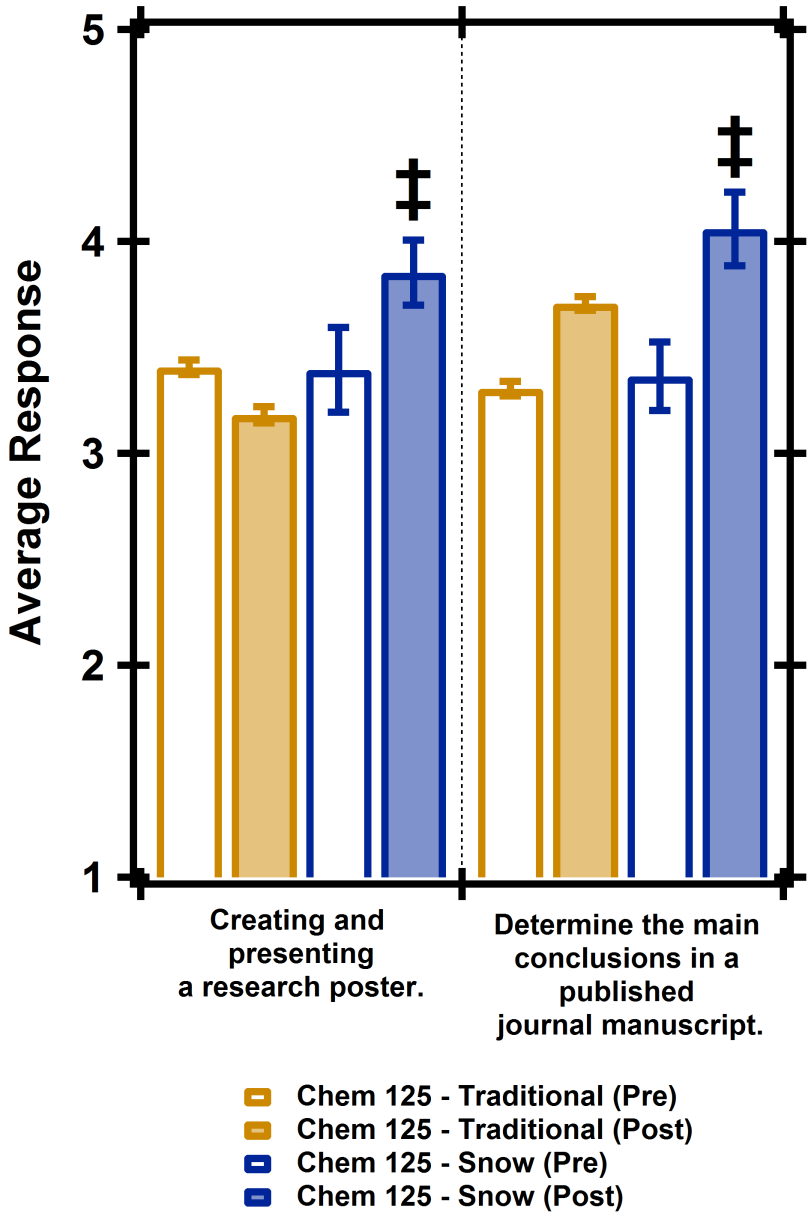

Figure 6—3. Average pre- and post-course responses to self-assessment survey questions regarding confidence in general research skills, on a scale of 1 being "not confident" to 5 being "very confident" and with error bars shown as standard error of the mean, for students in the Fall 2016 snow chemistry (Chem 125–Snow; N = 34) and traditional (Chem 125–Traditional; N = 920) general chemistry laboratory courses (control). ǂ indicates pre-course and post-course responses for students in the snow chemistry course that are statistically significant at the 95% confidence interval compared to the traditional general chemistry laboratory course students.

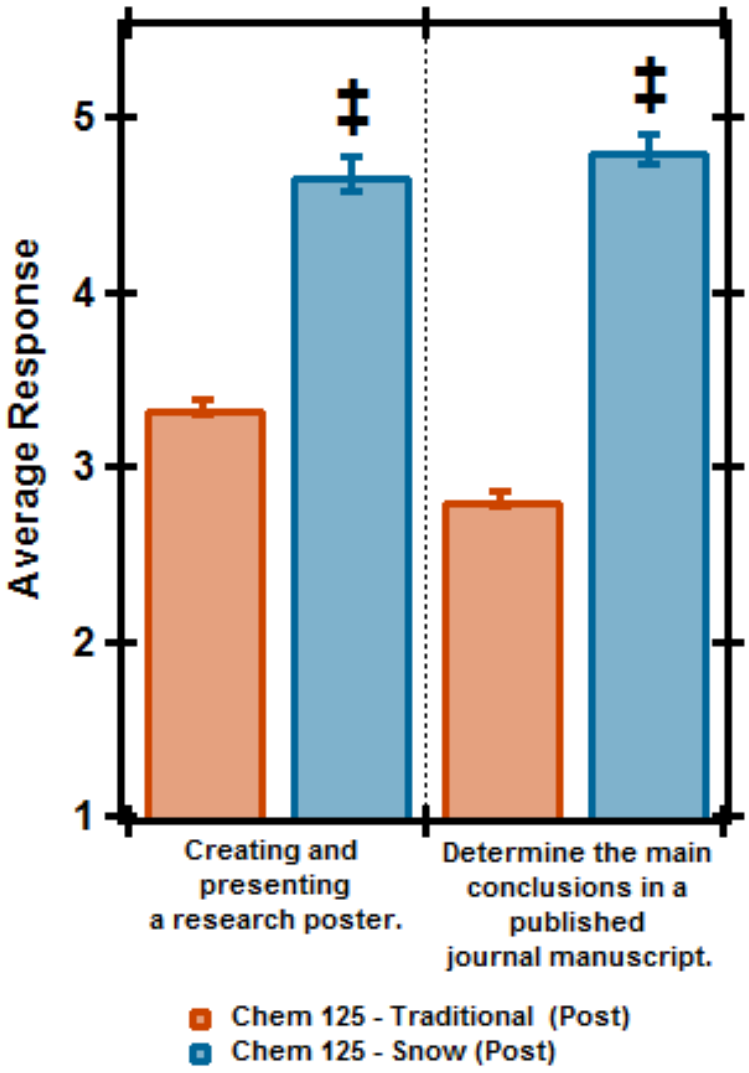

Figure 6—4. Average post-semester responses to self-assessment survey questions regarding confidence in general research skills, on a scale of 1 being "not confident" to 5 being "very confident", for students in the Fall 2015 snow chemistry (Chem 125–Snow) and traditional (Chem 125–Traditional, control) general chemistry laboratory courses. ǂ indicates responses for students in the snow chemistry course that are statistically significant at the 95% confidence interval compared to the traditional general chemistry laboratory course students.

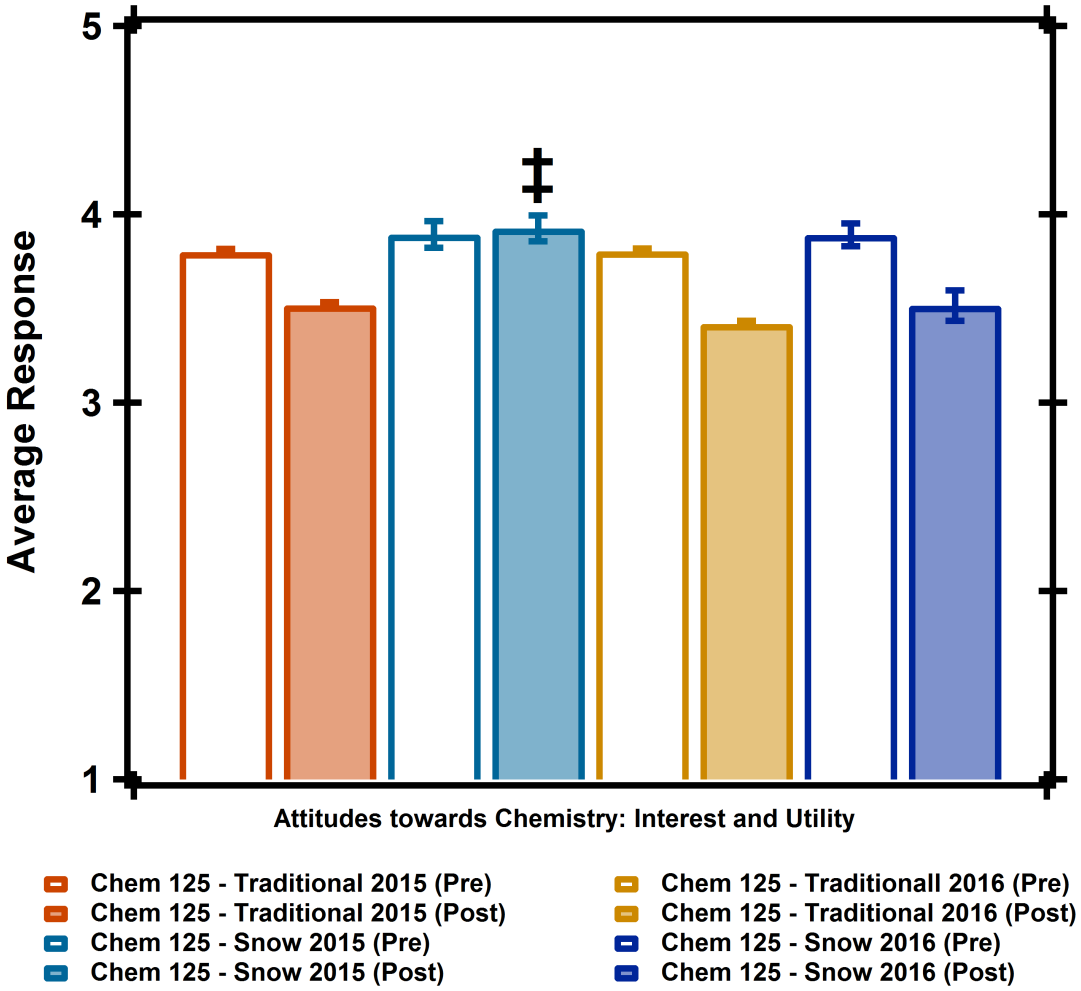

Figure 6—5. Average pre-course and post-course responses to survey questions regarding attitudes towards chemistry, on a scale of 1 being a less positive attitude to 5 being a more positive attitude and with error bars shown as standard error of the mean, for students in the Fall 2015 and 2016 snow chemistry (Chem 125–Snow; N = 34) and traditional (Chem 125–Traditional; N = 920) general chemistry laboratory courses (control). ǂ indicates pre-course and post-course responses for students in the snow chemistry course that are statistically significant at the 95% confidence interval compared to the traditional general chemistry laboratory course student.

For both years, the pre-course surveys in both Chem 125–Snow and Chem 125–Traditional showed no statistically significant differences ($p > 0.1$; $d < 0.15$). In the Fall 2015 post-course survey, Chem 125–Snow students responded with a significantly higher score ($p < 0.001$; $d > 0.5$) compared to the Chem 125–Traditional students, which exhibited a significant decrease in positive attitudes compared to pre-course ($p < 0.001$; $d > 0.5$). For Fall 2016, the post-course responses in both Chem 125-Snow and Chem 125-Traditional were significantly lower than the pre-course responses ($p < 0.001$, $d > 0.3$; $p < 0.001$, $d > 0.4$), respectively. While the Fall 2016 Chem 125-Snow post-course response was higher than Chem 125-Traditional, no statistical difference was discerned ($p > 0.1$; $d < 0.1$) (Figure 6—5). Similar post-course decreases in student attitudes have been reported, using the ASCI survey tool, for low-performing general chemistry students (Brandriet et al. 2011) and organic chemistry students (Mooring et al. 2016). Most notably, previous ASCI survey responses for general chemistry courses report male students having post-course attitude gains in contrast to their female counterparts who demonstrated post-course losses (Brandriet et al. 2011). Therefore, pervasive negative attitudes exhibited toward science by female students (Weinburgh 1995, Cheung 2007, Barmby et al. 2008) may have skewed the Chem 125 – Snow (female majority) survey results low, compared to the gender balanced Chem 125 – Traditional course. Continuing work by the Authentic Research Connection Program is investigating student outcomes in detail to examine potential long-term impacts of this CURE, including increased retention in STEM majors of participating students.

6.3.2. Student Feedback

As a part of the post-course survey process, students were asked two open-ended questions to assess the aspects of the course students viewed as positives, or those needing improvement. 35 student responses, collected between the Fall 2015 and 2016 semesters of Chem 125 – Snow were qualitatively analyzed by emergent and multiple coding, with the number of related responses for each thematic category and representative quotes provided here. In response to the first question ("What do you like most about the course? Why?"), the most common responses (15 responses) emphasized the integration of the research experience into all aspects of the course: *"I like the integration of research questions into the course because it makes what we are learning more applicable and interesting."* These responses demonstrate that the integration of research helps students establish a relationship between content and the real-

world (Kember et al. 2008, Williams and Williams 2011), while also highlighting the potential of CUREs to develop a larger population of students with interest in current research (Bakshi et al. 2016). Another common response subject focused on the relevancy of the course to students' life (9 responses): "*I liked how the topics were related to every day concepts and things that I care about like climate change and the environment.*" These response demonstrate that integration of environmental topics and research into courses helps students establish a relationship between content and the real-world (Kegley and Stacy 1993, Swan and Spiro 1995, Bachofer 2008, Kember et al. 2008, Williams and Williams 2011, Tomasik et al. 2013, Tomasik et al. 2014). Most other responses were related to the interactive nature of the laboratory course (8 responses): "*I liked the hands-on application of the topics learned in the course."* The consensus of student comments supports the quantitative student survey response data that the integration of the environmental research experience had a positive influence on their experience with chemistry.

Responses to the second question ("What would you change about the course? Why?") highlight the challenges of implementing a new laboratory course, especially one that is research-based. For example, the most common student responses were focused on the need for more guidance due to the challenges of the research experience (15 responses): "*More specific directions as to what we should be doing and how to approach the research assignment*" and "*By going over lab procedure a little bit more thoroughly*." These responses show that these students faced similar challenges, as those in previous CURE courses (Kowalski et al. 2016), due to the increased independent thought and effort required in a research experience. The open-ended nature of research requires course instructors in CUREs to offer increased encouragement in response to experimental difficulties to help students understand that failure is a part of science (Bakshi et al. 2016). The Fall 2015 responses guided revisions to the following year's course, with the additional structure (e.g. expansion of the research poster creation laboratory session) added to the course, yet the challenge of greater uncertainty in authentic research, compared to traditional experiments, still remains. Despite these challenges, none of the student responses to the second question mentioned the snow chemistry research focus as a reason for disliking the course, further supporting that integration of an environmental research experience had a positive influence.

6.4. Conclusions

A snow chemistry research-based general chemistry laboratory course was developed and piloted at the University of Michigan during Fall 2015 and 2016. First and second year students

learned traditional general chemistry laboratory concepts and skills through Arctic snow chemistry research (Pratt et al. 2013) during interconnected research-based laboratory experiments. These students conducted independent analyses of Arctic snow composition in a semester-long authentic research experience using ion chromatography, with results contributing to the PI's ongoing research. This work represents a successful combination of the pedagogical approaches of incorporating an environmental focus and research into the general chemistry laboratory curriculum through the CURE format (Auchincloss et al. 2014).

The structure of Chem 125 – Snow provides a framework for others to similarly transform their general chemistry laboratory curricula to incorporate authentic environmental chemistry research. This pilot implementation of the environmental chemistry CURE included exposure to scientific literature and data analysis, and culminated in the development of research questions, data interpretation, and the presentation of results through a public, volunteer judged poster symposium and a written manuscript, thus mirroring all steps of the research process. While this particular course focused on Arctic snow chemistry, the course could be adapted for analysis of other water-related research questions (e.g. increasing freshwater salinity due to road salt usage) (Dugan et al. 2017). A current advantage, and yet limitation, of this pilot course is its reliance on the resources of the PI's laboratory, which, in its current form, may limit the feasibility of future implementation of this course format by others (Lopatto et al. 2014). As discussed by Brownell et al. (2015), the implementation of CUREs, such as Chem 125 – Snow, can be challenging for larger enrollment settings due to higher costs, in-lab computer access, and the need for an increased number of research-trained instructors, compared to traditional laboratory courses. A particular challenge for scale-up, and yet a significant benefit (according to student surveys), of Chem 125 – Snow is Experiment 10, which involves student visits to the PI's laboratory for individual snow analyses using IC. In future work we will seek to determine best practices for incorporating environmental chemistry research into the curricula at primarily undergraduate institutions.

Student survey evaluation results showed that students in Chem 125 – Snow developed self-confidence in their understanding of the snow chemistry research topic and general research skills. Together with the increase in positive attitudes towards chemistry, these results are important as confidence and attitudes toward chemistry are both identified as key factors for retention in STEM (Dweck 1986, Graham et al. 2013). In addition, responses to open-ended questions revealed students appreciated that the research-based laboratory model provided real-

world applications of class material and that students were engaged by connections to the natural environment. The positive impacts on undergraduate students of this, and other, research-based introductory chemistry courses (Holme 1994, Hutchison and Atwood 2002, Ford et al. 2008, Richter-Egger et al. 2010, Clark et al. 2016) demonstrate that undergraduate students are capable of participating in, and benefiting from, research experiences at an early academic career stage. In addition, the leadership of the PI in the CURE provided access to a female research mentor for undergraduate women, an important step in increasing their retention in sciences (Wendel 2015). This general chemistry laboratory course thus demonstrates, like other implementations of CUREs in chemistry laboratory courses,(Clark et al. 2016, Kerr and Yan 2016) that a greater number of students can be exposed to the benefits of a research-experience through the CURE format, compared to traditional undergraduate research experiences in individual laboratories (Auchincloss et al. 2014, Rodenbusch et al. 2016).

6.5. Acknowledgments

Stephen M. McNamara, Dr. Siyuan Wang, and Dr. Katheryn Kolesar are thanked for their contributions as co-instructors. Dr. Julianne Vernon, Prof. John P. Wolfe, and Prof. Deborah Goldberg are thanked for their contributions to the course through the U-M Authentic Research Connection program, which was funded by the Howard Hughes Medical Institute (52008119) and is thanked for primary financial support of this work. Additional funding was provided by the U-M Department of Chemistry, the U-M Program in the Environment, and the National Science Foundation Arctic Research Support and Logistics Program. Ignatius Rigor (University of Washington) and the US Interagency Arctic Buoy Program are thanked for collection of the Arctic snow samples used during Fall 2015 and the TOC art photograph. Claire Mattson and Alicia Kevelin (U-M) are thanked for assistance in the collection of Arctic snow samples used during Fall 2016. Mark Hartwig, Evan Schwartz, Anna Leemon, and Alexa Watson (U-M) are acknowledged for their work as undergraduate assistants in the course. Ye Li and Scott Martin are acknowledged for their contributions as science librarians. Alexander Poniatowski (U-M) is acknowledged for helpful conversations and support of this course as the instructor of Chem 125-Traditional. Brian Coppola (U-M) is thanked for discussions.

Chapter 7 Determination of Chloride Content in Snow & Water Samples: Environmental Chemistry Research Based Laboratory Experiment

In preparation for submission to *Journal of Chemical Education*

7.1. Introduction

In the environment, chloride exists at concentrations that span several orders of magnitude, ranging from 0.1 mg/L in rainwater (Junge and Werby 1958, Post et al. 1991, Neal et al. 2007) to 35 g/L in seawater (Table 7—1) (Pilson 2013). Chloride in environmental waters can come from natural sources such as dissolved rocks and minerals (Lisensky and Reynolds 1991). In addition, anthropogenic sources, such as the application of salt to roads during winter for de-icing (Kolesar et al. 2018), can result in chloride accumulation in snow (Oliver et al. 1974, Mihailovic et al. 2014) and surface waters (Jackson and Jobbagy 2005, Dugan et al. 2017). The chloride content of natural waters is of interest to the environmental chemistry (Dugan et al. 2017) community because high concentrations of chloride can negatively impact ecosystems (Findlay and Kelly 2011) and damage metal structures (Fink 1960). The examination of chloride concentrations in environmental samples is an ideal topic for a research-based introductory chemistry laboratory experiment as it addresses active topics in the scientific community using locally accessible samples.

Chloride concentrations can be determined in the laboratory using the Mohr Method titration (Park 1958, Ibanez et al. 2008), involving the following precipitation reactions:

$$Ag^{+}_{(aq)} + Cl^{-}_{(aq)} \rightarrow AgCl_{(s)}$$

$$2Ag^{+}_{(aq)} + CrO_4^{2-}{}_{(aq)} \rightarrow Ag_2CrO_{4\ (s)}$$

A measured amount of a known concentration standard $Ag^{+}_{(aq)}$ solution is added to a sample of unknown $Cl^{-}_{(aq)}$ concentration with $CrO_4^{2-}{}_{(aq)}$ indicator added. After all $Cl^{-}_{(aq)}$ has reacted with the added $Ag^{+}_{(aq)}$ to form $AgCl_{(s)}$ (white precipitate), $Ag_2CrO_{4(s)}$ (red precipitate) forms and signals the endpoint of the titration. Lisensky and Reynolds (1991) presented an analytical chemistry laboratory experiment for the determination of chloride in freshwater samples using a potentiometric titration method. However, the potentiometric detection method requires specialized equipment with a relatively complex assembly (Lisensky and Reynolds 1991) and is a

Table 7—1. Environmental water sample chloride concentrations

Environmental Source	Concentration Range
Rain **(Junge and Werby 1958, Post et al. 1991, Neal et al. 2007)**	0.1 – 200 mg/L
Snow **(Oliver et al. 1974, Krnavek et al. 2012, Mihailovic et al. 2014)**	0.4 mg/L – 15 g/L
Freshwater lakes **(Chapra et al. 2012, Dugan et al. 2017)**	1 – 240 mg/L
Ground/drinking water **(Mullaney et al. 2009)**	3 – 250 mg/L
Stormwater/urban streams **(Corsi et al. 2010, Corsi et al. 2015)**	0.01 – 11 g/L
Seawater (Pilson 2013)	19.4 g/L

concept not typically introduced in introductory chemistry curriculum , which may challenge its implementation in the introductory undergraduate or high school laboratory.

With the National Research Council's 2012 Framework for K-12 Education (National Research Council 2012) and the Next Generation Science Standards (NGSS Lead States 2013) advocating for increased implementation of authentic science practices into the high school and undergraduate curricula, it is vital to present accessible research-based laboratory experiments to educators. Environmental chemistry is well suited for creating an exploratory laboratory experience more akin to authentic research as the samples under investigation are by nature not well-defined (Kegley and Stacy 1993, May et al. 2018). In addition, measuring the concentrations of chemical species in environmental samples engages students with real-world connections while providing a quantitative laboratory experiment experience (Lisensky and Reynolds 1991, Tabbutt 2000, Salido et al. 2003, Bachofer 2008, May et al. 2018). The Mohr Method utilizes low-cost, accessible laboratory equipment to determine chloride concentrations in environmental samples, and, with the authentic research-based experimental structure presented here, provides a means for integrating science practices outlined in recent science reform efforts (National Research Council 2012, NGSS Lead States 2013).

7.2. Experimental

7.2.1. Materials, Safety, & sample Handling

Using distilled or deionized water, the 5% chromate indicator solution is prepared with potassium chromate (K_2CrO_4), and the silver titrant solution (0.001 – 0.01 M) is prepared with silver nitrate ($AgNO_3$). All stock solutions should be prepared by the instructor using personal protective equipment (PPE) because $AgNO_3$ and K_2CrO_4 solutions are strong oxidizers that can cause injuries and stain skin. The required laboratory equipment includes burettes, glassware, polypropylene scoops, and polyethylene bags. To minimize ion loss during storage and sample contamination, it is recommended to collect samples in pre-cleaned polyethylene bags (Whirl-Pak, Nasco), freeze after collection, and then thaw immediately prior to analysis. All containers used for sample analysis are triple rinsed with deionized or distilled water to prevent contamination of samples with chloride. For the first implementation in a class of 30 students working in pairs, the total chemical and laboratory equipment per student cost is ~$15. However, this represents an upper cost limit as the consumable (chemicals, sample bags) costs for further iterations is less than $5 per student. PPE, including safety glasses, protective gloves, lab coat, long trousers, and covered shoes, must be worn during the experiment to prevent chemical exposure. Disposable nitrile gloves also prevent the contamination of samples with chloride.

7.2.2. Determination of Chloride Content in Environmental Samples

Pour the selected $AgNO_{3(aq)}$ solution into a 25 mL burette and record the position of the meniscus on the burette. Next, introduce approximately 3 drops of the 5% $K_2CrO_{4(aq)}$ solution to a 5 mL portion of the chloride-containing aqueous solution, yielding a yellow tint. Add the $AgNO_{3(aq)}$ solution from the burette into the sample in a dropwise manner, mixing the solution after every addition of $AgNO_{3(aq)}$ by manually swirling, or by the use of a stir bar and stir plate. As the $AgNO_{3(aq)}$ solution from the burette is added to the sample, an orange-red will start to appear, but will disappear with mixing. Continuously add the $AgNO_{3(aq)}$ titrant solution from the burette into the sample until the color change persists with stirring. The persistence of the color change indicates that all of the $Cl^-_{(aq)}$ in the sample reacted with the $Ag^+_{(aq)}$ from the titrant to form $AgCl_{(s)}$, and the $Ag^+_{(aq)}$ from the titrant is reacting with the $CrO_4^{2-}{}_{(aq)}$ added to the sample to form the red $Ag_2CrO_{4(s)}$. Repeat this process over 3 trials for each sample analyzed to ensure precision

of results. The students should compare the endpoint color of the triplicate titration solutions to maintain consistency in endpoint determination.

The ideal concentration of $AgNO_{3(aq)}$ titrant solution used is dependent on the range of concentrations expected for the particular environmental samples (Table 7—1). For $Cl^-_{(aq)}$ solutions ranging from 0.002 to 0.1 g/L, an $AgNO_{3(aq)}$ concentration of 0.001 M limits the titrant volume between 0.5 and 15 mL. Similarly, an $AgNO_{3(aq)}$ concentration of 0.01 M limits the titrant volume to 0.5 to 15 mL for $Cl^-_{(aq)}$ solutions ranging from 0.05 to 1.0 g/L. Using a higher concentration of $AgNO_{3(aq)}$ than recommended here results in small titrant volumes (<0.5 mL) needed to reach the end point; these are more difficult to measure reproducibly using standard 25 mL burettes with 0.1 mL graduations. Using a lower concentration of $AgNO_{3(aq)}$ results in larger titration volumes (>25 mL), which will require students to refill burettes. Solutions with $Cl^-_{(aq)}$ concentrations above 1.0 g/L, such as seawater (35 g/L), should be diluted to reduce the need for high volume or concentration $AgNO_{3(aq)}$ titrant.

7.3. Results & Discussion

This Mohr Method laboratory experiment to measure chloride in environmental samples was successfully implemented into the introductory undergraduate laboratory as a part of a semester-long course-based undergraduate research experience in Arctic snow chemistry (May et al. 2018). Through this experiment, the undergraduate students in this course were exposed to general chemistry concepts and laboratory skills, as well as snow chemistry fundamentals, needed to complete their semester-long research project (May et al. 2018). However, this experiment does not require a semester-long course for implementation and could provide a means for integration authentic science practices into undergraduate or high school curricula as a stand-alone research experience (National Research Council 2012, NGSS Lead States 2013). To extend this work and evaluate the ability of high school students to conduct this environmental chemistry research, this laboratory experiment was implemented in a professional development workshop for high school teachers held on the University of Michigan (U-M) campus through the Inter-professional STEM Learning Community (STEM-IPLC) program. On the first day of this workshop, three high school teachers participated in the experiment to familiarize themselves with the material. On the following day, the high school teachers guided a group of 16 volunteer high school students through the environmental chemistry research experience. The environmental chemistry research experience was completed in a 3 h session, with each hour devoted to individual sections focused

on: 1) formation of research questions, 2) laboratory experiment, and 3) synthesis of experimental results in the context of research questions. As demonstrated in previous integrations of research experiences into introductory undergraduate and high school courses, it was important in each of these sections for the instructor to provide the structure and guidance vital for the success of young researchers (Harris 1977, Newton et al. 2006, Ford et al. 2008, Canaria et al. 2012, Pueyo et al. 2013, May et al. 2018). While 3 h was sufficient to expose the high school students to science practices outlined in the Framework for K-12 Science Education (National Research Council 2012) through the research-based laboratory experiment, time constraints associated with the workshop limited portions of the research experience. Therefore, recommendations are presented for implementation in an extended time format, wherein individual classroom meetings are devoted to each section of the research experience.

The high school workshop began by establishing the broader context of the sources and impacts of chloride in the environment through a teacher-led discussion. However, if more time is available, students can independently investigate primary scientific literature using a scavenger hunt activity, which can reduce challenges associated with introducing young students to primary scientific literature (Lijek and Fankhauser 2016, May et al. 2018). This was successfully completed as one 3 h session in our introductory undergraduate laboratory (May et al. 2018). Following this introduction, the instructors focused on specific implications for the local environment, in this case an urban wintertime environment where road salt accumulates in snow. The teachers then engaged the students in the Framework for K-12 Science Education's science practice of "asking questions" (National Research Council 2012) by leading them to utilize their own life experiences living in a cold climate and their new understanding of chloride in the environment to develop research questions and hypotheses to test through the measurement of chloride concentrations in local snow. To aid in the high school students' formation of hypotheses, the instructors presented a general format of a hypothesis in the form of a "If _____, then _____, because _____" statement, wherein the "if" is followed by a statement of how the independent variable (in this case the sample location) will be manipulated, the "then" is followed by a statement of how the dependent variable (in this case the chloride concentration) is anticipated to respond to the change, and the "because" is followed by an explanation that links the variables. For example, the high school students utilized this format to hypothesize: If snow is closer to roadways where salt is applied, then the snow chloride concentration will be higher, because road salt composed primarily of sodium

chloride will be flung from the road by cars driving and deposit on the nearby snow. The high school students were then provided with local snow samples, collected by the instructional staff during a previous winter, to test their hypotheses. However, if additional time is available, this section of the research experience can include instructor-guided environmental sample collection planning, including the sample collection procedure and location(s) and time(s) of sample collection. Students can then collect samples during or outside of class sessions, dependent upon time availability and sampling site accessibility. In doing so, students would receive a deeper exposure to the "planning" portion of the Framework for K-12 Science Education's science practice of "planning and carrying out investigations" (National Research Council 2012).

The second section of the research experience focused on the measurement of chloride concentrations in the environmental samples. To introduce the concept of titration and associated calculations, the high school students completed a worksheet. After completing the worksheet, the teachers discussed practical experimental tips for titration, including reading the burette meniscus at eye level, as well as adding drops slowly from the burette and stirring the sample constantly. As a part of this discussion, the teachers demonstrated the ideal titration endpoint using a snow sample. Given the small color changes observed, this demonstration helps overcome potential challenges students may face in endpoint determination (Lisensky and Reynolds 1991). The endpoint is best visualized by comparison with a flask containing 5 mL of water with 3 drops of 5% $K_2CrO_{4(aq)}$ solution added, but with no $AgNO_{3(aq)}$ titrant solution introduced (Figure 7—1). In future implementations, it is recommended to demonstrate the endpoint with a solution of 0.004 g/L $Cl^-_{(aq)}$ titrated by 0.001 M $AgNO_{3(aq)}$ solution (Figure 7—1a) and a 0.5 g/L $Cl^-_{(aq)}$ solution titrated by 0.01 M $AgNO_{3(aq)}$ solution (Figure 7—1b) show differences in endpoint appearance based on concentration. The students will observe that the formation of the white $AgCl_{(s)}$ precipitate produces an opaquer final solution when the 0.01 M $AgNO_{3(aq)}$ titrant solution is used to measure higher concentration $Cl^-_{(aq)}$ solutions, compared to when the 0.001 M $AgNO_{3(aq)}$ titrant solution is used to measure lower concentration $Cl^-_{(aq)}$ solutions.

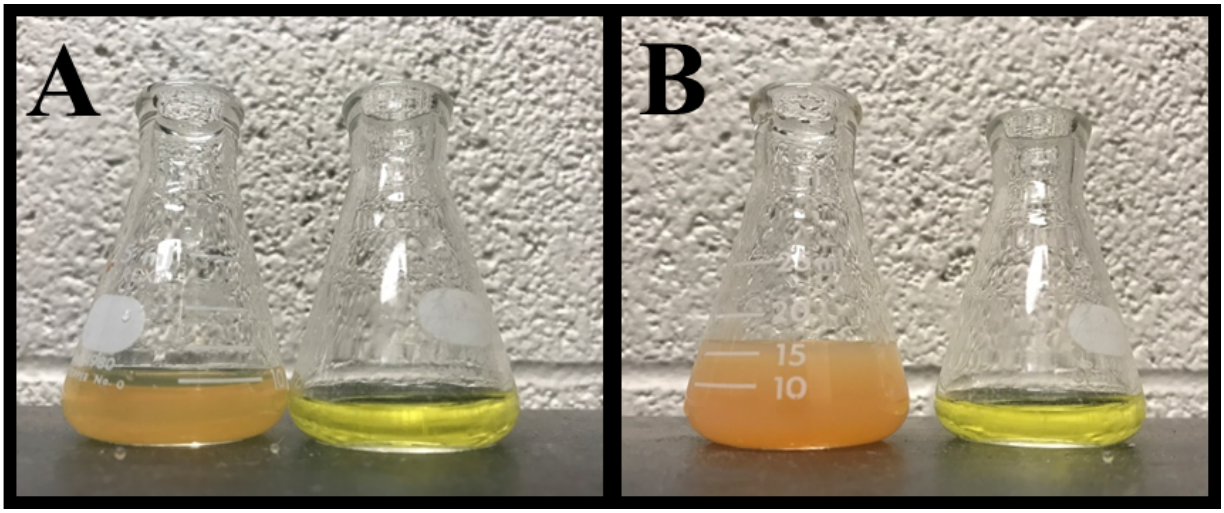

Figure 7—1. Comparison of starting solution color (yellow) and endpoint solution color (orange) for (A) 0.004 g/L $Cl^-_{(aq)}$ titrated by 0.001 M $AgNO_{3\,(aq)}$ and (B) 0.5 g/L $Cl^-_{(aq)}$ titrated by 0.01 M $AgNO_{3\,(aq)}$.

Students, working in pairs, measured the chloride concentration, in triplicate, of snow samples collected on the U-M campus from "Roadside" locations directly adjacent to a street where road salt was applied, as well as "Campus" locations surrounded by buildings and >100 m from any streets, but near sidewalks where deicing brine was applied. Snow chloride concentrations measured by the students ranged from 0.006 to 0.14 g/L, with higher chloride concentrations present in Roadside samples (0.05 ± 0.05 g/L) compared to Campus samples (0.02 ± 0.02 g/L). While this result was not statistically significant, it reflected the student-generated hypothesis that samples collected closer to roads would have higher chloride concentrations and could be further confirmed by a larger sample size (Figure 7—2). Only one sample collected away from the road (2/16/16 Campus) exhibited a higher chloride concentration (0.040 ± 0.005 g/L) than samples collected near roads; however, the sample collected near the roadway (2/16/16 Roadside) that same day was characterized by the highest chloride concentration measured across all samples (0.12 ± 0.02 g/L) (Figure 7—2). The high school students interpreted this to be the result of the snowpack remaining undisturbed preceding this date, leading to an accumulation of road salt-derived chloride in the snowpack, followed by heavy snowfall that diluted the concentration of chloride in subsequent samples, such as the 2/27/16 Roadside sample (0.012 ± 0.002 g/L). While 5 out of the 8 pairs of students had reasonable precision in their triplicate measurements (%

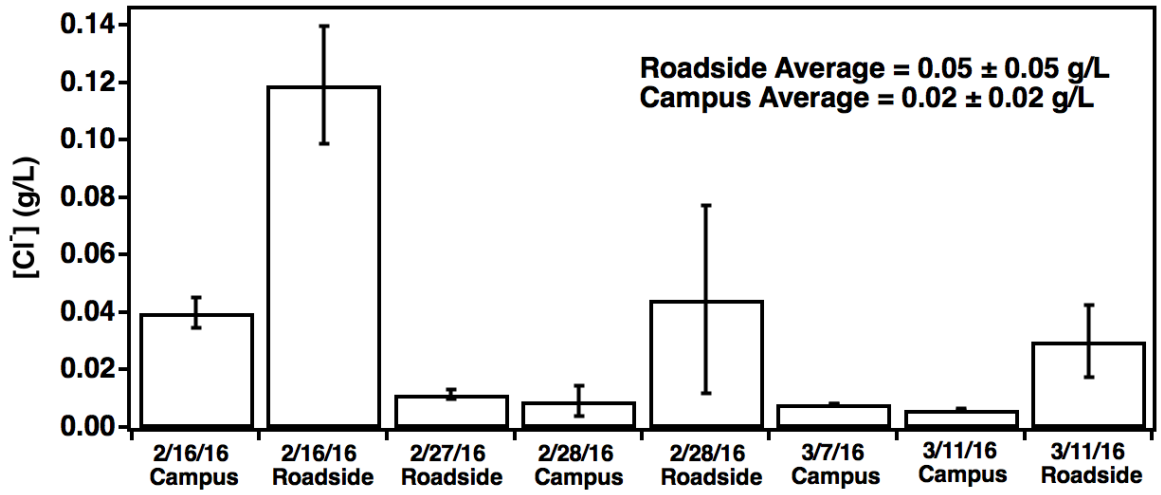

Figure 7—2. Snow chloride concentrations measured by high school students utilizing the Mohr Method for samples collected in Ann Arbor, MI near (Roadside) and away (Campus) from roads in February and March 2016.

standard deviation < 0.2), the remaining 3 pairs of students of reported low precision (% standard deviation = 0.4 – 0.7) (Figure 7—2). High school students may thus require more titration practice or instructional guidance to ensure higher precision. To complete this section of the research experience, the students entered individual snow sample data generated from their titrations into a shared spreadsheet to produce a dataset to be analyzed by the entire class. Through the process of measuring the chloride concentration of local snow samples, the students were engaged in the Framework for K-12 Science Education's science practice of "Planning and carrying out investigations" (National Research Council 2012).

While there was not sufficient time for testing with the high school workshop, calibration of the titration method using known concentration $Cl^-_{(aq)}$ solutions prepared by the instructor will improve the accuracy of the measured concentrations of the environmental samples in future implementations. The standard solutions may alternatively be made by students if there is further class time available, and this activity would be beneficial as even advanced chemistry students often struggle preparing simple solutions (Quigley 1991, Marino 1993, Wang 2000). However, given student challenges observed at the undergraduate level in solution preparation (May et al. 2018), it is recommended that students receive prior exposure to the preparation of solutions of known concentration through published exercises (Quigley 1991, Marino 1993, Wang 2000) prior

to preparing standard solutions for this laboratory experiment. An example calibration curve, produced by titrating prepared solutions of known chloride concentrations (0.002 to 1.0 g/L), is shown in (Figure 7—3). Results of this calibration show that measured $Cl^-_{(aq)}$ concentrations were biased high (slope > 1), especially when titrating lower concentration $Cl^-_{(aq)}$ solutions using lower concentration $AgNO_{3(aq)}$. It is recommended that students use data processing software (i.e. Microsoft Excel or Google Sheets) to generate the calibration curves to be used to calculate $Cl^-_{(aq)}$ concentrations. Incorporating the use of data processing (May et al. 2018), which is commonly employed across all scientific research fields, facilitates the classroom research experience by allowing calibration and sample class data to be compiled in an accessible spreadsheet in order for students to construct figures and make conclusions about their experimental results from a larger data set. This also exposes students to the science practice of "Using mathematics and computational thinking" from the Framework for K-12 Science Education (National Research Council 2012) and addresses the fact that students often matriculate into undergraduate science programs without prior spreadsheet experience (Schlotter 2013), which increases the time required to complete coursework and detracts from learning of chemistry (Rubin and Abrams 2015).

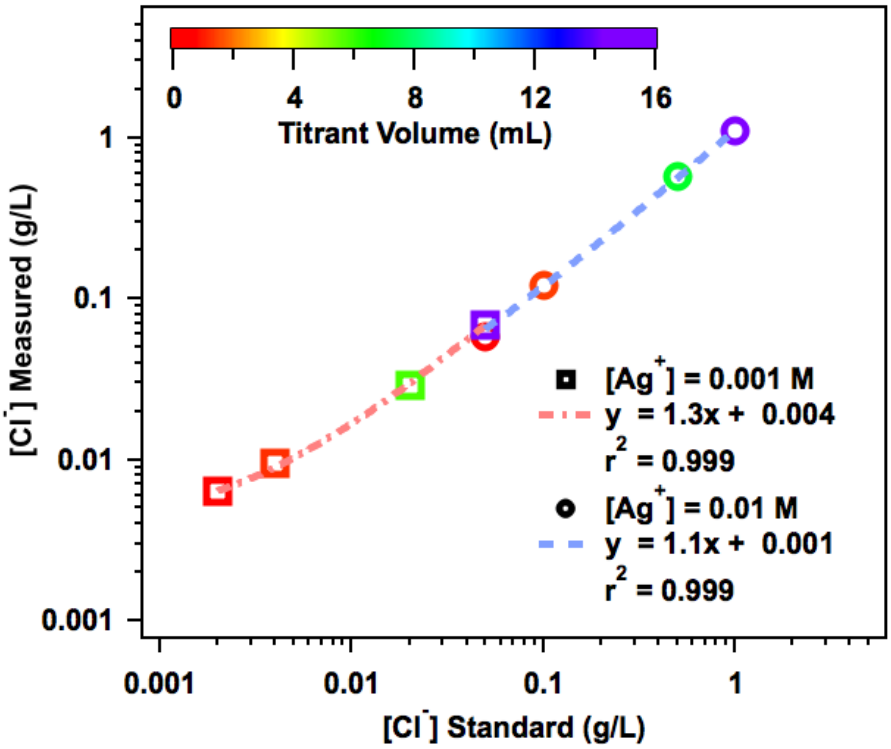

Figure 7—3. Chloride concentrations measured by titration using 0.001 M and 0.01 M $AgNO_{3\ (aq)}$ solutions versus known standard chloride concentrations, with linear fits and $AgNO_{3\ (aq)}$ volumes used shown.

In the third and final section of the research experience, the high school students converted their raw titration data to chloride concentrations, collaboratively interpreted the class data set, and constructed explanations for experimental results in the context of research questions and hypotheses established in the first section. The science practices of "Analyzing and interpreting data" and "Using mathematics and computational thinking" from the Framework for K-12 Science Education were thus integrated (National Research Council 2012). To aid the high school students in this process, the teachers presented a step-wise explanation of the process of translating raw data into chloride concentrations. In addition, the teachers led discussions on the construction of a narrative for presenting research results to help the high school students place their direct observations in context and inform their audience of the broader implications of their results. The high school students, again working in pairs, were given whiteboards to present their results and were shown a template to guide organization. This template included: a descriptive research title, a figure that best represents the main findings, and bulleted lists of research motivations, methods, conclusions in the context of their hypothesis, and ideas for future work. Students completed their research-based laboratory experience through the presentation of results to other class members who were encouraged to participate in a discussion by posing questions or alternate explanations. This portion of the research experience introduced the following science practices outlined in the Framework for K-12 Science Education: "Constructing explanations," "Engaging in argument from evidence," and "Obtaining, evaluating, and communicating information analyzing and interpreting data" (National Research Council 2012). While the implementation presented here was a standalone research experience, in future implementations this three-section structure could be iterated by utilizing the results of previous student analyses to inform development of new research questions and identification of other environmental samples to investigate.

7.4. Conclusion

An effective and inexpensive means for conducting classroom-based authentic research is shown through experimental (titration) determination of chloride in environmental samples over a range of chloride concentrations (>2 mg/L) (Table 7—1). This experiment engages students in fundamental introductory chemistry laboratory concepts, including stoichiometry, precipitation reactions, dilutions, titrations, and calibration curves, in an environmental chemistry research setting designed for the resources and educational level of high school and introductory undergraduate chemistry courses. The authentic research-based structure presented here, wherein

students use results from laboratory experimentation to address self-generated research questions, thus provides an accessible means for instructors to incorporate recent science reform efforts by engaging high school and introductory undergraduate students in authentic science practices (National Research Council 2012, NGSS Lead States 2013) in a manner that connects them with their local environment.

7.5. Acknowledgments

Stephen M. McNamara, Claire Mattson, and Alexa Watson are thanked for their contributions in the design, testing, and implementation of this experiment. The authors thank the U-M Authentic Research Connection program, funded by the Howard Hughes Medical Institute (52008119), and the U-M Third Century Initiative for financial support of the Inter-professional STEM Learning Community (STEM-IPLC) program. Funding for N.W. May and S.M. McNamara was provided by the Future Faculty Graduate Student Instructor Program at the U-M Department of Chemistry, a U-M Chemistry Summer Fellowship, and a U.S. Department of Education Graduate Assistance in Areas of National Need fellowship. Additional funding was provided by the U-M Chemistry Undergraduate Research Program. Siyuan Wang, Katheryn Kolesar, Madeline Parks, Charles Dershimer, and Ginger Shultz (U-M) are thanked for their assistance in the evaluation and implementation of this experiment.

Chapter 8 Conclusions and Future Directions

8.1. Conclusions

Wind-induced wave-breaking in marine and freshwater environments directly emit sea spray aerosol (SSA) and lake spray aerosol (LSA), respectively. The participation of individual wave-breaking particles in the formation of clouds, as well as their impact on air quality, is determined by their size, morphology, and chemical composition (i.e. physiochemical properties). Understanding the chemical composition of individual particles generated from wave-breaking in a variety of aquatic environments is crucial for determining their climate and human health effects. This dissertation focused on the measurement of the physiochemical properties of wave-breaking particles produced from both marine and freshwater environments, through a combination of ambient and laboratory-based studies that primarily employed single-particle chemical analysis techniques. In addition, this dissertation details effort, undertaken in response to calls for science education reform, to expose introductory undergraduate and high school students to the environmental chemistry research presented here.

Chapter 2 detailed the characterization of the first laboratory system constructed for the generation of aerosol from freshwater samples. To evaluate this new LSA generator, bubble and aerosol number size distributions were measured for salt solutions representative of freshwater ($CaCO_3$) and seawater (NaCl) at concentrations ranging from that of freshwater to seawater (0.05 - 35 g kg^{-1}), as well as synthetic seawater (inorganic), synthetic freshwater (inorganic), and a freshwater sample from Lake Michigan. Decreasing salt solution concentrations from seawater to freshwater led to greater bubble coalescence and the formation of larger bubbles, which generated larger particles and lower aerosol number concentrations. The systematic studies of particles produced from synthetic seawater and freshwater, as well as the Lake Michigan freshwater sample, indicate that LSA is characterized by a bimodal lognormal aerosol size distribution with a primary mode diameter larger than that of SSA, and a secondary mode diameter smaller than that of SSA. This new LSA generator offers a means to investigate a potentially important source of aerosol over bodies of freshwater that needs to be thoroughly characterized, as the sizes produced are

relevant to the direct scattering of solar radiation light scattering, as well as the formation of CCN and INP.

Chapter 3 discussed measurements of LSA produced in the laboratory using the newly characterized LSA generator from freshwater samples collected from Lake Michigan and Lake Erie during HAB and non-bloom conditions. The incorporation of biological material within the individual HAB-influenced LSA particles was examined by single-particle mass spectrometry, scanning electron microscopy with energy-dispersive X-ray spectroscopy, and fluorescence microscopy. Freshwater with higher blue-green algae content produced higher number fractions of individual LSA particles that contained biological material, showing that organic molecules of biological origin are incorporated in LSA from HABs. The number fraction of individual LSA particles containing biological material also increased with particle diameter (greater than 0.5 μm), a size dependence that is consistent with previous studies of sea spray aerosol impacted by phytoplankton blooms. Similar to sea spray aerosol, organic carbon markers were most frequently observed in individual LSA particles less than 0.5 μm in diameter. Understanding the transfer of biological material from freshwater to the atmosphere via LSA is crucial for determining health and climate effects of HABs.

Chapter 4 discussed the identification of individual SSA and LSA particles by single particle mass spectrometry and electron microscopy during a field study conducted at the University of Michigan Biological Station in northern Michigan. During the July 2014 sampling period, SSA comprised 34% and 20% of PM mass (0.5 – 2.0 μm) during two, separate multiday transport events from Hudson Bay and an average of 5% background outside these periods. LSA transported from Lake Michigan reached a maximum of 11% of PM mass (0.5 – 2 μm) during a daylong high wind event, but also contributed a 5% average background during 92% of the study. Air mass trajectory analysis determined that SSA and LSA were transported >700 km and >25 km from the nearest ocean and Great Lakes sources, respectively. The results presented here represent the furthest inland quantification of SSA particle mass contributions by single particle analysis and the first confirmation of inland transport of LSA.

Chapter 5 detailed measurements of the dependence of submicron (aerodynamic diameter < 1 μm) and supermicron (aerodynamic diameter 1-10 μm) sea salt mass concentrations on sea ice coverage and wind speed at Utqiaġvik, AK from 2006-2009. Consistent with a wind-dependent source, supermicron sea salt mass concentrations increased in the presence of nearby leads and

wind speeds greater than 4 m s^{-1}. Increased supermicron and submicron sea salt chloride depletion was observed for periods of low winds or a lack of nearby open water, consistent with transported sea salt influence. SSA produced from leads has the potential to alter cloud formation, as well as the chemical composition of the Arctic atmosphere and snowpack.

Chapter 6 described a new introductory general chemistry laboratory course that was developed to provide an authentic research experience on the impact of SSA produced from leads on Arctic snow chemistry. First and second year students learned general chemistry concepts and laboratory skills in the context of snow chemistry, while participating in the course-based undergraduate research experience (CURE). Students were guided through all steps of the research process, including research question development, data collection and processing, interpretation of results in the context of scientific literature, and both written and oral presentations. A key component of the course was an individual laboratory experiment in which snow samples from the Arctic were analyzed for pH and ion content. Assessment of the course via pre- and post-term surveys indicated that students, the majority of whom were women, experienced greater gains in confidence of research skills and general attitudes towards chemistry as compared to the traditional general chemistry laboratory course. This course represents a novel integration of environmental chemistry research into an introductory level chemistry laboratory course, and this approach has significant potential to increase student engagement in the sciences.

Chapter 7 detailed an introductory level, research-based laboratory experiment involving the determination of chloride concentration in environmental samples by the Mohr method. Chloride concentrations (>2 mg/L) in easily accessible environmental samples, including rainwater, snow, freshwater, seawater, groundwater, and stormwater, can be quantified through this titration experiment using standard laboratory equipment. This exploratory laboratory experiment is designed to incorporate authentic science practices through the process of asking questions and developing hypotheses, collecting environmental samples, measuring chloride content by titration, calculating chloride concentrations from experimental data, interpreting data, constructing explanations, and presenting results to others. This simple, effective, and inexpensive environmental chemistry laboratory experiment is proposed as a means for engaging high school and introductory undergraduate students in authentic science practices, as advocated by recent science education reform efforts.

8.2. Future Directions

8.2.1. Climate Impacts of Lake Spray Aerosol

While Chapters 2 and 3 explored the relationship between freshwater composition and the physiochemical properties of LSA (May et al. 2016, May et al. 2017), the resulting CCN and INP efficiencies of LSA are currently unknown. However, recent work has demonstrated that ice nucleating biological material is present in freshwater at 10^2–10^3 higher concentrations than in marine waters (Moffett 2016) and is linked to ice formation within the Great Lakes (D'Souza et al. 2013). Furthermore, a laboratory study demonstrated the INP viability of aerosolized freshwater bacteria (*Pseudomonas syringae*) (Pietsch et al. 2015), with a subsequent field study demonstrating that ice nucleating strains of *P. syringae* are present in freshwater lakes (Pietsch et al. 2017). Organic compounds and biological material aerosolized from marine algal blooms by bubble bursting (Matthias-Maser et al. 1999, Aller et al. 2005, McCluskey et al. 2017) impact the CCN and INP activities of SSA (DeMott et al. 2015, Wilson et al. 2015, Ladino et al. 2016, McCluskey et al. 2017, Vergara-Temprado et al. 2017). Organic compounds and biological material aerosolized from freshwater algal blooms, as identified in Chapter 3 (May et al. 2017), may have similar effects on CCN and INP activities of LSA. Therefore, direct measurements of the CCN and INP activities of LSA produced from freshwater of varied chemical and biological composition are needed. Previous laboratory studies of the relationship between seawater composition and SSA cloud formation can inform the approach to future studies of LSA climate properties. For example, Prather et al. (2013) demonstrated that following the addition of bacteria and ZoBell growth medium to natural seawater, the relative number fraction of OC-dominated SSA in the (d_a) 60–180 nm range increased from 0.26 to 0.85, and the measured mean activation diameter at which particles began to serve as CCN nearly doubled from 63 nm to 118 nm. Similarly, a laboratory study of SSA generated over the course of an algal bloom induced in a natural seawater sample demonstrated that increased chlorophyll-*a* led to an increase in INP number concentrations, measured online with a continuous flow diffusion chamber and offline with a droplet freezing method (DeMott et al. 2015). Initial LSA studies could thus mirror these previous laboratory studies of SSA cloud formation properties by generating aerosols from natural freshwater over the course of an induced algal bloom. Measurements of single particle physiochemical properties using ATOFMS and CCSEM-EDX, as demonstrated in Chapter 3, could then be coupled with CCN and INP activity measurements used in previous laboratory SSA

studies (Prather et al. 2013, DeMott et al. 2015). Such studies would expand the work undertaken by the SSA community to better understand the role aquatic environments play in regulating atmospheric chemistry and climate (Cochran et al. 2017) and improve parameterizations of LSA in regional climate models (Chung et al. 2011).

8.2.1. Aircraft Measurements of Lake Spray Aerosol

In addition to proposed laboratory experiments, measurements of the potential incorporation of LSA into clouds in the Great Lakes region are needed. This work is motivated by the previous identification of LSA in the ambient atmosphere in the Great Lakes region presented in Axson et al. (2016) and in Chapter 4, as well as the previous identification of calcium particles in Great Lakes region clouds (Lasher-Trapp et al. 2008, Twohy and Anderson 2008). The enhancement of cloud cover and precipitation resulting from transfer of heat and moisture from the surface of the Great Lakes (Scott and Huff 1996), known as lake effect, further motivates study of the role of LSA in cloud formation. An initial investigation of the potential incorporation of LSA in clouds in the ambient atmosphere over the Great Lakes was conducted over two days (July 9 and 12, 2016) of aircraft sampling on a Beechcraft Duchess twin-engine aircraft (Purdue University Airborne Laboratory for Atmospheric Research (ALAR)) over northern Lake Michigan. During both the July 9 and July 12 aircraft particle sampling, white capped waves were observed, and Lake Michigan wave heights peaked above 1 m, with wind speeds reaching over 9 m s^{-1}. Samples of atmospheric particles were collected on aluminum foil during multiple passages of the aircraft over the water through the same flightpath using a modified rotating drum impactor. For cloud water collection, a modified Mohnen slotted rod extended out of the top of the aircraft (Huebert et al. 1988). Following the method of Hill et al. (2007), cloud droplets were impacted onto Teflon rods, which are characterized by a 50% cutoff diameter of ~5.5 μm, and collected into glass vials (sample volume ranging from 5−15 mL each). For the July 9 flight, atmospheric particle sampling was conducted over a portion of northwest Lake Michigan in the area of Platte Bay from 11:59 AM – 12:39 PM eastern daylight time (EDT) at 100 meters above sea level (MASL) and then from 2:51 PM – 3:51 PM EDT at 300 MASL. Cloud water samples were not collected July 9 due to lack of cloud cover. For the July 12 flight, atmospheric particle sampling was conducted between from 2:51 PM – 3:51 PM EDT at 300 MASL over a portion of north Lake Michigan in the area of Manistique Bay between Thompson, MI and Seul Choix Point, MI. The cloud layer present on July 12 was near enough to the surface such that the aircraft could not safely fly below

and as a result the particle samples were collected above the cloud layer. Cloud water samples were used to produce particles in the laboratory using a nebulizer, and, for comparison, freshwater samples, collected from Lake Michigan at the time of aircraft sampling, were used to produce particles in the laboratory using the LSA generator presented in Chapter 2 (May et al. 2016).

From the July 2016 flights, ambient and laboratory generated particles were examined using SEM-EDX to identify LSA particles based on elemental composition and morphology. Preliminary results show that particles with strong Ca, C, and O peaks, indicative of $CaCO_3$, and a crystalline morphology, after drying on the substrate, were observed in in ambient particle samples, as well as in the particle samples generated from cloud-water and freshwater samples. This Ca-dominant elemental composition and cubic morphology is consistent with Great Lakes freshwater composition (Chapra et al. 2012) and previous measurements of LSA chemical composition (Axson et al. 2016, May et al. 2017). Preliminary CCSEM analysis was conducted on ambient atmospheric particles and particles nebulized from cloud water, both collected on July 12. LSA composed 9% and 7%, by number, of the total particles analyzed by CCSEM in the 0.7−5.0 μm size range. These results suggest that LSA participates in cloud formation over the Great Lakes. Additional bulk composition measurements of cloud water and Lake Michigan fresh water were conducted using ion chromatography (IC) and inductively couple plasma mass spectrometry (ICP-MS). However, an enhancement in bulk calcium concentration was not definitively observed by these techniques, likely because the cloud water samples were collected in glass, which can adsorb ions, and the blank concentrations were abnormally high. Therefore, in future LSA investigations using bulk cloud water analysis to investigate the impact of LSA should employ plastic collection materials, as well as observing precautions in regard to the purity of water and rinsing procedures used in blank collections. In addition, the low solubility of $CaCO_3$ may have impacted results. Further analysis of the differences in size-dependent chemical composition between ambient particle samples collected at multiple heights and within clouds during the July 2016 aircraft sampling, as well as laboratory experiments using the simultaneously collected freshwater, will improve our understanding of the role that fresh-water wave-breaking plays regional climate in the Great Lakes region.

8.2.2. Health Impacts of Lake Spray Aerosol

The Great Lakes have recently experienced some of the largest cyanotoxin producing harmful algal blooms (HABs) in recorded history due to an increased input of nutrients (Michalak

et al. 2013). In addition to posing a threat to water quality, HABs also have the potential to be detrimental to air quality if HAB toxins are included in the organic and biological component of LSA identified in Chapter 3. Previous work has demonstrated that aerosols produced by recreational activity in freshwater HABs can present a significant public health risk due to inhalation of cyanotoxins, presenting a variety of symptoms including gastrointestinal, respiratory, dermatologic, and allergic reactions, as well as acute hepatotoxicity or neurotoxicity (Cheng et al. 2007, Backer et al. 2008, Backer et al. 2010). The effects of cyanotoxin inhalation can last for days after only a brief exposure and are more potent than the effects from oral ingestion of contaminated water (Backer et al. 2010). Previous work on marine HABs has shown that wind-induced wave breaking during active blooms lead to detectable concentrations of aerosolized toxins within SSA (Cheng et al. 2005, Cheng et al. 2010, Kirkpatrick et al. 2011). However, little is known about how wind-induced wave breaking in freshwater HABs aerosolizes toxins and how this may affect regional inhalation exposure risk.

A combination of laboratory and field studies that incorporate measurements of aerosol physiochemical properties and human health effects are needed to understand the likely impacts of LSA produced from freshwater HABs on human health. As an initial study, the concentration of toxic compounds could be measured in LSA generated in the laboratory from freshwater collected during an active HAB and impacted onto filters, with analysis by liquid chromatography-mass spectrometry (LC/MS) (Maizels and Budde 2004, Gambaro et al. 2012) and enzyme linked immunosorbent assay (ELISA) techniques (Cheng et al. 2007, Backer et al. 2008, Backer et al. 2010). Once the incorporation of toxins into LSA has been confirmed in the laboratory, ambient atmospheric particle sampling next to freshwater bodies impacted by HABs during periods of high winds is proposed to assess the inhalation exposure risk of LSA. Such field studies could employ online analysis of LSA biological content by ATOFMS, as characterized in Chapter 3 (May et al. 2017), alongside bulk filter sampling for analysis by ELISA or LC/MS to confirm the incorporation of toxins (Maizels and Budde 2004, Cheng et al. 2007, Backer et al. 2008, Backer et al. 2010, Gambaro et al. 2012). The significance of such field studies would be vastly increased through the incorporation of direct measurements of health impacts. For example, Cheng et al. (2010) interviewed an asthma cohort for health symptoms after they spent 1 h on an ocean beach during aerosolized red tide events and non-exposure periods, with concurrent measurements of ambient aerosol concentration and hourly filter samples collected to determine brevotoxin and

NaCl concentrations. Similarly, Backer et al. (2010) offers an example for a comprehensive field study of the health impact of aerosolized freshwater HABs, with water samples, personal air samples, nasal swabs, and blood samples analyzed for microcystin concentrations, respectively. Laboratory and field studies that combine measurements of atmospheric particle composition with assessments of health impacts will expand our understanding of the impacts of freshwater HABs beyond traditional water quality concerns. In doing so, stakeholders in regions impacted by freshwater HABs will be further motivated to implement scientifically guided management plans to mitigate the predicted rise in freshwater HABs (Michalak et al. 2013).

8.2.3. Heterogeneous Reactions on Sea Spray Aerosol Produced from Leads

In Chapter 5, wind-dependent production of fresh SSA in the presence of local leads, as well as aged SSA during periods of full sea ice coverage and low wind speeds, was observed (May et al. 2016). While this multi-year study at Utqiaġvik, AK allowed a comprehensive investigation into the influences of sea ice coverage and wind speed on SSA in the coastal Arctic, there were significant limitations in the atmospheric chemistry sampling methodology that could be addressed in future studies. First, the bulk-filter based particle measurements used in this study were temporally limited, with submicron and supermicron particle sampling periods ranging from 1-11 days and 5-35 days, respectively. As shifts in sea ice and meteorology that impact SSA production often occur on much shorter time-scales, measurements of sea salt aerosol concentrations with higher time resolution are needed to fully understand the influence of SSA produced from leads (Kirpes et al. 2018). In addition, laboratory studies have shown that heterogeneous reactions on SSA can release gaseous halogen species, such as $HBr_{(g)}$ and $HCl_{(g)}$ (Saiz-Lopez and von Glasow 2012, Simpson et al. 2015), and evidence of heterogeneous reactions was observed in the aged SSA population measured in Chapter 5. However, no gas phase measurements were conducted as a part of the study presented in Chapter 5 and partitioning of halogens between the gas and particle phase has been minimally studied in the Arctic (Berg et al. 1983, Li et al. 1994, Langendörfer et al. 1999, Hara et al. 2002). Given decreasing multi-year sea ice extent and increasing ice fracturing (Stroeve et al. 2012), studies of the impacts of SSA produced from leads on ambient gas and particle composition in the Arctic are particularly needed in winter and early spring when sea ice coverage is at its maximum and local contributions to SSA were not previously present (Quinn et al. 2002).

A recently developed online atmospheric aerosol and trace gas IC technique – the URG Corp. 9000D Ambient Ion Monitor Ion Chromatography (AIM-IC) system (Markovic et al. 2012) could improve the time resolution of aerosol measurements and enable the study of heterogeneous reactions in the Arctic. By using the AIM-IC to perform online IC measurements, the sampling time will be reduced to the scale of hours, from the multi-day scale typical of filter sampling (Quinn et al. 2002, Markovic et al. 2012). In the AIM-IC, soluble gas-phase species, such as HCl and HBr, are first collected using a parallel plate wet denuder, while particles pass through due to their lower rate of diffusion. Soluble particle-phase species are subsequently collected in the particle supersaturation chamber where particles are grown in a steam chamber and collected as a solution by an inertial particle separator. The simultaneous measurement of gas and particle phase species allows for the study partitioning of species between particle and gas phases (Ellis et al. 2011, Markovic et al. 2012, VandenBoer et al. 2014, VandenBoer et al. 2014, Croft et al. 2016, Wentworth et al. 2016). Previous studies with the AIM-IC examined the partitioning of particulate NO_2^- and $HONO_{(g)}$ in California (VandenBoer et al. 2014, VandenBoer et al. 2014), as well as the partitioning of particulate NH_4^+ and $NH3_{(g)}$ in Ontario, Canada (VandenBoer et al. 2011, VandenBoer et al. 2012) and the summertime Canadian Arctic (Croft et al. 2016, Wentworth et al. 2016).

In order to reduce gas-particle partitioning artifacts that can occur in the sampling line, which is a particular issue in the Arctic, where outdoor temperatures of -40°C and indoor temperatures of 20 °C are common, modifications were made to the AIM-IC based on work described by Markovic et al. (2012) for reducing artifacts under mid-latitude sampling conditions. A heated chamber, with a short (0.3 m) inlet, was constructed: this contains the parallel plate wet denuder that collects gases and the particle super saturation chamber that collects aerosols. Gases and particles are thus immediately collected from the air flow into solution, reducing the partitioning of particle species into the gas phase due to the increase in temperature from the ambient atmosphere into the sampling chamber. To prevent freezing during the transfer of the aqueous phase gas and particle samples into the research laboratory for IC analysis, a custom heated sampling line was constructed (Clayborn Labs). The heated sampling line is regulated by an external temperature controller, features 2 layers of nomex felt insulation and industrial strength silicone fire-sleeve outer cover, and is capable of maintaining a constant temperature of 20 °C in -40 °C ambient temperature. The AIM-IC was further modified from its commercial configuration

by the replacement of the commercial LiBr internal standard with LiF to enable measurements ambient Br^- and the installation of concentrator columns for sample loading to reduce limit of detections (LODs). The modified AIM-IC was successfully deployed into the field on two separate occasions, summer 2016 at the University of Michigan Biological Station (temperature range = 3 to 33 °C) and winter 2018 in Kalamazoo (temperature range = -18 to 15 °C), with the second instance demonstrating that the heated sampling chamber and line could function at temperatures <0 °C.

In its commercial configuration, the AIM is operated at 1 h sampling intervals. However, particulate bromide, the lowest concentration species of interest in Utqiagvik, AK, is much less abundant (0.001-0.03 μg m^{-3}) than the concentration of atmospheric species previously measured by AIM-IC (> 0.05 μg m^{-3}) (Ellis et al. 2011, Markovic et al. 2012, VandenBoer et al. 2014, VandenBoer et al. 2014, Croft et al. 2016, Wentworth et al. 2016). By calculating theoretical AIM-IC loading based on aerosol concentration data from the NOAA Barrow Observatory filter data and experimentally-determined IC 3σ LOD, it was determined that one-hour sampling would not be sufficient to measure Arctic aerosol Br^-. An extended 12 h sampling period would increase the LOD (Br^- = 0.0025 μg m^{-3}) by over a factor of 10 compared to the traditional 1 h sampling period. In doing so, the estimated fraction of particulate Br^- samples below the LOD would be reduced to <15%. The improvement in LOD comes at the cost of time resolution; however, the 12 hour sampling time will be an improvement over the average multi-day filter sampling presented in Chapter 5 (May et al. 2016). The multi-hour sampling functionality of the AIM-IC was previously employed with success during its two deployments in Michigan, sampling at 2 h intervals during summer 2016 at the University of Michigan Biological Station and 3 h intervals during winter 2018 in Kalamazoo. Deployment of the AIM-IC in its modified configuration to Utqiagvik, AK will therefore enable the assessment of the level to which changes in sea ice extent and meteorology impact SSA concentrations, as well as their participation in heterogeneous reactions, with higher time resolution than traditional offline chromatography. Such measurements are vital in the rapidly changing Arctic, where warming induced sea ice loss is expected to drastically alter the composition and processes of the atmosphere (Struthers et al. 2011, Bhatt et al. 2014).

8.2.4. Environmental Chemistry Research in the High School Classroom

Translating research-based laboratory practices, such as the Arctic snow chemistry in the snow chemistry CURE presented in Chapter 6 (May et al. 2018) and the research laboratory

experiment established Chapter 7, into the high school chemistry classroom poses unique challenges for high school instructors. Teachers without scientific research experience feel unprepared to lead students in pedagogically risky activities that are central to inquiry based learning, such as student led question formulation, experimental design, and data representation (Singer et al. 2000, Windschitl 2003). Lack of direct research experience may also lead to misconceptions regarding what constitutes authentic science practices (Keys and Bryan 2001). Therefore, while the snow chemistry research laboratory experiment established in the previous chapter will be designed to be accessible to an introductory chemistry course, its implementation at the high school level should be examined to develop a model of best practices that will enable secondary science educators to easily integrate it into their classroom.

As an initial step, I helped lead a group of pre-service high school teachers through the snow chemistry laboratory experiment from Chapter 7 as a part of Inter-Professional STEM Learning Community (STEM-IPLC) program in the School of Education during winter 2016. Through the 3-week STEM-IPLC snow chemistry module the participating pre-service teachers followed the procedures and general research structure presented in Chapter 7 to investigate the effect of deicing practices on chloride content in snow by collecting and analyzing snow samples from their local environment. Qualitative data, primarily written reflections from the participating pre-service teachers, were collected and analyzed to identify major themes. In my preliminary analysis, the experience of analyzing environmental samples, which they collected, to address a real-world problem was identified as a particularly impactful experience. However, many participating teachers noted that increased scaffolding of the research experience would be needed prior to its implementation. The feedback received in this first iteration was used to improve further implementations of the snow chemistry laboratory experiment through the STEM-IPLC program, with reflections from participants again evaluated by qualitative analysis, such as a multi-day workshop that I helped design and implement in August 2017 with four secondary science teachers. The teachers conducted the snow chemistry research experiment presented in Chapter 7 under my guidance, revised it based on their experience and prior knowledge from high school teaching, and then led a group of volunteer high school students through the revised snow chemistry research experience. The teachers reflected on their experience at multiple points over the course of the workshop in written responses, with conversations amongst the teachers and educational researchers video recorded. Similar to the qualitative data collected winter 2016, these

materials will be analyzed to identify major themes. In the future, instructional kits containing all laboratory materials needed to perform the snow chemistry research experiment and guidelines of best practices for its implementation at the high school level will be distributed to a limited number of local high school science teachers. The effectiveness of this real-world implementation will be evaluated through feedback from the participating teachers and students. The expected result of this work will be the development of knowledge useful for introducing environmental chemistry research laboratory experiments into high school chemistry courses, which will support broader efforts to address the decline in students choosing to pursue academic degrees and careers in STEM.

Bibliography

"NASA Worldview." Retrieved Feb 2018, from https://worldview.earthdata.nasa.gov/.

"National Science Board. Science & Engineering Indicators, 2016." Retrieved Feb 2018, from https://www.nsf.gov/statistics/2016/nsb20161/#/

Allen, H. M., D. C. Draper, B. R. Ayres, A. Ault, A. Bondy, S. Takahama, R. L. Modini, K. Baumann, E. Edgerton, C. Knote, A. Laskin, B. Wang and J. L. Fry. Influence of crustal dust and sea spray supermicron particle concentrations and acidity on inorganic NO3- aerosol during the 2013 Southern Oxidant and Aerosol Study. *Atmospheric Chemistry and Physics.* **2015**, 15 (18), 10669-10685.

Aller, J. Y., M. R. Kuznetsova, C. J. Jahns and P. F. Kemp. The sea surface microlayer as a source of viral and bacterial enrichment in marine aerosols. *Journal of Aerosol Science.* **2005**, 36 (5-6), 801-812.

American Chemical Society, Committee on Professional Training,. Undergraduate Professional Education in Chemistry: ACS Guidelines and Evaluation Procedures for Bachelor's Degree Programs. **2015**. Washington, D.C.

Andreae, M. O. and D. Rosenfeld. Aerosol–cloud–precipitation interactions. Part 1. The nature and sources of cloud-active aerosols. *Earth-Science Reviews.* **2008**, 89 (1-2), 13-41.

Andren, A. W., A. W. Elzerman and D. E. Armstrong. Chemical and Physical Aspects of Surface Organic Microlayers in Freshwater Lakes. *Journal of Great Lakes Research.* **1976**, 2, 101-110.

Atkinson, M. J. and C. Bingman. Elemental composition of commercial seasalts. *Journal of Aquariculture and Aquatic Sciences.* **1997**, 8 (2), 39-43.

Auchincloss, L. C., S. L. Laursen, J. L. Branchaw, K. Eagan, M. Graham, D. I. Hanauer, G. Lawrie, C. M. McLinn, N. Pelaez, S. Rowland, M. Towns, N. M. Trautmann, P. Varma-Nelson, T. J. Weston and E. L. Dolan. Assessment of course-based undergraduate research experiences: a meeting report. *CBE Life Sciences Education.* **2014**, 13 (1), 29-40.

Ault, A. P. and J. L. Axson. Atmospheric Aerosol Chemistry: Spectroscopic and Microscopic Advances. *Analytical Chemistry.* **2017**, 89 (1), 430-452.

Ault, A. P., T. L. Guasco, J. Baltrusaitis, O. S. Ryder, J. V. Trueblood, D. B. Collins, M. J. Ruppel, L. A. Cuadra-Rodriguez, K. A. Prather and V. H. Grassian. Heterogeneous reactivity of

nitric acid with nascent sea spray aerosol: large differences observed between and within individual particles. *The Journal of Physical Chemistry Letters.* **2014**, 2493-2500.

Ault, A. P., T. L. Guasco, J. Baltrusaitis, O. S. Ryder, J. V. Trueblood, D. B. Collins, M. J. Ruppel, L. A. Cuadra-Rodriguez, K. A. Prather and V. H. Grassian. Heterogeneous Reactivity of Nitric Acid with Nascent Sea Spray Aerosol: Large Differences Observed between and within Individual Particles. *The Journal of Physical Chemistry Letters.* **2014**, 5 (15), 2493-2500.

Ault, A. P., T. L. Guasco, O. S. Ryder, J. Baltrusaitis, L. A. Cuadra-Rodriguez, D. B. Collins, M. J. Ruppel, T. H. Bertram, K. A. Prather and V. H. Grassian. Inside versus outside: ion redistribution in nitric acid reacted sea spray aerosol particles as determined by single particle analysis. *Journal of the American Chemical Society.* **2013**, 135 (39), 14528-14531.

Ault, A. P., T. L. Guasco, O. S. Ryder, J. Baltrusaitis, L. A. Cuadra-Rodriguez, D. B. Collins, M. J. Ruppel, T. H. Bertram, K. A. Prather and V. H. Grassian. Inside versus outside: ion redistribution in nitric acid reacted sea spray aerosol particles as determined by single particle analysis. *Journal of the American Chemical Society.* **2013**, 135 (39), 14528-14531.

Ault, A. P., R. C. Moffet, J. Baltrusaitis, D. B. Collins, M. J. Ruppel, L. A. Cuadra-Rodriguez, D. Zhao, T. L. Guasco, C. J. Ebben, F. M. Geiger, T. H. Bertram, K. A. Prather and V. H. Grassian. Size-dependent changes in sea spray aerosol composition and properties with different seawater conditions. *Environmental Science & Technology.* **2013**, 47 (11), 5603-5612.

Ault, A. P., M. J. Moore, H. Furutani and K. A. Prather. Impact of emissions from the Los Angeles port region on San Diego air quality. *Environmental Science & Technology.* **2009**, 43 (10), 3500-3506.

Ault, A. P., T. M. Peters, E. J. Sawvel, G. S. Casuccio, R. D. Willis, G. A. Norris and V. H. Grassian. Single-particle SEM-EDX analysis of iron-containing coarse particulate matter in an urban environment: sources and distribution of iron within Cleveland, Ohio. *Environmental Science & Technology.* **2012**, 46 (8), 4331-4339.

Ault, A. P., C. R. Williams, A. B. White, P. J. Neiman, J. M. Creamean, C. J. Gaston, F. M. Ralph and K. A. Prather. Detection of Asian dust in California orographic precipitation. *J. Geophys. Res.* **2011**, 116 (D16), D16205.

Ault, A. P., D. Zhao, C. J. Ebben, M. J. Tauber, F. M. Geiger, K. A. Prather and V. H. Grassian. Raman microspectroscopy and vibrational sum frequency generation spectroscopy as probes of the bulk and surface compositions of size-resolved sea spray aerosol particles. *Physical Chemistry Chemical Physics.* **2013**, 15 (17), 6206-6214.

Axson, J. L., N. W. May, I. D. Colon-Bernal, K. A. Pratt and A. P. Ault. Lake Spray Aerosol: A Chemical Signature from Individual Ambient Particles. *Environmental Science & Technology.* **2016**, 50 (18), 9835-9845.

Axson, J. L., H. Shen, A. L. Bondy, C. C. Landry, J. Welz, J. M. Creamean and A. P. Ault. Transported Mineral Dust Deposition Case Study at a Hydrologically Sensitive Mountain Site: Size and Composition Shifts in Ambient Aerosol and Snowpack. *Aerosol and Air Quality Resarch.* **2016**, 16 (3), 555-567.

Bachofer, S. J. Sampling the Soils Around a Residence Containing Lead-Based Paints: An X-ray Fluorescence Experiment. *Journal of Chemical Education.* **2008**, 85 (7), 980.

Backer, L. C., W. Carmichael, B. Kirkpatrick, C. Williams, M. Irvin, Y. Zhou, T. B. Johnson, K. Nierenberg, V. R. Hill, S. M. Kieszak and Y. S. Cheng. Recreational exposure to low concentrations of microcystins during an algal bloom in a small lake. *Marine Drugs.* **2008**, 6 (2), 389-406.

Backer, L. C., S. V. McNeel, T. Barber, B. Kirkpatrick, C. Williams, M. Irvin, Y. Zhou, T. B. Johnson, K. Nierenberg, M. Aubel, R. LePrell, A. Chapman, A. Foss, S. Corum, V. R. Hill, S. M. Kieszak and Y. S. Cheng. Recreational exposure to microcystins during algal blooms in two California lakes. *Toxicon.* **2010**, 55 (5), 909-921.

Bakshi, A., L. E. Patrick and E. W. Wischusen. A Framework for Implementing Course-Based Undergraduate Research Experiences (CUREs) in Freshman Biology Labs. *The American Biology Teacher.* **2016**, 78 (6), 448-455.

Baldwin, R. G. The climate for undergraduate teaching and learning in STEM fields. *New Directions for Teaching and Learning.* **2009**, 2009 (117), 9-17.

Bangera, G. and S. E. Brownell. Course-based undergraduate research experiences can make scientific research more inclusive. *CBE Life Sciences Education.* **2014**, 13 (4), 602-606.

Barmby, P., P. M. Kind and K. Jones. Examining Changing Attitudes in Secondary School Science. *International Journal of Science Education.* **2008**, 30 (8), 1075-1093.

Barrie, L. A. and M. J. Barrie. Chemical components of lower tropospheric aerosols in the high arctic: six years of observations. *Journal of Atmospheric Chemistry.* **1990**, 11, 211-226.

Barrie, L. A., R. Staebler, D. Toom, B. Georgi, G. Denhartog, S. Landsberger and D. Wu. Arctic Aerosol Size-Segregated Chemical Observations in Relation to Ozone Depletion during Polar Sunrise Experiment 1992. *Journal of Geophysical Research: Atmospheres.* **1994**, 99 (D12), 25439-25451.

Bauer, C. F. Attitude toward Chemistry: A Semantic Differential Instrument for Assessing Curriculum Impacts. *Journal of Chemical Education.* **2008**, 85 (10), 1440.

Berg, W. W., P. D. Sperry, K. A. Rahn and E. S. Gladney. Atmospheric bromine in the Arctic. *Journal of Geophysical Research: Oceans.* **1983**, 88 (C11), 6719-6736.

Bhatt, U. S., D. A. Walker, J. E. Walsh, E. C. Carmack, K. E. Frey, W. N. Meier, S. E. Moore, F.-J. W. Parmentier, E. Post, V. E. Romanovsky and W. R. Simpson. Implications of Arctic

Sea Ice Decline for the Earth System. *Annual Review of Environment and Resources.* **2014**, 39 (1), 57-89.

Biddanda, B. A. and J. B. Cotner. Love Handles in Aquatic Ecosystems: The Role of Dissolved Organic Carbon Drawdown, Resuspended Sediments, and Terrigenous Inputs in the Carbon Balance of Lake Michigan. *Ecosystems.* **2002**, 5 (5), 431-445.

Bigg, E. K. and C. Leck. The composition of fragments of bubbles bursting at the ocean surface. *Journal of Geophysical Research.* **2008**, 113 (D11).

Blanchard, D. C. The electrification of the atmosphere by particles from bubbles in the sea. *Progress in Oceanography.* **1963**, 1, 73-202.

Blanchard, D. C. and L. D. Syzdek. Concentration of bacteria in jet drops from bursting bubbles. *Journal of Geophysical Research.* **1972**, 77 (27), 5087-5099.

Blanchard, D. C. and L. D. Syzdek. Electrostatic collection of jet and film drops. *Limnology and Oceanography.* **1975**, 20 (5), 762-774.

Blanchard, D. C. and A. H. Woodcock. Bubble Formation and Modification in the Sea and its Meteorological Significance. *Tellus.* **1957**, 9 (2), 145-158.

Blenkinsopp, C. E. and J. R. Chaplin. Void fraction measurements and scale effects in breaking waves in freshwater and seawater. *Coastal Engineering.* **2011**, 58 (5), 417-428.

Bondy, A. L., B. Wang, A. Laskin, R. L. Craig, M. V. Nhliziyo, S. B. Bertman, K. A. Pratt, P. B. Shepson and A. P. Ault. Inland Sea Spray Aerosol Transport and Incomplete Chloride Depletion: Varying Degrees of Reactive Processing Observed during SOAS. *Environmental Science & Technology.* **2017**, 51 (17), 9533-9542.

Boucher, O., D. Randall, P. Artaxo, C. Bretherton, G. Feingold, P. Forster, V.-M. Kerminen, Y. Kondo, H. Liao, U. Lohmann, P. Rasch, S. K. Satheesh, S. Sherwood, B. Stevens and X. Y. Zhang. "Clouds and Aerosols". Climate Change 2013: The Physical Science Basis. Contribution of Working Group I to the Fifth Assessment Report of the Intergovernmental Panel on Climate Change. **2013**. T. F. Stocker, D. Qin, G.-K. Plattner et al. Cambridge, United Kingdom and New York, NY, USA, Cambridge University Press**,** 571–658.

Bowyer, P. A. Video measurements of near-surface bubble spectra. *Journal of Geophysical Research: Oceans.* **2001**, 106 (C7), 14179-14190.

Brandriet, A. R., X. Xu, S. L. Bretz and J. E. Lewis. Diagnosing changes in attitude in first-year college chemistry students with a shortened version of Bauer's semantic differential. *Chemistry Education Research and Practice.* **2011**, 12 (2), 271-278.

Bressette, A. R. and G. W. Breton. Using Writing to Enhance the Undergraduate Research Experience. *Journal of Chemical Education.* **2001**, 78 (12), 1626.

Brook, R. D., B. Franklin, W. Cascio, Y. Hong, G. Howard, M. Lipsett, R. Luepker, M. Mittleman, J. Samet and S. C. Smith. Air pollution and cardiovascular disease. *Circulation.* **2004**, 109 (21), 2655-2671.

Brooks, S. D. and D. C. O. Thornton. Marine Aerosols and Clouds. *Annual Review of Marine Science.* **2018**, 10 (1), 289-313.

Brownell, S. E., D. S. Hekmat-Scafe, V. Singla, P. Chandler Seawell, J. F. Conklin Imam, S. L. Eddy, T. Stearns and M. S. Cyert. A high-enrollment course-based undergraduate research experience improves student conceptions of scientific thinking and ability to interpret data. *CBE Life Sciences Education.* **2015**, 14 (2), 14:ar21.

Browse, J., K. S. Carslaw, S. R. Arnold, K. Pringle and O. Boucher. The scavenging processes controlling the seasonal cycle in Arctic sulphate and black carbon aerosol. *Atmospheric Chemistry and Physics.* **2012**, 12 (15), 6775-6798.

Browse, J., K. S. Carslaw, G. W. Mann, C. E. Birch, S. R. Arnold and C. Leck. The complex response of Arctic aerosol to sea-ice retreat. *Atmospheric Chemistry and Physics.* **2014**, 14 (14), 7543-7557.

Burrows, S. M., O. Ogunro, A. A. Frossard, L. M. Russell, P. J. Rasch and S. M. Elliott. A physically based framework for modeling the organic fractionation of sea spray aerosol from bubble film Langmuir equilibria. *Atmospheric Chemistry and Physics.* **2014**, 14 (24), 13601-13629.

Cahill, J. F., T. K. Darlington, C. Fitzgerald, N. G. Schoepp, J. Beld, M. D. Burkart and K. A. Prather. Online analysis of single cyanobacteria and algae cells under nitrogen-limited conditions using aerosol time-of-flight mass spectrometry. *Analytical Chemistry.* **2015**, 87 (16), 8039-8046.

Cahill, R. A. Illinois State Geological Survey. **1981**. Champaign, IL.

Calvo, A., C. Alves, A. Castro, V. Pont, A. Vicente and R. Fraile. Research on aerosol sources and chemical composition: past, current and emerging issues. *Atmospheric Research.* **2013**, 120, 1-28.

Calvo, A. I., C. Alves, A. Castro, V. Pont, A. M. Vicente and R. Fraile. Research on aerosol sources and chemical composition: Past, current and emerging issues. *Atmospheric Research.* **2013**, 120-121, 1-28.

Canaria, J. A., A. M. Schoffstall, D. J. Weiss, R. M. Henry and S. B. Braun-Sand. A Model for an Introductory Undergraduate Research Experience. *Journal of Chemical Education.* **2012**, 89 (11), 1371-1377.

Carey, W. M., J. W. Fitzgerald, E. C. Monahan and Q. Wang. Measurement of the sound produced by a tipping trough with fresh and salt water. *The Journal of the Acoustical Society of America.* **1993**, 93 (6), 3178.

Carmichael, W. W. and G. L. Boyer. Health impacts from cyanobacteria harmful algae blooms: Implications for the North American Great Lakes. *Harmful Algae.* **2016**, 54, 194-212.

Carpenter, N. E. and T. M. Pappenfus. Teaching Research: A Curriculum Model That Works. *Journal of Chemical Education.* **2009**, 86 (8), 940.

Carroll, M. A., S. B. Bertman and P. B. Shepson. Overview of the Program for Research on Oxidants: PHotochemistry, Emissions, and Transport (PROPHET) summer 1998 measurements intensive. *Journal of Geophysical Research.* **2001**, 106 (D20), 24275.

Chalbot, M. C., B. McElroy and I. G. Kavouras. Sources, trends and regional impacts of fine particulate matter in southern Mississippi valley: significance of emissions from sources in the Gulf of Mexico coast. *Atmospheric Chemistry and Physics.* **2013**, 13 (7), 3721-3732.

Chapra, S. C., A. Dove and G. J. Warren. Long-term trends of Great Lakes major ion chemistry. *Journal of Great Lakes Research.* **2012**, 38 (3), 550-560.

Chase, A. M., H. A. Clancy, R. P. Lachance, B. M. Mathison, M. M. Chiu and G. C. Weaver. Improving critical thinking via authenticity: the CASPiE research experience in a military academy chemistry course. *Chemistry Education Research and Practice.* **2017**, 18 (1), 55-63.

Chen, X. STEM Attrition: College Students' Paths Into and Out of STEM Fields **2013**. Washington, DC.

Cheng, Y. S., T. A. Villareal, Y. Zhou, J. Gao, R. Pierce, J. Naar and D. G. Baden. Characterization of Red Tide Aerosol on the Texas Coast. *Harmful Algae.* **2005**, 4 (1), 87-94.

Cheng, Y. S., Y. Zhou, C. M. Irvin, B. Kirkpatrick and L. C. Backer. Characterization of aerosols containing microcystin. *Marine Drugs.* **2007**, 5 (4), 136-150.

Cheng, Y. S., Y. Zhou, C. M. Irvin, R. H. Pierce, J. Naar, L. C. Backer, L. E. Fleming, B. Kirkpatrick and D. G. Baden. Characterization of Marine Aerosol for Assessment of Human Exposure to Brevetoxins. *Environmental Health Perspectives.* **2005**, 113 (5), 638-643.

Cheng, Y. S., Y. Zhou, R. H. Pierce, M. Henry and D. G. Baden. Characterization of Florida red tide aerosol and the temporal profile of aerosol concentration. *Toxicon.* **2010**, 55 (5), 922-929.

Cheung, D. Students' Attitudes Toward Chemistry Lessons: The Interaction Effect between Grade Level and Gender. *Research in Science Education.* **2007**, 39 (1), 75-91.

Chi, J. W., W. J. Li, D. Z. Zhang, J. C. Zhang, Y. T. Lin, X. J. Shen, J. Y. Sun, J. M. Chen, X. Y. Zhang, Y. M. Zhang and W. X. Wang. Sea salt aerosols as a reactive surface for inorganic and organic acidic gases in the Arctic troposphere. *Atmospheric Chemistry and Physics.* **2015**, 15 (19), 11341-11353.

Chinn, C. A. and B. A. Malhotra. Epistemologically authentic inquiry in schools: A theoretical framework for evaluating inquiry tasks. *Science Education.* **2002**, 86 (2), 175-218.

Chung, S. H., B. M. Basarab and T. M. VanReken. Regional impacts of ultrafine particle emissions from the surface of the Great Lakes. *Atmospheric Chemistry and Physics.* **2011**, 11 (24), 12601-12615.

Clark, T. M., R. Ricciardo and T. Weaver. Transitioning from Expository Laboratory Experiments to Course-Based Undergraduate Research in General Chemistry. *Journal of Chemical Education.* **2016**, 93 (1), 56-63.

Cochran, R. E., O. S. Ryder, V. H. Grassian and K. A. Prather. Sea Spray Aerosol: The Chemical Link between the Oceans, Atmosphere, and Climate. *Accounts of Chemical Research.* **2017**, 50 (3), 599-604.

Cohen, A. J., M. Brauer, R. Burnett, H. R. Anderson, J. Frostad, K. Estep, K. Balakrishnan, B. Brunekreef, L. Dandona, R. Dandona, V. Feigin, G. Freedman, B. Hubbell, A. Jobling, H. Kan, L. Knibbs, Y. Liu, R. Martin, L. Morawska, C. A. Pope, H. Shin, K. Straif, G. Shaddick, M. Thomas, R. van Dingenen, A. van Donkelaar, T. Vos, C. J. L. Murray and M. H. Forouzanfar. Estimates and 25-year trends of the global burden of disease attributable to ambient air pollution: an analysis of data from the Global Burden of Diseases Study 2015. *The Lancet.* **2017**, 389 (10082), 1907-1918.

Collins, D. B., A. P. Ault, R. C. Moffet, M. J. Ruppel, L. A. Cuadra-Rodriguez, T. L. Guasco, C. E. Corrigan, B. E. Pedler, F. Azam, L. I. Aluwihare, T. H. Bertram, G. C. Roberts, V. H. Grassian and K. A. Prather. Impact of marine biogeochemistry on the chemical mixing state and cloud forming ability of nascent sea spray aerosol. *Journal of Geophysical Research: Atmospheres.* **2013**, 118 (15), 8553-8565.

Collins, D. B., D. F. Zhao, M. J. Ruppel, O. Laskina, J. R. Grandquist, R. L. Modini, M. D. Stokes, L. M. Russell, T. H. Bertram, V. H. Grassian, G. B. Deane and K. A. Prather. Direct aerosol chemical composition measurements to evaluate the physicochemical differences between controlled sea spray aerosol generation schemes. *Atmospheric Measurement Techniques.* **2014**, 7 (11), 3667-3683.

Corsi, S. R., L. A. De Cicco, M. A. Lutz and R. M. Hirsch. River chloride trends in snow-affected urban watersheds: increasing concentrations outpace urban growth rate and are common among all seasons. *Sci Total Environ.* **2015**, 508, 488-497.

Corsi, S. R., D. J. Graczyk, S. W. Geis, N. L. Booth and K. D. Richards. A fresh look at road salt: aquatic toxicity and water-quality impacts on local, regional, and national scales. *Environ Sci Technol.* **2010**, 44 (19), 7376-7382.

Cory, R. M., T. W. Davis, G. J. Dick, T. Johengen, V. J. Denef, M. A. Berry, S. E. Page, S. B. Watson, K. Yuhas and G. W. Kling. Seasonal Dynamics in Dissolved Organic Matter, Hydrogen Peroxide, and Cyanobacterial Blooms in Lake Erie. *Frontiers in Marine Science.* **2016**, 3.

Craig, V. S. J., B. W. Ninham and R. M. Pashley. Effect of electrolytes on bubble coalescence. *Nature.* **1993**, 364 (6435), 317-319.

Craig, V. S. J., B. W. Ninham and R. M. Pashley. The effect of electrolytes on bubble coalescence in water. *The Journal of Physical Chemistry.* **1993**, 97 (39), 10192-10197.

Creamean, J. M., K. J. Suski, D. Rosenfeld, A. Cazorla, P. J. DeMott, R. C. Sullivan, A. B. White, F. M. Ralph, P. Minnis, J. M. Comstock, J. M. Tomlinson and K. A. Prather. Dust and Biological Aerosols from the Sahara and Asia Influence Precipitation in the Western U.S. *Science.* **2013**, 339 (6127), 1572-1578.

Croft, B., G. R. Wentworth, R. V. Martin, W. R. Leaitch, J. G. Murphy, B. N. Murphy, J. K. Kodros, J. P. Abbatt and J. R. Pierce. Contribution of Arctic seabird-colony ammonia to atmospheric particles and cloud-albedo radiative effect. *Nat Commun.* **2016**, 7, 13444.

Custard, K. D., A. R. W. Raso, P. B. Shepson, R. M. Staebler and K. A. Pratt. Production and Release of Molecular Bromine and Chlorine from the Arctic Coastal Snowpack. *ACS Earth and Space Chemistry.* **2017**, 1 (3), 142-151.

D'Souza, N. A., Y. Kawarasaki, J. D. Gantz, R. E. Lee, Jr., B. F. Beall, Y. M. Shtarkman, Z. A. Kocer, S. O. Rogers, H. Wildschutte, G. S. Bullerjahn and R. M. McKay. Diatom assemblages promote ice formation in large lakes. *The ISME journal.* **2013**, 7 (8), 1632-1640.

Dall'Osto, M., D. C. S. Beddows, R. P. Kinnersley, R. M. Harrison, R. J. Donovan and M. R. Heal. Characterization of individual airborne particles by using aerosol time-of-flight mass spectrometry at Mace Head, Ireland. *Journal of Geophysical Research: Atmospheres.* **2004**, 109 (D21).

Danowitz, A. M., R. C. Brown, C. D. Jones, A. Diegelman-Parente and C. E. Taylor. A Combination Course and Lab-Based Approach To Teaching Research Skills to Undergraduates. *Journal of Chemical Education.* **2016**, 93 (3), 434-438.

Deane, G. B. Sound generation and air entrainment by breaking waves in the surf zone. *The Journal of the Acoustical Society of America.* **1997**, 102 (5), 2671.

Deane, G. B. and M. D. Stokes. Air Entrainment Processes and Bubble Size Distributions in the Surf Zone. *Journal of Physical Oceanography.* **1999**, 29 (7), 1393-1403.

Deane, G. B. and M. D. Stokes. Scale dependence of bubble creation mechanisms in breaking waves. *Nature.* **2002**, 418 (6900), 839-844.

Delene, D. J. and J. A. Ogren. Variability of Aerosol Optical Properties at Four North American Surface Monitoring Sites. *Journal of the Atmospheric Sciences.* **2002**, 59 (6), 1135-1150.

DeMott, P. J., T. C. Hill, C. S. McCluskey, K. A. Prather, D. B. Collins, R. C. Sullivan, M. J. Ruppel, R. H. Mason, V. E. Irish, T. Lee, C. Y. Hwang, T. S. Rhee, J. R. Snider, G. R. McMeeking, S. Dhaniyala, E. R. Lewis, J. J. Wentzell, J. Abbatt, C. Lee, C. M. Sultana,

A. P. Ault, J. L. Axson, M. Diaz Martinez, I. Venero, G. Santos-Figueroa, M. D. Stokes, G. B. Deane, O. L. Mayol-Bracero, V. H. Grassian, T. H. Bertram, A. K. Bertram, B. F. Moffett and G. D. Franc. Sea spray aerosol as a unique source of ice nucleating particles. *Proceedings of the National Academy of Sciences.* **2015**, 113 (21), 5797-5803.

DeMott, P. J., T. C. J. Hill, C. S. McCluskey, K. A. Prather, D. B. Collins, R. C. Sullivan, M. J. Ruppel, R. H. Mason, V. E. Irish, T. Lee, C. Y. Hwang, T. S. Rhee, J. R. Snider, G. R. McMeeking, S. Dhaniyala, E. R. Lewis, J. J. B. Wentzell, J. Abbatt, C. Lee, C. M. Sultana, A. P. Ault, J. L. Axson, M. Diaz Martinez, I. Venero, G. Santos-Figueroa, M. D. Stokes, G. B. Deane, O. L. Mayol-Bracero, V. H. Grassian, T. H. Bertram, A. K. Bertram, B. F. Moffett and G. D. Franc. Sea spray aerosol as a unique source of ice nucleating particles. *Proceedings of the National Academy of Sciences.* **2016**, 113 (21), 5797-5803.

Desai, A. R., J. A. Austin, V. Bennington and G. A. McKinley. Stronger winds over a large lake in response to weakening air-to-lake temperature gradient. *Nature Geoscience.* **2009**, 2 (12), 855-858.

Dillner, D. K., R. F. Ferrante, J. P. Fitzgerald and M. J. Schroeder. Integrated Laboratories: Laying the Foundation for Undergraduate Research Experiences. *Journal of Chemical Education.* **2011**, 88 (12), 1623-1629.

Domine, F., R. Sparapani, A. Ianniello and H. J. Beine. The origin of sea salt in snow on Arctic sea ice and in coastal regions. *Atmospheric Chemistry and Physics.* **2004**, 4 (9/10), 2259-2271.

Doubrawa, P., R. J. Barthelmie, S. C. Pryor, C. B. Hasager, M. Badger and I. Karagali. Satellite winds as a tool for offshore wind resource assessment: The Great Lakes Wind Atlas. *Remote Sensing of Environment.* **2015**, 168, 349-359.

Douglas, T. A., F. Domine, M. Barret, C. Anastasio, H. J. Beine, J. Bottenheim, A. Grannas, S. Houdier, S. Netcheva, G. Rowland, R. Staebler and A. Steffen. Frost flowers growing in the Arctic ocean-atmosphere-sea ice-snow interface: 1. Chemical composition. *Journal of Geophysical Research: Atmospheres.* **2012**, 117.

Dreessen, J., J. Sullivan and R. Delgado. Observations and impacts of transported Canadian wildfire smoke on ozone and aerosol air quality in the Maryland region on June 9-12, 2015. *J Air Waste Manag Assoc.* **2016**, 66 (9), 842-862.

Druckenmiller, M. L., H. Eicken, M. A. Johnson, D. J. Pringle and C. C. Williams. Toward an integrated coastal sea-ice observatory: System components and a case study at Barrow, Alaska. *Cold Regions Science and Technology.* **2009**, 56 (2-3), 61-72.

Dugan, H. A., S. L. Bartlett, S. M. Burke, J. P. Doubek, F. E. Krivak-Tetley, N. K. Skaff, J. C. Summers, K. J. Farrell, I. M. McCullough, A. M. Morales-Williams, D. C. Roberts, Z. Ouyang, F. Scordo, P. C. Hanson and K. C. Weathers. Salting our freshwater lakes. *Proceedings of the National Academy of Sciences.* **2017**, 114 (17), 4453-4458.

Dunstan, M. and P. Bassinger. An Innovative Model: Undergraduate Poster Sessions by Health Professional Majors as a Method for Communicating Chemistry in Context. *Journal of Chemical Education.* **1997**, 74 (9), 1067.

Dusek, U., G. P. Frank, L. Hildebrandt, J. Curtius, J. Schneider, S. Walter, D. Chand, F. Drewnick, S. Hings, D. Jung, S. Borrmann and M. O. Andreae. Size matters more than chemistry for cloud-nucleating ability of aerosol particles. *Science.* **2006**, 312 (5778), 1375-1378.

Dweck, C. S. Motivational processes affecting learning. *American Psychologist.* **1986**, 41 (10), 1040-1048.

Eicken, H., J. Jones, R. Mv, C. Kambhamettu, F. J. Meyer, A. Mahoney and M. L. Druckenmiller. Environmental security in arctic ice-covered seas: From strategy to tactics of hazard identification and emergency response. *Marine Technolology Society Journal.* **2011**, 45 (3), 37-48.

Ellis, R. A., J. G. Murphy, M. Z. Markovic, T. C. VandenBoer, P. A. Makar, J. Brook and C. Mihele. The influence of gas-particle partitioning and surface-atmosphere exchange on ammonia during BAQS-Met. *Atmospheric Chemistry and Physics.* **2011**, 11 (1), 133-145.

Facchini, M. C., M. Rinaldi, S. Decesari, C. Carbone, E. Finessi, M. Mircea, S. Fuzzi, D. Ceburnis, R. Flanagan, E. D. Nilsson, G. de Leeuw, M. Martino, J. Woeltjen and C. D. O'Dowd. Primary submicron marine aerosol dominated by insoluble organic colloids and aggregates. *Geophysical Research Letters.* **2008**, 35 (17).

Ferrer-Vinent, I. J., M. Bruehl, D. Pan and G. L. Jones. Introducing Scientific Literature to Honors General Chemistry Students: Teaching Information Literacy and the Nature of Research to First-Year Chemistry Students. *Journal of Chemical Education.* **2015**, 92 (4), 617-624.

Fierce, L., T. C. Bond, S. E. Bauer, F. Mena and N. Riemer. Black carbon absorption at the global scale is affected by particle-scale diversity in composition. *Nature Communications.* **2016**, 7.

Findlay, S. E. and V. R. Kelly. Emerging indirect and long-term road salt effects on ecosystems. *Annals of the New York Academy of Sciences.* **2011**, 1223, 58-68.

Fink, F. W. Corrosion of Metals in Sea Water. **1960**, 27, 27-39.

Ford, J. R., C. Prudenté and T. A. Newton. A Model for Incorporating Research into the First-Year Chemistry Curriculum. *Journal of Chemical Education.* **2008**, 85 (7), 929.

Forestieri, S. D., G. C. Cornwell, T. M. Helgestad, K. A. Moore, C. Lee, G. A. Novak, C. M. Sultana, X. Wang, T. H. Bertram, K. A. Prather and C. D. Cappa. Linking variations in sea spray aerosol particle hygroscopicity to composition during two microcosm experiments. *Atmospheric Chemistry and Physics.* **2016**, 16 (14), 9003-9018.

Freeman, S., S. L. Eddy, M. McDonough, M. K. Smith, N. Okoroafor, H. Jordt and M. P. Wenderoth. Active learning increases student performance in science, engineering, and

mathematics. *Proceedings of the National Academy of Sciences.* **2014**, 111 (23), 8410-8415.

Fuentes, E., H. Coe, D. Green, G. de Leeuw and G. McFiggans. Laboratory-generated primary marine aerosol via bubble-bursting and atomization. *Atmospheric Measurement Techniques.* **2010**, 3 (1), 141-162.

Fuhs, G. W. Microbiota in Surface Films: an Historical Perspective. *Journal of Great Lakes Research.* **1982**, 8 (2), 312-315.

Furlan, P. Y., H. Kitson and C. Andes. Chemistry, Poetry, and Artistic Illustration: An Interdisciplinary Approach to Teaching and Promoting Chemistry. *Journal of Chemical Education.* **2007**, 84 (10), 1625.

Furutani, H., M. Dall'osto, G. C. Roberts and K. A. Prather. Assessment of the relative importance of atmospheric aging on CCN activity derived from field observations. *Atmospheric Environment.* **2008**, 42 (13), 3130-3142.

Gambaro, A., E. Barbaro, R. Zangrando and C. Barbante. Simultaneous quantification of microcystins and nodularin in aerosol samples using high-performance liquid chromatography/negative electrospray ionization tandem mass spectrometry. *Rapid Communications in Mass Spectrometry.* **2012**, 26 (12), 1497-1506.

Gard, E., J. E. Mayer, B. D. Morrical, T. Dienes, D. P. Fergenson and K. A. Prather. Real-time analysis of individual atmospheric aerosol particles: Design and performance of a portable ATOFMS. *Analytical Chemistry.* **1997**, 69 (20), 4083-4091.

Gard, E. E. Direct Observation of Heterogeneous Chemistry in the Atmosphere. *Science.* **1998**, 279 (5354), 1184-1187.

Gard, E. E., M. J. Kleeman, D. S. Gross, L. S. Hughes, J. O. Allen, B. D. Morrical, D. P. Fergenson, T. Dienes, M. E. Galli, R. J. Johnson, G. R. Cass and K. A. Prather. Direct observation of heterogeneous chemistry in the atmosphere. *Science.* **1998**, 279 (5354), 1184-1187.

Gaston, C. J., K. A. Pratt, X. Qin and K. A. Prather. Real-Time detection and mixing state of methanesulfonate in single particles at an inland urban location during a phytoplankton bloom. *Environmental Science & Technology.* **2010**, 44 (5), 1566-1572.

Gibson, E. R., P. K. Hudson and V. H. Grassian. Aerosol chemistry and climate: Laboratory studies of the carbonate component of mineral dust and its reaction products. *Geophysical Research Letters.* **2006**, 33 (13).

Gobler, C. J., J. M. Burkholder, T. W. Davis, M. J. Harke, T. Johengen, C. A. Stow and D. B. Van de Waal. The dual role of nitrogen supply in controlling the growth and toxicity of cyanobacterial blooms. *Harmful Algae.* **2016**, 54, 87-97.

Gong, S. L., L. A. Barrie and M. Lazare. Canadian Aerosol Module (CAM): A size-segregated simulation of atmospheric aerosol processes for climate and air quality models - 2. Global

sea-salt aerosol and its budgets. *Journal of Geophysical Research: Atmospheres.* **2002**, 107 (D24).

Graham, M. J., J. Frederick, A. Byars-Winston, A. B. Hunter and J. Handelsman. Science education. Increasing persistence of college students in STEM. *Science.* **2013**, 341 (6153), 1455-1456.

Grammatika, M. and W. B. Zimmerman. Microhydrodynamics of flotation processes in the sea surface layer. *Dynamics of Atmospheres and Oceans.* **2001**, 34 (2–4), 327-348.

Griffith, A. L. Persistence of women and minorities in STEM field majors: Is it the school that matters? *Economics of Education Review.* **2010**, 29 (6), 911-922.

Grythe, H., J. Ström, R. Krejci, P. Quinn and A. Stohl. A review of sea-spray aerosol source functions using a large global set of sea salt aerosol concentration measurements. *Atmospheric Chemistry and Physics.* **2014**, 14 (3), 1277-1297.

Guasco, T. L., L. A. Cuadra-Rodriguez, B. E. Pedler, A. P. Ault, D. B. Collins, D. Zhao, M. J. Kim, M. J. Ruppel, S. C. Wilson, R. S. Pomeroy, V. H. Grassian, F. Azam, T. H. Bertram and K. A. Prather. Transition metal associations with primary biological particles in sea spray aerosol generated in a wave channel. *Environmental Science & Technology.* **2014**, 48 (2), 1324-1333.

Gunsch, M. J., R. M. Kirpes, K. R. Kolesar, T. E. Barrett, S. China, R. J. Sheesley, A. Laskin, A. Wiedensohler, T. Tuch and K. A. Pratt. Contributions of transported Prudhoe Bay oil field emissions to the aerosol population in Utqiaġvik, Alaska. *Atmospheric Chemistry and Physics.* **2017**, 17 (17), 10879-10892.

Gunsch, M. J., N. W. May, M. Wen, C. L. H. Bottenus, D. J. Gardner, T. M. VanReken, S. B. Bertman, P. K. Hopke, A. P. Ault and K. A. Pratt. Ubiquitous influence of wildfire emissions and secondary organic aerosol on summertime atmospheric aerosol in the forested Great Lakes region. *Atmospheric Chemistry and Physics.* **2018**, 18 (5), 3701-3715.

Gustafsson, M. E. R. and L. G. Franzén. Inland transport of marine aerosols in southern Sweden. *Atmospheric Environment.* **2000**, 34 (2), 313-325.

Hanauer, D. I., M. J. Graham and G. F. Hatfull. A Measure of College Student Persistence in the Sciences (PITS). *CBE Life Sciences Education.* **2016**, 15 (4), ar54.

Hara, K., K. Osada, M. Kido, M. Hayashi, K. Matsunaga, Y. Iwasaka, T. Yamanouchi, G. Hashida and T. Fukatsu. Chemistry of sea-salt particles and inorganic halogen species in Antarctic regions: Compositional differences between coastal and inland stations. *Journal of Geophysical Research: Atmospheres.* **2004**, 109 (D20).

Hara, K., K. Osada, K. Matsunaga, Y. Iwasaka, T. Shibata and K. Furuya. Atmospheric inorganic chlorine and bromine species in Arctic boundary layer of the winter/spring. *Journal of Geophysical Research: Atmospheres.* **2002**, 107 (D18).

Harris, S. P. Science research in the high school: An impossible dream? *Journal of Chemical Education.* **1977**, 54 (9), 526.

Hawkins, L. N. and L. M. Russell. Polysaccharides, Proteins, and Phytoplankton Fragments: Four Chemically Distinct Types of Marine Primary Organic Aerosol Classified by Single Particle Spectromicroscopy. *Advances in Meteorology.* **2010**, 2010, 1-14.

Held, A., I. M. Brooks, C. Leck and M. Tjernström. On the potential contribution of open lead particle emissions to the central Arctic aerosol concentration. *Atmospheric Chemistry and Physics.* **2011**, 11 (7), 3093-3105.

Held, A., D. A. Orsini, P. Vaattovaara, M. Tjernström and C. Leck. Near-surface profiles of aerosol number concentration and temperature over the Arctic Ocean. *Atmospheric Measurement Techniques.* **2011**, 4 (8), 1603-1616.

Henry, C. L., C. N. Dalton, L. Scruton and V. S. J. Craig. Ion-Specific Coalescence of Bubbles in Mixed Electrolyte Solutions. *The Journal of Physical Chemistry C.* **2007**, 111 (2), 1015-1023.

Hill, K. A., P. B. Shepson, E. S. Galbavy, C. Anastasio, P. S. Kourtev, A. Konopka and B. H. Stirm. Processing of atmospheric nitrogen by clouds above a forest environment. *Journal of Geophysical Research.* **2007**, 112 (D11).

Holme, T. A. Providing Motivation for the General Chemistry Course through Early Introduction of Current Research Topics. *Journal of Chemical Education.* **1994**, 71 (11), 919.

Huebert, B. J., S. Vanbramer and K. L. Tschudy. Liquid cloudwater collection using modified Mohnen slotted rods. *Journal of Atmospheric Chemistry.* **1988**, 6 (3), 251-263.

Hultin, K. A. H., E. D. Nilsson, R. Krejci, E. M. Mårtensson, M. Ehn, Å. Hagström and G. de Leeuw. In situ laboratory sea spray production during the Marine Aerosol Production 2006 cruise on the northeastern Atlantic Ocean. *Journal of Geophysical Research.* **2010**, 115 (D6).

Hutchison, A. R. and D. A. Atwood. Research with First- and Second-Year Undergraduates: A New Model for Undergraduate Inquiry at Research Universities. *Journal of Chemical Education.* **2002**, 79 (1), 125.

Ibanez, J. G., M. Hernandez-Esparaza, C. Doria-Serrano, A. Fregoso-Infante and M. M. Singh. Environmental Chemistry: Microscale Laboratory Experiments. **2008**. New York, NY, Springer.

Ittekkot, V. Variations of dissolved organic matter during a plankton bloom: qualitative aspects, based on sugar and amino acid analyses. *Marine Chemistry.* **1982**, 11 (2), 143-158.

Jackson, R. B. and E. G. Jobbagy. From icy roads to salty streams. *Proceedings of the National Academy of Sciences.* **2005**, 102 (41), 14487-14488.

Jacobi, H. W., D. Voisin, J. L. Jaffrezo, J. Cozic and T. A. Douglas. Chemical composition of the snowpack during the OASIS spring campaign 2009 at Barrow, Alaska. *Journal of Geophysical Research: Atmospheres.* **2012**, 117.

Jacobson, M. Z. Strong radiative heating due to the mixing state of black carbon in atmospheric aerosols. *Nature.* **2001**, 409, 695.

Jayarathne, T., C. M. Sultana, C. Lee, F. Malfatti, J. L. Cox, M. A. Pendergraft, K. A. Moore, F. Azam, A. V. Tivanski, C. D. Cappa, T. H. Bertram, V. H. Grassian, K. A. Prather and E. A. Stone. Enrichment of Saccharides and Divalent Cations in Sea Spray Aerosol During Two Phytoplankton Blooms. *Environmental Science & Technology.* **2016**, 50 (21), 11511-11520.

Johnson, B. D. and P. J. Wangersky. Microbubbles: Stabilization by monolayers of adsorbed particles. *Journal of Geophysical Research: Oceans.* **1987**, 92 (C13), 14641-14647.

Junge, C. E. and R. T. Werby. The Concentration of Chloride, Sodium, Potassium, Calcium, and Sulfate in Rain Water over the United States. *Journal of Meteorology.* **1958**, 15 (5), 417-425.

Keene, W. C., H. Maring, J. R. Maben, D. J. Kieber, A. A. P. Pszenny, E. E. Dahl, M. A. Izaguirre, A. J. Davis, M. S. Long, X. L. Zhou, L. Smoydzin and R. Sander. Chemical and physical characteristics of nascent aerosols produced by bursting bubbles at a model air-sea interface. *Journal of Geophysical Research: Atmospheres.* **2007**, 112 (D21).

Keene, W. C., A. A. P. Pszenny, J. N. Galloway and M. E. Hawley. Sea-Salt Corrections and Interpretation of Constituent Ratios in Marine Precipitation. *Journal of Geophysical Research: Atmospheres.* **1986**, 91 (D6), 6647-6658.

Keene, W. C., R. Sander, A. A. P. Pszenny, R. Vogt, P. J. Crutzen and J. N. Galloway. Aerosol pH in the marine boundary layer. *Journal of Aerosol Science.* **1998**, 29 (3), 339-356.

Kegley, S. E. and A. M. Stacy. Environmental Chemistry in the Freshman Laboratory. *Journal of Chemical Education.* **1993**, 70 (2), 151.

Kember, D., A. Ho and C. Hong. The importance of establishing relevance in motivating student learning. *Active Learning in Higher Education.* **2008**, 9 (3), 249-263.

Kennedy, J. H. Poster presentations for evaluating laboratory coursework. *Journal of Chemical Education.* **1985**, 62 (12), 1104.

Kerr, M. A. and F. Yan. Incorporating Course-Based Undergraduate Research Experiences into Analytical Chemistry Laboratory Curricula. *Journal of Chemical Education.* **2016**, 93 (4), 658-662.

Keys, C. W. and L. A. Bryan. Co-constructing inquiry-based science with teachers: Essential research for lasting reform. *Journal of Research in Science Teaching.* **2001**, 38 (6), 631-645.

Kharas, G. B. A New Investigative Sophomore Organic Laboratory Involving Individual Research Projects. *Journal of Chemical Education.* **1997**, 74 (7), 829.

Khlystov, A., C. Stanier and S. N. Pandis. An Algorithm for Combining Electrical Mobility and Aerodynamic Size Distributions Data when Measuring Ambient Aerosol Special Issue ofAerosol Science and Technologyon Findings from the Fine Particulate Matter Supersites Program. *Aerosol Science and Technology.* **2004**, 38 (sup1), 229-238.

Kientzler, C. F., A. B. Arons, D. C. Blanchard and A. H. Woodcock. Photographic Investigation of the Projection of Droplets by Bubbles Bursting at a Water Surface. *Tellus.* **1954**, 6 (1), 1-7.

King, S. M., A. C. Butcher, T. Rosenoern, E. Coz, K. I. Lieke, G. de Leeuw, E. D. Nilsson and M. Bilde. Investigating primary marine aerosol properties: CCN activity of sea salt and mixed inorganic-organic particles. *Environmental Science & Technology.* **2012**, 46 (19), 10405-10412.

Kirkpatrick, B., L. E. Fleming, J. A. Bean, K. Nierenberg, L. C. Backer, Y. S. Cheng, R. Pierce, A. Reich, J. Naar, A. Wanner, W. M. Abraham, Y. Zhou, J. Hollenbeck and D. G. Baden. Aerosolized Red Tide Toxins (Brevetoxins) and Asthma: Continued health effects after 1 hour beach exposure. *Harmful Algae.* **2011**, 10 (2), 138-143.

Kirpes, R. M., A. L. Bondy, D. Bonanno, R. C. Moffet, B. Wang, A. Laskin, A. P. Ault and K. A. Pratt. Secondary sulfate is internally mixed with sea spray aerosol and organic aerosol in the winter Arctic. *Atmospheric Chemistry and Physics.* **2018**, 18 (6), 3937-3949.

Kolesar, K. R., C. N. Mattson, P. K. Peterson, N. W. May, R. K. Prendergast and K. A. Pratt. Increases in wintertime PM2.5 sodium and chloride linked to snowfall and road salt application. *Atmospheric Environment.* **2018**, 177, 195-202.

Kopp, R. E. and D. L. Mauzerall. Assessing the climatic benefits of black carbon mitigation. *Proceedings of the National Academy of Sciences.* **2010**, 107 (26), 11703-11708.

Kowalski, J. R., G. C. Hoops and R. J. Johnson. Implementation of a Collaborative Series of Classroom-Based Undergraduate Research Experiences Spanning Chemical Biology, Biochemistry, and Neurobiology. *CBE Life Sciences Education.* **2016**, 15 (4).

Krnavek, L., W. R. Simpson, D. Carlson, F. Domine, T. A. Douglas and M. Sturm. The chemical composition of surface snow in the Arctic: Examining marine, terrestrial, and atmospheric influences. *Atmospheric Environment.* **2012**, 50, 349-359.

Ladino, L. A., J. D. Yakobi-Hancock, W. P. Kilthau, R. H. Mason, M. Si, J. Li, L. A. Miller, C. L. Schiller, J. A. Huffman, J. Y. Aller, D. A. Knopf, A. K. Bertram and J. P. D. Abbatt. Addressing the ice nucleating abilities of marine aerosol: A combination of deposition mode laboratory and field measurements. *Atmospheric Environment.* **2016**, 132, 1-10.

Langendörfer, U., E. Lehrer, D. Wagenbach and U. Platt. Observation of filterable bromine variabilities during Arctic tropospheric ozone depletion events in high (1 hour) time resolution. *Journal of Atmospheric Chemistry.* **1999**, 34 (1), 39-54.

Lasher-Trapp, S., S. Anderson-Bereznicki, A. Shackelford, C. H. Twohy and J. G. Hudson. An Investigation of the Influence of Droplet Number Concentration and Giant Aerosol Particles upon Supercooled Large Drop Formation in Wintertime Stratiform Clouds. *Journal of Applied Meteorology and Climatology.* **2008**, 47 (10), 2659-2678.

Laskin, A. and J. P. Cowin. Automated single-particle SEM/EDX analysis of submicrometer particles down to 0.1 μm. *Analytical Chemistry.* **2001**, 73 (5), 1023-1029.

Laskin, A., M. J. Iedema and J. P. Cowin. Quantitative Time-Resolved Monitoring of Nitrate Formation in Sea Salt Particles Using a CCSEM/EDX Single Particle Analysis. *Environmental Science & Technology.* **2002**, 36 (23), 4948-4955.

Laskina, O., H. S. Morris, J. R. Grandquist, A. D. Estillore, E. A. Stone, V. H. Grassian and A. V. Tivanski. Substrate-Deposited Sea Spray Aerosol Particles: Influence of Analytical Method, Substrate, and Storage Conditions on Particle Size, Phase, and Morphology. *Environmental Science & Technology.* **2015**, 49 (22), 13447-13453.

Leck, C. and E. K. Bigg. Aerosol production over remote marine areas - A new route. *Geophysical Research Letters.* **1999**, 26 (23), 3577-3580.

Leck, C., M. Norman, E. K. Bigg and R. Hillamo. Chemical composition and sources of the high Arctic aerosol relevant for cloud formation. *Journal of Geophysical Research: Atmospheres.* **2002**, 107 (D12).

Leck, C. and C. Persson. Seasonal and short-term variability in dimethyl sulfide, sulfur dioxide and biogenic sulfur and sea salt aerosol particles in the arctic marine boundary layer during summer and autumn. *Tellus B.* **1996**, 48 (2).

Leck, C. and E. Svensson. Importance of aerosol composition and mixing state for cloud droplet activation over the Arctic pack ice in summer. *Atmospheric Chemistry and Physics.* **2015**, 15 (5), 2545-2568.

Lee, C., C. M. Sultana, D. B. Collins, M. V. Santander, J. L. Axson, F. Malfatti, G. C. Cornwell, J. R. Grandquist, G. B. Deane, M. D. Stokes, F. Azam, V. H. Grassian and K. A. Prather. Advancing Model Systems for Fundamental Laboratory Studies of Sea Spray Aerosol Using the Microbial Loop. *The Journal of Physical Chemistry A.* **2015**, 119 (33), 8860-8870.

Legrand, M., X. Yang, S. Preunkert and N. Theys. Year-round records of sea salt, gaseous, and particulate inorganic bromine in the atmospheric boundary layer at coastal (Dumont d'Urville) and central (Concordia) East Antarctic sites. *Journal of Geophysical Research: Atmospheres.* **2016**, 121 (2), 997-1023.

Leiserowitz, A., E. Maibach and C. Roser-Renouf. Global Warming's Six Americas 2009: An Audience Segmentation. **2008**.

Leiserowitz, A., E. Maibach, C. Roser-Renouf and J. Hmielowski. Global Warming's Six Americas, March 2012 & November 2011. **2012**.

Leiserowitz, A., M. N. Smith and J. R. Marlon. Americans' Knowledge of Climate Change. **2010**. Yale Project on Climate Change Communication.

Lelieveld, J., J. S. Evans, M. Fnais, D. Giannadaki and A. Pozzer. The contribution of outdoor air pollution sources to premature mortality on a global scale. *Nature.* **2015**, 525 (7569), 367-371.

Lessard, R. R. and S. A. Zieminski. Bubble Coalescence and Gas Transfer in Aqueous Electrolytic Solutions. *Industrial & Engineering Chemistry Fundamentals.* **1971**, 10 (2), 260-269.

Lewis, E. R. and S. E. Schwartz. Sea Salt Aerosol Production: Mechanisms, Methods, Measurements, and Models - A Critical Review. **2004**. Washington D.C., American Geophysical Union. **152**.

Lewis, S. E. Investigating the Longitudinal Impact of a Successful Reform in General Chemistry on Student Enrollment and Academic Performance. *Journal of Chemical Education.* **2014**, 91 (12), 2037-2044.

Li, S. M., Y. Yokouchi, L. A. Barrie, K. Muthuramu, P. B. Shepson, J. W. Bottenheim, W. T. Sturges and S. Landsberger. Organic and inorganic bromine compounds and their composition in the Arctic troposphere during polar sunrise. *Journal of Geophysical Research: Atmospheres.* **1994**, 99 (D12), 25415-25428.

Liao, J., L. G. Huey, Z. Liu, D. J. Tanner, C. A. Cantrell, J. J. Orlando, F. M. Flocke, P. B. Shepson, A. J. Weinheimer, S. R. Hall, K. Ullmann, H. J. Beine, Y. Wang, E. D. Ingall, C. R. Stephens, R. S. Hornbrook, E. C. Apel, D. Riemer, A. Fried, R. L. Mauldin, J. N. Smith, R. M. Staebler, J. A. Neuman and J. B. Nowak. High levels of molecular chlorine in the Arctic atmosphere. *Nature Geoscience.* **2014**, 7 (2), 91-94.

Lieb-Lappen, R. M. and R. W. Obbard. The role of blowing snow in the activation of bromine over first-year Antarctic sea ice. *Atmospheric Chemistry and Physics.* **2015**, 15 (13), 7537-7545.

Lijek, R. S. and S. C. Fankhauser. Using Scavenger Hunts to Familiarize Students with Scientific Journal Articles. *Journal of Microbiology & Biology Education.* **2016**, 17 (1), 125-128.

Linn, M. C., E. Palmer, A. Baranger, E. Gerard and E. Stone. Education. Undergraduate research experiences: impacts and opportunities. *Science.* **2015**, 347 (6222), 1261757.

Lisensky, G. and K. Reynolds. Chloride in natural waters: An environmental application of a potentiometric titration. *Journal of Chemical Education.* **1991**, 68 (4), 334.

Logan, J. L., R. Quiñones and D. P. Sunderland. Poster Presentations: Turning a Lab of the Week into a Culminating Experience. *Journal of Chemical Education.* **2015**, 92 (1), 96-101.

Lohmann, U. and J. Feichter. Global indirect aerosol effects: a review. *Atmospheric Chemistry and Physics.* **2005**, 5 (3), 715-737.

Lopatto, D., C. Hauser, C. J. Jones, D. Paetkau, V. Chandrasekaran, D. Dunbar, C. MacKinnon, J. Stamm, C. Alvarez, D. Barnard, J. E. Bedard, A. E. Bednarski, S. Bhalla, J. M. Braverman, M. Burg, H. M. Chung, R. J. DeJong, J. R. DiAngelo, C. Du, T. T. Eckdahl, J. Emerson, A. Frary, D. Frohlich, A. L. Goodman, Y. Gosser, S. Govind, A. Haberman, A. T. Hark, A. Hoogewerf, D. Johnson, L. Kadlec, M. Kaehler, S. C. Key, N. P. Kokan, O. R. Kopp, G. A. Kuleck, J. Lopilato, J. C. Martinez-Cruzado, G. McNeil, S. Mel, A. Nagengast, P. J. Overvoorde, S. Parrish, M. L. Preuss, L. D. Reed, E. G. Regisford, D. Revie, S. Robic, J. A. Roecklien-Canfield, A. G. Rosenwald, M. R. Rubin, K. Saville, S. Schroeder, K. A. Sharif, M. Shaw, G. Skuse, C. D. Smith, M. Smith, S. T. Smith, E. P. Spana, M. Spratt, A. Sreenivasan, J. S. Thompson, M. Wawersik, M. J. Wolyniak, J. Youngblom, L. Zhou, J. Buhler, E. Mardis, W. Leung, C. D. Shaffer, J. Threlfall and S. C. Elgin. A central support system can facilitate implementation and sustainability of a Classroom-based Undergraduate Research Experience (CURE) in Genomics. *CBE Life Sciences Education.* **2014**, 13 (4), 711-723.

Machina, K. and A. Gokhale. Maintaining Positive Attitudes toward Science and Technology in First-Year Female Undergraduates: Peril and promise. *International Journal of Science Education.* **2010**, 32 (4), 523-540.

Mahaffy, P. G., T. A. Holme, L. Martin-Visscher, B. E. Martin, A. Versprille, M. Kirchhoff, L. McKenzie and M. Towns. Beyond "Inert" Ideas to Teaching General Chemistry from Rich Contexts: Visualizing the Chemistry of Climate Change (VC3). *Journal of Chemical Education.* **2017**, 94 (8), 1027-1035.

Mahoney, A. R., H. Eicken, A. G. Gaylord and R. Gens. Landfast sea ice extent in the Chukchi and Beaufort Seas: The annual cycle and decadal variability. *Cold Regions Science and Technology.* **2014**, 103, 41-56.

Mahowald, N., S. Albani, J. F. Kok, S. Engelstaeder, R. Scanza, D. S. Ward and M. G. Flanner. The size distribution of desert dust aerosols and its impact on the Earth system. *Aeolian Research.* **2014**, 15, 53-71.

Maizels, M. and W. L. Budde. A LC/MS method for the determination of cyanobacteria toxins in water. *Analytical Chemistry.* **2004**, 76 (5), 1342-1351.

Makowski Giannoni, S., K. Trachte, R. Rollenbeck, L. Lehnert, J. Fuchs and J. Bendix. Atmospheric salt deposition in a tropical mountain rainforest at the eastern Andean slopes of south Ecuador – Pacific or Atlantic origin? *Atmospheric Chemistry and Physics.* **2016**, 16 (15), 10241-10261.

Manders, A. M. M., M. Schaap, X. Querol, M. F. M. A. Albert, J. Vercauteren, T. A. J. Kuhlbusch and R. Hoogerbrugge. Sea salt concentrations across the European continent. *Atmospheric Environment.* **2010**, 44 (20), 2434-2442.

Marino, F. General chemistry lab time to learn solutions. *Journal of Chemical Education.* **1993**, 70 (5), 407.

Marino, R., S. Clarkson, P. A. Mills, W. V. Sweeney and S. DeMeo. Using Poster Sessions as an Alternative to Written Examination—The Poster Exam. *Journal of Chemical Education.* **2000**, 77 (9), 1158.

Marion, J. W., J. Lee, J. R. Wilkins, 3rd, S. Lemeshow, C. Lee, E. J. Waletzko and T. J. Buckley. In vivo phycocyanin flourometry as a potential rapid screening tool for predicting elevated microcystin concentrations at eutrophic lakes. *Environmental Science & Technology.* **2012**, 46 (8), 4523-4531.

Markovic, M. Z., T. C. VandenBoer and J. G. Murphy. Characterization and optimization of an online system for the simultaneous measurement of atmospheric water-soluble constituents in the gas and particle phases. *Journal of Environmental Monitoring.* **2012**, 14 (7), 1872-1884.

Marple, V. A., K. L. Rubow and S. M. Behm. A Microorifice Uniform Deposit Impactor (MOUDI): Description, Calibration, and Use. *Aerosol Science and Technology.* **1991**, 14 (4), 434-446.

Maslanik, J., J. Stroeve, C. Fowler and W. Emery. Distribution and trends in Arctic sea ice age through spring 2011. *Geophysical Research Letters.* **2011**, 38 (13).

Matthias-Maser, S., J. Brinkmann and W. Schneider. The size distribution of marine atmospheric aerosol with regard to primary biological aerosol particles over the South Atlantic Ocean. *Atmospheric Environment.* **1999**, 33 (21), 3569-3575.

Matz, R. L., E. D. Rothman, J. S. Krajcik and M. M. Banaszak Holl. Concurrent enrollment in lecture and laboratory enhances student performance and retention. *Journal of Research in Science Teaching.* **2012**, 49 (5), 659-682.

May, N. W., J. L. Axson, A. Watson, K. A. Pratt and A. P. Ault. Lake spray aerosol generation: a method for producing representative particles from freshwater wave breaking. *Atmospheric Measurement Techniques.* **2016**, 9 (9), 4311-4325.

May, N. W., S. M. McNamara, S. Wang, K. R. Kolesar, J. Vernon, J. P. Wolfe, D. Goldberg and K. A. Pratt. Polar Plunge: Semester-Long Snow Chemistry Research in the General Chemistry Laboratory. *Journal of Chemical Education.* **2018**.

May, N. W., N. E. Olson, M. Panas, J. L. Axson, P. S. Tirella, R. M. Kirpes, R. L. Craig, M. J. Gunsch, S. China, A. Laskin, A. P. Ault and K. A. Pratt. Aerosol Emissions from Great Lakes Harmful Algal Blooms. *Environmental Science & Technology.* **2017**.

May, N. W., N. E. Olson, M. Panas, J. L. Axson, P. S. Tirella, R. M. Kirpes, R. L. Craig, M. J. Gunsch, S. China, A. Laskin, A. P. Ault and K. A. Pratt. Aerosol Emissions from Great Lakes Harmful Algal Blooms. *Environmental Science & Technology.* **2018**, 52 (2), 397-405.

May, N. W., P. K. Quinn, S. M. McNamara and K. A. Pratt. Multi-Year Study of the Dependence of Sea Salt Aerosol on Wind Speed and Sea Ice Conditions in the Coastal Arctic. *Journal of Geophysical Research: Atmospheres.* **2016**.

McCluskey, C. S., T. C. J. Hill, F. Malfatti, C. M. Sultana, C. Lee, M. V. Santander, C. M. Beall, K. A. Moore, G. C. Cornwell, D. B. Collins, K. A. Prather, T. Jayarathne, E. A. Stone, F. Azam, S. M. Kreidenweis and P. J. DeMott. A Dynamic Link between Ice Nucleating Particles Released in Nascent Sea Spray Aerosol and Oceanic Biological Activity during Two Mesocosm Experiments. *Journal of the Atmospheric Sciences.* **2017**, 74 (1), 151-166.

McInnes, L. M., D. S. Covert, P. K. Quinn and M. S. Germani. Measurements of chloride depletion and sulfur enrichment in individual sea-salt particles collected from the remote marine boundary layer. *Journal of Geophysical Research.* **1994**, 99 (D4), 8257.

Mensah-Attipoe, J., S. Saari, A. M. Veijalainen, P. Pasanen, J. Keskinen, J. T. Leskinen and T. Reponen. Release and characteristics of fungal fragments in various conditions. *Science of the Total Environment.* **2016**, 547, 234-243.

Meyers, P. A. and O. E. Kawka. Fractionation of Hydrophobic Organic Materials in Surface Microlayers. *Journal of Great Lakes Research.* **1982**, 8 (2), 288-298.

Michalak, A. M., E. J. Anderson, D. Beletsky, S. Boland, N. S. Bosch, T. B. Bridgeman, J. D. Chaffin, K. Cho, R. Confesor, I. Daloglu, J. V. Depinto, M. A. Evans, G. L. Fahnenstiel, L. He, J. C. Ho, L. Jenkins, T. H. Johengen, K. C. Kuo, E. Laporte, X. Liu, M. R. McWilliams, M. R. Moore, D. J. Posselt, R. P. Richards, D. Scavia, A. L. Steiner, E. Verhamme, D. M. Wright and M. A. Zagorski. Record-setting algal bloom in Lake Erie caused by agricultural and meteorological trends consistent with expected future conditions. *Proceedings of the National Academy of Sciences.* **2013**, 110 (16), 6448-6452.

Mihailovic, A., V. Vasic, J. Ninkov, S. Eric, N. Ralevic, T. Nemes and A. Antic. Multivariate analysis of metals content in urban snow near traffic lanes in Novi Sad, Serbia. *Journal of the Serbian Chemical Society.* **2014**, 79 (2), 265-276.

Mihok, M., J. T. Keiser, J. M. Bortiatynski and T. E. Mallouk. An Environmentally Focused General Chemistry Laboratory. *Journal of Chemical Education.* **2006**, 83 (2), 250.

Moffet, R. C. and K. A. Prather. In-situ measurements of the mixing state and optical properties of soot with implications for radiative forcing estimates. *Proceedings of the National Academy of Sciences.* **2009**, 106 (29), 11872-11877.

Moffet, R. C., X. Qin, T. Rebotier, H. Furutani and K. A. Prather. Chemically segregated optical and microphysical properties of ambient aerosols measured in a single-particle mass spectrometer. *Journal of Geophysical Research.* **2008**, 113 (D12).

Moffett, B. F. Fresh water ice nuclei. *Fundamental and Applied Limnology / Archiv für Hydrobiologie.* **2016**, 188 (1), 19-23.

Monahan, E. C. Fresh Water Whitecaps. *Journal of the Atmospheric Sciences.* **1969**, 26 (5), 1026-1029.

Monahan, E. C. and I. G. O'Muircheartaigh. Whitecaps and the passive remote sensing of the ocean surface. *International Journal of Remote Sensing.* **1986**, 7 (5), 627-642.

Monahan, E. C. and C. R. Zietlow. Laboratory Comparisons of Fresh-Water and Salt-Water Whitecaps. *Journal of Geophysical Research.* **1969**, 74 (28), 6961-&.

Monahan, E. C. and C. R. Zietlow. Laboratory comparisons of fresh-water and salt-water whitecaps. *Journal of Geophysical Research.* **1969**, 74 (28), 6961-6966.

Mooring, S. R., C. E. Mitchell and N. L. Burrows. Evaluation of a Flipped, Large-Enrollment Organic Chemistry Course on Student Attitude and Achievement. *Journal of Chemical Education.* **2016**, 93 (12), 1972-1983.

Msagati, T. A., B. A. Siame and D. D. Shushu. Evaluation of methods for the isolation, detection and quantification of cyanobacterial hepatotoxins. *Aquatic Toxicology.* **2006**, 78 (4), 382-397.

Mullaney, J. R., D. L. Lorenz and A. D. Arntson. Chloride in Groundwater and Surface Water in Areas Underlain by the Glacial Aquifer System, Northern United States: U.S. Geological Survey Scientific Investigations Report 2009–5086. **2009**.

Murphy, D. M. The design of single particle laser mass spectrometers. *Mass Spectrometry Reviews.* **2007**, 26 (2), 150-165.

Murphy, D. M., J. R. Anderson, P. K. Quinn, L. M. McInnes, F. J. Brechtel, S. M. Kreidenweis, A. M. Middlebrook, M. Pósfai, D. S. Thomson and P. R. Buseck. Influence of sea-salt on aerosol radiative properties in the SouthernOcean marine boundary layer. *Nature.* **1998**, 392 (6671), 62-65.

Nagda, B. A., S. R. Gregerman, J. Jonides, W. von Hippel and J. S. Lerner. Undergraduate student-faculty research partnerships affect student retention. *The Review of Higher Education.* **1998**, 22, 55-72.

National Research Council. Transforming Undergraduate Education in Science, Mathematics, Engineering, and Technology. **1999**. Washington, DC, The National Academies Press.

National Research Council. Successful K-12 STEM Education: Identifying Effective Approaches in Science, Technology, Engineering, and Mathematics. **2011**. Washington, DC, The National Academies Press.

National Research Council. A Framework for K-12 Science Education: Practices, Crosscutting Concepts, and Core Ideas. **2012**. Washington, DC, The National Academies Press.

Neal, M., C. Neal, H. Wickham and S. Harman. Determination of bromide, chloride, fluoride, nitrate and sulphate by ion chromatography: comparisons of methodologies for rainfall, cloud water and river waters at the Plynlimon catchments of mid-Wales. *Hydrol. Earth Syst. Sci.* **2007**, 11 (1), 294-300.

Neubauer, K. R., M. V. Johnston and A. S. Wexler. On-line analysis of aqueous aerosols by laser desorption ionization. *International Journal of Mass Spectrometry and Ion Processes.* **1997**, 163 (1-2), 29-37.

Newberg, J. T., B. M. Matthew and C. Anastasio. Chloride and bromide depletions in sea-salt particles over the northeastern Pacific Ocean. *Journal of Geophysical Research: Atmospheres.* **2005**, 110 (D6), n/a-n/a.

Newton, T. A., H. J. Tracy and C. Prudenté. A Research-Based Laboratory Course in Organic Chemistry. *Journal of Chemical Education.* **2006**, 83 (12), 1844.

NGSS Lead States. Next Generation Science Standards: For States, By States. **2013**. Washington, DC.

Nguyen, Q. T., K. H. Kjær, K. I. Kling, T. Boesen and M. Bilde. Impact of fatty acid coating on the CCN activity of sea salt particles. *Tellus B: Chemical and Physical Meteorology.* **2017**, 69 (1), 1304064.

Nilsson, E. D. and Ü. Rannik. Turbulent aerosol fluxes over the Arctic Ocean: 1. Dry deposition over sea and pack ice. *Journal of Geophysical Research: Atmospheres.* **2001**, 106 (D23), 32125-32137.

Nilsson, E. D., U. Rannik, E. Swietlicki, C. Leck, P. P. Aalto, J. Zhou and M. Norman. Turbulent aerosol fluxes over the Arctic Ocean 2. Wind-driven sources from the sea. *Journal of Geophysical Research: Atmospheres.* **2001**, 106 (D23), 32139-32154.

Norman, A. L., L. A. Barrie, D. Toom-Sauntry, A. Sirois, H. R. Krouse, S. M. Li and S. Sharma. Sources of aerosol sulphate at Alert: Apportionment using stable isotopes. *Journal of Geophysical Research: Atmospheres.* **1999**, 104 (D9), 11619-11631.

Norris, S. J., I. M. Brooks, G. de Leeuw, A. Sirevaag, C. Leck, B. J. Brooks, C. E. Birch and M. Tjernström. Measurements of bubble size spectra within leads in the Arctic summer pack ice. *Ocean Science.* **2011**, 7 (1), 129-139.

O'Dowd, C. D., M. C. Facchini, F. Cavalli, D. Ceburnis, M. Mircea, S. Decesari, S. Fuzzi, Y. J. Yoon and J. P. Putaud. Biogenically driven organic contribution to marine aerosol. *Nature.* **2004**, 431 (7009), 676-680.

O'Dowd, C. D., B. Langmann, S. Varghese, C. Scannell, D. Ceburnis and M. C. Facchini. A combined organic-inorganic sea-spray source function. *Geophysical Research Letters.* **2008**, 35 (1).

O'Dowd, C. D., M. H. Smith, I. E. Consterdine and J. A. Lowe. Marine aerosol, sea-salt, and the marine sulphur cycle: a short review. *Atmospheric Environment.* **1997**, 31 (1), 73-80.

Oliver, B. G., J. B. Milne and N. LaBarre. Chloride and Lead in Urban Snow. *Journal (Water Pollution Control Federation).* **1974**, 46 (4), 766-771.

Olson, S. and D. G. Riordan. Engage to Excel: Producing One Million Additional College Graduates with Degrees in Science, Technology, Engineering, and Mathematics. Report to the President. **2012**.

Osborne, J., S. Simon and S. Collins. Attitudes towards science: A review of the literature and its implications. *International Journal of Science Education.* **2003**, 25 (9), 1049-1079.

Overland, J. E. and M. Wang. When will the summer Arctic be nearly sea ice free? *Geophysical Research Letters.* **2013**, 40 (10), 2097-2101.

Pakkanen, T. A. Study of formation of coarse particle nitrate aerosol. *Atmospheric Environment.* **1996**, 30 (14), 2475-2482.

Park, B. A statistical comparison of the gravimetric, Mohr, and Fajans methods for chloride. *Journal of Chemical Education.* **1958**, 35 (10).

Patterson, J. P., D. B. Collins, J. M. Michaud, J. L. Axson, C. M. Sultana, T. Moser, A. C. Dommer, J. Conner, V. H. Grassian, M. D. Stokes, G. B. Deane, J. E. Evans, M. D. Burkart, K. A. Prather and N. C. Gianneschi. Sea Spray Aerosol Structure and Composition Using Cryogenic Transmission Electron Microscopy. *ACS Central Science.* **2016**, 2 (1), 40-47.

Pham, D. Q., R. E. O'Brien, M. Fraund, D. Bonanno, O. Laskina, C. Beall, K. A. Moore, S. Forestieri, X. Wang, C. Lee, C. M. Sultana, V. H. Grassian, C. D. Cappa, K. A. Prather and R. C. Moffet. Biological Impacts on Carbon Speciation and Morphology of Sea Spray Aerosol. *ACS Earth and Space Chemistry.* **2017**, 1 (9), 551-561.

Pietsch, R. B., R. F. David, L. C. Marr, B. Vinatzer and D. G. Schmale. Aerosolization of Two Strains (Ice+ and Ice–) ofPseudomonas syringaein a Collison Nebulizer at Different Temperatures. *Aerosol Science and Technology.* **2015**, 49 (3), 159-166.

Pietsch, R. B., B. A. Vinatzer and D. G. Schmale. Diversity and Abundance of Ice Nucleating Strains of Pseudomonas syringae in a Freshwater Lake in Virginia, USA. *Frontiers in Microbiology.* **2017**, 8 (318).

Pilson, M. E. Q. An Introduction to the Chemistry of the Sea. **2013**. Cambridge, Cambridge University Press.

Pöhlker, C., J. A. Huffman and U. Pöschl. Autofluorescence of atmospheric bioaerosols – fluorescent biomolecules and potential interferences. *Atmospheric Measurement Techniques.* **2012**, 5 (1), 37-71.

Polissar, A. V., P. K. Hopke and J. M. Harris. Source Regions for Atmospheric Aerosol Measured at Barrow, Alaska. *Environmental Science & Technology.* **2001**, 35 (21), 4214-4226.

Pope, C. A. and D. W. Dockery. Health effects of fine particulate air pollution: lines that connect. *Journal of the Air & Waste Management Association.* **2006**, 56 (6), 709-742.

Pöschl, U. Atmospheric aerosols: composition, transformation, climate and health effects. *Angew Chem Int Ed Engl.* **2005**, 44 (46), 7520-7540.

Pöschl, U. Atmospheric Aerosols: Composition, Transformation, Climate and Health Effects. *Angewandte Chemie.* **2005**, 44 (46), 7520 - 7540.

Pöschl, U. and M. Shiraiwa. Multiphase Chemistry at the Atmosphere–Biosphere Interface Influencing Climate and Public Health in the Anthropocene. *Chemical Reviews.* **2015**, 115 (10), 4440-4475.

Post, D., H. A. Bridgman and G. P. Ayers. Fog and rainwater composition in rural SE Australia. *Journal of Atmospheric Chemistry.* **1991**, 13 (1), 83-95.

Prather, K. A., T. H. Bertram, V. H. Grassian, G. B. Deane, M. D. Stokes, P. J. Demott, L. I. Aluwihare, B. P. Palenik, F. Azam, J. H. Seinfeld, R. C. Moffet, M. J. Molina, C. D. Cappa, F. M. Geiger, G. C. Roberts, L. M. Russell, A. P. Ault, J. Baltrusaitis, D. B. Collins, C. E. Corrigan, L. A. Cuadra-Rodriguez, C. J. Ebben, S. D. Forestieri, T. L. Guasco, S. P. Hersey, M. J. Kim, W. F. Lambert, R. L. Modini, W. Mui, B. E. Pedler, M. J. Ruppel, O. S. Ryder, N. G. Schoepp, R. C. Sullivan and D. Zhao. Bringing the ocean into the laboratory to probe the chemical complexity of sea spray aerosol. *Proceedings of the National Academy of Sciences.* **2013**, 110 (19), 7550-7555.

Prather, K. A., C. D. Hatch and V. H. Grassian. Analysis of atmospheric aerosols. *Annual Review of Analytical Chemistry.* **2008**, 1, 485-514.

Prather, K. A., T. Nordmeyer and K. Salt. Real-time characterization of individual aerosol particles using time-of-flight mass spectrometry. *Analytical Chemistry.* **1994**, 66 (9), 1403-1407.

Pratt, K. A., K. D. Custard, P. B. Shepson, T. A. Douglas, D. Pohler, S. General, J. Zielcke, W. R. Simpson, U. Platt, D. J. Tanner, L. Gregory Huey, M. Carlsen and B. H. Stirm. Photochemical production of molecular bromine in Arctic surface snowpacks. *Nature Geoscience.* **2013**, 6 (5), 351-356.

Pratt, K. A., P. J. DeMott, J. R. French, Z. Wang, D. L. Westphal, A. J. Heymsfield, C. H. Twohy, A. J. Prenni and K. A. Prather. In situ detection of biological particles in cloud ice-crystals. *Nature Geoscience.* **2009**, 2 (6), 398-401.

Pratt, K. A., J. E. Mayer, J. C. Holecek, R. C. Moffet, R. O. Sanchez, T. P. Rebotier, H. Furutani, M. Gonin, K. Fuhrer, Y. Su, S. Guazzotti and K. A. Prather. Development and characterization of an aircraft aerosol time-of-flight mass spectrometer. *Analytical Chemistry.* **2009**, 81 (5), 1792-1800.

Pratt, K. A. and K. A. Prather. Real-time, single-particle volatility, size, and chemical composition measurements of aged urban aerosols. *Environmental Science & Technology.* **2009**, 43 (21), 8276-8282.

Pratt, K. A. and K. A. Prather. Mass spectrometry of atmospheric aerosols—Recent developments and applications. Part II: On-line mass spectrometry techniques. *Mass spectrometry reviews.* **2012**, 31 (1), 17-48.

Pratt, K. A., C. H. Twohy, S. M. Murphy, R. C. Moffet, A. J. Heymsfield, C. J. Gaston, P. J. DeMott, P. R. Field, T. R. Henn, D. C. Rogers, M. K. Gilles, J. H. Seinfeld and K. A. Prather. Observation of playa salts as nuclei in orographic wave clouds. *Journal of Geophysical Research.* **2010**, 115 (D15).

Pueyo, N. C., A. G. Raub, S. Jackson, M. M. Metz, A. C. Mount, K. L. Naughton, A. L. Eaton, N. M. Thomas, P. Hastings, J. Greaves, B. Blumberg, T. J. Collins and S. G. Sogo. Oxidation of Ethidium using TAML Activators: A Model for High School Research Performed in Partnership with University Scientists. *J Chem Educ.* **2013**, 90 (3), 326-331.

Qin, X., P. V. Bhave and K. A. Prather. Comparison of two methods for obtaining quantitative mass concentrations from aerosol time-of-flight mass spectrometry measurements. *Analytical Chemistry.* **2006**, 78 (17), 6169-6178.

Qin, X., K. A. Pratt, L. G. Shields, S. M. Toner and K. A. Prather. Seasonal comparisons of single-particle chemical mixing state in Riverside, CA. *Atmospheric Environment.* **2012**, 59, 587-596.

Quigley, M. N. Student preparation of standard solutions. *Journal of Chemical Education.* **1991**, 68 (6), 505.

Quinn, P. K., T. S. Bates, K. S. Schulz, D. J. Coffman, A. A. Frossard, L. M. Russell, W. C. Keene and D. J. Kieber. Contribution of sea surface carbon pool to organic matter enrichment in sea spray aerosol. *Nature Geoscience.* **2014**, 7 (3), 228-232.

Quinn, P. K., D. J. Coffman, V. N. Kapustin, T. S. Bates and D. S. Covert. Aerosol optical properties in the marine boundary layer during th First Aerosol Characterization Experiment (ACE 1) and the underlying chemical and physical aerosol properties. *Journal of Geophysical Research.* **1998**, 103 (D13), 16547-16563.

Quinn, P. K., D. B. Collins, V. H. Grassian, K. A. Prather and T. S. Bates. Chemistry and related properties of freshly emitted sea spray aerosol. *Chemical Reviews.* **2015**, 115 (10), 4383-4399.

Quinn, P. K., T. L. Miller, T. S. Bates, J. A. Ogren, E. Andrews and G. E. Shaw. A 3-year record of simultaneously measured aerosol chemical and optical properties at Barrow, Alaska. *Journal of Geophysical Research: Atmospheres.* **2002**, 107 (D11).

Radke, L. F., P. V. Hobbs and J. E. Pinnons. Observations of Cloud Condensation Nuclei, Sodium-Containing Particles, Ice Nuclei and the Light-Scattering Coefficient Near Barrow, Alaska. *Journal of Applied Meteorology.* **1976**, 15 (9), 982-995.

Raines, B. J., C. G. Gomez and K. R. Williams. Posters—Old Tool, New Tech. *Journal of Chemical Education.* **2005**, 82 (8), 1118.

Rankin, A. M., V. Auld and E. W. Wolff. Frost flowers as a source of fractionated sea salt aerosol in the polar regions. *Geophysical Research Letters.* **2000**, 27 (21), 3469-3472.

Repeta, D. J., T. M. Quan, L. I. Aluwihare and A. Accardi. Chemical characterization of high molecular weight dissolved organic matter in fresh and marine waters. *Geochimica et Cosmochimica Acta.* **2002**, 66 (6), 955-962.

Resch, F. "Oceanic Air Bubbles as Generators of Marine Aerosols". Oceanic Whitecaps. **1986**. E. Monahan and G. Niocaill, Springer Netherlands. **2,** 101-112.

Richter-Egger, D. L., J. P. Hagen, F. C. Laquer, N. F. Grandgenett and R. D. Shuster. Improving Student Attitudes about Science by Integrating Research into the Introductory Chemistry Laboratory: Interdisciplinary Drinking Water Analysis. *Journal of Chemical Education.* **2010**, 87 (8), 862-868.

Riemer, N. and M. West. Quantifying aerosol mixing state with entropy and diversity measures. *Atmospheric Chemistry and Physics.* **2013**, 13 (22), 11423-11439.

Robelia, B., K. McNeill, K. Wammer and F. Lawrenz. Investigating the Impact of Adding an Environmental Focus to a Developmental Chemistry Course. *Journal of Chemical Education.* **2010**, 87 (2), 216-220.

Rodenbusch, S. E., P. R. Hernandez, S. L. Simmons and E. L. Dolan. Early Engagement in Course-Based Research Increases Graduation Rates and Completion of Science, Engineering, and Mathematics Degrees. *CBE Life Sciences Education.* **2016**, 15 (2).

Rosenfeld, D., M. O. Andreae, A. Asmi, M. Chin, G. Leeuw, D. P. Donovan, R. Kahn, S. Kinne, N. Kivekäs, M. Kulmala, W. Lau, K. S. Schmidt, T. Suni, T. Wagner, M. Wild and J. Quaas. Global observations of aerosol-cloud-precipitation-climate interactions. *Reviews of Geophysics.* **2014**, 52 (4), 750-808.

Rubin, S. J. and B. Abrams. Teaching Fundamental Skills in Microsoft Excel to First-Year Students in Quantitative Analysis. *Journal of Chemical Education.* **2015**, 92 (11), 1840-1845.

Russell, S. C., G. Czerwieniec, C. Lebrilla, H. Tobias, D. P. Fergenson, P. Steele, M. Pitesky, J. Horn, A. Srivastava, M. Frank and E. E. Gard. Toward understanding the ionization of biomarkers from micrometer particles by bio-aerosol mass spectrometry. *Journal of the American Society for Mass Spectrometry.* **2004**, 15 (6), 900-909.

Russell, S. H., M. P. Hancock and J. McCullough. Benefits of Undergraduate Research Experiences. *Science.* **2007**, 316 (5824), 548-549.

Ryder, O. S., A. P. Ault, J. F. Cahill, T. L. Guasco, T. P. Riedel, L. A. Cuadra-Rodriguez, C. J. Gaston, E. Fitzgerald, C. Lee, K. A. Prather and T. H. Bertram. On the Role of Particle Inorganic Mixing State in the Reactive Uptake of N2O5 to Ambient Aerosol Particles. *Environmental Science & Technology.* **2014**, 48 (3), 1618-1627.

Ryder, O. S., N. R. Campbell, H. Morris, S. Forestieri, M. J. Ruppel, C. Cappa, A. Tivanski, K. Prather and T. H. Bertram. Role of Organic Coatings in Regulating N2O5 Reactive Uptake to Sea Spray Aerosol. *The Journal of Physical Chemistry A.* **2015**, 119 (48), 11683-11692.

Saiz-Lopez, A. and R. von Glasow. Reactive halogen chemistry in the troposphere. *Chem Soc Rev.* **2012**, 41 (19), 6448-6472.

Salido, A., C. Atterholt, J. R. Bacon and D. J. Butcher. An Environmental Focus Using Inductively Coupled Plasma-Optical Emission Spectrometry and Ion Chromatography. *Journal of Chemical Education.* **2003**, 80 (1), 22.

Salter, M. E., E. D. Nilsson, A. Butcher and M. Bilde. On the seawater temperature dependence of the sea spray aerosol generated by a continuous plunging jet. *Journal of Geophysical Research: Atmospheres.* **2014**, 119 (14), 9052-9072.

Salter, M. E., P. Zieger, J. C. Acosta Navarro, H. Grythe, A. Kirkevåg, B. Rosati, I. Riipinen and E. D. Nilsson. An empirically derived inorganic sea spray source function incorporating sea surface temperature. *Atmospheric Chemistry and Physics.* **2015**, 15 (19), 11047-11066.

Santos, M. D., L. Dawidowski, P. Smichowski, A. G. Ulke and D. Gómez. Factors controlling sea salt abundances in the urban atmosphere of a coastal South American megacity. *Atmospheric Environment.* **2012**, 59, 483-491.

Schlotter, N. E. A Statistics Curriculum for the Undergraduate Chemistry Major. *Journal of Chemical Education.* **2013**, 90 (1), 51-55.

Schneider, C. A., W. S. Rasband and K. W. Eliceiri. NIH Image to ImageJ: 25 years of image analysis. *Nature Methods.* **2012**, 9 (7), 671-675.

Scott, R. W. and F. A. Huff. Impacts of the Great Lakes on Regional Climate Conditions. *Journal of Great Lakes Research.* **1996**, 22 (4), 845-863.

Scott, W. D. and Z. Levin. Open channels in sea ice (leads) as ion sources. *Science.* **1972**, 177 (4047), 425-426.

Seguin, A. M., A.-L. Norman and L. Barrie. Evidence of sea ice source in aerosol sulfate loading and size distribution in the Canadian High Arctic from isotopic analysis. *Journal of Geophysical Research: Atmospheres.* **2014**, 119 (2), 1087-1096.

Seinfeld, J. H. and S. N. Pandis. Atmospheric chemistry and physics: from air pollution to climate change. **2016**. Hoboken, New Jersey, John Wiley & Sons.

Sellegri, K., C. D. O'Dowd, Y. J. Yoon, S. G. Jennings and G. de Leeuw. Surfactants and submicron sea spray generation. *Journal of Geophysical Research: Atmospheres.* **2006**, 111 (D22), n/a-n/a.

Serreze, M. C. and J. Stroeve. Arctic sea ice trends, variability and implications for seasonal ice forecasting. *Philososphical Transactions A.* **2015**, 373 (2045).

Seymour, E. and N. M. Hewitt. Talking about leaving: Why undergraduates leave the sciences. **1997**. Boulder, Colo., Westview Press.

Shaw, G. E. Aerosol chemical components in Alaska air masses: 2. Sea salt and marine product. *Journal of Geophysical Research.* **1991**, 96 (D12), 22369.

Shedlosky-Shoemaker, R. and J. M. Fautch. Who Leaves, Who Stays? Psychological Predictors of Undergraduate Chemistry Students' Persistence. *Journal of Chemical Education.* **2015**, 92 (3), 408-414.

Sheesley, R. J., J. J. Schauer, E. Bean and D. Kenski. Trends in Secondary Organic Aerosol at a Remote Site in Michigan's Upper Peninsula. *Environmental Science & Technology.* **2004**, 38 (24), 6491-6500.

Shen, H., T. M. Peters, G. S. Casuccio, T. L. Lersch, R. R. West, A. Kumar, N. Kumar and A. P. Ault. Elevated Concentrations of Lead in Particulate Matter on the Neighborhood-Scale in Delhi, India As Determined by Single Particle Analysis. *Environmental Science & Technology.* **2016**, 50 (10), 4961-4970.

Shepson, P. B., P. A. Ariya, C. J. Deal, D. J. Donaldson, T. A. Douglas, B. Loose, T. Maksym, P. A. Matrai, L. M. Russell, B. Saenz, J. Stefels and N. Steiner. Changing polar environments: Interdisciplinary challenges. *Eos, Transactions American Geophysical Union.* **2012**, 93 (11), 117.

Shortlidge, E. E., G. Bangera and S. E. Brownell. Faculty Perspectives on Developing and Teaching Course-Based Undergraduate Research Experiences. *BioScience.* **2016**, 66 (1), 54-62.

Shuchman, R. A., G. Leshkevich, M. J. Sayers, T. H. Johengen, C. N. Brooks and D. Pozdnyakov. An algorithm to retrieve chlorophyll, dissolved organic carbon, and suspended minerals from Great Lakes satellite data. *Journal of Great Lakes Research.* **2013**, 39, 14-33.

Silva, B., T. Rivas, E. Garciarodeja and B. Prieto. Distribution of ions of marine origin in Galicia (NW Spain) as a function of distance from the sea. *Atmospheric Environment.* **2007**, 41 (21), 4396-4407.

Simpson, W. R. Halogens in the coastal snow pack near Barrow, Alaska: Evidence for active bromine air-snow chemistry during springtime. *Geophysical Research Letters.* **2005**, 32 (4).

Simpson, W. R., S. S. Brown, A. Saiz-Lopez, J. A. Thornton and R. Glasow. Tropospheric halogen chemistry: sources, cycling, and impacts. *Chemical Reviews.* **2015**, 115 (10), 4035-4062.

Singer, J., R. W. Marx, J. Krajcik and J. Clay Chambers. Constructing Extended Inquiry Projects: Curriculum Materials for Science Education Reform. *Educational Psychologist.* **2000**, 35 (3), 165-178.

Sinniah, K. and K. Piers. Ion chromatography: Analysis of ions in pond waters. *Journal of Chemical Education.* **2001**, 78 (3), 358-362.

Sirois, A. and L. A. Barrie. Arctic lower tropospheric aerosol trends and composition at Alert, Canada: 1980–1995. *Journal of Geophysical Research.* **1999**, 104 (D9), 11599.

Sisak, M. E. Poster Sessions as a Learning Technique. *Journal of Chemical Education.* **1997**, 74 (9), 1065.

Slade, J. H., T. M. VanReken, G. R. Mwaniki, S. Bertman, B. Stirm and P. B. Shepson. Aerosol production from the surface of the Great Lakes. *Geophysical Research Letters.* **2010**, 37 (18).

Slauenwhite, D. E. and B. D. Johnson. Bubble shattering: Differences in bubble formation in fresh water and seawater. *Journal of Geophysical Research.* **1999**, 104 (C2), 3265.

Smith, V. H. Eutrophication of freshwater and coastal marine ecosystems a global problem. *Environmental Science and Pollution Research.* **2003**, 10 (2), 126-139.

Song, X.-H., P. K. Hopke, D. P. Fergenson and K. A. Prather. Classification of Single Particles Analyzed by ATOFMS Using an Artificial Neural Network, ART-2A. *Analytical Chemistry.* **1999**, 71 (4), 860-865.

Sovechles, J. M. and K. E. Waters. Effect of ionic strength on bubble coalescence in inorganic salt and seawater solutions. *AIChE Journal.* **2015**, 61 (8), 2489-2496.

Spak, S. N. and T. Holloway. Seasonality of speciated aerosol transport over the Great Lakes region. *Journal of Geophysical Research.* **2009**, 114 (D8).

Spiel, D. E. The number and size of jet drops produced by air bubbles bursting on a fresh water surface. *Journal of Geophysical Research.* **1994**, 99 (C5), 10289.

Spiel, D. E. The sizes of the jet drops produced by air bubbles bursting on sea- and fresh-water surfaces. *Tellus B.* **1994**, 46 (4), 325-338.

Squier, C., J. Renaud and S. C. Larsen. Integration of a Communicating Science Module into an Advanced Chemistry Laboratory Course. *Journal of Chemical Education.* **2006**, 83 (7), 1029.

Stains, M., J. Harshman, M. K. Barker, S. V. Chasteen, R. Cole, S. E. DeChenne-Peters, M. K. Eagan, Jr., J. M. Esson, J. K. Knight, F. A. Laski, M. Levis-Fitzgerald, C. J. Lee, S. M. Lo, L. M. McDonnell, T. A. McKay, N. Michelotti, A. Musgrove, M. S. Palmer, K. M. Plank, T. M. Rodela, E. R. Sanders, N. G. Schimpf, P. M. Schulte, M. K. Smith, M. Stetzer, B. Van Valkenburgh, E. Vinson, L. K. Weir, P. J. Wendel, L. B. Wheeler and A. M. Young. Anatomy of STEM teaching in North American universities. *Science.* **2018**, 359 (6383), 1468-1470.

Steffen, M. M., B. S. Belisle, S. B. Watson, G. L. Boyer and S. W. Wilhelm. Status, causes and controls of cyanobacterial blooms in Lake Erie. *Journal of Great Lakes Research.* **2014**, 40 (2), 215-225.

Stein, A. F., R. R. Draxler, G. D. Rolph, B. J. B. Stunder, M. D. Cohen and F. Ngan. NOAA's HYSPLIT Atmospheric Transport and Dispersion Modeling System. *Bulletin of the American Meteorological Society.* **2015**, 96 (12), 2059-2077.

Stokes, M. D., G. B. Deane, K. Prather, T. H. Bertram, M. J. Ruppel, O. S. Ryder, J. M. Brady and D. Zhao. A Marine Aerosol Reference Tank system as a breaking wave analogue for the production of foam and sea-spray aerosols. *Atmospheric Measurement Techniques.* **2013**, 6 (4), 1085-1094.

Stroeve, J., M. Serreze, M. Holland, J. Kay, J. Malanik and A. Barrett. The Arctic's rapidly shrinking sea ice cover: a research synthesis. *Climatic Change.* **2012**, 110 (3-4), 1005-1027.

Stroeve, J. C., M. C. Serreze, M. M. Holland, J. E. Kay, J. Malanik and A. P. Barrett. The Arctic's rapidly shrinking sea ice cover: a research synthesis. *Climatic Change.* **2011**, 110 (3-4), 1005-1027.

Struthers, H., A. M. L. Ekman, P. Glantz, T. Iversen, A. Kirkevag, E. M. Martensson, O. Seland and E. D. Nilsson. The effect of sea ice loss on sea salt aerosol concentrations and the radiative balance in the Arctic. *Atmospheric Chemistry and Physics.* **2011**, 11 (7), 3459-3477.

Sturges, W. T. and L. A. Barrie. Chlorine, Bromine and Iodine in Arctic Aerosols. *Atmospheric Environment.* **1988**, 22 (6), 1179-1194.

Sullivan, R. C., S. A. Guazzotti, D. A. Sodeman and K. A. Prather. Direct observations of the atmospheric processing of Asian mineral dust. *Atmospheric Chemistry and Physics.* **2007**, 7 (5), 1213-1236.

Sullivan, R. C., M. J. Moore, M. D. Petters, S. M. Kreidenweis, G. C. Roberts and K. A. Prather. Timescale for hygroscopic conversion of calcite mineral particles through heterogeneous reaction with nitric acid. *Physical Chemistry Chemical Physics.* **2009**, 11 (36), 7826-7837.

Sultana, C. M., H. Al-Mashat and K. A. Prather. Expanding Single Particle Mass Spectrometer Analyses for the Identification of Microbe Signatures in Sea Spray Aerosol. *Analytical Chemistry.* **2017**, 89 (19), 10162-10170.

Sultana, C. M., D. B. Collins and K. A. Prather. Effect of Structural Heterogeneity in Chemical Composition on Online Single-Particle Mass Spectrometry Analysis of Sea Spray Aerosol Particles. *Environmental Science & Technology.* **2017**.

Sultana, C. M., G. C. Cornwell, P. Rodriguez and K. A. Prather. FATES: a flexible analysis toolkit for the exploration of single-particle mass spectrometer data. *Atmospheric Measurement Techniques.* **2017**, 10 (4), 1323-1334.

Swan, J. A. and T. G. Spiro. Context in Chemistry: Integrating Environmental Chemistry with the Chemistry Curriculum. *Journal of Chemical Education.* **1995**, 72 (11), 967.

Tabbutt, F. D. Water: A Powerful Theme for an Interdisciplinary Course. *Journal of Chemical Education.* **2000**, 77 (12), 1594.

The Boyer Commission on Educating Undergraduates in the Research University. Reinventing Undergraduate Education: A Blueprint for America's Research Universities. **1998**.

Tjernström, M., C. E. Birch, I. M. Brooks, M. D. Shupe, P. O. G. Persson, J. Sedlar, T. Mauritsen, C. Leck, J. Paatero, M. Szczodrak and C. R. Wheeler. Meteorological conditions in the central Arctic summer during the Arctic Summer Cloud Ocean Study (ASCOS). *Atmospheric Chemistry and Physics.* **2012**, 12 (15), 6863-6889.

Tomasik, J. H., K. E. Cottone, M. T. Heethuis and A. Mueller. Development and Preliminary Impacts of the Implementation of an Authentic Research-Based Experiment in General Chemistry. *Journal of Chemical Education.* **2013**, 90 (9), 1155-1161.

Tomasik, J. H., D. LeCaptain, S. Murphy, M. Martin, R. M. Knight, M. A. Harke, R. Burke, K. Beck and I. D. Acevedo-Polakovich. Island Explorations: Discovering Effects of Environmental Research-Based Lab Activities on Analytical Chemistry Students. *Journal of Chemical Education.* **2014**, 91 (11), 1887-1894.

Twohy, C. H. and J. R. Anderson. Droplet nuclei in non-precipitating clouds: composition and size matter. *Environmental Research Letters.* **2008**, 3 (4), 045002.

U.S. Department of Education. STEM 2026: A Vision for Innovation in STEM Education. **2016**.

Udisti, R., U. Dayan, S. Becagli, M. Busetto, D. Frosini, M. Legrand, F. Lucarelli, S. Preunkert, M. Severi, R. Traversi and V. Vitale. Sea spray aerosol in central Antarctica. Present atmospheric behaviour and implications for paleoclimatic reconstructions. *Atmospheric Environment.* **2012**, 52, 109-120.

Uno, I., K. Eguchi, K. Yumimoto, T. Takemura, A. Shimizu, M. Uematsu, Z. Liu, Z. Wang, Y. Hara and N. Sugimoto. Asian dust transported one full circuit around the globe. *Nature Geoscience.* **2009**, 2 (8), 557-560.

Valavanidis, A., K. Fiotakis and T. Vlachogianni. Airborne Particulate Matter and Human Health: Toxicological Assessment and Importance of Size and Composition of Particles for Oxidative Damage and Carcinogenic Mechanisms. *Journal of Environmental Science and Health, Part C.* **2008**, 26 (4), 339-362.

VandenBoer, T. C., M. Z. Markovic, A. Petroff, M. F. Czar, N. Borduas and J. G. Murphy. Ion chromatographic separation and quantitation of alkyl methylamines and ethylamines in atmospheric gas and particulate matter using preconcentration and suppressed conductivity detection. *J Chromatogr A.* **2012**, 1252, 74-83.

VandenBoer, T. C., M. Z. Markovic, J. E. Sanders, X. Ren, S. E. Pusede, E. C. Browne, R. C. Cohen, L. Zhang, J. Thomas, W. H. Brune and J. G. Murphy. Evidence for a nitrous acid (HONO) reservoir at the ground surface in Bakersfield, CA, during CalNex 2010. *Journal of Geophysical Research: Atmospheres.* **2014**, 119 (14), 9093-9106.

VandenBoer, T. C., A. Petroff, M. Z. Markovic and J. G. Murphy. Size distribution of alkyl amines in continental particulate matter and their online detection in the gas and particle phase. *Atmospheric Chemistry and Physics.* **2011**, 11 (9), 4319-4332.

VandenBoer, T. C., C. J. Young, R. K. Talukdar, M. Z. Markovic, S. S. Brown, J. M. Roberts and J. G. Murphy. Nocturnal loss and daytime source of nitrous acid through reactive uptake and displacement. *Nature Geoscience.* **2014**, 8 (1), 55-60.

VanReken, T. M., G. R. Mwaniki, H. W. Wallace, S. N. Pressley, M. H. Erickson, B. T. Jobson and B. K. Lamb. Influence of air mass origin on aerosol properties at a remote Michigan forest site. *Atmospheric Environment.* **2015**, 107, 35-43.

Vergara-Temprado, J., B. J. Murray, T. W. Wilson, amp, apos, D. Sullivan, J. Browse, K. J. Pringle, K. Ardon-Dryer, A. K. Bertram, S. M. Burrows, D. Ceburnis, P. J. DeMott, R. H. Mason, amp, apos, C. D. Dowd, M. Rinaldi and K. S. Carslaw. Contribution of feldspar and marine organic aerosols to global ice nucleating particle concentrations. *Atmospheric Chemistry and Physics.* **2017**, 17 (5), 3637-3658.

Vernon, J., D. Goldberg and J. Wolfe. Engaging Students in Authentic Research in Introductory Chemistry and Biology Laboratories. **2016**. New Orleans, Louisiana.

Veron, F. Ocean Spray. *Annual Review of Fluid Mechanics.* **2015**, 47 (1), 507-538.

Versprille, A., A. Zabih, T. A. Holme, L. McKenzie, P. Mahaffy, B. Martin and M. Towns. Assessing Student Knowledge of Chemistry and Climate Science Concepts Associated with Climate Change: Resources To Inform Teaching and Learning. *Journal of Chemical Education.* **2017**, 94 (4), 407-417.

Walz, K. A. and S. C. Kerr. "Holes" in Student Understanding: Addressing Prevalent Misconceptions Regarding Atmospheric Environmental Chemistry. *Journal of Chemical Education.* **2007**, 84 (10), 1693.

Wang, J., X. Bai, H. Hu, A. Clites, M. Colton and B. Lofgren. Temporal and Spatial Variability of Great Lakes Ice Cover, 1973–2010*. *Journal of Climate.* **2012**, 25 (4), 1318-1329.

Wang, M. R. An Introductory Laboratory Exercise on Solution Preparation: A Rewarding Experience. *Journal of Chemical Education.* **2000**, 77 (2), 249.

Wang, X., G. B. Deane, K. A. Moore, O. S. Ryder, M. D. Stokes, C. M. Beall, D. B. Collins, M. V. Santander, S. M. Burrows, C. M. Sultana and K. A. Prather. The role of jet and film drops in controlling the mixing state of submicron sea spray aerosol particles. *Proceedings of the National Academy of Sciences.* **2017**, 114 (27), 6978-6983.

Warner, D. L., E. C. Brown and S. E. Shadle. Laboratory Instrumentation: An Exploration of the Impact of Instrumentation on Student Learning. *Journal of Chemical Education.* **2016**, 93 (7), 1223-1231.

Weinburgh, M. Gender differences in student attitudes toward science: A meta-analysis of the literature from 1970 to 1991. *Journal of Research in Science Teaching.* **1995**, 32 (4), 387-398.

Wendel, J. Working toward gender parity in the geosciences. *EOS Trans. AGU.* **2015**, 96, doi:10.10209/12015EO031573.

Wentworth, G. R., J. G. Murphy, B. Croft, R. V. Martin, J. R. Pierce, J.-S. Côté, I. Courchesne, J.-É. Tremblay, J. Gagnon, J. L. Thomas, S. Sharma, D. Toom-Sauntry, A. Chivulescu, M. Levasseur and J. P. D. Abbatt. Ammonia in the summertime Arctic marine boundary layer: sources, sinks, and implications. *Atmospheric Chemistry and Physics.* **2016**, 16 (4), 1937-1953.

Whelan, R. J. and R. N. Zare. Teaching Effective Communication in a Writing-Intensive Analytical Chemistry Course. *Journal of Chemical Education.* **2003**, 80 (8), 904.

Wieman, C. Why Not Try a Scientific Approach to Science Education? *Change: The Magazine of Higher Learning.* **2007**, 39 (5), 9-15.

Williams, E. T. and F. B. Bramwell. Introduction to Research: A new course for chemistry majors. *Journal of Chemical Education.* **1989**, 66 (7), 565.

Williams, J., M. de Reus, R. Krejci, H. Fischer and J. Ström. Application of the variability-size relationship to atmospheric aerosol studies: estimating aerosol lifetimes and ages. *Atmospheric Chemistry and Physics.* **2002**, 2 (2), 133-145.

Williams, K. C. and C. C. Williams. Five Key Ingredients for Improving Student Motivation. *Research in Higher Education Journal.* **2011**, 12, 1-23.

Wilson, T. W., L. A. Ladino, P. A. Alpert, M. N. Breckels, I. M. Brooks, J. Browse, S. M. Burrows, K. S. Carslaw, J. A. Huffman, C. Judd, W. P. Kilthau, R. H. Mason, G. McFiggans, L. A. Miller, J. J. Najera, E. Polishchuk, S. Rae, C. L. Schiller, M. Si, J. V. Temprado, T. F. Whale, J. P. Wong, O. Wurl, J. D. Yakobi-Hancock, J. P. Abbatt, J. Y. Aller, A. K. Bertram,

D. A. Knopf and B. J. Murray. A marine biogenic source of atmospheric ice-nucleating particles. *Nature.* **2015**, 525 (7568), 234-238.

Wimpfheimer, T. Peer-Evaluated Poster Sessions: An Alternative Method to Grading General Chemistry Laboratory Work. *Journal of Chemical Education.* **2004**, 81 (12), 1775.

Windschitl, M. Inquiry projects in science teacher education: What can investigative experiences reveal about teacher thinking and eventual classroom practice? *Science Education.* **2003**, 87 (1), 112-143.

Wise, M. E., E. J. Freney, C. A. Tyree, J. O. Allen, S. T. Martin, L. M. Russell and P. R. Buseck. Hygroscopic behavior and liquid-layer composition of aerosol particles generated from natural and artificial seawater. *Journal of Geophysical Research.* **2009**, 114 (D3).

Wood, S. A. and D. R. Dietrich. Quantitative assessment of aerosolized cyanobacterial toxins at two New Zealand lakes. *Journal of Environmental Monitoring.* **2011**, 13 (6), 1617-1624.

Woodcock, A. H. Note Concerning Human Respiratory Irritation Associated with High Concentrations of Plankton and Mass Mortality of Marine Organisms. *Journal of Marine Research.* **1948**, 7 (1), 56-62.

Xu, X. and J. E. Lewis. Refinement of a Chemistry Attitude Measure for College Students. *Journal of Chemical Education.* **2011**, 88 (5), 561-568.

Yan, Y.-d. and G. J. Jameson. Application of the Jameson Cell technology for algae and phosphorus removal from maturation ponds. *International Journal of Mineral Processing.* **2004**, 73 (1), 23-28.

Yang, X., J. A. Pyle and R. A. Cox. Sea salt aerosol production and bromine release: Role of snow on sea ice. *Geophysical Research Letters.* **2008**, 35 (16).

Yin, Y., Z. Levin, T. G. Reisin and S. Tzivion. The effects of giant cloud condensation nuclei on the development of precipitation in convective clouds — a numerical study. *Atmospheric Research.* **2000**, 53 (1-3), 91-116.

Yu, G. H., S. Park and K. H. Lee. Source contributions and potential source regions of size-resolved water-soluble organic carbon measured at an urban site over one year. *Environmental Science: Processes & Impacts.* **2016**, 18 (10), 1343-1358.

Zábori, J., M. Matisāns, R. Krejci, E. D. Nilsson and J. Ström. Artificial primary marine aerosol production: a laboratory study with varying water temperature, salinity, and succinic acid concentration. *Atmospheric Chemistry and Physics.* **2012**, 12 (22), 10709-10724.

Zaveri, R. A., J. C. Barnard, R. C. Easter, N. Riemer and M. West. Particle-resolved simulation of aerosol size, composition, mixing state, and the associated optical and cloud condensation nuclei activation properties in an evolving urban plume. *Journal of Geophysical Research: Atmospheres.* **2010**, 115 (D17).

Zhang, Z. Direct determination of thickness of sea surface microlayer using a pH microelectrode at original location. *Science in China Series B*. **2003**, 46 (4), 339.

Zhu, Y., H. N. OĞUz and A. Prosperetti. On the mechanism of air entrainment by liquid jets at a free surface. *Journal of Fluid Mechanics.* **2000**, 404, 151-177.